



Clarke, Cassie J. (2015) *An investigation into the role of the initiator methionine transfer RNA in cell migration and tumour growth*. PhD thesis.

<http://theses.gla.ac.uk/6913/>

Copyright and moral rights for this work are retained by the author

A copy can be downloaded for personal non-commercial research or study, without prior permission or charge

This work cannot be reproduced or quoted extensively from without first obtaining permission in writing from the author

The content must not be changed in any way or sold commercially in any format or medium without the formal permission of the author

When referring to this work, full bibliographic details including the author, title, awarding institution and date of the thesis must be given

Enlighten:Theses
<http://theses.gla.ac.uk/>
theses@gla.ac.uk

**An investigation into the role of the initiator
methionine transfer RNA in cell migration and
tumour growth**

Cassie J. Clarke

M.Sci.

Submitted in fulfilment of the requirements for the
Degree of Doctor of Philosophy

Institute of Cancer Sciences
College of Medical, Veterinary and Life Sciences
University of Glasgow

September 2015

Abstract

Control of cellular tRNA repertoires can drive specific programmes of translation to favour the maintenance of proliferative or differentiated phenotypes. tRNA_i^{Met} is the initiator methionine tRNA, responsible for recognising the start codon and initiating translation. We have investigated how increased expression of tRNA_i^{Met} can influence cell behaviour, using both immortalised cell lines *in vitro* and mouse models *in vivo*.

Levels of tRNA_i^{Met} are increased in carcinoma-associated fibroblasts compared to normal fibroblasts. To understand the cellular effects of tRNA_i^{Met} overexpression in more detail we generated immortalised mouse embryonic fibroblasts (iMEFs) that overexpressed tRNA_i^{Met} (iMEF.tRNA_i^{Met}) or an empty vector as control (iMEF.Vector). Full characterisation of iMEF.Vector and iMEF.tRNA_i^{Met} cell lines showed that overexpression of tRNA_i^{Met} did not affect cell size, energy metabolism, cell spreading, rate of cellular protein synthesis or proliferation. Increased expression of tRNA_i^{Met} did, however, have marked effects on cell migration; with iMEF.tRNA_i^{Met} cells migrating approximately 1.5 fold faster than iMEF.Vector controls when assessing both directional and random migration. This tRNA_i^{Met}-driven increase in cell speed was dependent on the levels of phosphorylated eIF2 α , indicating that fibroblast migration might be influenced by tRNA_i^{Met} in the ternary complex. Furthermore, the ability of tRNA_i^{Met} to increase cell migration depended on the ability of integrin $\alpha_5\beta_1$ to bind its extracellular ligand fibronectin. However, despite the robust and reproducible role of both phospho-eIF2 α and integrin $\alpha_5\beta_1$ in this process, the way in which these are mechanistically linked to tRNA_i^{Met} levels is yet to be determined.

To investigate whether increased stromal tRNA_i^{Met} expression may contribute to tumour progression, we utilised a mouse that expressed additional copies of the tRNA_i^{Met} gene (2+tRNA_i^{Met} mouse), and performed syngeneic allografts into these animals. Subcutaneous allograft tumours of a number of different cancer cell lines became more vascularised and grew significantly more rapidly in 2+tRNA_i^{Met} mice by comparison with tumours grown in littermate control animals. The extracellular matrix (ECM) that was deposited by fibroblasts from 2+tRNA_i^{Met} mice was found to support enhanced endothelial cell and fibroblast migration. We used SILAC mass spectrometry to compare the secretome of iMEF.Vector and

iMEF.tRNA_i^{Met} cell lines and found that overexpression of tRNA_i^{Met} significantly increased synthesis and secretion of certain types of collagen, in particular collagen II. Moreover, knockdown of collagen II using siRNA and CRISPR approaches opposed the ability of tRNA_i^{Met} overexpressing fibroblasts to deposit a pro-migratory ECM. We used the prolyl hydroxylase inhibitor, ethyl-3,4-dihydroxybenzoate (DHB), to determine whether collagen synthesis contributed to the ability of tRNA_i^{Met} to drive a pro-tumorigenic stroma *in vivo*. Administration of DHB had no effect on the growth of syngeneic allografts in wild-type mice, but opposed the ability of 2+tRNA_i^{Met} animals to support increased angiogenesis and tumour growth. Collectively these data indicate that increased expression of tRNA_i^{Met} contributes to tumour progression by enhancing the ability of stromal fibroblasts to synthesise and secrete a collagen II-rich ECM that supports endothelial cell migration and angiogenesis.

Taken together these data provide evidence that the tRNAome, and in particular cellular levels of tRNA_i^{Met}, influence both the migration of fibroblasts and the composition of their secretome in a way that promotes the generation of a microenvironment supportive of endothelial cell migration, angiogenesis and tumour growth.

Table of contents

Abstract	2
List of Tables	9
List of Figures	10
Acknowledgements	13
Author's Declaration	14
Abbreviations	15
Chapter 1 Introduction	18
1.1 The regulation of gene expression	18
1.2 General transcription	18
1.3 RNA polymerase III.....	19
1.3.1 Pol III machinery	19
1.3.2 Pol III transcription	20
1.3.2.1 Initiation	20
1.3.2.2 Elongation and termination.....	21
1.3.2.3 Regulation of Pol III transcription	22
1.3.3 Pol III products	23
1.4 Transfer RNAs	24
1.4.1 Transcription	25
1.4.2 Modification	27
1.4.3 Aminoacylation.....	28
1.4.4 Turnover.....	28
1.4.5 tRNAome	29
1.4.6 Canonical function.....	30
1.4.6.1 Protein synthesis	30
1.4.7 Non-canonical functions	33
1.4.7.1 Targeting proteins for degradation.....	33
1.4.7.2 Nutrient deprivation response	33
1.4.7.3 Apoptosis	34
1.4.8 tRNA derived fragments	34
1.4.9 tRNA expression in disease	34
1.5 Protein synthesis.....	36
1.5.1 Control of translation initiation	36
1.5.2 The influence of untranslated regions	37

1.5.2.1	Internal ribosome entry sites.....	37
1.5.2.2	Upstream open reading frames	38
1.5.2.3	5' UTR structure.....	38
1.5.3	Localised translation	39
1.6	Translational control in cancer.....	41
1.7	The tumour microenvironment	42
1.8	Cancer-associated fibroblasts	43
1.8.1	Secretion of soluble factors.....	44
1.8.2	Extracellular Matrix	46
1.8.2.1	Collagen	47
1.8.2.2	Fibronectin	50
1.8.2.3	Additional ECM components	52
1.8.2.4	Matrix degradation.....	54
1.8.2.5	Mechanical properties of the ECM.....	55
1.9	Cell migration	56
1.9.1	Single cell migration	57
1.9.2	Multicellular streaming	57
1.9.3	Collective migration.....	57
1.9.4	Integrin cell surface receptors	58
1.9.4.1	Integrin trafficking.....	59
1.9.4.2	ECM and trafficking.....	63
1.10	PhD Objectives	63
Chapter 2	Materials and methods	65
2.1	Materials	65
2.1.1	Reagents	65
2.1.2	Solutions	67
2.1.3	Kits	67
2.1.4	Primers	68
2.1.5	Plasmids.....	68
2.1.6	siRNA.....	68
2.1.7	Primary antibodies	68
2.1.8	Secondary antibodies	69
2.2	Methods	69
2.2.1	2+tRNA _i ^{Met} mice.....	69
2.2.2	Allograft models	69

2.2.2.1	Melanocyte allograft	69
2.2.2.2	Lewis lung carcinoma allograft	70
2.2.2.3	B16 melanoma allograft	70
2.2.2.4	Lewis lung carcinoma allograft with ethyl-3,4-dihydroxybenzoate treatment.....	70
2.2.3	Cloning	71
2.2.3.1	tRNA _i ^{Met} expression vector	71
2.2.3.2	Collagen II CRISPR expression vector	72
2.2.4	Cell culture	72
2.2.4.1	Immortalised cell lines	72
2.2.4.2	Primary cell lines.....	73
2.2.4.3	Transient transfection.....	73
2.2.4.4	siRNA transfection	74
2.2.4.5	Drug treatments.....	74
2.2.5	Cell proliferation assay	74
2.2.6	Flow cytometry	74
2.2.7	Cell metabolism assay	75
2.2.8	RNA extraction	75
2.2.9	RNA-Sequencing.....	76
2.2.9.1	Sample preparation	76
2.2.9.2	Sequencing and data analysis	77
2.2.10	cDNA synthesis	77
2.2.11	qRT-PCR	78
2.2.12	Western blotting	78
2.2.13	Immunoprecipitation	79
2.2.14	Capture-ELISA	80
2.2.15	Internalisation assays	80
2.2.16	Recycling assays.....	81
2.2.17	Immunofluorescence	81
2.2.18	Metabolic labelling	82
2.2.19	SILAC based mass spectrometry	82
2.2.19.1	Secretome	83
2.2.19.2	Cellular proteome	83
2.2.20	ECM generation	84
2.2.20.1	ECM derived from control and tRNA _i ^{Met} overexpressing cells	84

2.2.20.2	ECM derived from conditioned media treated cells.....	85
2.2.20.3	ECM derived from microvesicle free conditioned media	85
2.2.20.4	ECM derived from conditioned media from siRNA treated cells	85
2.2.21	Immunostaining	85
2.2.22	Atomic force microscopy	86
2.2.23	Migration assays.....	86
2.2.23.1	Directional migration	86
2.2.23.2	Random migration	86
2.2.24	Breast cancer tissue microarray & immunohistochemistry	87
2.2.25	Statistics	87
Chapter 3	The influence of tRNA _i ^{Met} levels on fibroblast behaviour	89
3.1	Introduction	89
3.2	Results.....	91
3.2.1	Generation of tRNA _i ^{Met} overexpressing immortalised fibroblast cell lines	91
3.2.2	Overexpression of tRNA _i ^{Met} does not affect cellular protein synthesis.	91
3.2.3	Overexpression of tRNA _i ^{Met} does not affect cell proliferation	92
3.2.4	Overexpression of tRNA _i ^{Met} does not affect energy metabolism	94
3.2.5	Overexpression of tRNA _i ^{Met} does not affect cell spreading.....	96
3.2.6	Overexpression of tRNA _i ^{Met} increases cell migration	97
3.2.7	Overexpression of tRNA _i ^{Met} increases cell migration through a mechanism that does not involve synthesis of collagen II	99
3.2.8	tRNA _i ^{Met} -driven fibroblast migration is dependent on ternary complex formation	101
3.2.9	tRNA _i ^{Met} -driven cell migration is dependent on integrin $\alpha_5\beta_1$ - fibronectin association.....	107
3.3	Discussion	114
Chapter 4	Increased tRNA _i ^{Met} drives cell migration and tumour growth via non-cell autonomous mechanisms	119
4.1	Introduction	119
4.2	Results.....	121
4.2.1	Expression of tRNA _i ^{Met} in cancer-associated fibroblasts.....	121
4.2.2	Increased expression of tRNA _i ^{Met} in the host animal promotes growth and angiogenesis of allografted tumours	123
4.2.3	Fibroblasts isolated from 2+tRNA _i ^{Met} transgenic mice deposit a pro-migratory ECM.....	126

4.2.4	tRNA _i ^{Met} supports deposition of pro-migratory ECM via release of secreted factors.....	128
4.2.5	tRNA _i ^{Met} drives a secretome that is enriched in collagen II and collagen-modifying enzymes.....	134
4.2.6	Collagen II secretion is required for tRNA _i ^{Met} to drive production of pro-tumourigenic ECM	140
4.2.7	Collagen II expression in human cancer	143
4.3	Discussion	147
	Chapter 5 Final Discussion	156
	Appendices.....	162
	Appendix I: Secretome dataset.....	162
	Appendix II: Cellular proteome dataset.....	165
	Appendix II: RNA-Sequencing dataset	170
	References	181

List of Tables

Table 1-1- Major eukaryotic RNA polymerases and their products.	18
Table 1-2- RNA codon table.	25
Table 1-3- The collagen family members.	48
Table 1-4- Integrin heterodimers and their ligands.	59
Table 1-5- Integrin trafficking pathways associated with human disease processes.	62
Table 2-1- Reagents and suppliers	67
Table 2-2- Recipes of solutions	67
Table 2-3- Kits and suppliers.....	68
Table 2-4- qRT-PCR primer sequences	68
Table 2-5- Expression vectors.....	68
Table 2-6- siRNA used for siRNA knock-down experiments	68
Table 2-7- Primary antibodies	69
Table 2-8- Secondary antibodies	69

List of Figures

Figure 1-1- RNA Polymerase III promoter types.	21
Figure 1-2- Regulation of Pol III transcription.	23
Figure 1-3- tRNA processing.	27
Figure 1-4- The process of eukaryotic translation initiation.	31
Figure 1-5- The process of elongation in eukaryotic protein synthesis.	32
Figure 1-6- Exposure to cell stresses inhibits global protein synthesis through P- eIF2 α	37
Figure 1-7- Tumour promoting soluble factors secreted from CAFs.	46
Figure 1-8- Collagen biosynthesis.	49
Figure 1-9- Fibronectin structure.	51
Figure 1-10- Model of mesenchymal-like cell migration through the ECM.	56
Figure 1-11- Rab GTPase control of integrin trafficking.	61
Figure 3-1- Overexpression of tRNA _i ^{Met} in immortalised mouse embryonic fibroblasts.	91
Figure 3-2- tRNA _i ^{Met} does not affect the rate of cellular protein synthesis.	92
Figure 3-3- tRNA _i ^{Met} does not affect the rate of cell proliferation.	93
Figure 3-4- tRNA _i ^{Met} does not affect cell viability, granularity or size.	94
Figure 3-5- tRNA _i ^{Met} does not affect energy metabolism.	96
Figure 3-6- tRNA _i ^{Met} does not affect cell spreading.	97
Figure 3-7- Overexpression of tRNA _i ^{Met} increases speed of cell migration.	98
Figure 3-8- Conditioned media from tRNA _i ^{Met} overexpressing cells does not affect cell migration.	99
Figure 3-9- siRNA of collagen II does not affect tRNA _i ^{Met} -driven fibroblast migration.	100
Figure 3-10- Endogenous levels of phospho-eIF2 α are unchanged by overexpression of tRNA _i ^{Met}	101
Figure 3-11- The tRNA _i ^{Met} driven increase in cell speed can be recapitulated by increasing levels of phospho-eIF2 α in control cells.	103
Figure 3-12- The tRNA _i ^{Met} driven increase in cell speed is influenced by manipulating levels of the ternary complex.	104
Figure 3-13- Cycloheximide does not inhibit tRNA _i ^{Met} -driven cell migration. ...	106
Figure 3-14- Fibronectin negates the increase in cell migration driven by tRNA _i ^{Met}	107

Figure 3-15- tRNA _i ^{Met} -driven cell migration is opposed by an integrin α_5 blocking antibody.	108
Figure 3-16- tRNA _i ^{Met} -driven cell migration is opposed by siRNA of integrin α_5	109
Figure 3-17- tRNA _i ^{Met} -driven cell migration is opposed by blockade of the RGD site in fibronectin.....	110
Figure 3-18- tRNA _i ^{Met} overexpression does not influence integrin $\alpha_5\beta_1$ expression.	111
Figure 3-19- No significant difference in integrin $\alpha_5\beta_1$ localisation following tRNA _i ^{Met} overexpression.	112
Figure 3-20- Investigation of integrin α_5 internalisation and recycling following tRNA _i ^{Met} overexpression.	113
Figure 3-21- Model of the effect of tRNA _i ^{Met} overexpression on fibroblast behaviour.	118
Figure 4-1- Changes in expression of specific tRNAs in cancer-associated fibroblasts and normal fibroblasts.	122
Figure 4-2- The 2+tRNA _i ^{Met} transgenic mouse model.	124
Figure 4-3- Increased expression of tRNA _i ^{Met} in the host animal promotes angiogenesis and growth of allografted tumours.	125
Figure 4-4- Fibroblasts isolated from 2+tRNA _i ^{Met} transgenic mice deposit a pro-migratory ECM.	127
Figure 4-5- tRNA _i ^{Met} supports deposition of pro-migratory ECM via release of secreted factor(s).....	129
Figure 4-6- No consistent difference in the thickness or stiffness of the pro-migratory ECM generated in the presence of conditioned media from tRNA _i ^{Met} overexpressing cells.	130
Figure 4-7- Microvesicles are not the secreted factor required for tRNA _i ^{Met} to support deposition of pro-migratory ECM.	131
Figure 4-8- Conditioned media from tRNA _i ^{Met} overexpressing cells is not able to influence the migratory characteristics of pre-assembled ECM.	132
Figure 4-9- ECM derived from tRNA _i ^{Met} -overexpressing cells promotes increased migration of fibroblasts but negates the difference in migration between iMEF.Vector and iMEF.tRNA _i ^{Met}	133
Figure 4-10- Integrin $\alpha_5\beta_1$ -fibronectin interaction does not influence fibroblast migration on ECM derived from control or tRNA _i ^{Met} overexpressing cells.....	134

Figure 4-11- tRNA _i ^{Met} drives a secretome that is enriched in collagen II and collagen-modifying enzymes.	136
Figure 4-12- RNA sequencing following tRNA _i ^{Met} overexpression.	139
Figure 4-13- Collagen II secretion is required for tRNA _i ^{Met} to drive production of a pro-migratory ECM.	141
Figure 4-14- CRISPR gene editing methods indicate that collagen II secretion is required for tRNA _i ^{Met} to drive production of a pro-migratory ECM.	142
Figure 4-15- The prolyl hydroxylase inhibitor, DHB, opposes the ability of tRNA _i ^{Met} to drive production of a pro-tumourigenic ECM.	143
Figure 4-16- Collagen II expression in a breast cancer tissue microarray.	146
Figure 4-17- Schematic representation of the non-cell autonomous effects of tRNA _i ^{Met} overexpression.	155
Figure 5-1- Proposed model of the tRNA _i ^{Met} effect on tumour progression.	156

Acknowledgements

I would like to thank Jim Norman for his supervision and guidance throughout my PhD, and all the members of R20 and R21 for all of their help and support. I am especially grateful to Joanna Birch and Louise Mitchell for their input and advice, and for keeping me sane over the last 4 years, and to Kirsteen Campbell and Liane McGlynn for their feedback and encouragement throughout the writing process. I am also thankful to Bob White for providing me with the initial opportunity to join the Beatson Institute, and I would like to thank Cancer Research UK for providing the funds and resources for my research.

The progress I have made throughout my time at the Beatson would not have been possible without the collaborators and services that have contributed to this work. I would therefore like to extend my thanks to David Sumpton for his proteomic expertise, Billy Clark and Andy Keith for their molecular services, Ann Hedley for her bioinformatics input, Margaret O'Prey and Tom Gilbey for their help with microscopy and FACS, Colin Nixon and his team for their histology services, Karen Blyth for her *in vivo* advice, and the BSU/BRU staff for their practical support with the *in vivo* models.

I am eternally grateful to my husband, Ben, for all of his love and support, and for always being there for me, and to my fur children Logan and Victor who never fail to put a smile on my face. A very special thank you goes to my Mum, for always believing in me and encouraging me to be the best that I can be, her love and guidance has made me the person that I am today. My friend Roslyn has also been an amazing support, and I can't thank her enough for all the bubbles, chats, and laughter. I would also like to thank my Grandma for her honesty and advice, and finally I would like to dedicate this thesis to the memory of my Grandad. I miss you very much Grandad, and I hope you are proud of me.

Author's Declaration

I declare that, except where explicit reference is made to the contribution of others, this thesis is the result of my own work and has not been submitted for any other degree at the University of Glasgow or any other institution.

Cassie Clarke

Abbreviations

aaRS	Aminoacyl-tRNA synthetase
Abi3bp	Abi gene family, member 3 (NESH) binding protein
ADAM	A disintegrin and metalloproteinase
ADAMTS	A disintegrin and metalloproteinase with thrombospondin type 1 motif
AFM	Atomic force microscopy
Ala	Alanine
Arg	Arginine
Arp2/3	Actin-related protein 2/3
Asn	Asparagine
Asp	Aspartate
Atp1b1	ATPase, Na ⁺ /K ⁺ transporting, beta 1 polypeptide
Bdp1	B double prime 1
Brf1	TFIIIB-related factor 1
Brf2	TFIIIB-related factor 2
CAF	Cancer-associated fibroblast
CLIC3	Chloride intracellular channel 3
Col2a1	Collagen, type II, alpha 1
CRISPR	Clustered Regularly Interspaced Short Palindromic Repeats
Cys	Cysteine
DHB	Ethyl-3,4-dihydroxybenzoate
Dkk2	Dickkopf homolog 2
DSE	Distal sequence element
ECM	Extracellular matrix
EGF	Epidermal growth factor
EMT	Epithelial to mesenchymal transition
ER	Endoplasmic reticulum
ER	Estrogen receptor
ERK	Extracellular signal-regulated kinase
FA	Focal adhesion
FACIT	Fibril-associated collagens with interrupted triple helices
FACS	Fluorescence activated cell sorting
FAK	Focal adhesion kinase
FAP	Fibroblast-activation protein
Fbxo2	F-box protein 2
FERM	Four-point-one, ezrin, radixin, moesin domain
FGF	Fibroblast growth factor
FMT	Fibroblast to myofibroblast transdifferentiation
FPKM	Fragments per kilobase of exon per million reads
GAG	Glycosaminoglycan
GARS	Glycyl-tRNA synthetase
GBM	Glioblastoma multiforme
GCN5	General control of amino acid synthesis protein 5
GEF	Guanine nucleotide exchange factor
Gln	Glutamine
Glu	Glutamate

Gly	Glycine
HAT	Histone acetyltransferase
HGF	Hepatocyte growth factor
His	Histidine
HPRT	hypoxanthine phosphoribosyltransferase
HUVEC	Human umbilical vein endothelial cells
iCAF	Immortalised human mammary cancer-associated fibroblast
IE	Intermediate element
IHC	Immunohistochemistry
Ile	Isoleucine
iMEF	Immortalised mouse embryonic fibroblast
iNF	Immortalised human normal fibroblast
IRES	Internal ribosome entry sites
Kctd12b	potassium channel tetramerisation domain containing 12b
LC-MS	Liquid chromatography-mass spectrometry
Leu	Leucine
LLC	Lewis lung carcinoma
LOX	Lysyl oxidase
Lys	Lysine
MACIT	Membrane-associated collagens with interrupted triple helices
MCS	Multiple cloning site
MEF	Primary mouse embryonic fibroblast
MELAS	Mitochondrial encephalomyopathy, lactic acidosis, and stroke-like episodes
Meox1	Mesenchyme homeobox 1
MERRF	Myoclonic epilepsy with red tagged fibers
Met	Methionine
miRNA	Micro-RNA
MM	Multiple myeloma
MMP	Matrix metalloproteinases
MSC	Mesenchymal stem cells
mTOR	Mammalian target of rapamycin
mt-tRNA	Mitochondrial transfer RNA
MULTIPLEXIN	Mutiple triple-helix domains and interruptions
MV	Microvesicles
MW	Molecular weight
NDLB	Nondenaturing lysis buffer
NF	Normal fibroblast
NT	Non-targeting siRNA
OFP	Orange fluorescent protein
PABP	Poly-A binding protein
Pappa	Pregnancy-associated plasma protein A
PCH	<i>Pontocerebellar hypoplasia</i>
PDGF	Platelet-derived growth factor
PERK	Protein <i>kinase</i> RNA-like endoplasmic reticulum <i>kinase</i>
PFA	Paraformaldehyde
Phe	Phenylalanine
PI	Propidium Iodide
PIC	Pre-initiation complex

PKB	Protein Kinase B / Akt
PKC	Protein Kinase C
PKR	Protein Kinase R
Plk1	Polo-like kinase 1
Pol I	RNA Polymerase I
Pol II	RNA Polymerase II
Pol III	RNA Polymerase III
Pro	Proline
PRTE	Pyrimidine-rich translational elements
PSE	Proximal sequence element
qRT-PCR	Quantitative real time polymerase chain reaction
Rb	Retinoblastoma protein
RCP	Rab-coupling protein
RGD	Arginine-Glycine-Aspartate sequence
RNA-Seq	RNA sequencing
ROS	Reactive oxygen species
rRNA	Ribosomal RNA
RT	Room temperature
RTD	Rapid tRNA Decay pathway
RTK	Receptor tyrosine kinase
SDF-1	Stromal-derived factor
Ser	Serine
SFRP	Secreted-frizzled related protein
SILAC	Stable isotope labelling by amino acids in cell culture
snRNA	Small nuclear RNA
snRNP	Small nuclear ribonucleoprotein
SRP	Signal recognition particle
TAF	Transacting factor
T-ALL	T-cell acute lymphoblastic leukaemia
TBP	TATA-binding protein
TC	Ternary complex
TGF- β	Transforming growth factor- β
Thr	Threonine
TMA	Tissue microarray
TME	Tumour microenvironment
TOP	Terminal oligopyrimidine tracts
tRF	Transfer RNA derived fragment
tRNA	Transfer RNA
tRNA _i ^{Met}	Initiator methionine transfer RNS
TSP	Tumour stroma percentage
TSS	Transcription start site
Tyr	Tyrosine
uORF	Upstream open reading frame
UTR	Untranslated region
Val	Valine
VEGF	Vascular endothelial growth factor
WASH	WASP and SCAR homologue complex
WT	Wild type

Chapter 1 Introduction

1.1 The regulation of gene expression

The control of gene expression is a fundamental aspect of both health and disease that is governed by a number of highly sophisticated mechanisms. The initial pioneering work into the structure of DNA by Watson, Crick, Wilkins and Franklin provided the early suggestion of “a possible copying mechanism for genetic material” (Watson and Crick, 1953), and the consequent transcription of DNA into RNA and translation of RNA to protein are well established processes that play key roles in regulating gene expression (Crick, 1970). Advances in epigenetics, in addition to progress in understanding post-transcriptional and post-translational modifications, continue to add additional layers of complexity to these processes, and it is now apparent that what may once have been considered basic biology is actually anything but, as investigating the intricacy of transcriptional and translational regulation again comes to the fore-front of biological research (Gingold et al., 2014, Rubio et al., 2014, Truitt et al., 2015).

1.2 General transcription

In order to express the information stored within the genome, genes must first be transcribed from DNA to RNA by an RNA polymerase. In eukaryotes three major RNA Polymerases have evolved, each catalysing the transcription of a specific set of genes (Table 1-1).

RNA Polymerase	Product	Gene Product Abbreviation	Function
Pol I	ribosomal RNA	rRNA	ribosome
Pol II	messenger RNA	mRNA	protein coding
	small nucleolar micro RNA	snRNA miRNA	pre-mRNA splicing gene expression
	transfer RNA	tRNA	adaptor molecule
Pol III	specific rRNA	5S rRNA	ribosome
	specific snRNA	U6 snRNA	pre-mRNA splicing
	other small RNAs	Inc. MRP, 7SL	various

Table 1-1- Major eukaryotic RNA polymerases and their products.

In plants two additional nuclear RNA polymerases have also been identified, namely RNA polymerase IV and V, which are related to RNA polymerase II and encode non-coding RNAs involved in gene silencing (Haag and Pikaard, 2011).

Eukaryotic cells also express a specific RNA polymerase responsible solely for the transcription of the mitochondrial genome, encoding the 13 transcripts required for the components of the electron transport chain in addition to the 2 rRNAs and 22 tRNAs required for their translation (reviewed in (Arnold et al., 2012)).

Of the main RNA polymerases, RNA Polymerase II (Pol II) is responsible for transcription of all protein-coding genes and some non-coding RNA products such as microRNAs (miRNA) and small nuclear RNAs (snRNA). RNA Polymerase I (Pol I) is dedicated only to production of ribosomal RNA (rRNA), and this occurs through transcription of a large 47S pre-rRNA template which is then processed into mature 5.8S, 18S and 28S rRNAs to form essential components of the ribosomal machinery (Moss and Stefanovsky, 2002, Moore and Steitz, 2002). RNA Polymerase III (Pol III) is responsible for transcription of small non-coding RNAs, including transfer RNAs (tRNAs) and 5S rRNA, and in collaboration with Pol I, transcribes essential components of the protein synthesis machinery (White, 1998). The level of Pol III transcription, therefore, tends to be coordinated with regulation of cell growth, and so is increased in conditions supportive of proliferation and inhibited in times of stress.

1.3 RNA polymerase III

1.3.1 Pol III machinery

Pol III is a large multi-subunit enzyme, composed of 17 subunits with a total mass of 600 - 700kDa (White, 2001, Dieci et al., 2007). Dedicated to the transcription of small structural and catalytic RNAs, Pol III can initiate transcription through interaction with its associated transcription factors TFIIC and TFIIB. TFIIC is composed of 6 subunits (TFIIC220, TFIIC110, TFIIC102, TFIIC90, TFIIC63 and TFIIC35) that come together in two major subdomains connected by a flexible linker, with the intrinsic histone acetyltransferase (HAT) activity of TFIIC220, TFIIC110 and TFIIC90 being central to their role in Pol III transcription (Hsieh et al., 1999a, Hsieh et al., 1999b, Kundu et al., 1999). TFIIB is a complex of 3 independent subunits composed of TBP (TATA-binding protein), Bdp, and BRF1 or BRF2 (TFIIB-related factor 1 or 2) (Wang and Roeder, 1995), and gene structure determines which Pol III specific factors are recruited.

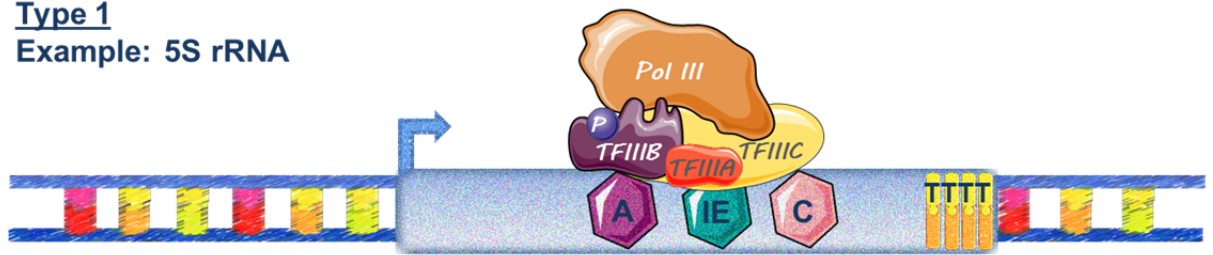
1.3.2 Pol III transcription

1.3.2.1 Initiation

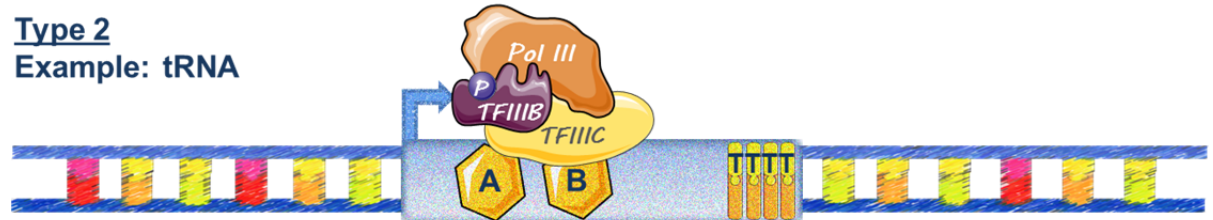
Initiation of Pol III transcription can occur at three different promoter types (Figure 1-1) (Dieci et al., 2007, Schramm and Hernandez, 2002). For type 1 and type 2 promoters, the promoter sequence is positioned within the transcribed region. Type 1 structures are only found within 5S rRNA genes and consist of a pair of conserved motifs (A box and C box) separated by an intermediate element sequence (IE). To initiate transcription at type 1 promoters, TFIIIC recognises and binds to the A and C box internal promoter sequences and this is assisted by an additional transcription factor, TFIIIA, which can bind the IE. TFIIIB can then associate upstream of the transcription start site (TSS) to enable recruitment of Pol III and formation of the pre-initiation complex (PIC). Type 2 promoters are found in all tRNA genes (with the exception of tRNA^{Sec}_{Cys}). They initiate transcription in a similar manner to that described for type 1 promoters, with the exception of TFIIIA requirement and the internal promoters recognised by TFIIIC are defined as A and B box sequences. For both type 1 and type 2 promoters TFIIIB is composed of TBP, Bdp and BRF1, and the rate-limiting step of PIC formation is TFIIIB recruitment (Oler et al., 2010, Moqtaderi and Struhl, 2004). However, at type 3 promoters a variant TFIIIB is required, which is comprised of TBP, Bdp and BRF2 subunits. Type 3 genes include U6, and this gene structure is reminiscent of that found in protein-coding genes. External promoter sequences upstream of the TSS include a distal sequence element (DSE), proximal sequence element (PSE) and a TATA box. TFIIIB binds the TATA box to recruit a multi subunit complex known as SNAP_C to the PSE, and this then enables Pol III to bind the TSS. Following recruitment of additional factors, including Oct-1 and STAF at the DSE, the PIC can then initiate Pol III transcription (Dieci et al., 2007, Schramm and Hernandez, 2002). A transcription bubble is formed as the helicase activity of the polymerase unwinds the double-stranded DNA to expose the template strand, ribonucleotides are then incorporated into a complementary RNA transcript, and TFIIIB releases Pol III allowing elongation to begin (Kassavetis et al., 1990, White, 2002).

Type 1

Example: 5S rRNA

**Type 2**

Example: tRNA

**Type 3**

Example: U6

**Figure 1-1- RNA Polymerase III promoter types.**

A schematic representation of the three types of Pol III promoter. Type I promoters, eg 5S rRNA, have internal A and C block promoters separated by an intermediate element (IE), and Pol III binding is aided by the transcription factors TFIIC, TFIIA, and TFIIB (consisting of BRF1, Bdp and TBP). Type 2 promoters, eg tRNAs, have two internal A and B box sequences that function as internal promoters, and are bound as above but without the requirement for TFIIA. Type 3 promoters, eg U6 RNA, are more similar to protein coding genes and have a distal sequence element (DSE), a proximal sequence element (PSE) and a TATA box, and are bound by a TFIIB variant consisting of BRF2, Bdp1 and TBP, in addition to a SNAP_C multi-protein complex and Pol III. Image made using items from Image Bank in Servier Medical Art.

1.3.2.2 Elongation and termination

Pol III transcription generates non-coding RNAs that are generally less than 300 base pairs (bp) in length, and so it requires no additional accessory factors (Schramm and Hernandez, 2002, Canella et al., 2010). Elongation is followed by termination, which is signalled by a short run of thymine residues. The poly-T signal pauses the polymerase causing catalytic inactivation and backtracking which commits the enzyme to termination and enables release of the newly synthesised RNA (Nielsen et al., 2013).

1.3.2.3 Regulation of Pol III transcription

The rate of Pol III transcription is tightly linked to the rate of cell growth and proliferation. For cells to be able to grow and divide they need to accumulate mass, and as the majority of a cell's dry mass is protein, the Pol III mediated transcription of essential components of the protein synthesis machinery is regulated in-line with cell growth requirements. Serum and increased nutrient availability therefore increase Pol III transcription, while growth arrest and other cell stresses oppose it (Clarke et al., 1996, Mauck and Green, 1974).

The level of Pol III transcription can be regulated in a number of different ways. The short length of Pol III products means that assignment of control to the elongation step would be insufficiently effective, and so the rate-limiting step of Pol III transcription tends to be PIC formation in initiation. Increased expression of TFIIC and TFIIIB are associated with increased Pol III activity (White, 2004), and phosphorylation of BRF1 by a number of different kinases, including ERK and PLK1 (Polo-like kinase 1), is also thought to increase TFIIIB's binding affinity for TFIIC to increase the rates of Pol III transcription (Fairley et al., 2012, Felton-Edkins et al., 2003).

Specific regulators are also able to bind and modulate components of the Pol III machinery (Figure 1-2). Through its association with BRF1, c-Myc can localise to tRNA genes and recruit the co-factors GCN5 and TRRAP to promote Pol III transcription (Gomez-Roman et al., 2003, Kenneth et al., 2007). Overexpression of c-Myc, therefore, increases the rate of Pol III transcription (Aaronson, 1991, Johnson et al., 2008, Gomez-Roman et al., 2006). Retinoblastoma protein (Rb) and p53 can also bind TFIIIB, but their association is inhibitory to Pol III transcription, as they block the interaction between TFIIC and TFIIIB to prevent the recruitment of Pol III to its promoters (White et al., 1996, Cairns and White, 1998). Maf1 is another repressor of Pol III transcription, and this inhibition can occur through its ability to associate with both TFIIIB and Pol III (Boguta, 2013). Maf1 activity is regulated by its phosphorylation status (Pluta et al., 2001). Inactivation of Maf1 by mTOR-dependent phosphorylation increases Pol III transcription in response to nutrient availability (Kantidakis et al., 2010, Boguta, 2013), and increased growth driven by aberrant TORC1 activity can be blocked in mutant BRF1 cells (Marshall et al., 2012). The level of Pol III-mediated

transcription is therefore intricately linked to the rate of protein synthesis and cell growth, and the abnormal Pol III activity which is reported as a common feature of cancer cells is therefore not surprising considering its regulation by a number of well-characterised tumour promoters and suppressors (Figure 1-2) (White, 2004).

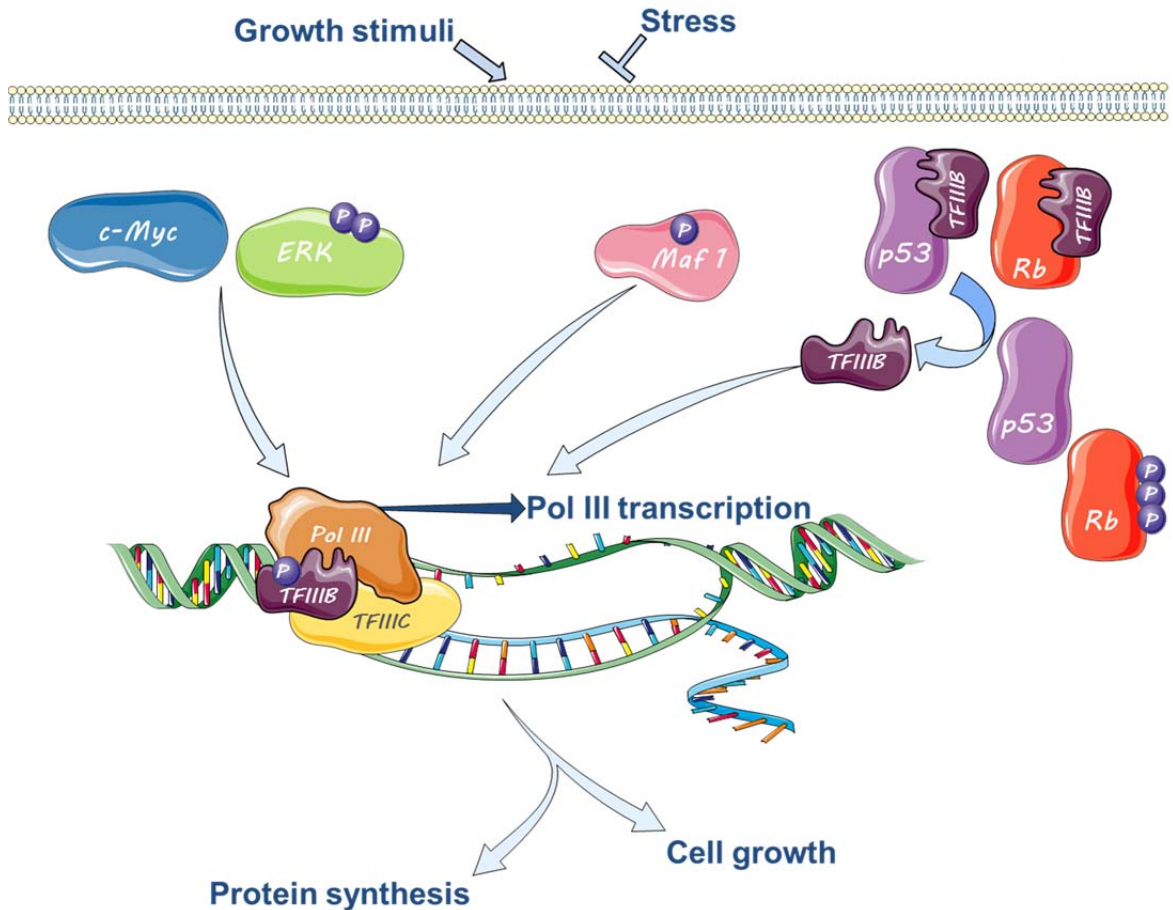


Figure 1-2- Regulation of Pol III transcription.

Pol III-mediated transcription is regulated by a variety of different factors, and is increased in response to growth stimuli. Phosphorylation of Pol III specific transcription factors by kinases such as ERK can increase the affinity of TFIIB for the Pol III machinery, whilst c-Myc can recruit histone acetyltransferases (HATs) to increase gene expression. Negative regulators of Pol III transcription include Maf1, p53 and Rb, and release of repression by these factors can increase Pol III transcription. Pol III transcribes essential components of the protein synthesis machinery, and as a consequence is associated with processes such as cell growth. Image made using items from Image Bank in Servier Medical Art.

1.3.3 Pol III products

Although all the products transcribed by Pol III are small non-coding RNAs, they can have a number of versatile functions within the cell including roles in RNA

processing and protein localisation, in addition to more well-known functions in ribosome biogenesis and protein synthesis.

U6 is a small nuclear RNA (snRNA) that forms the RNA component of the small nuclear ribonucleoprotein (snRNP). This RNA-protein complex associates with other snRNPs and additional proteins to form the spliceosome, and is responsible for splicing pre-mRNA (Will and Luhrmann, 2011).

7SL is the RNA component of the signal recognition particle (SRP) ribonucleoprotein complex (Walter and Blobel, 1982). Once bound to its 6 associated protein subunits, the SRP complex facilitates trafficking of newly synthesised proteins into the endoplasmic reticulum (ER) and can also play a role in post-translational sorting (Shan and Walter, 2005, Abell et al., 2004).

5S rRNA is an essential component of the large subunit of the ribosome, and its expression is coordinated with the transcription of the other rRNAs produced by Pol I. Ribosomal RNA conducts most of the functional and catalytic roles of the ribosome, while the associated ribosomal proteins are mainly required to provide structural support (Moore and Steitz, 2002).

Transfer RNAs (tRNAs) are some of the most abundant Pol III products (Dieci et al., 2007), and as they function as adaptor molecules in protein synthesis, they have long been considered housekeepers that recognise codons of the mRNA and bring the corresponding amino acids to the translation machinery (Hoagland et al., 1958). However, recent work has suggested that tRNAs play a much more complex role in translational control (Gingold et al., 2014), and so further investigating tRNA biology could be of great value in understanding the complexities of gene expression.

1.4 Transfer RNAs

There are currently 516 annotated genes known to encode nuclear tRNAs dispersed throughout the human genome, and 22 known mitochondrial tRNA genes (Genomic tRNA database, (Lowe and Eddy, 1997)). They can be categorised into 61 isoacceptor classes depending on the anticodon they contain, and into 21 isotypes depending on the amino acid they decode (20 standard

amino acids plus selenocysteine) (Dittmar et al., 2006). For example, tRNAs with the anticodons AAG and CAG can both specify leucine, and are therefore of the same isotype. However, the difference in their anticodon sequence means they belong to different isoacceptor classes. Since there are only 61 possible anticodons specified by the triplet code (Table 1-2), there are many tRNA species in the same isoacceptor family that have sequence differences throughout the body of the tRNA.

		Second Letter				
		U	C	A	G	
First Letter	U	UUU Phe UUC UUA Leu UUG	UCU UCC Ser UCA UCG	UAU Tyr UAC UAA Stop UAG	UGU Cys UGC UGA Stop UGG Trp	U C A G
	C	CUU CUC Leu CUA CUG	CCU CCC Pro CCA CCG	CAU His CAC CAA Gln CAG	CGU CGC Arg CGA CGG	U C A G
	A	AUU Ile AUC AUA AUG Met	ACU ACC Thr ACA ACG	AAU Asn AAC AAA Lys AAG	AGU Ser AGC AGA Arg AGG	U C A G
	G	GUU GUC Val GUA GUG	GCU GCC Ala GCA GCG	GAU Asp GAC GAA Glu GAG	GGU GGC Gly GGA GGG	U C A G
						Third Letter

Table 1-2- RNA codon table.

The genetic code describing the codons encoding each of the standard amino acids.

1.4.1 Transcription

tRNA genes are highly transcribed, producing 3 million new tRNAs per yeast cell division cycle compared to around 60,000 mRNAs (Ares et al., 1999, Waldron and Lacroute, 1975). tRNA synthesis begins with Pol III-mediated transcription in the nucleus from type 2 promoters (as described in 1.3.2), and the pre-tRNA generated is then processed into a mature transcript (White, 2002). This occurs through RNase P and RNase Z cleavage at the 5' and 3' ends respectively, and a CCA sequence is then added to the 3' end by a nucleotidyl-transferase (Frank and Pace, 1998, Ceballos and Vioque, 2007). Splicing occurs, for intron-containing tRNAs, through reactions with tRNA-splicing endonucleases, and this

is invariably performed adjacent to the anticodon loop between positions 37 and 38 of the tRNA (Tocchini-Valentini et al., 2009). Nucleotides can then be modified and this acts not only to stabilise the tRNA but also has functional consequences, as will be described further in 1.4.2 (Figure 1-3). Nuclear export to the cytoplasm is mediated by the Ran-GTPase pathway and Xpo-t, a member of the Ran-binding β -importin family (Kutay et al., 1998, Arts et al., 1998). Xpo-t directly binds the tRNA and associates with Ran-GTP, allowing the Ran-GTP:Xpo-t:tRNA complex to move through the nuclear pores to the cytoplasm, where increased Ran-GAP activity hydrolyses Ran-GTP to Ran-GDP, facilitating dissociation of the complex and tRNA release. The tRNA is then available to be charged with its cognate amino acid via an aminoacylation reaction that will also be described in more detail later in the text (1.4.3). Subsequent data, however, have suggested that the process is not necessarily this simple and that, at least in yeast, splicing can occur out-with the nucleus (Yoshihisa et al., 2003), movement between the nucleus and the cytoplasm can be bidirectional, and aminoacylation does not only occur in the cytoplasm (Hopper and Shaheen, 2008, Lund and Dahlberg, 1998).

Mature tRNAs are 70 to 100 nucleotides in length with a cloverleaf secondary structure and a complex L-shaped tertiary structure. The main functional regions of the tRNA are the anticodon, which reads the codons of the mRNA, and the 3' CCA nucleotides which enable attachment of the corresponding amino acid. The tRNA anticodon is located at positions 34, 35 and 36 of the tRNA, and position 34 can pair with various nucleotides through wobble and non-Watson-Crick interactions at the third position of the mRNA codon, allowing for the degeneracy of the genetic code (Agris et al., 2007). Other regions important in defining the identity of a tRNA include sequences within the acceptor stem and the D, T and variable loops (Goodenbour and Pan, 2006). In addition to differences in sequence, tRNA bases can also be highly modified, with 105 different chemical modifications of tRNAs currently described that primarily have structural and stabilising roles (The RNA modification database <http://mods.rna.albany.edu/home>).

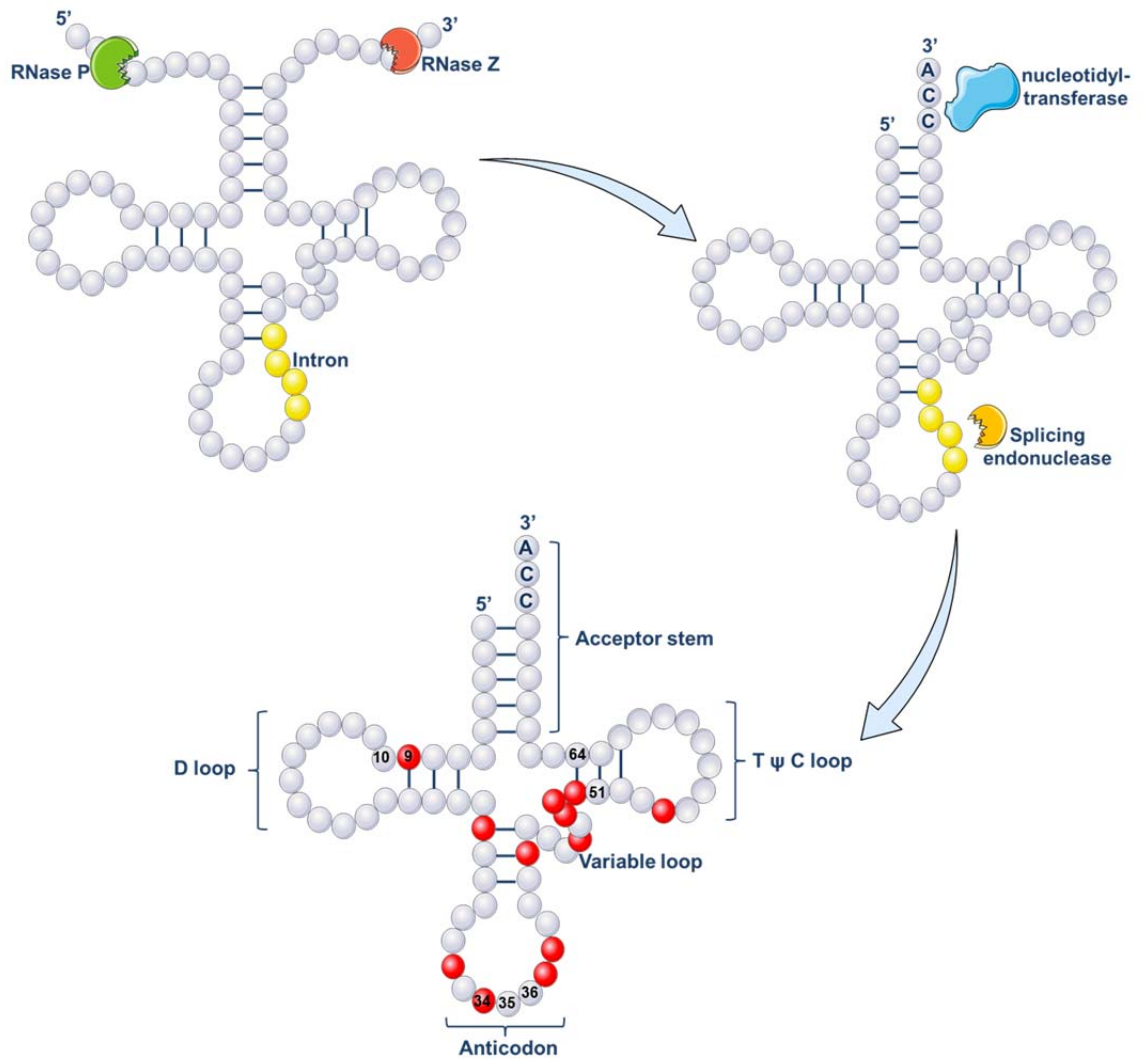


Figure 1-3- tRNA processing.

Schematic representation of the processes that occur in generation of a mature tRNA. The pre-tRNA is processed by RNase P and Z, and a 3' CCA then added by a tRNA nucleotidyl-transferase. Splicing can occur in intron containing tRNAs, and the bases that are commonly modified are highlighted in red. The functional domains important in specifying tRNA identity are also identified, and numbers refer to the nucleotide positions. Image made using items from Image Bank in Servier Medical Art.

1.4.2 Modification

The post-transcriptional modification of selected tRNA nucleotides is an important part of the tRNA maturation process that is essential for correct tRNA structure, function and stability. There are a number of specific bases that are commonly modified (as represented in Figure 1-3) and tRNAs that lack the correct modifications are targeted to degradation pathways (Phizicky and Hopper, 2010). For example, modifications at position 37 (adjacent to the anticodon loop) can stabilise codon:anticodon interactions to prevent frameshifts in translation (El Yacoubi et al., 2012), modifications at position 34

(the wobble position of the anticodon) are important in decoding the degeneracy of the amino acid code, and modifications in the main body of the tRNA tend to have structural and stabilising roles (Novoa et al., 2012). Common modifications at the wobble position include incorporation of thiol, hydroxyl and methyl groups on uridine (U), and adenosine-to-inosine (A-to-I) editing, while the 2'-O-ribose phosphate modification at position 64 of tRNA^{Met} distinguishes the initiator methionine tRNA (tRNA_i^{Met}) from the elongator methionine tRNA (tRNA_e^{Met}) (Astrom and Bystrom, 1994). Correct tRNA modifications are therefore important in specifying the identity of tRNAs to maintain correct aminoacylation reactions and fidelity in protein synthesis.

1.4.3 Aminoacylation

By recognising embedded identity elements within the tRNA, including discriminatory bases, unique base-pair interactions and specific modifications, aminoacyl-tRNA synthetases (aaRSs) charge tRNA molecules with their corresponding amino acid, and this process is completed via a two-step reaction. The first stage consumes ATP to activate the amino acid with an active phosphate moiety to form an aminoacyl-adenylate intermediate, and in the second phase the charged amino acid is covalently attached to the 3'-CCA of the corresponding tRNA (Beuning and Musier-Forsyth, 1999). aaRSs are categorised into two classes, Class I are monomeric and aminoacylate the 2'-OH of a terminal adenosine nucleotide on the tRNA, while Class II aaRSs are oligomeric and generally aminoacylate the 3'-OH of the terminal adenosine (Pang et al., 2014). Both classes of aaRSs have proofreading abilities and are able to edit amino acid loading errors via hydrolytic domains in their catalytic core, and so represent the final but important step of tRNA biosynthesis to generate a mature charged tRNA for use in translation.

1.4.4 Turnover

Mature tRNAs are very stable, with half-lives reported to range from 50 hours in chicken muscle (Nwagwu and Nana, 1980) to 3 days in avian liver (Kanerva and Maenpaa, 1981). However, two pathways are now known to monitor tRNA quality and modulate turnover. The first pathway ensures the integrity of pre-tRNAs by nuclear surveillance, and allows pre-tRNAs that are not modified in the correct

manner to be degraded from the 3' end by the nuclear exosome (Kadaba et al., 2004). The other pathway is specific to mature tRNAs and is known as the Rapid tRNA Decay (RTD) pathway. In this instance mutated tRNAs, or tRNAs with a destabilised structure, are degraded from the 5' end via a reaction catalysed by the 5'-3' exonucleases Rat1 and Xrn1 (Chernyakov et al., 2008). Furthermore, the nucleotidyl transferase that catalyses addition of the 3' CCA sequence to tRNAs can also add a CCACCA sequence to tRNAs with unstable structures to prevent aminoacylation and mark them for degradation via the RTD pathway (Wilusz et al., 2011). These turnover pathways provide a quality control mechanism to ensure that only mature, stable and functional tRNAs are available to engage with the protein synthesis machinery.

1.4.5 tRNAome

Modification, aminoacylation and targeted degradation are essential to produce functional tRNAs for synonymous decoding. However, the specific complement of tRNAs expressed within a cell (the tRNAome) varies depending on the cell type and its requirements. The degeneracy of the genetic code enables bias in codon use and the efficiency at which a given codon is translated depends upon the amount of activated cognate amino acid available. The abundance of tRNAs corresponding to those codons can therefore determine the speed of translation (Tuller et al., 2010). Thus, transcripts with a codon bias towards highly expressed tRNAs have increased expression levels, and increased translation of proteins can be artificially induced by mutating sequences to improve their codon-tRNA complement (Percudani et al., 1997, Tuller et al., 2007, Mahlab et al., 2012). Furthermore, because controlling ribosome density along the length of the transcript can influence co-translational protein folding, codon bias and tRNA abundance can not only effect the overall speed of translation but also the kinetics of protein folding and final protein structure (O'Brien et al., 2014). Whilst codon use correlates with tRNA gene copy number in non-complex organisms (Iben and Maraia, 2012), work has now shown that in human cells epigenetic modification of tRNA genes, and the consequent levels of tRNA transcription, drive changes in expression of particular pools of tRNAs to subsequently influence specific patterns of gene expression through increasing the translational efficiency of particular pathways (Gingold et al., 2014). tRNAs are therefore not just housekeeping components of the translation machinery, as

precise coordination of their expression levels with codon-usage in transcripts they are translating adds another level of control to the regulation of protein synthesis.

1.4.6 Canonical function

1.4.6.1 Protein synthesis

The canonical and most well-defined function of tRNAs is their role in translation, where they operate as adaptor molecules to read mRNA codons and bring the corresponding amino acid to the translation machinery. The process of translation is divided into four stages: initiation, elongation, termination and recycling, with each step involving the coordinated action of multiple binding partners.

The first stage of translation initiation requires assembly of the ternary complex (TC), which is composed of eIF2 + GTP + the initiator methionine tRNA ($\text{tRNA}_i^{\text{Met}}$). With the aid of other initiation factors (including eIFs 1A and 3), the TC is able to bind the 40S ribosomal subunit to form the 43S pre-initiation complex. eIF4E can then bind the 5' cap of the mRNA, and in conjunction with eIF4A, eIF4B and eIF4H, unwinds structures within the 5' UTR. Additional factors, including eIF4G and poly (A) binding protein (PABP), bind the 3' poly (A) tail of the mRNA and load it onto the 43S pre-initiation complex. This complex is then able to sequentially scan the 5' mRNA region to search for the correct start codon. Following anticodon:codon base pairing of $\text{tRNA}_i^{\text{Met}}$ and the start codon, the GTP of the TC is then hydrolysed by eIF2 and eIF5. eIF2 is then able to release the tRNA into the P site of the 40S subunit, and eIFs 1A, 3 and 5 can dissociate. This enables eIF2-GDP to dissociate from the 40S ribosomal subunit, allowing eIF5B-GTP to facilitate binding of the 60S ribosomal subunit to the 40S- $\text{tRNA}_i^{\text{Met}}$ -mRNA complex. Upon GTP hydrolysis, eIF5B is released from the complex, marking the end of translation initiation and the beginning of elongation (Kapp and Lorsch, 2004) (Figure 1-4).

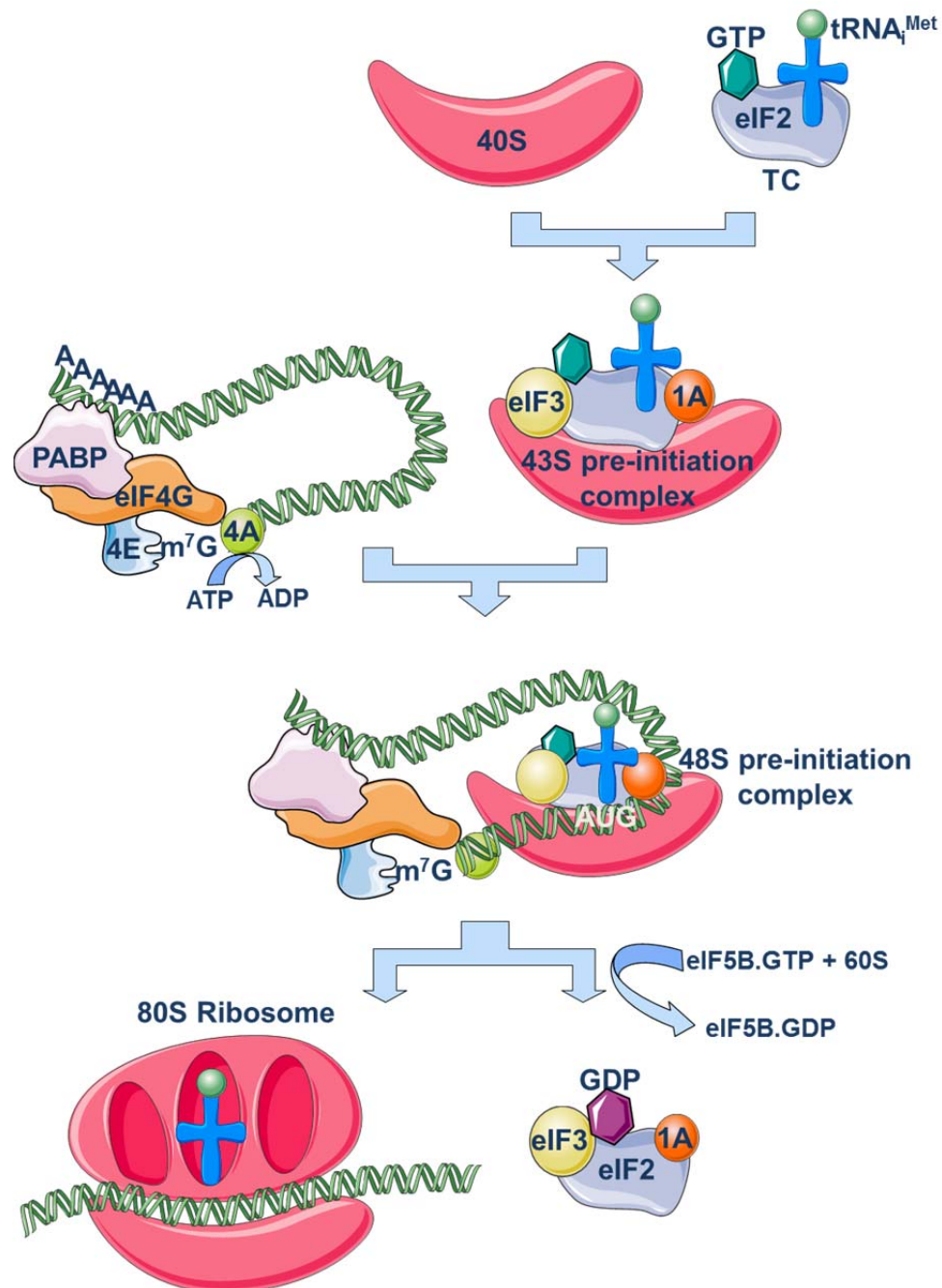


Figure 1-4- The process of eukaryotic translation initiation.

The ternary complex (TC) is composed of eIF2, GTP and tRNA^{Met}. Initiation factors eIF3 and 1A enable the TC to bind the 40S ribosomal subunit to form the 43S pre-initiation complex. eIF4E binds the 5' cap of the mRNA, and additional initiation factors including eIF4A, 4B and 4H unwind the 5' UTR. Poly (A) binding protein (PABP) and eIF4G can bind the 3' Poly (A) tail of the mRNA to assist ribosomal loading, and the 48S pre-initiation complex is formed. Following base pairing of the tRNA^{Met} anticodon with the start codon, the GTP of the TC is hydrolysed, tRNA^{Met} is released into the P site of the 40S ribosomal subunit and the initiation factors can dissociate. eIF5B-GTP assists binding of the 60S ribosomal subunit and upon GTP hydrolysis eIF5B is released from the initiation complex (Klann and Dever, 2004). Image made using items from Image Bank in Servier Medical Art.

At the start of elongation, a peptidyl tRNA sits in the ribosomal P site. An aminoacyl-tRNA is brought to the vacant A site by eEF1A-GTP and when correct anticodon:codon base pairing occurs the aminoacyl-tRNA is released into the A

site by eEF1A's GTPase activity and conformational changes in the small ribosomal subunit. A ribosomal peptidyl transferase catalyses peptide bond formation between the amino acids situated in the A and P sites. The complex is then translocated, so that the deacylated tRNA is moved to the E site, the peptidyl tRNA sits within the P site, and the mRNA is shifted by three nucleotides so that the next mRNA codon is in the ribosomal A site (Kapp and Lorsch, 2004) (Figure 1-5).

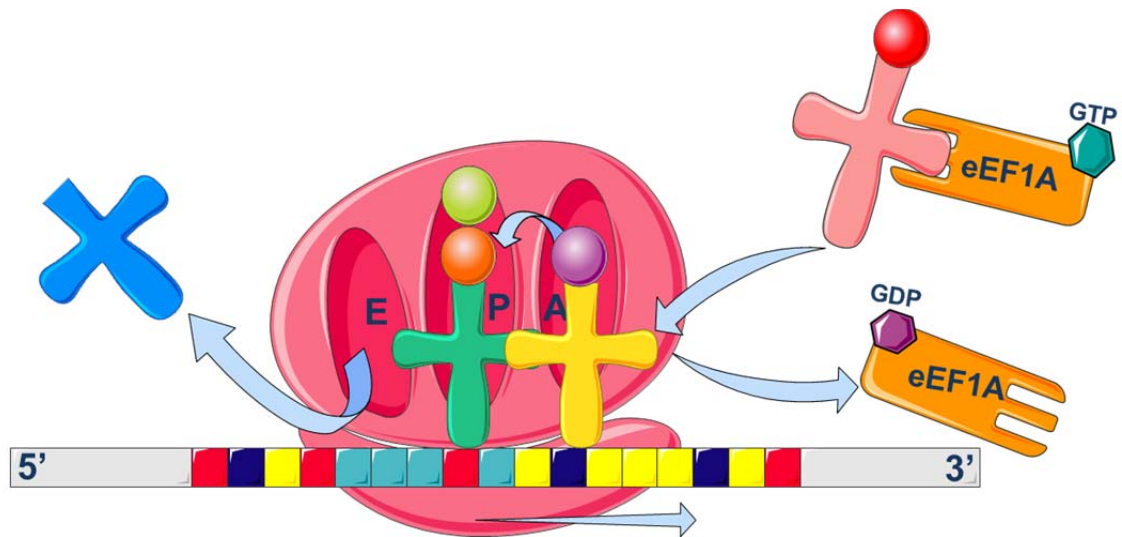


Figure 1-5- The process of elongation in eukaryotic protein synthesis.

Aminoacyl-tRNAs are brought to the vacant A site of the ribosome by the elongation factor eEF1A, and are released into the A site by conformational changes and GTP hydrolysis following suitable anticodon:codon base pairing between the tRNA and mRNA. A peptide bond is formed between the amino acids in the P and the A site, and the complex translocated to allow the deacylated tRNA to be released from the E site and the cycle repeated until a stop codon is detected within the A site. Image made using items from Image Bank in Servier Medical Art.

The elongation cycle is repeated until a stop codon is detected in the A site. The peptidyl transferase centre of the ribosome catalyses the release of the synthesised polypeptide by hydrolysing the ester bond that links the polypeptide chain to the P site tRNA, and this process is assisted by Class I and Class II release factors. The ribosomal subunits can then be recycled for further rounds of translation initiation, although the precise mechanism of recycling in eukaryotes is still unclear (Kapp and Lorsch, 2004).

1.4.7 Non-canonical functions

In addition to their well-characterised participation in protein synthesis, a number of other functional roles for tRNAs have been described within eukaryotic cells. Observations that these processes can be stress-induced, or part of programmed cellular processes, demonstrates that tRNAs are more than just translational adaptor molecules required for the synthesis of proteins.

1.4.7.1 Targeting proteins for degradation

Aminoacylated tRNAs are able to donate their associated amino acid for N-terminal conjugation reactions to proteins being marked for degradation. The N-rule pathway is used in regulated proteolysis, based on the fact that the half-life of a protein can be determined by the identity of its N-terminal amino acid residue. Aminoacyl-tRNA transferases can recognise destabilising residues and transfer specific amino acids from tRNAs to particular proteins to enable their delivery to the proteasome (Mogk et al., 2007). Regulated degradation of proteins in this way not only removes misfolded or abnormal proteins, but is also used in a number of physiological processes including the regulation of DNA repair pathways and cardiovascular development (Varshavsky, 2011).

1.4.7.2 Nutrient deprivation response

Uncharged tRNAs can also have functional effects and are involved in the nutrient deprivation response in both yeast and mice. In yeast, increased levels of uncharged tRNAs provide an amino acid starvation signal, and this is detected by GCN2 (Wek et al., 1995). Binding of uncharged tRNAs to GCN2 activates the GCN2 kinase domain, enabling phosphorylation of the translation initiation factor eIF2 (Dong et al., 2000, Dever et al., 1992). Phosphorylation of eIF2 inhibits TC formation, therefore inhibiting protein synthesis and limiting amino acid consumption in starved cells. Similar processes can also occur in mice to control feeding behaviour and maintain amino acid homeostasis (Maurin et al., 2005, Hao et al., 2005). Thus cytoplasmic accumulation of uncharged tRNAs acts as a basic mechanism in nutritional stress management and enables activation of stress response pathways.

1.4.7.3 Apoptosis

Intrinsic apoptosis pathways are characterised by cytochrome c release and caspase activation. In such pathways, mitochondrial cytochrome c that has been released into the cytosol can bind Apaf-1 which can then assemble into the apoptosome complex. This recruits caspase 9, which, once activated by autoproteolytic activity, can activate effector caspases to induce cell death (Riedl and Salvesen, 2007). tRNAs are able to bind cytochrome c and impair its association with Apaf-1, blocking apoptosome formation and inhibiting caspase-9 activation (Mei et al., 2010b). This provides a mechanism to regulate sensitivity to apoptosis and could also provide a way for cells to develop apoptotic resistance.

1.4.8 tRNA derived fragments

A number of recent publications have also highlighted how tRNAs can be processed into smaller fragments, and how these tRNA derived fragments (tRFs) may have specific functional effects within the cell including roles in translational inhibition, long-distance signalling and acting as guide RNAs. tRNAs can be cleaved in the anticodon loop to produce tRFs by the stress activated ribonuclease angiogenin, and the resulting tRFs are able to inhibit protein synthesis by displacing eIF4G/eIF4A from the 5' cap of mRNAs to activate a protective stress response (Ivanov et al., 2011). Smaller tRFs may also be generated through cleavage of the 3' and 5' ends of the tRNAs, and this can occur through a number of mechanisms including RNase Z cleavage and Dicer-dependent processing (Haussecker et al., 2010). These smaller tRFs are able to associate with argonaute proteins, and may have roles in regulating gene expression through RNA-silencing mechanisms. And so, in addition to the effects of charged and uncharged tRNAs, the directed cleavage of tRNAs into defined fragments represents another way in which these ancient molecules have evolved to influence gene expression.

1.4.9 tRNA expression in disease

Expression and mutation of tRNAs and tRNA processing enzymes have been linked to a diverse range of disease states, and this can be attributed to a number of different mechanisms; including compromised aminoacylation and effects on

tRNA modification, folding and splicing. Mitochondrial tRNA (mt-tRNA) genes have been described as “hotspots” for mutation, with over 200 mt-tRNA mutations currently linked to disease processes (Abbott et al., 2014). The two most characterised disorders associated with mt-tRNA mutations are mitochondrial encephalomyopathy, lactic acidosis, and stroke-like episodes (MELAS) and myoclonic epilepsy with red tagged fibers (MERRF). These disorders are due to mutations in mt-tRNA^{Leu} and mt-tRNA^{Lys} respectively, both of which effect wobble position modifications to disrupt correct decoding by the mitochondrial ribosome (Suzuki et al., 2011). Tissues that are highly dependent on mitochondrial ATP production, such as the heart, can also be sensitive to mt-tRNA mutations, and a number of cases of cardiomyopathy have been found to be owing to mt-tRNA mutations (Shin et al., 2000, Taylor et al., 2003, Hollingsworth et al., 2012). With regard to nuclear encoded tRNAs and their associated enzymes, mutations in the tRNA splicing machinery have been associated with Pontocerebellar hypoplasia (PCH, a neurodegenerative disorder characterised by defective growth, development and brainstem/cerebellum function) (Budde et al., 2008), and mutations in the aaRS glycyl-tRNA synthetase (GARS) gene are responsible for Charcot-Marie-Tooth disease (Antonellis et al., 2003), although the underlying mechanisms are not fully understood.

Pol III mediated transcription of tRNAs is under the control of a number of well described oncogenic/tumour suppressor pathways (Figure 1-2), and increased Pol III activity in cancer is well documented across a number of different cancer types (Winter et al., 2000, Chen et al., 1997). As a consequence, tRNA expression is increased in a variety of cancers (Daly et al., 2005, Pavon-Eternod et al., 2009, Zhou et al., 2009). Moreover, increased levels of tRNAs and tRFs have been shown to drive increased cell growth and proliferation (Pavon-Eternod et al., 2013, Rideout et al., 2012, Lee et al., 2009a). Specifically, increased levels of the initiator methionine tRNA, tRNA_i^{Met}, in human epithelial cells was found to promote cell proliferation (Pavon-Eternod et al., 2013), while an extra copy of the tRNA_i^{Met} gene was also able to increase growth in *Drosophila* larvae (Rideout et al., 2012). With regard to tRFs, a fragment derived from the 3' end of Ser-TGA pre-tRNA was also found to have increased expression in cancer cell lines, with expression levels tightly correlating with proliferation rate, and impaired proliferation observed when expression of the fragment was knocked

down (Lee et al., 2009a). These observations collectively suggest that tRNA levels themselves could influence the increased growth and proliferation seen in carcinogenesis. Furthermore, recent work characterising the tRNAome has also demonstrated that proliferating cells can change the repertoire of tRNAs they express to direct specific programmes of translation (Gingold et al., 2014). These data suggested that expression of specific complements of tRNAs could increase the efficiency of translational pathways associated with cellular proliferation, and essentially help to channel a cell into a more proliferative state. Further understanding the mechanisms by which tRNA expression can affect the rate of protein synthesis may therefore provide insight into how aberrant tRNA expression could influence disease progression.

1.5 Protein synthesis

1.5.1 Control of translation initiation

The rate limiting step of eukaryotic translation is thought to be the initiation of protein synthesis, and the canonical model of cap-dependent translation is described previously (Figure 1-4). This multi-step process is highly regulated and can be controlled by a number of different mechanisms, the most common being the phosphorylation state of the initiation factor eIF2 (Krishnamoorthy et al., 2001). eIF2 is a heterotrimeric protein that, when loaded with GTP by the guanine nucleotide exchange factor (GEF) eIF2B, associates with tRNA_i^{Met} to form the TC, which enables association with the small ribosomal subunit to generate the 43S pre-initiation complex required for global initiation of translation. However, when eIF2 is phosphorylated on serine 51 of its α subunit, it becomes a competitive inhibitor of eIF2B, preventing GDP-GTP exchange and therefore reducing global translation rates by decreasing the amount of TC available (Krishnamoorthy et al., 2001). Phosphorylation of eIF2 α is stimulated in response to cell stress, and is performed by a variety of kinases including GCN2, PERK, HRI and PKR depending on the nature of the stress (Dever et al., 1992, Kline et al., 2006, Sequeira et al., 2007). This consequently enables suppression of global protein synthesis, and increases translation of specific transcripts to allow the cell to respond to the stress or external cue (Figure 1-6). These specific transcripts must therefore have distinguishing features to enable their selective

translation, and this information tends to be found within the untranslated regions.

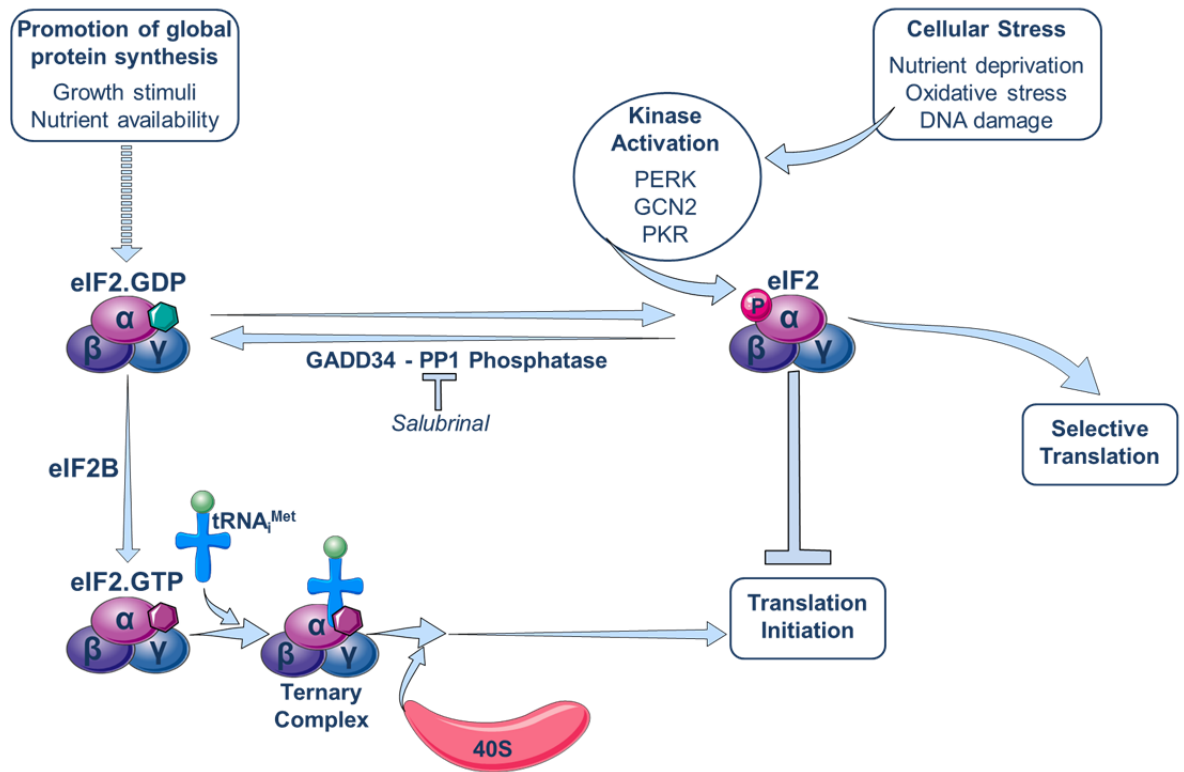


Figure 1-6- Exposure to cell stresses inhibits global protein synthesis through P-eIF2 α .

Protein kinases such as PERK and GCN2 can phosphorylate eIF2 α and inhibit eIF2 α activity, whilst GADD34 can recruit Protein Phosphatase 1 (PP1) to dephosphorylate eIF2 α . Salubrinal is a drug that can inhibit PP1 to block eIF2 α dephosphorylation. Phosphorylation of eIF2 α sequesters the initiation factor away from ternary complex formation, decreasing amounts of ternary complex available for global protein synthesis, and as a result drives only the translation of specific transcripts required under conditions of cellular stress. Image made using items from Image Bank in Servier Medical Art.

1.5.2 The influence of untranslated regions

The rate of translation initiation is not only dependent on the assembly of the translation initiation machinery, but also on the structure of the flanking untranslated regions (UTRs). Particular features of these regions, whether they be structural or sequence specific, are able to influence translational efficiency and hence provide another means to regulate gene expression.

1.5.2.1 Internal ribosome entry sites

Internal ribosome entry sites (IRES) were originally identified in viruses, but have since been identified in approximately 10% of eukaryotic mRNAs (Mitchell et al., 2005). They are structured RNA elements found in many stress-response mRNAs

and, in association with transacting factors, can facilitate binding of the mRNA to the 40S ribosomal subunit to enable translation when cap-dependent initiation is compromised (Spriggs et al., 2008). c-Myc is known to contain a well characterised IRES motif and this has been shown to be important in maintaining increased levels of c-Myc translation during conditions of ER stress in multiple myeloma (MM) (Shi et al., 2015). A number of other oncogenes and growth factors also contain IRES sites within their 5' UTR, leading to the hypothesis that selective translation of these factors through IRES-mediated mechanisms could contribute to the survival of cancer cells under stressful conditions (Holcik, 2004).

1.5.2.2 Upstream open reading frames

Upstream open reading frames (uORFs) are in-frame start and stop codons that occur in the 5' UTR, and the presence of numerous uORFs has the tendency to be inhibitory under conditions of normal global protein synthesis. Cap-dependent translation initiation relies on scanning of the 5' UTR for the AUG start codon. When conditions are optimal, translation is initiated at the first uORF, and the ribosome can then continue to scan and reinitiate translation at downstream uORFs by recruitment of additional TC. Because subsequent uORFs tend to overlap with coding sequence, this process is usually inhibitory to translation of the correct coding sequence. However, in conditions of increased phospho-eIF2 α and consequent decreased TC formation, re-initiating ribosomes are less likely to recruit TC to subsequent uORFs due to decreased TC availability, therefore allowing translation of the correct coding sequence. Examples of genes regulated in this way include the stress induced transcription factor ATF4 (Blais et al., 2004) which has been described as a master regulator of genes for adaptive functions (B'Chir et al., 2013), and GADD34, which provides a feedback mechanism to control absolute levels of phospho-eIF2 α (Lee et al., 2009b).

1.5.2.3 5' UTR structure

5' UTRs tend to have an average length of 100 to 220 nucleotides (Pesole et al., 2001). However, significantly longer 5' UTRs can be found in transcripts encoding transcription factors, proto-oncogenes, growth factors and their receptors, and these tend to be poorly translated under normal conditions

(Davuluri et al., 2000). GC content and short repeat sequences can further contribute to secondary structure and add additional complexity to 5' UTRs. Stable secondary structures can resist the helicase activity of eIF4A (Rozen et al., 1990), and this can significantly affect the ability of the translation initiation machinery to scan from the 5' m7G cap structure through the UTR in search for the translation start site. Terminal oligopyrimidine (TOP) motifs, pyrimidine-rich translational elements (PRTE), and other regulatory sequence motifs within the 5' UTR can also affect the assembly of the translation initiation machinery (Hsieh et al., 2012, Thoreen et al., 2012). Complex 5' UTRs are therefore another effective mechanism to control efficient translation initiation and protein synthesis under normal conditions.

1.5.3 Localised translation

In addition to the structure of mRNAs, transcript localisation can also play an important role in directing protein synthesis. While the signal recognition particle (SRP) can facilitate localised translation on the ER, RNA localisation sequences (found within UTRs) and transacting factor (TAF)-mediated mRNA localisation can also dictate the intracellular position of RNA molecules (Oleynikov and Singer, 1998). mRNA-mediated localised translation is an important mechanism for organising cellular architecture and function, and coordination between mRNA distribution and consequent protein localisation is seen throughout *Drosophila* embryogenesis (Lecuyer et al., 2007). Targeting of mRNAs to the site of protein synthesis can save cellular energy, as transported mRNA transcripts can subsequently be translated into numerous protein molecules, whilst also minimising inappropriate protein-protein interactions and facilitating specific associations for protein complex assembly (Liao et al., 2015).

The most studied form of localised protein synthesis is that found in neurons. Although the majority of protein synthesis occurs within the soma of the neuron, axons can be up to 1 metre in length, and so the site of action of certain proteins may be some distance from the soma, and this could place considerable demands on the protein transport machinery. Polyribosomes have been found at the base of dendritic spines (Steward and Levy, 1982), and metabolic labelling experiments have shown *de novo* protein synthesis in both axons and dendrites

(Torre and Steward, 1992). Such localised protein synthesis can influence growth cone adaptation, gradient sensing and directional turning of axons (Leung et al., 2006, Ming et al., 2002, Piper et al., 2005, Yao et al., 2006), and so this may underlie a number of fundamental neuronal processes.

Specific mRNA localisation has also been found in the cell protrusions of fibroblasts and tumour cells (Mili et al., 2008, Stuart et al., 2008), and components of the translation machinery are found at the leading edge of migrating cells consistent with a role of localised protein synthesis in cell migration (Willett et al., 2010, Willett et al., 2011, Willett et al., 2013). Local translation of β -actin has been studied in migrating cells, and its localisation requires an intact actin cytoskeleton in addition to activation of Rho and its downstream effector myosin IIB (Liao et al., 2015). Rho-regulated transport of translationally silent β -actin mRNA by myosin II motor-mediated transport is thought to occur along actin filament tracts (Kislauskis et al., 1994, Latham et al., 1994, Latham et al., 2001). A short nucleotide sequence in the 3' UTR of β -actin acts as a localisation signal, and the transcript is bound by ZBP1/IMP1 to repress its synthesis through the transportation process (Ross et al., 1997). Local β -actin translation in cell protrusions can consequently effect cell motility, and the translation elongation factor EF1 α can also bind to actin mRNA and increase its translational efficiency (Perez and Kinzy, 2014), linking the actin cytoskeleton to the protein synthesis machinery (Woods et al., 2005, Woods et al., 2002). Tumour cell migration and invasion can consequently be influenced by expression of transacting factors that facilitate mRNA transport, with ZBP1/IMP1 levels correlating with poor prognosis in ovarian cancer through mechanisms that can stabilise transcripts associated with both cell proliferation and migration (Kobel et al., 2007, Vikesaa et al., 2006, Weidensdorfer et al., 2009). The localisation of protein synthesis therefore represents another means by which translational control can influence cellular behaviour. Moreover, these particular effects on cell migration and invasion indicate that translational control is a mechanism that could contribute to tumour progression through supporting the increased cell motility displayed during metastatic dissemination.

1.6 Translational control in cancer

Development of cancer is a multistep process, and the original hallmarks described by Hanahan and Weinberg form a framework of six distinct but complementary processes that enable normal cells to become tumourigenic, namely sustained proliferation, evasion of growth suppression, activation of invasive and metastatic processes, replicative immortality, induction of angiogenesis and resistance to cell death (Hanahan and Weinberg, 2000). This paradigm has now been updated to include reprogrammed energy metabolism and evasion of immune destruction into the process of cancer development (Hanahan and Weinberg, 2011). Control of translation plays an important role in each of these processes, with regulation of both global and directed protein synthesis contributing to cancer development and progression. In general, increased cancer cell proliferation requires increased rates of protein synthesis and ribosomal number (Johnson et al., 1976), and in neoplastic tissues enlarged nucleoli (the sites of ribosomal RNA synthesis and ribosome assembly) are often considered to be indicative of malignancy (Gani, 1976). Active polyribosome fractions from proliferating cells contain an additional 2-5% of unique mRNAs that are absent in quiescent cells (Getz et al., 1976), indicating that selective translation is also associated with altered patterns of gene expression, and this could contribute to transformation.

The phosphorylation state of the initiation factor eIF2 α dictates availability of the TC and, as a consequence, can regulate the balance of global and selective translation. Its contribution to cancer progression is complicated, with some studies showing that tumourigenesis in mice is promoted by inhibiting phospho-eIF2 α levels (Donze et al., 1995, Koromilas et al., 1992b) while others find that modifying the levels of phospho-eIF2 α has no impact on cancer development (Tejada et al., 2009, Yang et al., 1995, Abraham et al., 1999). The role of eIF2 α in tumourigenesis may therefore depend on the cancer type and stage, with increased phosphorylation of eIF2 α perhaps playing a role in the early stages of cancer cell survival to protect against stresses such as hypoxia (Bi et al., 2005, Koritzinsky et al., 2006), whilst in the later stages of disease progression decreased phospho-eIF2 α may promote increased global protein synthesis and aberrant expression of a number of pathways to increase tumour cell growth.

The interaction between ribosomes and mRNA is coordinated by a number of different initiation and elongation factors, and the expression of each of them provides another opportunity to regulate translation. eIF4F is a core complex required for cap-dependent translation, and is composed of eIF4E (cap binding protein), eIF4A (ATP-dependent RNA helicase) and eIF4G (scaffolding protein) (Sonenberg and Hinnebusch, 2009). eIF4E activity is regulated by its availability, which can be controlled through phosphorylation by eIF4G-associated kinases and expression of eIF4E inhibitory binding proteins (4E-BPs). Regulation of eIF4E expression through phosphorylation of 4E-BP1 enables TORC1 to influence translational control (Hsieh et al., 2012), and eIF4E overexpression has been found to promote increased translation of a subset of mRNAs that have specific structures within their 5' UTRs to drive transformation and tumourigenesis (Koromilas et al., 1992a, Hsieh et al., 2012). An eIF4A-dependent mechanism of translational control has also been described in T-cell acute lymphoblastic leukaemia (T-ALL) (Wolfe et al., 2014). These workers found that transcripts that were sensitive to the expression of eIF4A possessed G-quadruplex structures in their 5'UTRs. These transcripts included oncogenes and transcriptional regulators such as Myc, Notch and Bcl-2, and indicated that RNA G-quadruplexes in the 5' UTR were associated with eIF4A-dependent oncogene translation in cancer. The binding of eIF4E to eIF4G can also stimulate the helicase activity of eIF4A to increase the rate of translation (Feoktistova et al., 2013). Increased availability of eIF4E and eIF4A can therefore promote increased formation and activity of eIF4F to enhance the translation of transcripts that are normally poorly transcribed due to the presence of inhibitory structures in and around their translational start site. Oncogenes tend to have a number of inhibitory features within their UTRs (Willis, 1999), and so increased expression of initiation factors in disease can increase the favoured translation of oncoproteins, providing a mechanism to enable cancer cells to drive their own growth and proliferation to contribute to tumour progression.

1.7 The tumour microenvironment

Tumours have a complex architecture and are composed of multiple cell types in addition to cancer cells; these include cancer stem cells, inflammatory cells, endothelial cells, pericytes, and fibroblasts (Hanahan and Weinberg, 2011). However, in addition to uncontrolled tumour growth due to aberrant control of

autonomous gene expression pathways, the surrounding tumour microenvironment (TME) also plays an integral role in carcinogenesis. The TME is a domain that supports the relationship between tumours and their stromal neighbours, and is composed of a complex collection of different cell types within an extracellular scaffold. Mesenchymal stem cells, immune cells, endothelial cells, capillaries and fibroblasts are all found within the extracellular matrix (ECM), and all are able to contribute to the TME to influence cancer progression. Communication between tumours and their microenvironments is reciprocal, with tumour cells releasing extracellular signals to influence their surroundings, while the TME can also activate specific gene expression pathways within cancer cells to influence proliferation, migration and invasion, in addition to contributing to immune evasion mechanisms. The importance of this relationship has been reinforced by the advent of a number of therapeutic strategies aimed at targeting the tumour stroma (Tchou and Conejo-Garcia, 2012, Hofmeister et al., 2008, Li et al., 2012), and highlights the need to understand how components of the TME can contribute to tumour progression.

1.8 Cancer-associated fibroblasts

Fibroblasts are the most common type of cell found in connective tissue, and they are predominantly responsible for synthesis of the ECM within which they reside (Tarin and Croft, 1969). Fibroblasts are elongated spindle-shaped cells with extended processes that can acquire an activated phenotype in response to a number of stimuli, including injury and growth factors, to become more myofibroblast-like (Gabbiani et al., 1971). These activated, myofibroblast-like fibroblasts, commonly express markers such as α -smooth muscle actin and fibroblast-activation protein (FAP), and are characterised by their increased ECM deposition and changes in the complement of matrix-degrading enzymes they secrete to remodel the surrounding ECM (Kalluri and Zeisberg, 2006). In addition to contributing to the physical structure of the TME, activated fibroblasts can also secrete growth factors to provide proliferative signals to surrounding epithelial cells (Tomasek et al., 2002), which contribute to normal physiological processes such as tissue re-modelling during development and wound healing.

Cancer-associated fibroblasts (CAFs) are activated fibroblasts that are found in association with cancer cells. CAFs are thought to arise through myofibroblast

transdifferentiation (FMT) of resident normal stromal fibroblasts (Untergasser et al., 2005) which can be stimulated through release of growth factors such as transforming growth factor- β (TGF- β) and platelet-derived growth factor (PDGF) from cancer cells (Anderberg et al., 2009, Ronnov-Jessen and Petersen, 1993). CAFs may also be derived from malignant epithelial cells via epithelial to mesenchymal transition (EMT); a process through which epithelial cells lose their apical basal polarity and adhesive properties in favour of a more migratory and invasive phenotype (Petersen et al., 2003). Another reported source of CAFs is mesenchymal stem cells (MSCs), which although normally resident in bone marrow can be attracted to the TME where they are able to differentiate into cells with a more myofibroblast-like phenotype (Direkze et al., 2004, Mishra et al., 2008).

CAFs are one of the most abundant cell types in the TME and, in addition to having a multi-faceted role in tumour progression, their relatively stable genome (by comparison with cancer cells which commonly display gross chromosomal abnormalities) has also made them an attractive target for potential cancer therapies (Cirri and Chiarugi, 2012). They have a higher proliferative activity than normal fibroblasts (NFs) and secrete an altered ECM that is characteristic of the desmoplastic stroma found in advanced carcinomas (Kalluri and Zeisberg, 2006). Their ability to influence tumour growth and development can occur through a number of different mechanisms, including secretion of growth promoting soluble factors, and deposition of a matrix that facilitates tumour progression.

1.8.1 Secretion of soluble factors

The pro-tumourigenic properties of CAFs were initially investigated using tumour allograft models in immunodeficient mice. In these studies, tumour growth was assessed following co-injection of tumour cells with fibroblasts which had been isolated from tumour or surrounding tissue (Orimo et al., 2005, Olumi et al., 1999, Hwang et al., 2008). Tumours grew faster when mixed with CAFs compared to co-injection with fibroblasts from surrounding tissue, owing to CAF secreted factors acting in a paracrine fashion to promote tumour growth. Specifically, CAFs were shown to secrete stromal-derived factor (SDF-1), a cytokine that can bind the CXCR4 receptor on the surface of cancer cells to

stimulate their growth (Orimo et al., 2005, Ao et al., 2007). Further work has also demonstrated that CAFs secrete increased levels of transforming growth factor beta 1 (TGF- β 1), which can have paracrine effects on tumour cells, promoting both their growth and invasion, and autocrine effects on CAFs themselves, promoting FMT and enabling maintenance of an activated CAF phenotype (San Francisco et al., 2004, Rosenthal et al., 2004). Furthermore, SDF-1 can also play a role in neo-angiogenesis (Orimo et al., 2005), and so in collaboration with additional secreted angiogenic factors, such as fibroblast growth factor 2 (FGF-2) and vascular endothelial growth factor (VEGF) (Fukumura et al., 1998), can increase the vascularisation of growing tumours. Tumour cell invasion can also be promoted by CAF secreted hepatocyte growth factor (HGF) (De Wever et al., 2004). HGF activates the receptor tyrosine kinase (RTK) Met, and signalling downstream of this RTK can lead to a number of pro-tumourigenic processes including the increased motility of cancer cells (Maulik et al., 2002), the secretion of factors such as uPA and uPAR which are involved in ECM degradation (Nishimura et al., 2003), and the protection of tumours from apoptosis (Provencal et al., 2010). Other CAF-secreted factors such as secreted-frizzled related protein (SFRP-1) can also have anti-apoptotic roles (Joesting et al., 2005). CAF-secreted soluble factors are also able to influence the immune response to tumour growth, with tenascin-C secretion having immunosuppressive functions through inhibition of monocyte migration and T lymphocyte adhesion (Hauzenberger et al., 1999, Loike et al., 2001), while they can also activate specific pro-inflammatory signatures to regulate the innate and adaptive immune response (reviewed in (Harper and Sainson, 2014)). CAFs can therefore secrete a cocktail of pro-tumourigenic soluble factors to support increased tumour growth and progression through a number of different mechanisms (Figure 1-7).

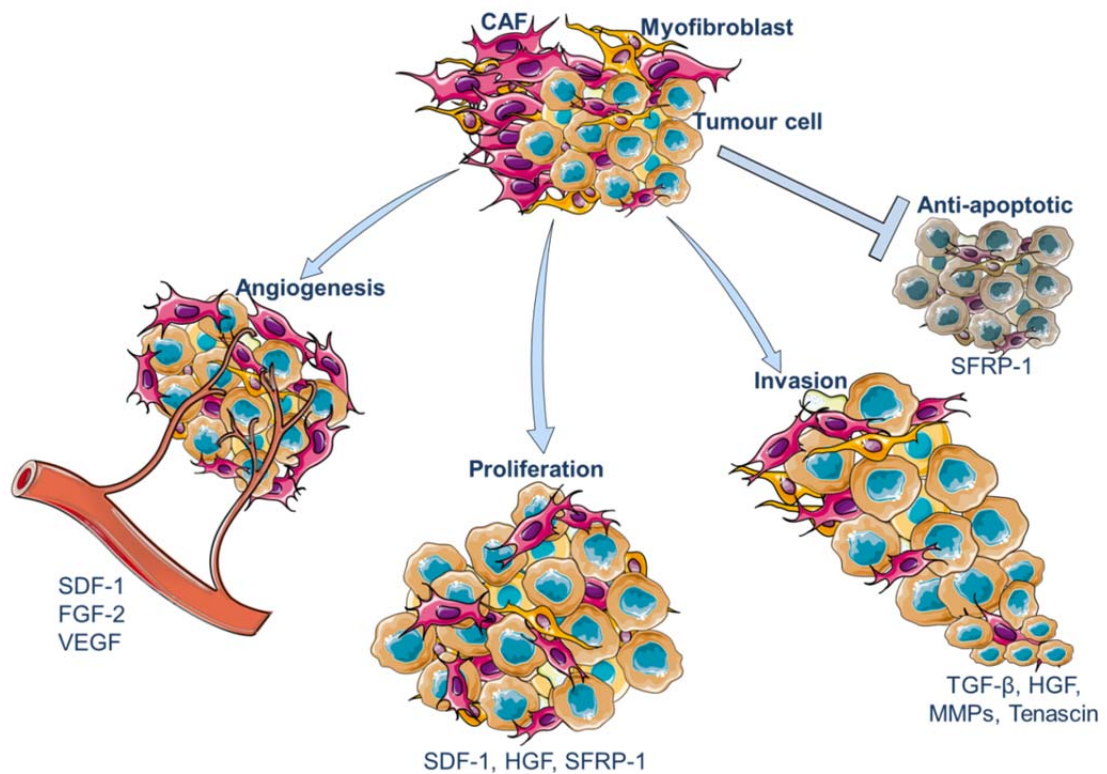


Figure 1-7- Tumour promoting soluble factors secreted from CAFs.

CAFs can secrete a number of soluble components to influence tumour growth through a variety of different mechanisms. Pro-angiogenic factors include stromal-derived factor 1 (SDF-1), fibroblast growth factor 2 (FGF-2) and vascular endothelial growth factor (VEGF). Other components such as hepatocyte growth factor (HGF), secreted-frizzled related protein (SFRP-1) can directly induce increased proliferation of cancer cells, while transforming growth factor beta 1 (TGF- β 1) and tenascin-C are among the molecules that can induce cancer cell invasion and metastasis. Factors such as SFRP-1 have also been shown to prevent tumour cell death. Figure adapted from (Shimoda et al., 2010). Image made using items from Image Bank in Servier Medical Art.

1.8.2 Extracellular Matrix

The ECM provides a scaffold of structural support whilst also providing a reservoir of molecules that act as biochemical and biomechanical cues to the cells around them. Fibroblasts, chondrocytes and osteoblasts all have the ability to secrete ECM, with each cell type producing matrix of different composition depending on the tissue of origin. The ECM is a dynamic structure that is subject to regulation at many levels including its deposition, degradation and remodelling (Page-McCaw et al., 2007). The ECM secreted by CAFs has been implicated as a major player in the tumorigenic process, and this can be attributed to a number of observations indicating that the tumour ECM differs from its normal counterpart in a number of ways; including alterations to its physical structure and ability to bind and present soluble growth factors, in addition to the composition of ECM proteins that are deposited.

1.8.2.1 Collagen

Collagen is one of the most abundant fibrous protein found in the ECM, and is composed of a superfamily of 28 members in total, with each collagen having a common triple helix structural motif (Table 1-3) (Ricard-Blum, 2011, Fang et al., 2014).

Collagen Type	α chains	Molecular species	Class	Distribution
I	$\alpha 1(I), \alpha 2(I)$	$[\alpha 1(I)]_2 \alpha 2(I)$	Fibril	Widespread, non-cartilaginous
II	$\alpha 1(II)$	$[\alpha 1(II)]_3$	Fibril	Cartilage, vitreous
III	$\alpha 1(III)$	$[\alpha 1(III)]_3$	Fibril	Co-distributed with collagen I, skin, vessels, intestine
IV	$\alpha 1(IV), \alpha 2(IV), \alpha 3(IV), \alpha 4(IV), \alpha 5(IV), \alpha 6(IV)$	$[\alpha 1(IV)]_2, \alpha 2(IV) \alpha 3(IV), \alpha 4(IV), \alpha 5(IV) [\alpha 5(IV)]_2, \alpha 6(IV)$	Network	Basement membrane
V	$\alpha 1(V), \alpha 2(V), \alpha 3(V), \alpha 4(V)$	$[\alpha 1(V)]_2, \alpha 2(V) [\alpha 1(V)]_3 [\alpha 1(V)]_2, \alpha 4(V) \alpha 1(V), \alpha 2(V), \alpha 3(V),$	Fibril	Co-distributed with collagen I, bone, dermis, cornea, placenta
VI	$\alpha 1(VI), \alpha 2(VI), \alpha 3(VI), \alpha 4(VI), \alpha 5(VI), \alpha 6(V)$	$\alpha 1(VI), \alpha 2(VI), \alpha 3(VI) \alpha 1(VI), \alpha 2(VI) \alpha 4(VI)$	Network	Widespread, muscle, bone, cartilage, cornea, dermis
VII	$\alpha 1(VII)$	$[\alpha 1(VII)]_3$	FACIT	Dermis, bladder
VIII	$\alpha 1(VIII), \alpha 2(VIII)$	$[\alpha 1(VIII)]_2, \alpha 2(VIII) [\alpha 2(VIII)]_2, \alpha 1(VIII) [\alpha 1(VIII)]_3 [\alpha 3(VIII)]_3$	Network	Widespread, dermis, heart, kidney
IX	$\alpha 1(IX), \alpha 2(IX), \alpha 3(IX)$	$\alpha 1(IX), \alpha 2(IX), \alpha 3(IX)$	FACIT	Co-distributed with collagen II, cartilage, cornea, vitreous
X	$\alpha 1(X)$	$[\alpha 1(X)]_3$	Network	Hypertrophic cartilage
XI	$\alpha 1(XI), \alpha 2(XI), \alpha 3(XI)$	$\alpha 1(XI), \alpha 2(XI), \alpha 3(XI) \alpha 1(XI), \alpha 1(V), \alpha 3(XI)$	Fibril	Co-distributed with collagen II, cartilage, intervertebral disc
XII	$\alpha 1(XII)$	$[\alpha 1(XII)]_3$	FACIT	Co-distributed with collagen I, dermis, tendon
XIII	$\alpha 1(XIII)$	$[\alpha 1(XIII)]_3$	MACIT	Endothelial cells, dermis, eye, heart
XIV	$\alpha 1(XIV)$	$[\alpha 1(XIV)]_3$	FACIT	Widespread & co-distributed collagen I, bone, dermis, cartilage
XV	$\alpha 1(XV)$	$[\alpha 1(XV)]_3$	Multiplexin	Between collagen fibrils close to basement membrane
XVI	$\alpha 1(XVI)$	$[\alpha 1(XVI)]_3$	FACIT	Integrated into collagen fibrils & fibrillin-1 microfibrils

XVII	$\alpha 1(\text{XVII})$	$[\alpha 1(\text{XVII})]_3$	MACIT	Hemidesmosomes in epithelia
XVIII	$\alpha 1(\text{XVIII})$	$[\alpha 1(\text{XVIII})]_3$	Multiplexin	Associated with basement membrane
XIX	$\alpha 1(\text{XIX})$	$[\alpha 1(\text{XIX})]_3$	FACIT	Rare, localised to basement membrane
XX	$\alpha 1(\text{XX})$	$[\alpha 1(\text{XX})]_3$	FACIT	Widespread, cornea
XXI	$\alpha 1(\text{XXI})$	$[\alpha 1(\text{XXI})]_3$	FACIT	Widespread, stomach
XXII	$\alpha 1(\text{XXII})$	$[\alpha 1(\text{XXII})]_3$	FACIT	Tissue junctions
XXIII	$\alpha 1(\text{XXIII})$	$[\alpha 1(\text{XXIII})]_3$	MACIT	Limited distribution, heart, retina
XXIV	$\alpha 1(\text{XXIV})$	$[\alpha 1(\text{XXIV})]_3$	Fibril	Homology to fibril forming collagens, bone, cornea
XXV	$\alpha 1(\text{XXV})$	$[\alpha 1(\text{XXV})]_3$	MACIT	Brain, heart, testis
XXVI	$\alpha 1(\text{XXVI})$	$[\alpha 1(\text{XXVI})]_3$	FACIT	Testis, ovary
XXVII	$\alpha 1(\text{XXVII})$	$[\alpha 1(\text{XXVII})]_3$	Fibril	Homology to fibril forming collagens, cartilage
XXVIII	$\alpha 1(\text{XXVIII})$	$[\alpha 1(\text{XXVIII})]_3$	Network	Component of basement membrane around Schwann cells

Table 1-3- The collagen family members.

Fibril-associated collagens with interrupted triple helices (FACIT), Membrane-associated collagens with interrupted triple helices (MACIT), Multiple triple-helix domains and interruptions (MULTIPLEXINS). Adapted from (Ricard-Blum, 2011, Fang et al., 2014).

Fibrillar collagens are synthesised in defined ways (Figure 1-8), starting with the translation of an initial pre-pro-peptide which is then post-translationally modified in the endoplasmic reticulum (ER). Following removal of the signal peptide the collagen propeptide is formed, and lysine and proline residues can be hydroxylated via an enzymatic reaction that requires ascorbate as a co-factor. Consequent glycosylation of hydroxyl-lysines allows formation of an α -chain with a left-handed polyproline II helical twist. Three α -chains can then wind together into a right handed triple helix, with a one residue stagger between adjacent α chains, to form the procollagen triple helix. The sequence repeats of Gly-X-Y stabilise the triple helix, where Gly is Glycine, and X and Y are most often proline and 4-hydroxyproline respectively. The procollagen is then transferred to the Golgi apparatus where it is further modified and packaged for secretion into the extracellular space. The large size and rigid structure of procollagen necessitates a requirement for specialised transport vesicles, and the ubiquitin ligase CUL3-KLHL12 consequently attaches ubiquitin to SEC31 of the SEC13-31 complex to modify COPII coated vesicles and thus enable encapsulation of large procollagen cargoes (Jin et al., 2012, Saito et al., 2009). Once outside the cell, collagen-specific peptidases remove the N- and C-

terminal peptides to produce insoluble tropocollagen, and crosslinking by extracellular enzymes such as lysyl oxidase (LOX) helps assemble the collagen into large fibrils (Figure 1-8) (Brodsky and Persikov, 2005, Ricard-Blum, 2011, Fang et al., 2014).

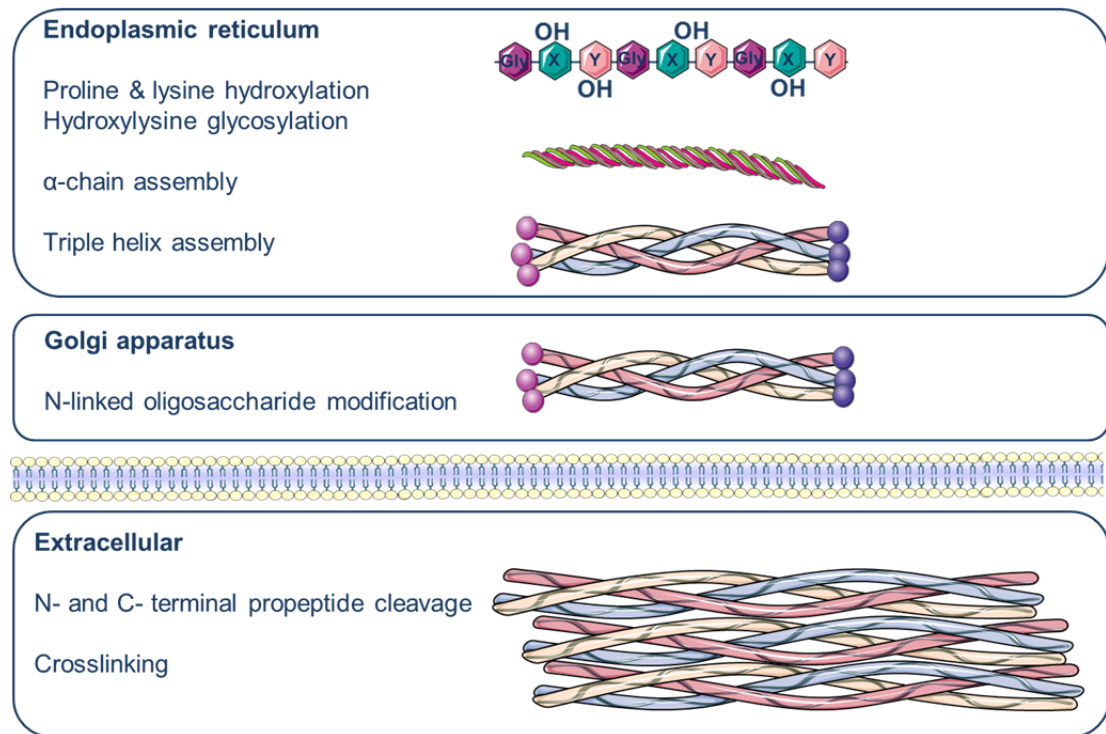


Figure 1-8- Collagen biosynthesis.

Every third residue of the collagen triple helical sequence is glycine (Gly), followed most frequently by proline (X) and 4-hydroxyproline (Y). Following modification in the endoplasmic reticulum, an α chain is formed from a left handed polyproline II helix. Three α chains form a right handed triple helix to generate the secondary structure of the collagen triple helix. This is further modified in the Golgi compartment and then packaged for secretion into the ECM. The N- and C- terminal propeptides are then cleaved and the fibrils cross-linked by extracellular enzymes. Image made using items from Image Bank in Servier Medical Art.

The architecture of the collagen scaffold is severely altered in tumours, in ways that include increased deposition of fibrillar collagens and linearization, thickening and alignment of fibres (Zhu et al., 1995, Huijbers et al., 2010). These structures can provide efficient tracks to facilitate increased cell migration and metastasis of cancer cells (Wyckoff et al., 2007). Increased expression of enzymes such as LOX results in increased collagen crosslinking and matrix stiffness and this is also associated with increased tumour aggressiveness (Erler et al., 2009). Increased matrix stiffness can have a number of effects, including enhancing tumour cell adhesion and migration (Erler et al., 2006, Erler and Giaccia, 2006), and further details of how the physical properties of the matrix can influence tumourigenesis will be discussed later in the text (1.8.2.5).

However, the construction of a rigid collagen matrix is also dependent on other factors, including the initial deposition of fibronectin, another major ECM protein that plays an important role in both health and disease (Velling et al., 2002, Shi et al., 2010).

1.8.2.2 Fibronectin

Fibronectin can be classified into two forms; plasma fibronectin that is secreted by hepatocytes and which circulates in the blood, and cellular fibronectin that is abundant in the fibrillar matrix of most tissues. Fibronectin is a key component of the ECM which is secreted as a large glycoprotein and assembled via cell-mediated processes into fibrils (Singh et al., 2010). Although the product of a single gene, alternative splicing of fibronectin can generate multiple variants that can each contribute to protein solubility and stability (Schwarzbauer and DeSimone, 2011). Fibronectin is a dimer composed of two nearly identical subunits. Each monomer is a modular protein of three different types of repeating unit (Type I, II and III) which contain binding motifs to mediate intramolecular interactions to facilitate self-assembly, in addition to enabling interactions with other ECM proteins and cell surface receptors. Disulphide bonds between modules stabilise a folded tertiary structure, and antiparallel C-terminal disulphide bonds enable dimer formation (Figure 1-9) (Singh et al., 2010, Mouw et al., 2014). Fibronectin is secreted as a soluble covalent dimer and this structure is necessary for its subsequent fibrillogenesis (Schwarzbauer, 1991).

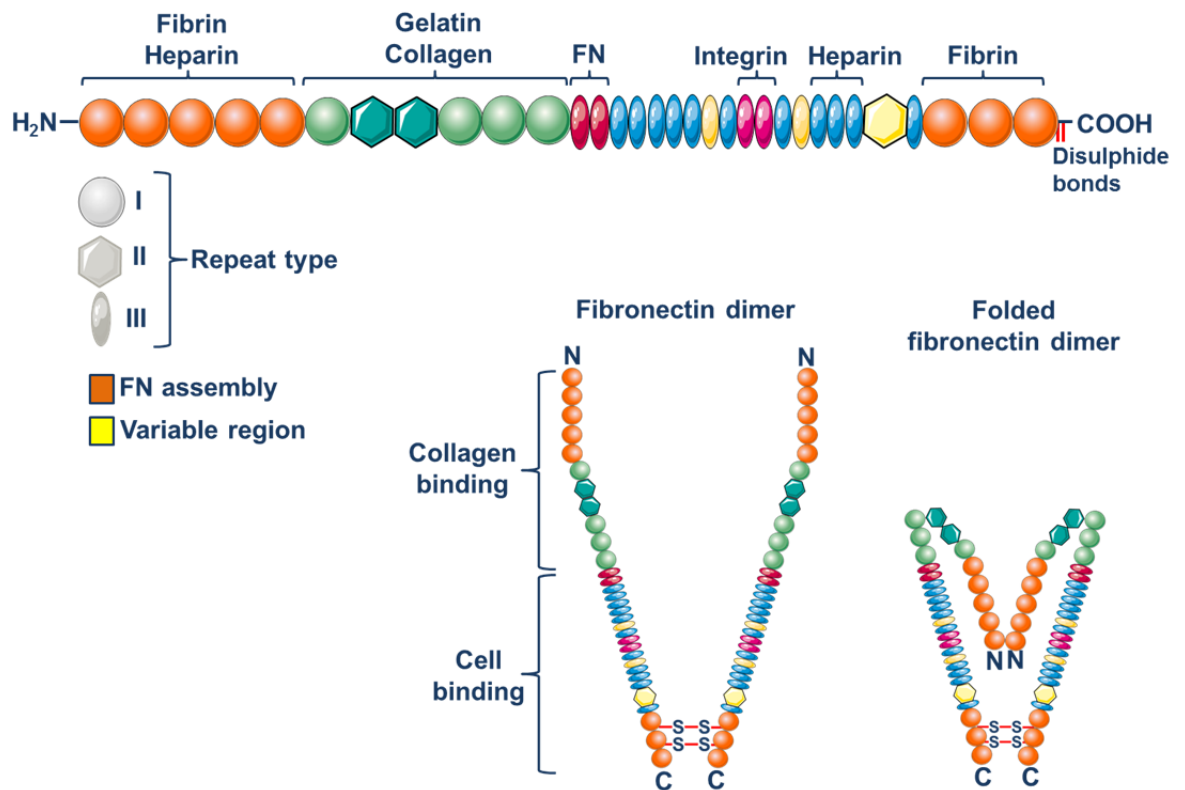


Figure 1-9- Fibronectin structure.

The fibronectin (FN) molecule is composed of three types of repeating unit, and the regions containing binding motifs to specific proteins and/or receptors are described. Domains required to initiate self-assembly are the RGD domain (highlighted as integrin binding domain) and the N and C terminal regions highlighted in orange. The FN dimer forms through C terminal disulphide bonds, and the folded fibronectin molecule through ionic interactions between type III domains in neighbouring molecules. Application of mechanical force can reveal cryptic sites for additional FN molecule binding and cell surface receptor interaction. Figure adapted from (Mouw et al., 2014). Image made using items from Image Bank in Servier Medical Art.

Fibril assembly is mediated by interactions between the RGD sequence (Arg-Gly-Asp) of fibronectin's integrin-binding domain to cell surface receptors; with integrin $\alpha_5\beta_1$ being the primary receptor for soluble fibronectin (Huveneers et al., 2008). Binding of fibronectin dimers to integrin $\alpha_5\beta_1$ leads to receptor clustering and activation, which promotes further intermolecular interactions between additional fibronectin molecules, and exerts forces to change its molecular conformation to reveal cryptic sites that promote the assembly of an insoluble fibrillar fibronectin matrix (Mouw et al., 2014, Singh et al., 2010). Other members of the integrin receptor family can also contribute to matrix assembly, as can additional transmembrane proteins including members of the Syndecan family (Klass et al., 2000, Stepp et al., 2010). Syndecan-4, for example, can control integrin recycling (Bass et al., 2011, Morgan et al., 2013) and modulate cell adhesion and migration (Bass et al., 2007b, Bass et al., 2007a, Bass et al., 2008), all of which can influence fibril assembly. Cell contractility

and tension are also important in mediating fibrillogenesis and maintaining the fibronectin matrix architecture, and activation of focal adhesion kinase (FAK) and downstream Rho GTPase signalling pathways by integrin-fibronectin associations can be evoked to maintain cell-matrix force interactions (Ilic et al., 2004, Yoneda et al., 2007).

Continued deposition and end-to-end assembly can lengthen and thicken fibronectin fibres, and the density and rigidity of these fibrils can influence the deposition and structure of the collagen matrix (Egeblad et al., 2010, Velling et al., 2002, Shi et al., 2010). In fact, the assembly of a collagen I matrix *in vivo* actively requires fibronectin fibrillogenesis (Kadler et al., 2008, Sottile and Hocking, 2002) and specific binding of collagen's $\alpha 1$ chain to fibronectin's gelatin binding domain is necessary for deposition of collagen I into the ECM (Kleinman et al., 1978, McDonald et al., 1982). The initial deposition of fibronectin has subsequently been shown to be an early step in the formation of the pre-metastatic niche (Kaplan et al., 2005), whilst upregulation of fibronectin expression can also increase cell proliferation (Williams et al., 2008, Zheng et al., 2007) and induce cancer cell invasion (Tang et al., 2015b).

1.8.2.3 Additional ECM components

Proteoglycans are heavily glycosylated proteins composed of a core protein covalently linked to one or more glycosaminoglycan (GAG) chains. Primarily found in cartilage and the neural ECM (Bandtlow and Zimmermann, 2000, Knudson and Knudson, 2001), proteoglycans are classified by their relative size and associated GAG chains, with major GAGs including chondroitin sulphate and hyaluronan. In addition to being an abundant structural component of the ECM, they are also able to regulate the activity of other molecules, including facilitating the activation of matrix metalloproteinases to enhance tumour cell invasion and promote metastasis (Iida et al., 2007).

Laminins are large glycoproteins that consist of globular laminin-type epidermal growth factor (EGF)-like repeats and α -helical domains. These heterotrimeric proteins are formed through association of an α , β and γ chain that come together through triple-helical coiled-coil domains to form cross-shaped, Y-shaped or rod-shaped conformations (Timpl and Brown, 1994). They are a major

component of basal lamina, can associate with collagen IV and fibronectin networks, and are known to mediate cell adhesion and migration in addition to triggering pro-metastatic signalling pathways (Pal et al., 2014).

Fibrinogen is a major adhesive glycoprotein that is normally converted to fibrin, by thrombin, in blood clot formation. However deposition of fibrinogen, without subsequent conversion to fibrin, is commonly found in the tumour stroma (Brown et al., 1988, Costantini et al., 1991, Rybarczyk and Simpson-Haidaris, 2000). The aberrant deposition of fibrinogen can alter the migration of cancer cells and directly stimulate pro-inflammatory cytokine release from surrounding stromal cells (Masamune et al., 2009).

Osteopontin is a phosphorylated glycoprotein that has roles in biomineralisation, bone remodelling and immune modulation (Choi et al., 2008, Wang and Denhardt, 2008). Overexpression of osteopontin is found in a number of different tumour types including those originating in the breast and ovary (Wong et al., 2001, Brown et al., 1992) and it has also been proposed for biomarker use in cancer detection (Kim et al., 2002). Its chemotactic properties can mediate immune cell infiltration and cytokine production (Giachelli and Steitz, 2000), whilst its ability to interact with various cell surface receptors, such as $\alpha_v\beta_3$, has also been shown to mediate increased cell migration and invasion (Ellison et al., 1998).

Tenascins are a family of extracellular matrix glycoproteins composed of 4 members, namely tenascin-C, -R, -X and -W, that have important roles in embryonic development and tissue remodelling (Jones and Jones, 2000). Tenascin-C is one of the most studied family members, especially in its relation to cancer progression, and its expression has been found to correspond to metastatic niche formation (Oskarsson et al., 2011), and cancer cell invasiveness via regulation of EMT (Takahashi et al., 2013). Tenascin-W is also known as tenascin-N, and this family member has been proposed as a marker of the cancer stroma (Degen et al., 2008) while it has also been shown to stimulate cell migration (Scherberich et al., 2005).

Thrombospondins are also involved in embryonic development and tissue remodelling. A family of 5 members, they have multifunctional roles in

mediating interactions between cells and the surrounding microenvironment (Ghajar et al., 2013). Thrombospondin-1 and -2 (TSP-1 and TSP-2) play important roles in balancing anti-angiogenic and pro-angiogenic stimuli during cancer progression (Naumov et al., 2006, Ren et al., 2006), while TSP-1 can also activate TGF- β in the tumour microenvironment (Harpel et al., 2001) to further contribute to the complex and interdependent pathways that promote tumour progression.

1.8.2.4 Matrix degradation

The ECM is a highly dynamic structure and in order for it to be remodelled it must be amenable to degradation. This can be performed by a variety of proteases, with two major groups being the matrix metalloproteinases (MMPs) and the 'disintegrin and metalloproteinase with thrombospondin motif' (ADAMTS) family.

The MMP family is composed of 28 members, and they are able to target a wide range of extracellular proteins (Lu et al., 2011). MMP-1 has selectivity for collagen III, whereas MMP-8 and MMP-13 target collagen I and II respectively, while MMP-3 and -10 target proteoglycans, fibronectin and laminin. MMP-2 and MMP-9 can both expose a cryptic epitope within collagen IV to promote angiogenesis (Hangai et al., 2002, Xu et al., 2001). Cross-talk also occurs between MMPs and other specific pathways, with MMP-9 and VEGF expression being simultaneously induced by regulators such as hypoxia-inducible factor (HIF-1) to promote angiogenesis (Hiratsuka et al., 2002), while cleavage of the ECM by endopeptidases can also release embedded VEGF to further promote vascularity (Park et al., 1993).

ADAMTS proteinases are also a large family, consisting of 19 members in total. In addition to degrading the ECM they are also able to activate proteinase precursors (Cawston and Young, 2010). Tumour promoting and inhibiting roles have been described for members of the ADAMTS family dependent upon their function in the TME (Kelwick et al., 2015). ADAMTS1 is commonly up-regulated in metastatic cancers, and its ability to increase tumour growth and metastatic burden in mouse models has been attributed to its capacity to cleave ECM proteins and inhibit tumour cell apoptosis (Ricciardelli et al., 2011).

Cleavage of the ECM by endopeptidases can consequently have a number of biological functions, from degrading matrix components to remodel the ECM and thus modify the cell-ECM interface, to liberating growth factors and promoting angiogenesis, all of which can contribute to tumour progression.

1.8.2.5 Mechanical properties of the ECM

The physical properties of the ECM have important ramifications for cell behaviour. ECM stiffening may be induced by increased collagen deposition and increased collagen crosslinking, which is primarily conducted by LOX and LOX-like enzymes (Erler et al., 2006, Paszek et al., 2005). Such changes in architecture are often associated with increased thickness, alignment and linearisation of fibres (Conklin et al., 2011). In addition to tensile forces, increased deposition of GAGs such as hyaluronan may increase the interstitial pressure within the matrix due to repulsion of its negatively charged chains and water molecule retention (Kultti et al., 2014), and this provides another means to influence the mechanical properties of the matrix.

The rigidity of the ECM can influence cell adhesion, proliferation and migration. Work on glioblastoma multiforme (GBM) has shown that tumour cells have increased rates of spreading, increased rates of proliferation and increased migration speeds on ECM substrates that are more rigid than those with similarity to normal brain tissue (Ulrich et al., 2009). The biomechanical properties of the matrix can also influence how cells perceive and respond to external forces. Increased matrix stiffness is able to enhance Rho-activated cell tension to promote focal adhesion (FA) assembly and increase ERK activation, and this can drive transformation (Paszek et al., 2005). The focal adhesion complex is composed of clusters of integrin receptors, adaptors and signalling proteins, and functions as a mechanosensor linking the cellular cytoskeleton with the ECM, facilitating conformational changes to apply traction force to the surrounding environment (del Rio et al., 2009, Sawada et al., 2006). The physical composition of the ECM can therefore have important ramifications for how cells are able to perceive and respond to their external environment, and is consequently another major factor that can influence cell migration.

1.9 Cell migration

Cell migration is pivotal to many processes including embryonic development, angiogenesis and wound healing, and the ECM surrounding cells can either inhibit or promote cell migration depending on the cell type and its mechanism of movement. In general, cell migration occurs through repeated cycles of leading edge protrusion, adhesion, cell body translocation and retraction of the cell rear (Figure 1-10). However, in practice cells can migrate in a number of different ways, including single cell migration, multicellular streaming and collective migration, with the selected mode depending on the cell type and its response to the external microenvironment.

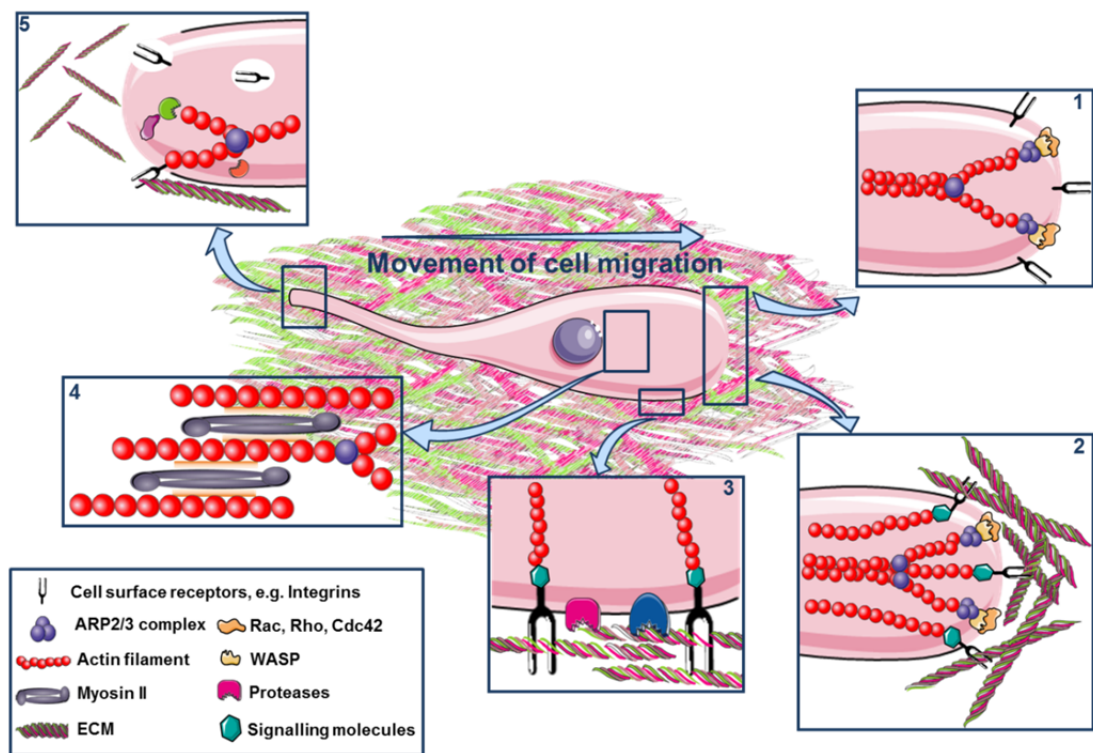


Figure 1-10- Model of mesenchymal-like cell migration through the ECM.

(1) Cell protrusion at the leading edge. Actin filaments grow by polymerisation and coupling with the ARP2/3/WASP complex. Extensions are further formed and supported through engagement of adaptor proteins, cell surface proteins and other molecules such as Rac, Cdc42 and Rho. (2) ECM interaction and focal adhesion formation. Cell surface integrin receptors bind the ECM and cluster at the cell membrane. Clustered integrins can recruit adaptor and signalling molecules through their intracellular domains, including tensin and focal adhesion kinase (FAK). This can further recruit other signalling and regulatory molecules, such as vinculin and Rho-family GTPases. (3) Localised proteolysis. Surface proteases are recruited to the binding sites to cleave ECM components to assist migration through the matrix and create active soluble endopeptidases to further facilitate degradation. (4) Cell body contraction. Active myosin II binds actin filaments to generate actomyosin contraction. (5) Detachment of trailing edge. Focal contact disassembly occurs by a number of mechanisms, including actin binding and severing proteins and cytoplasmic proteases that cleave focal adhesion components. Cell surface receptors can be internalised and trafficked for recycling or degradation. Figure adapted from (Friedl and Wolf, 2003). Image made using items from Image Bank in Servier Medical Art.

1.9.1 Single cell migration

Cells can lose their cell-cell contacts and migrate as individual cells. This is particularly relevant for metastatic dissemination of cancer cells were, for example, local increases in TGF- β can enable breast cancer cells to switch from cohesive to single cell migration to promote haematogenous metastasis (Giampieri et al., 2009). Single cell migration can be amoeboid or mesenchymal in type. Mesenchymal-like cell migration follows the mechanisms outlined in Figure 1-10, and tends to be used by cells that have a fibroblast-like spindle-shaped morphology that are dependent on integrin-mediated dynamics for their motility. Amoeboid migration, on the other-hand, uses a less adhesive gliding type of movement, and is supported by cortical filamentous actin and more short-lived weak interactions (Friedl and Wolf, 2003).

1.9.2 Multicellular streaming

Cells with amoeboid like morphologies can migrate in streams, as cells follow each other in single file without cohesive cell-cell junctions. This kind of migration is particularly relevant *in vivo*, and can occur in correlation with a vascularised microenvironment as blood vessels can function as pre-defined cell tracks (Patsialou et al., 2013). Coordinated cell streaming can enhance transendothelial migration and intravasation of tumour cells to promote cancer cell metastasis (Roussos et al., 2011) and so is a key migration mechanism used in invasive cancer progression.

1.9.3 Collective migration

Collective cell migration occurs when cells move in cohesive groups, and is commonly seen during embryonic development and in the sprouting of endothelial cells for new blood vessel formation (Davidson and Keller, 1999, Collen et al., 2003). Cell-cell adhesions linking groups of moving cells can cause assembly of cortical actin filaments along cell junctions, to essentially form a large multicellular contractile body (Hegerfeldt et al., 2002). Leading cells are able to generate a path, and migratory traction can consequently tow trailing cells (Friedl et al., 1995). By moving in a larger cell mass, cells are able to

increase local concentrations of pro-migratory factors, and more motile cells can promote migration and invasion of less mobile cell types.

1.9.4 Integrin cell surface receptors

Cells use transmembrane receptors to bind and respond to the surrounding ECM and facilitate their migration through it, and one of the major classes required for cell adhesion and migration are the integrin receptors (Hynes, 1987). Integrins are a diverse family of heterodimeric receptors that are generally composed of a non-covalently linked α and β subunit, with each subunit having a large extracellular domain, a single membrane spanning domain, and a short cytoplasmic tail (Hynes, 2002). Heterodimerisation generates 24 known types of receptor that can engage and respond to various and overlapping ECM components (Table 1-4).

Ligand	Receptor	Common distribution
Collagen	$\alpha_{10}\beta_1$	Chondrocytes
	$\alpha_2\beta_1$	Chondrocytes, endothelial cells, fibroblasts
	$\alpha_1\beta_1$	Chondrocytes, epithelial cells
	$\alpha_{11}\beta_1$	Mesenchymal non-muscle cells
Fibronectin	$\alpha_5\beta_1$	Fibroblasts, chondrocytes, endothelial cells
	$\alpha_8\beta_1$	Smooth muscle cells
	$\alpha_v\beta_1$	Fibroblasts, osteoclasts, smooth muscle cells
	$\alpha_v\beta_6$	Epithelial cells
	$\alpha_v\beta_3$	Endothelial cells, epithelial cells
	$\alpha_{11b}\beta_3$	Platelets
Laminin	$\alpha_{10}\beta_1$	Chondrocytes
	$\alpha_2\beta_1$	Keratinocytes, chondrocytes, endothelial cells
	$\alpha_1\beta_1$	Chondrocytes, epithelial cells
	$\alpha_7\beta_1$	Differentiated muscle cells
	$\alpha_6\beta_4$	Endothelial cells
	$\alpha_6\beta_1$	Chondrocytes, endothelial cells
	$\alpha_3\beta_1$	Keratinocytes
Fibrinogen	$\alpha_v\beta_3$	Endothelial cells, epithelial cells
	$\alpha_v\beta_5$	Endothelial cells, epithelial cells, platelets
	$\alpha_v\beta_6$	Epithelial cells
	$\alpha_{11b}\beta_3$	Platelets
Osteopontin	$\alpha_v\beta_1$	Fibroblasts, osteoclasts, smooth muscle cells
	$\alpha_v\beta_3$	Endothelial cells, fibroblasts, epithelial cells
	$\alpha_v\beta_5$	Endothelial cells, epithelial cells, platelets
Tenascin	$\alpha_v\beta_3$	Endothelial cells, epithelial cells
	$\alpha_v\beta_6$	Endothelial cells
	$\alpha_2\beta_1$	Keratinocytes, chondrocytes, endothelial cells
	$\alpha_9\beta_1$	Keratinocytes, endothelial cells
Thrombospondin	$\alpha_v\beta_3$	Endothelial cells, epithelial cells
	$\alpha_v\beta_5$	Endothelial cells, epithelial cells, platelets
Vitronectin	$\alpha_v\beta_1$	Fibroblasts, osteoclasts, smooth muscle cells
	$\alpha_v\beta_3$	Endothelial cells, epithelial cells
	$\alpha_v\beta_5$	Endothelial cells, epithelial cells, platelets

$\alpha_v\beta_6$	Epithelial cells
$\alpha_v\beta_8$	Uterus, kidney, brain, ovary, placenta
$\alpha_1\beta_1$	Chondrocytes, epithelial cells

Table 1-4- Integrin heterodimers and their ligands.

Integrin-ligand interactions for some of the most common components of the ECM (Humphries et al., 2006, Niu and Chen, 2011).

Integrins provide a link between the ECM and the cell's cytoskeleton, and hence are important for most types of cell migration. Integrins can exist in three different conformational states; an inactive bent conformation with a low affinity for ECM ligands, a primed extended conformation which still has a closed head-piece and low ligand affinity, and an active extended head-piece with high ligand affinity (Luo et al., 2007). Despite lacking enzymatic activity, they are able to initiate 'outside in' signalling through ligand binding to the external domain and consequent recruitment of signalling molecules such as FAK, or by influencing how growth factors such as EGFR or FGFR can respond to their ligands (Walker et al., 2005). Alternatively, cells can also trigger 'inside-out' signalling, where the integrin receptors are switched from low-affinity inactive states to high-affinity active conformations through association of β -integrin cytoplasmic tails with FERM-domain containing proteins such as talin and kindlin (Moser et al., 2009, Wegener et al., 2007). Integrin signalling is highly regulated at a number of different levels, including ligand binding, intracellular signalling and receptor trafficking, all of which can affect how cells migrate (Caswell and Norman, 2006).

1.9.4.1 Integrin trafficking

Integrins can be endocytosed from the cell surface into early endosomes via a number of different mechanisms; these can be clathrin-dependent or independent, caveolin-mediated, or macropinosytotic (Gu et al., 2011, De Franceschi et al., 2015). Once internalised, integrins are sorted for degradation or recycled back to the cell surface by a number of distinct mechanisms that are controlled by small GTPases, and the pathway that they take can influence cell migration. Members of the Ras superfamily of small GTPases which are involved in integrin trafficking include those of the Rho, Rab and Arf groups. The Rho GTPases include Rho, Rac and Cdc42, and these members tend to influence integrin trafficking and cell motility through regulation of actin cytoskeleton dynamics (Ridley, 2006). The role played by the Rab and Arf GTPases in integrin

trafficking are more direct than those played by the Rho subfamily, and involve the dynamic recycling and trafficking of internalised receptors to the plasma membrane. Recycling through a Rab-4 dependent pathway can promote rapid delivery of integrins back to the plasma membrane, while longer recycling routes include recycling to Rab-11-positive perinuclear recycling compartments prior to returning to the cell surface (Caswell and Norman, 2006, Morgan et al., 2009, Scita and Di Fiore, 2010, De Franceschi et al., 2015). For example, integrin $\alpha_v\beta_3$ can be trafficked through the Rab-4 dependent short loop pathway, as the receptor is rapidly trafficked from early endosomes back to the plasma membrane through a mechanism dependent on growth factor induced autophosphorylation of PKD1 and its recruitment to the cytoplasmic tail of β_3 (Roberts et al., 2001, Roberts et al., 2004, White et al., 2007). Integrin $\alpha_5\beta_1$ on the other-hand can be sorted from early endosomes into recycling endosomes via the Rab-11 dependent long loop (Roberts et al., 2004). In this case receptors are trafficked to the Rab-11 positive perinuclear recycling compartment (PNRC) before being returned to the plasma membrane, and this can be regulated by a number of different kinases including PKB/Akt (Roberts et al., 2004) and PKC ϵ (Ivaska et al., 2005), in addition to actin related proteins such as Arp2/3 (Actin-related protein 2/3) and WASH (WASP and SCAR homologue) (Duleh and Welch, 2012, Zech et al., 2011) (Figure 1-11).

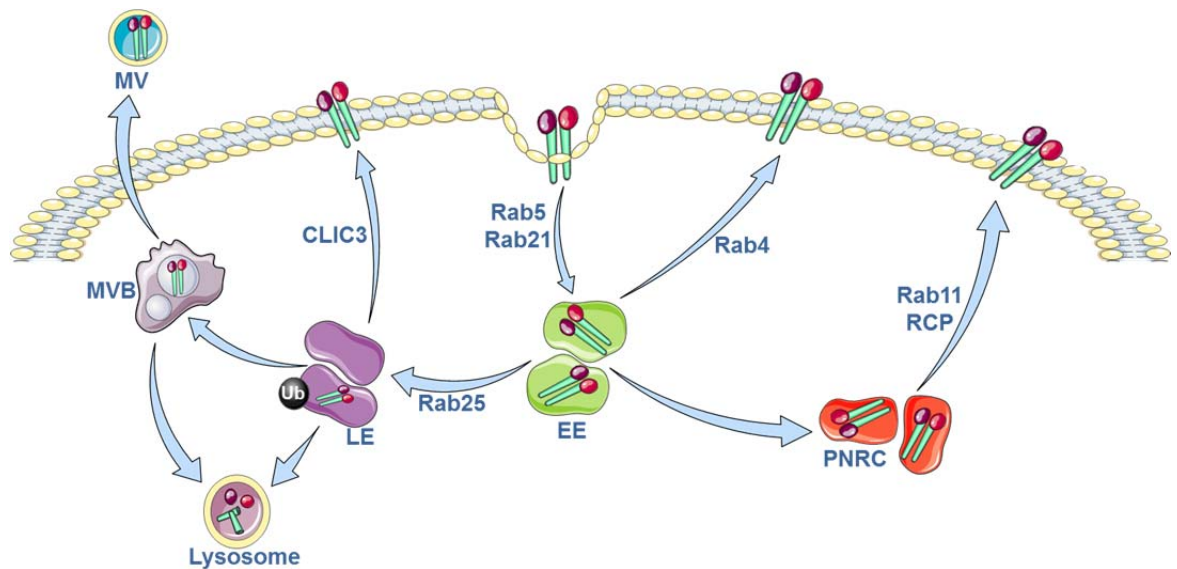


Figure 1-11- Rab GTPase control of integrin trafficking.

Integrins can be internalised into early endosomes (EE) by a number of different mechanisms, which can be regulated by Rab-21. Following internalisation they can then be trafficked by a number of different pathways. The short-loop pathway is mediated by Rab-4 to traffick integrins back to the cell surface, and the long loop pathway by Rab-11 and RCP mediated processes through the perinuclear recycling compartment (PNRC). Integrins can also be trafficked to the late endosome (LE), where they can be transported back to the plasma membrane in a Rab-25 dependent process, sorted and secreted in microvesicles (MV) via the multivesicular body (MVB), or are targeted for lysosomal degradation by ubiquitination. Image made using items from Image Bank in Servier Medical Art.

These recycling pathways enable adhesion turnover and replenishment of cell surface integrins, and they have important influences on the control of cell migration and invasion. The Rab-11 effector RCP (Rab-coupling protein) controls the recycling of integrin $\alpha_5\beta_1$ and receptor RTKs. RCP-driven recycling of $\alpha_5\beta_1$ to leading edge protrusions increases the fibronectin-dependent migration of cancer cells, with increased invasive behaviour not owing to differences in adhesive function but to $\alpha_5\beta_1$ and RCP's effect on the trafficking of RTKs such as EGFR1 and activation of the pro-invasive PKB/Akt pathway (Caswell et al., 2008). Mutant p53 can also activate RCP-dependent trafficking of integrins and RTKs to promote invasion (Muller et al., 2009, Muller et al., 2013), and RCP-dependent trafficking can also influence Rho GTPase function to regulate invasion, by suppressing Rac and promoting RhoA activity through phosphorylation of RacGAP1 (Jacquemet et al., 2013).

Differential receptor trafficking can also occur, where distinct heterodimers for the same ligand are trafficked through different pathways to regulate the activity of each other. In the case of the fibronectin receptors, the activity of

$\alpha_v\beta_3$ suppresses $\alpha_5\beta_1$ recycling (White et al., 2007, Morgan et al., 2009), and this can also influence cell migration. Recycling of $\alpha_v\beta_3$ is associated with directional migration and invasion into ECM containing low fibronectin concentrations through pathways that are dependent on Rac activation, whereas $\alpha_5\beta_1$ recycling can induce random migration through the Rho-ROCK-Cofilin pathway in matrices with high fibronectin abundance (White et al., 2007, De Franceschi et al., 2015, Morgan et al., 2013, Danen et al., 2005). Control of integrin trafficking is therefore an integral regulator of cell migration, and aberrant activity of such pathways can result in the increased migratory effect seen in metastatic cancers (Table 1-5).

Integrin Receptor	Associated Molecule	Trafficking Step	Biological Process	Disease Association
$\alpha_5\beta_1$	Rab25	Recycling	Invasion	Ovarian cancer, breast cancer, colon cancer, intestinal neoplasia
$\alpha_5\beta_1$	RCP	Recycling	Invasion Metastasis	Breast cancer, mutant p53 carcinomas, head and neck squamous carcinoma
$\alpha_5\beta_1$	CLIC3	Recycling	Invasion	Ovarian cancer, pancreatic cancer, breast cancer
$\alpha_5\beta_1, \alpha_6$	GIPC1	Endocytosis	Invasion Metastasis Vascular-development	Breast cancer, ovarian cancer, gastric cancer, pancreatic cancer
$\alpha_5\beta_1, \alpha_v\beta_3$	PRKD1	Recycling	Proliferation Invasion	Breast cancer, prostate cancer, gastrointestinal cancer, skin cancer
$\alpha_3\beta_1, \alpha_5\beta_1,$	STX6 VAMP3	Recycling	Proliferation	Breast, colon, liver, pancreatic, prostate, bladder, skin, testicular, tongue, cervical, lung and gastric cancers
$\alpha_5\beta_1, \alpha_2\beta_1$ $\alpha_v\beta_3, \alpha_6\beta_4$	Rab11	Recycling	Invasion Metastasis	Skin carcinogenesis, Barrett's dysplasia, mutant p53 carcinomas
$\alpha_v\beta_6$	HAX1	Endocytosis	Transformation Invasion Metastasis	Breast cancer, colon cancer, oral cancer
$\alpha_9\beta_1$	Arf6	Recycling	Tissue repair	Axonal development, regeneration peripheral nervous system
$\alpha_1, \alpha_2, \alpha_5$ α_6, β_1	Rab21	Endocytosis	Migration Cytokinesis	Prostate cancer, lung cancer

Table 1-5- Integrin trafficking pathways associated with human disease processes.

A summary of some of the known associations between human pathophysiological conditions and integrin receptor trafficking pathways. GAIP interacting protein C1 (GIPC1), Rab coupling protein (RCP), Chloride intracellular channel protein 3 (CLIC3), Protein Kinase D1 (PRKD1), Synaptophysin 6 (STX6), Vesicle-associated membrane protein 3 (VAMP3), HS1 associated protein (HAX1). Table adapted from (De Franceschi et al., 2015).

1.9.4.2 ECM and trafficking

Integrin trafficking plays a pivotal role in the dynamic formation and disassembly of adhesions that mediate cell migration, however ECM components can also be internalised into the cells during transmembrane receptor endocytosis. Endopeptidases can co-localise with integrins and adhesion complexes to cleave ECM components and enable co-uptake of the matrix upon receptor internalisation (Galvez et al., 2002, Shi and Sottile, 2011). Ligand-bound receptors can be targeted to lysosomes for degradation, however in cancers that have increased expression of the lysosomal protein CLIC3, ligand-bound integrins were found not to be degraded but recycled to the plasma membrane to promote increased levels of cell invasion and metastasis (Dozynkiewicz et al., 2012). In environments with low fibronectin levels, internalised fibronectin can be re-secreted from late endosomes and lysosomes to further promote cell migration by providing an autocrine substrate to enable cells to increase their own motility (Sung and Weaver, 2011). Recent data has also shown that ligand-bound integrins can be trafficked to late endosomes to support mTOR signalling (Rainero et al., 2015). The interaction between mTORC1 and integrin trafficking is particularly interesting, and suggests a link between ECM internalisation, nutrient signalling and cell migration. Furthermore, given mTORC1's key role in controlling selectivity of protein synthesis, in particular translation initiation and elongation, this observation may indicate a potential mechanistic connection between the turnover and internalisation of the ECM and the synthesis of cellular and secreted proteins. All of these factors can contribute to increased cancer cell invasion and metastasis, and so further understanding the role of the ECM in cell migration and tumour growth is an important area of research that could have a major impact on the development of future cancer therapies.

1.10 PhD Objectives

Understanding how cells can sense, respond, influence and migrate through their microenvironments is fundamental to understanding how cancer cells can grow, disseminate and metastasise. It is metastasis rather than primary tumour growth that causes the majority of human cancer deaths, and so unravelling the molecular basis of this process is essential to provide the necessary knowledge required to generate targeted and effective therapies.

Control of gene expression is pivotal to a large range of cell processes from cell migration to ECM secretion, and as a consequence is subject to regulation by a number of highly complex and complicated mechanisms. The translation of mRNA into protein can be regulated at a number of different levels including global upregulation/downregulation of the total amount of protein produced, to more subtle shifts in the translational efficiency of particular transcripts. Transfer RNAs are key adaptor molecules which are required to read codons of the mRNA and bring the appropriate amino acid to the translation machinery. Moreover, it is clear that the tRNA repertoire differs markedly between cells that are rapidly proliferating and those that are terminally differentiated or quiescent. Whilst cells express a large number of different tRNAs, the initiator methionine tRNA ($\text{tRNA}_i^{\text{Met}}$) is of particular interest, as only this tRNA can recognise and bind the start codon to initiate translation. Increased levels of tRNAs are found across a variety of cancer types, however it is currently unknown whether this is a cause or a consequence of tumourigenesis, or what role, if any, this might play in tumour progression. The objective of this work is therefore to understand whether increased expression of one particular tRNA, $\text{tRNA}_i^{\text{Met}}$, could influence cell behaviour, with a specific interest in understanding whether $\text{tRNA}_i^{\text{Met}}$ expression could affect cell migration and tumour growth.

Chapter 2 Materials and methods

2.1 Materials

2.1.1 Reagents

Reagent	Supplier
0.45µm filter	Gilson
1.5mL microcentrifuge tubes	Eppendorf
1.5mL RNase free microcentrifuge tubes	Life Technologies
1Kb Plus DNA Ladder	Life Technologies
1mL syringe	Becton Dickinson
2% gelatin	Sigma
25G needle	Becton Dickinson
AEBSF	Melford Laboratories
Agarose	Sigma
Ampicillin	Sigma
Aprotinin	Sigma
Ascorbic Acid	Sigma
BglII	New England Biolabs
BSA	First link
Casyton	Roche
Cell lifter	Corning
Chloroform	Sigma
Citric acid	Sigma
Clal	New England Biolabs
Coomassie gel stain	Expedeon
Dialysed foetal calf serum	PAA
DMEM minus methionine and cysteine	Life Technologies
DMEM/F12 media	Life Technologies
DMSO	Fisher Scientific
DNase1	Roche
DTT	Melford Laboratories
Dulbecco's Modified Eagle Medium (DMEM)	Life Technologies
Dynabeads anti-mouse	Life Technologies
EasyTag Express Protein Labelling Max ³⁵ S	PerkinElmer
ECL Western blotting substrate	Pierce
EcoRI	New England Biolabs
EDTA	Sigma
EGTA	Sigma
Ethanol	VWR
Falcon tissue culture 6 well plates	BD Biosciences
Falcon tissue culture dishes (10 & 15cm ²)	BD Biosciences
Fibronectin	Sigma
Foetal Calf Serum	PAA

Full-Range Rainbow Ladder	Amersham
Fungizone	Life Technologies
Glass bottom 3cm dishes	Maktek
Glutaraldehyde	Sigma
Glycerol	Fisher Scientific
Glycine	Sigma
Hpal	New England Biolabs
Hybond-P PVDF membrane	GE Healthcare
Hydrogen peroxide	Sigma
Hygromycin	Life Technologies
Igepal CA-630	Fluka
Iodoacetamide (IAA)	Sigma
Leupeptin	Melford
L-Glutamine	Life Technologies
Maxisorp 96 well microtiter plates	Life Technologies
MesNa	Fluka
Milk powder	Marvel
Na ₂ CO ₃	Fisher Scientific
Na ₂ HPO ₄	Fisher Scientific
Na ₃ VO ₄	Fisher Scientific
NaCl	Fisher Scientific
NaF	Sigma
NaHCO ₃	Fisher Scientific
NaN ₃	Sigma
NaOH	Fisher Scientific
NH ₄ OH	Sigma
Nunc tissue culture plates	TCS biologicals
NuPAGE MES SDS running buffer	Life Technologies
NuPAGE MOPS SDS running buffer	Life Technologies
NuPAGE pre-cast gels (4-12% & 10%)	Life Technologies
NuPAGE sample buffer	Life Technologies
NuPAGE transfer buffer	Life Technologies
Odyssey blocking buffer	Licor
Ortho-phenylenediamine	Sigma
Parafilm wrap	Fisher Scientific
Paraformaldehyde (PFA)	Electron Microscopy Sciences
PBS containing calcium and magnesium	Sigma
Penicillin/Streptomycin	Life Technologies
PerfeCTa SYBR Green Fast Mix	Quanta
Propan-2-ol	Fisher Scientific
Propidium Iodide	Sigma
RNase free water	Sigma
Salubrinal	Calbiochem
Scintillation fluid	National Diagnostics
SDS	Fisher Scientific
SILAC DMEM	Lonza
SILAC labelled amino acids	Cambridge Isotope Laboratories

siRNA	Dharmacon
SnaBI	New England Biolabs
Strataclean beads	Agilent
Streptavidin-conjugated HRP	GE Healthcare
Sulfo-NHS-SS-Biotin	Pierce
Super RX medical x-ray film	Fuji
TOP10 OneShot chemically competent cells	Life Technologies
TransIT-LT1 transfection reagent	Mirus
Trichloroacetic acid (TCA)	Sigma
Tris HCl	Melford
Triton-X100	Sigma
Trizol	Life Technologies
Trypsin	Life Technologies
Tween-20	Sigma
Vectashield mounting media + DAPI	Vector laboratories
Whatman GF/C 2.5cm filter paper	GE Healthcare
XF base medium	Seahorse Biosciences
β -mercaptoethanol	Sigma

Table 2-1- Reagents and suppliers

2.1.2 Solutions

Solution	Recipe
1% SDS lysis buffer	1% SDS (v/v), 50mM Tris-HCl pH7.0, 0.1M DTT
4% SDS lysis buffer	4% SDS (v/v), 0.1M Tris-HCl pH7.4, 0.1M DTT
Biotin reduction buffer	50mM Tris-HCl pH7.4, 10mM NaCl, pH8.6 at 4 °C
ELISA coating buffer	0.05M Na ₂ CO ₃ , pH9.6 at 4 °C
ELISA development reagent	0.56 mg/mL ortho-phenylenediamine , 25.4mM Na ₂ HPO ₄ , 12.3mM citric acid, pH5.4 with 0.003% H ₂ O ₂
Extraction buffer	10mM NH ₄ OH, 0.5% Triton-X100 (v/v) in PBS with calcium and magnesium
FACS buffer	PBS, 1% BSA (v/v), 0.5 μ g/mL propidium iodide
LB Broth	85mM NaCl, 1% bacto-trypton (w/v), 0.5% yeast extract (w/v)
NDLB	50mM Tris-HCl pH7.0, 150mM NaCl, 10mM NaF, 1mM Na ₃ VO ₄ , 5mM EDTA, 5mM EGTA, 1.5% Triton-X100 (v/v), 0.75% Igepal CA-630 (v/v)
PBS-T	PBS, 0.1% Tween-20 (v/v)
TBS	10mM Tris-HCl pH7.4, 150mM NaCl
TBS-T	TBS, 0.1% Tween-20 (v/v)

Table 2-2- Recipes of solutions

2.1.3 Kits

Kit	Supplier
Agilent RNA 6000 Pico Kit	Agilent
Amaxa Nucleofector Kit R	Lonza
GeneArt CRISPR Nuclease Vector with OFP Reporter Kit	Life Technologies

Mini Elute Gel Extraction Kit	Qiagen
Quantitech Reverse Transcription Kit	Qiagen
Qubit Protein Assay	Life Technologies
Rapid Ligation Kit	Roche
RiboZero Magnetic Kit	Illumina
RNeasy MinElute Cleanup Kit	Qiagen
XF Cell Mitochondrial Stress Test	Seahorse Bioscience

Table 2-3- Kits and suppliers

2.1.4 Primers

Primer	Sequence
5S rRNA Forward	CAGCACCCGGTATTCCCAGG
5S rRNA Reverse	GGCATACCACCTGAACGC
ARPP P0 Forward	GCACTGGAAGTCCAACACTTC
ARPP P0 Reverse	TGAGGTCTCCTTGGTGAACAC
Collagen II Forward	GGGTCACAGAGGTTACCCAG
Collagen II Reverse	ACCAGGGGAACCACTCTCAC
tRNA ^{Ile} Forward	GCGCGCCGGTTAGCTCAG
tRNA ^{Ile} Reverse	CCCGTACGGGGATCGAAC
tRNA _i ^{Met} Forward	AGAGTGCGCAGCGGAAG
tRNA _i ^{Met} Reverse	AGCAGAGGATGGTTTCGATCC

Table 2-4- qRT-PCR primer sequences

2.1.5 Plasmids

Plasmid	Supplier
pGEM easy T	Promega
pLPCX	Clontech
pLHCX	Clontech

Table 2-5- Expression vectors

2.1.6 siRNA

Target	siRNA	Supplier
Collagen II	ON-TARGET plus Col2a1 siRNA L-043139-01-0005	Dharmacon
Integrin alpha 5	ON-TARGET plus Itga5 siRNA L-060502-01-0005	Dharmacon
Non-targeting(NT)	siGENOME control pool NT #1 D-001206-13-50	Dharmacon

Table 2-6- siRNA used for siRNA knock-down experiments

2.1.7 Primary antibodies

Protein	Host	Antibody	Technique (dilution)	Supplier
Collagen II	Rabbit	AB21291	Western blot (1:1000), Immunostaining ECM	Abcam

			(1:100), IHC of TMA (1:300)	
Integrin α_5	Rat	553319	ELISA (1:100), IF (1:100)	BD Pharmingem
Integrin α_5	Rabbit	AB1921	Western blot (1:5000)	Chemicon
Integrin β_1	Rat	550531	ELISA (1:100)	BD Pharmingen
P-eIF2 α	Rabbit	44728G	Western blot (1:1000)	Life Technologies
TfR	Rat	553264	ELISA (1:100)	BD Pharmingem
β -actin	Mouse	A1978	Western blot (1:10,000)	Sigma

Table 2-7- Primary antibodies

2.1.8 Secondary antibodies

Antibody	Host	Technique (dilution)	Supplier
Alexa-fluor 488 α -rat	Goat	IF (1:200)	Life Technologies
HRP α -mouse	Goat	Western blot (1:1000)	Sigma
HRP α -rabbit	Goat	Western blot (1:1000)	Sigma
IRDye 680CW α -rabbit	Donkey	Western blot (1:10,000)	LI-COR
IRDye 800CW α -mouse	Donkey	Western blot (1:10,000)	LI-COR
IRDye 800CW α -rabbit	Donkey	Immunostaining ECM (1:10,000) Western blot (1:10,000)	LI-COR

Table 2-8- Secondary antibodies

2.2 Methods

2.2.1 2+tRNA_i^{Met} mice

The 2+tRNA_i^{Met} mouse was generated by the Transgenic Technology group at the CR-UK Beatson Institute, Glasgow. Briefly, two copies of the murine tRNA_i^{Met} gene (tRNA78), including ~140bp of flanking sequence, were targeted to the HPRT locus of HM1 embryonic stem cells, and used to generate chimeric mice. 2+tRNA_i^{Met} transgenic offspring were derived by crosses to C57Bl/6 mice.

2.2.2 Allograft models

2.2.2.1 Melanocyte allograft

1x10⁶ transformed melanocytes (Tyr::NrasQ61K;INK4a-/-) were injected subcutaneously into littermatched WT or 2+tRNA_i^{Met} transgenic male mice and tumour size monitored 3 times per week. Mice were culled once tumours reached 15x15mm size, and survival plotted by Kaplan-Meier analysis.

2.2.2.2 Lewis lung carcinoma allograft

This experiment was conducted by the Reynolds lab, Institute of Cancer Research, London. 1×10^6 Lewis lung carcinoma cells were injected subcutaneously into the right flank of littermatched WT or 2+tRNA_i^{Met} transgenic male mice. All tumours were harvested 21 days post injection and final tumour volume was measured as $(L \times W \times W)/2$, where L is the longest dimension and W is the shortest dimension. Tumours were paraformaldehyde (PFA) fixed and immunohistochemistry (IHC) performed for endomucin to enable blood vessel identification. Vessels were counted across the entire tumour section and are reported as vessels per mm².

2.2.2.3 B16 melanoma allograft

This experiment was conducted by the Reynolds lab, Institute of Cancer Research, London. 0.5×10^6 B16 F0 mouse melanoma cells were injected subcutaneously into the right flank of littermatched WT or 2+tRNA_i^{Met} transgenic male mice. Mice were culled and tumours harvested 22 days from the day the tumour was a measurable 3x3mm size. Tumours were skinned, and final tumour volume was measured as $(L \times W \times W)/2$, where L is the longest dimension and W is the shortest dimension. Tumours were PFA fixed and IHC performed for endomucin to enable blood vessel identification. Vessels were counted across the entire tumour section and are reported as vessels per mm².

2.2.2.4 Lewis lung carcinoma allograft with ethyl-3,4-dihydroxybenzoate treatment

This experiment was conducted by the Reynolds lab, Institute of Cancer Research, London. 1×10^6 Lewis lung carcinoma cells were injected subcutaneously into littermatched WT or 2+tRNA_i^{Met} transgenic male mice, followed by daily dosing with 40mg/kg ethyl-3,4-dihydroxybenzoate (DHB). Tumours were harvested 21 days post injection and final tumour volume measured as $(L \times W \times W)/2$, where L is the longest dimension and W is the shortest dimension. Tumours were PFA fixed and IHC performed for endomucin to enable blood vessel identification. Vessels were counted across the entire tumour section and are reported as vessels per mm².

2.2.3 Cloning

2.2.3.1 tRNA_i^{Met} expression vector

A construct containing tRNA_i^{Met} (pGEM.tRNA_i^{Met}) was kindly provided by the White lab (formerly CR-UK Beatson Institute, now University of York, UK). As the pGEM easy T vector provided was a bacterial expression vector, tRNA_i^{Met} was subcloned into a mammalian expression vector in which the cytomegalovirus (CMV) promoter was removed to allow Pol III transcription of the tRNA from its own internal promoters without interference from Pol II at the upstream CMV promoter.

Fragments containing tRNA_i^{Met} were digested out of the pGEM.tRNA_i^{Met} construct using EcoRI and ligated into the multiple cloning site (MCS) of the EcoRI digested pLPCX vector. Briefly, 1µg of DNA was digested with EcoRI and the fragments separated by gel electrophoresis (1.5% agarose gel at 90V for 75 minutes). The digested vector and insert were then purified from the gel using a Mini Elute Gel Extraction Kit and ligated using a 1:2 molar ratio of vector to insert and a Rapid Ligation Kit, all exactly as per manufacturer's instructions.

The pLPCX.tRNA_i^{Met} construct and pLHCX final destination vector were digested using BglII and ClaI, and then gel purified and ligated as described above to produce the pLHCX.tRNA_i^{Met} containing vector. To make the corresponding pLHCX empty vector control minus the Pol II CMV promoter, the pLHCX vector was digested with HpaI and SnaBI, gel purified, and then religated.

Transformation of TOP10 chemically competent *E.coli* was conducted to propagate the constructs. In short, 2µL of the ligation reaction was added to a vial of TOP10 cells and incubated on ice for 15 minutes. Vials were heat-shocked for 30 seconds at 42°C and then placed back on ice for 2 minutes. 250µL pre-warmed LB broth was added to each vial, followed by horizontal shaking at 37°C for 1 hour at 225rpm. 50µL and 200µL of each transformation was then spread onto pre-warmed agar selective plates (containing 100µg/mL ampicillin) and incubated at 37°C overnight. Individual colonies were picked and propagated in 5mL LB broth + 100µg/mL ampicillin by incubating at 37°C with shaking at 225rpm for 6 hours. This culture was then diluted 1:500 into 200mL LB broth +

100µg/mL ampicillin, and incubated at 37°C with shaking at 225rpm overnight. Bacterial cells were harvested by centrifugation at 4000rpm for 20 minutes at 4°C. Pellets were maxiprepmed and sequenced by the Molecular Technology Service, CR-UK Beatson Institute, Glasgow.

2.2.3.2 Collagen II CRISPR expression vector

Single-stranded oligonucleotides were designed to exon 1 of collagen II (Top strand oligo 5'-3': CCTCGGGGCTCCCCAGTCGCGTTTT, Bottom strand oligo 5'-3': GCGACTGGGGAGCCCCGAGGCGGTG), annealed to make double stranded oligos and ligated into the linearised GeneArt CRISPR Nuclease Vector exactly as per manufacturer's instructions. The construct was then transformed, propagated and sequenced as described in 2.2.3.1.

2.2.4 Cell culture

2.2.4.1 Immortalised cell lines

Immortalised mouse embryonic fibroblasts (iMEFs) previously made using the 3T3 method were kindly provided by the White lab (formerly CR-UK Beatson Institute, now University of York, UK) and cultured in DMEM supplemented with 10% FBS, 200µM L-Glutamine, 100U/mL penicillin streptomycin, 0.25µg/mL fungizone. Stable cell lines expressing pLHCX.tRNA_i^{Met} and corresponding empty vector control were made by transfection using 1x10⁵ cells per well in a 6 well plate with 2.5µg construct and TransIT-LT1 transfection reagent, exactly as per manufacturer's instructions. Selection of stable pools was performed in full growth media supplemented with 250µg/mL hygromycin. Stable pLHCX.tRNA_i^{Met} iMEFs were also transfected with the collagen II CRISPR construct, or corresponding empty GeneArt vector control, using 1x10⁶ cells per 10cm² dish with 15µg construct and TransIT-LT1 transfection reagent exactly as per manufacturer's instructions. Transfected cells were selected using fluorescence activated cell sorting (FACS) of orange fluorescent protein (OFP) expressing cells.

For continued culture, cells were grown at 37°C/5%CO₂ and passaged every 2 - 3 days. To passage cells, media was removed, cells were washed in PBS, and incubated in 0.25% trypsin for 5 minutes at 37°C/5%CO₂. After visualising cell

detachment by light microscopy, cells were resuspended in full growth media and plated at the required density in new tissue culture dishes.

Cryofreezing was conducted for long term storage. Cells were trypsinised and resuspended as described above, and then centrifuged at 1000rpm for 5 minutes at room temperature (RT). Pelleted cells were then resuspended in freezing media (Complete growth media minus selective antibiotics + 10% FBS + 10% DMSO). Four 1mL freezing vials were obtained per 80 - 90% confluent 15cm² tissue culture dish. Vials were initially frozen at -80°C using a Mr Frosty Freezing Container, as per manufacturer's instructions, and then transferred to liquid nitrogen for long term storage.

2.2.4.2 Primary cell lines

Primary breast fibroblasts derived from human breast tumour or surrounding tissue were kindly gifted by the Reynolds Lab (Institute of Cancer Research, London, UK). Cells were cultured in DMEM/F12 media supplemented with 10% FBS, 200µM L-Glutamine, 100U/mL penicillin streptomycin and 0.25µg/mL fungizone. Cells were passaged and cryopreserved as described for immortalised cell lines for a maximum of 2 passages (2.2.4.1).

Primary mouse embryonic fibroblasts (MEFs) were isolated from E13 - E15 littermatched WT or 2+tRNA_i^{Met} embryos. After sterile dissection from the yolk sac and removal of the foetal liver and head, the embryo was disaggregated by forceful pipetting, cells pelleted by centrifugation, and resuspended in DMEM supplemented with 10% FBS, 200µM L-Glutamine, 100U/mL penicillin streptomycin, 0.25µg/mL fungizone and 50µM β-mercaptoethanol. Cells were plated on 0.1% gelatin coated dishes and incubated at 37°C/5%CO₂ until 80% confluent. Cells were passaged once as described for immortalised cells at a 1:3 splitting ratio (2.2.4.1), with 1 plate being used for cryopreservation and the remaining cells used as described in the results chapters.

2.2.4.3 Transient transfection

iMEFs were transiently transfected with a GADD34 containing construct (kindly gifted from the Willis lab, MRC toxicology unit, Leicester, UK) in a 6 well plate using 2.5µg construct and TransIT-LT1 reagent as per manufacturer's

instructions, with one exception. Cells were plated at 1×10^5 cells per well and left to adhere for 4 hours prior to transfection, as opposed to an overnight incubation.

2.2.4.4 siRNA transfection

iMEFs were transfected with 5nM integrin α_5 siRNA, 10nM collagen II siRNA, or corresponding concentration of non-targeting (NT) siRNA, using the Amaxa Nucleofector system with solution R and programme T-20 exactly as per manufacturer's instructions. One nucleofection reaction was conducted per 80 - 90% confluent 15cm^2 dish, with each reaction being replated into a new 10cm^2 dish. Cells were then used experimentally as described in the results chapters.

2.2.4.5 Drug treatments

iMEF cells were plated at 1×10^5 cells per well in a 6 well tissue culture plate and incubated at $37^\circ\text{C}/5\%\text{CO}_2$ for 2 hours to adhere. Cells were then treated with $75\mu\text{M}$ salubrinal, or 0.35% DMSO as control. For migration experiments, cells were incubated at $37^\circ\text{C}/5\%\text{CO}_2$ in the presence of drug or control for 2 further hours prior to 17 hours of timelapse microscopy. In the case of western blot, cells were incubated at $37^\circ\text{C}/5\%\text{CO}_2$ overnight prior to lysis.

2.2.5 Cell proliferation assay

iMEFs were plated at 1×10^5 cells per well in a 6 well tissue culture plate and incubated at $37^\circ\text{C}/5\%\text{CO}_2$. Media was refreshed every other day and total cell number was counted every day for 4 days, at which time the cells had reached 90% confluence. To count cell number, cells were trypsinised and resuspended in growth media as described in 2.2.4.1 and then total cell number measured using a Casy Cell Counter (Innovatis), as per manufacturer's instructions

2.2.6 Flow cytometry

iMEF cells were trypsinised and resuspended as described in 2.2.4.1, counted using a Casy Cell Counter and 1×10^6 cells centrifuged at 1000rpm for 5 minutes at RT. Pelleted cells were resuspended in FACS buffer, transferred to FACS tubes and placed on ice until analysis by flow cytometry using FACSCalibur (BD

Biosciences) and FlowJo Single Cell Analysis Software as per manufacturer's instructions.

2.2.7 Cell metabolism assay

An XF Cell Mitochondrial Stress Test was conducted using the XFp Extracellular Flux Analyser as per manufacturer's instructions. Briefly, cells were plated at 5000, 10,000 and 20,000 cells per well in a 96 well plate, and incubated at 37°C/5%CO₂ overnight. Assay medium was made by supplementing XF base medium with 1nM pyruvate, 2mM glutamine and 25mM glucose, and adjusting the media to pH7.4. Oligomycin and FCCP were prepared at 100µM and Rotenone/Antimycin A at 50µM, all three drugs were prepared in assay media, and then loaded into the supplied cartridge ports. The cell culture media was removed from cells, and the cells washed twice with PBS. Assay media was then added and the cells incubated at 37°C (No CO₂) for 30 minutes prior to running the XF Cell Mitochondrial Stress Test in the XF Extracellular Flux Analyser (Seahorse Bioscience) as per manufacturer's instructions.

2.2.8 RNA extraction

Cells at 80 - 90% confluence were washed twice with PBS, scraped into Trizol (1mL per 10cm² tissue culture dish), snap frozen on dry ice and stored at -80°C until use. Prior to use, samples were thawed and incubated at RT for 5 minutes to allow dissociation of nucleoprotein complexes. 200µL chloroform was added per 1mL Trizol used, samples were vortexed for 15 seconds, and centrifuged at 13,000rpm for 15 minutes at 4°C. The upper aqueous layer was then transferred to a fresh tube and an equal volume of isopropanol added. The tubes were then vortexed for 10 seconds and incubated at RT for 10 minutes. The samples were then centrifuged at 13,000rpm for 10 minutes at 4°C. The RNA pellet was then washed by adding 1mL 75% ethanol and centrifuging the samples at 13,000rpm for 5 minutes at 4°C. The supernatant was removed, and the pellet left to air dry for 15 minutes. The pellet was then resuspended in 20µL RNase-free water, pre-warmed to 50°C, and samples incubated at 50°C for 15 minutes. After brief vortexing, samples were incubated at 50°C for a further 5 minutes, and then transferred to ice. The RNA concentration was determined by measurement of

the $A_{260}:A_{280}$ ratio using a NanoDrop spectrophotometer (Thermo Scientific), and the RNA stored at -80°C .

2.2.9 RNA-Sequencing

For the RNA-Sequencing (RNA-Seq) of iMEF.Vector and iMEF.tRNA_i^{Met} cells, 1×10^6 cells were plated in 10cm^2 tissue culture dishes and incubated at $37^{\circ}\text{C}/5\%\text{CO}_2$ for 48 hours. For the RNA-Seq of iMEF.Vector cells treated with iMEF.Vector and iMEF.tRNA_i^{Met} conditioned media, 1×10^6 iMEF.Vector cells were plated in 10cm^2 tissue culture dishes and incubated at $37^{\circ}\text{C}/5\%\text{CO}_2$ for 2 hours to adhere. Media was then removed and replaced with conditioned media from iMEF.Vector and iMEF.tRNA_i^{Met} cells. The conditioned media was prepared by filtration through a $0.45\mu\text{m}$ filter and 1:1 dilution with full growth media before being added to the iMEF.Vector cells. The iMEF.Vector cells were incubated with the conditioned media for 48 hours at $37^{\circ}\text{C}/5\%\text{CO}_2$.

2.2.9.1 Sample preparation

RNA was extracted from the above cells as described in 2.2.8. Samples were then ribodepleted using the RiboZero Magnetic Kit as per manufacturer's instructions. Briefly, the magnetic beads of the RiboZero kit were washed with RNase-free water and resuspended in Resuspension Solution with RiboGuard RNase Inhibitor. $4\mu\text{g}$ RNA was added to the Ribo-Zero rRNA Reaction Buffer and Removal Solution and incubated at 68°C for 10 minutes, followed by RT incubation for 5 minutes. The probe-hybridised RNA samples were then added to the washed magnetic beads, vortexed for 10 seconds, and incubated at RT for 5 minutes. Tubes were incubated at 50°C for 5 minutes and then transferred to a magnetic stand. The supernatant, containing the RNA sample depleted of rRNA, was transferred to a new RNase-free microcentrifuge tube and the RNA purified using the following modified protocol of the RNeasy MinElute Cleanup Kit. The RNA sample volume was adjusted to $100\mu\text{L}$ with RNase-free water and $350\mu\text{L}$ Buffer RLT added. Following mixing, $550\mu\text{L}$ 100% ethanol was added and the samples mixed gently by pipetting. The samples were transferred to an RNeasy MinElute spin column and centrifuged at $10,000\text{rpm}$ for 15 seconds. The flow through was discarded and the process repeated. The spin column was then transferred to a new collection tube, $500\mu\text{L}$ Buffer RPE was added to the spin

column followed by centrifugation at 10,000rpm for 15 seconds, to wash the column membrane. The flow through was discarded and 500µL 80% ethanol added to the spin column and the samples centrifuged at 10,000 rpm for 2 minutes. The spin column was then transferred to a new collection tube, with the lid of the spin column open, and centrifuged at 13,000 rpm for 5 minutes. The spin column was then placed in a new RNase-free microcentrifuge tube and 12µL RNase-free water added directly to the spin column. Samples were centrifuged at 13,000rpm for 1 minute to elute the RNA. The removal of ribosomal RNA was determined by showing the lack of 18S and 28S rRNA peaks on the RNA quality trace using the RNA 6000 Pico Kit and Bioanalyzer (Agilent Technologies) exactly as per manufacturer's instructions.

2.2.9.2 Sequencing and data analysis

RNA-Seq was performed by Billy Clark, Molecular Technology Service, CR-UK Beatson Institute, Glasgow. Briefly, an Illumina TruSeq RNA Sample Prep Kit was used to prepare the samples, and sequencing was performed on the NextSeq500 platform using a High Output 75 cycle kit. Data was analysed by Ann Hedley, Bioinformatics, CR-UK Beatson Institute, Glasgow.

2.2.10 cDNA synthesis

cDNA was prepared using a Quantitech Reverse Transcription Kit as per manufacturer's instructions. In cases where the cDNA was being used to assess the expression of tRNAs, cDNA was prepared using 5, 10 and 20ng of RNA as template, to ensure the reaction was quantitative. In cases where the cDNA was being used to assess the expression of Pol II transcribed genes, 1µg of RNA was used as template. In each case, 2µL genomic DNA wipeout buffer was added to the RNA in a total volume of 14µL, samples were incubated at 42°C for 2 minutes and then transferred to ice. A reverse transcription mix of 1µL Quantiscript reverse transcriptase + 4µL Quantiscript RT buffer + 1µL RT primer mix was then added to each sample, followed by incubation for 15 minutes at 42°C and then 3 minutes at 95°C to inactivate the reverse transcriptase. Controls containing no reverse transcriptase were included to ensure there was no genomic DNA contamination. cDNA was stored at -20°C.

2.2.11 qRT-PCR

Gene expression analysis (qRT-PCR) was conducted using SyBr green and the BioRad CFX platform in a 96 well plate set-up. A total reaction volume of 10 μ L per well was used, containing a 1:20 dilution of cDNA template + 1x PerfeCTa SYBR Green Fast Mix + 0.5 μ M forward primer + 0.5 μ M reverse primer (primer details provided in 2.1.4). Samples were plated in duplicate. In order to calculate reaction efficiency and enable quantification, standard curves were generated using serially diluted cDNA from combined samples. A no template control was also included to test for primer dimer formation. Reactions were conducted using a 3 step protocol, corresponding to 95 $^{\circ}$ C for 3 mins, followed by 40 cycles of 95 $^{\circ}$ C for 20 seconds, 60 $^{\circ}$ C for 20 seconds and 72 $^{\circ}$ C for 20 seconds, with a final extension step of 72 $^{\circ}$ C for 5 minutes and a melt curve from 65 $^{\circ}$ C to 95 $^{\circ}$ C in 0.5 $^{\circ}$ C increments. Data was collected and analysed in CFX Manager Software (BioRad).

2.2.12 Western blotting

After cells had reached 80 - 90% confluence, media was aspirated, the cells were placed on ice and washed in ice-cold PBS. Cells were lysed into either 1% SDS buffer or NDLB supplemented with protease inhibitors (50 μ g/mL leupeptin + 50 μ g/mL aprotinin + 1mM AEBSF), as specified in the figure legends. For cell lysis, 150 μ L buffer was added per 10cm² dish, the cells were scraped from the dish using a cell lifter, transferred into a 1.5mL microcentrifuge tube, passed through a 25G needle 5 times and centrifuged at 13,000rpm for 10 minutes, 4 $^{\circ}$ C. The supernatant was removed and used immediately or stored at -20 $^{\circ}$ C (in cases where phospho-proteins were being detected samples were always used immediately).

SDS-PAGE electrophoresis was used to resolve protein samples. Samples were reduced in 1x NuPAGE sample buffer + 0.1M DTT at 95 $^{\circ}$ C for 5 minutes and then loaded onto 4-12% or 10% pre-cast Novex Bis-Tris gels with MES or MOPs running buffer. The gel type and buffer used was dependent on the protein size and separation needed. Electrophoresis was performed at 120V until required separation was reached, as determined by visual separation of the full-range rainbow ladder.

The proteins were transferred from the gel to PVDF membrane by wet transfer using the NuPage transfer system and NuPage transfer buffer, at 40V for 2 hours. The membrane was blocked in 4% milk, or 4% BSA for phospho-antibodies, with gentle rocking at RT for 1 hour. The membrane was then incubated with the appropriate primary antibody diluted in 1% milk or 1% BSA (dependent on blocking solution used), at 4°C overnight with gentle shaking. The membrane was then washed three times with TBS-T, with gentle rocking for 10 minutes per wash. Following this, the membrane was incubated with the appropriate secondary antibody for 1 hour at RT with gentle shaking. The membranes were then washed three times for 10 minutes with TBS-T, and the blots then developed. In the case of integrin α_5 detection, the secondary antibody was HRP conjugated and the membranes were incubated in ECL solution for 3 minutes followed by transfer to a film cassette and detection by autoradiography using x-ray film and a Kodak X-Omat 488 x-ray processor. For the phospho-eIF2 α blots, IRDye secondary antibodies and the LI-COR Aeries infrared imaging system was used for visualisation.

2.2.13 Immunoprecipitation

Magnetic dynabeads were coupled with the primary antibody of interest by one wash in PBS + 0.1% BSA, followed by incubation with antibody diluted in ice-cold PBS + 0.1% BSA. 1.5 μ g of antibody was used for each lysate undergoing immunoprecipitation. The dynabeads and antibody were then mixed for 1 hour at 4°C on a rotating wheel. Cells at 80-90% confluency were surface labelled with Sulfo-NHS-SS-Biotin, by aspirating their media, placing them on ice, washing them twice with ice-cold PBS, adding 0.13mg/mL Sulfo-NHS-SS-Biotin and rocking the cells gently for 1 hour at 4°C. Cells were then placed back on ice, washed twice with ice-cold PBS, PBS removed, and cells scraped into NDLB supplemented with protease inhibitors (50 μ g/mL leupeptin + 50 μ g/mL aprotinin + 1mM AEBSF) using 100 μ L buffer per 10cm² plate. The lysate was passed through a 25G needle 5 times, centrifuged at 13,000rpm for 10 minutes at 4°C, the supernatant removed and protein concentration determined using a Qubit Protein Assay and Qubit Fluorometer exactly as per manufacturer's instructions (Life Technologies). The antibody-incubated dynabeads were then washed once in PBS and incubated with 500 μ g of each protein lysate. The dynabeads and lysates were mixed for 2 hours at 4°C on a rotating wheel. The bead slurry was

then washed four times in NDLB and the beads resuspended in 1x non-reducing NuPAGE loading buffer. The proteins were removed from the beads by incubating at 95°C for 10 minutes, resolved by SDS-PAGE electrophoresis, and visualised by western blot with streptavidin-conjugated HRP detection, as described in 2.2.12.

2.2.14 Capture-ELISA

Maxisorp 96 well microtiter plates were incubated with 50µL/well of primary antibody, diluted in ELISA coating buffer, overnight at 4°C with gentle shaking. Plates were washed once with PBS-T and blocked in 0.1% PBS-T + 5% BSA for 1 hour at RT with gentle shaking. Cells at 80-90% confluency were surface labelled with Sulfo-NHS-SS-Biotin, by aspirating their media, placing them on ice, washing them twice with ice-cold PBS, adding 0.13mg/mL Sulfo-NHS-SS-Biotin and rocking the cells gently for 1 hour at 4°C. Cells were then placed back on ice, washed twice with ice-cold PBS, PBS removed, and the cells scraped into NDLB supplemented with protease inhibitors (50µg/mL leupeptin + 50µg/mL aprotinin + 1mM AEBSF) using 100µL buffer per 10cm² plate. The lysate was passed through a 25G needle 5 times, centrifuged at 13,000rpm for 10 minutes at 4°C the supernatant removed and serial dilutions of the protein lysate made in NDLB. The BSA blocking solution was removed from the plate, the plate was washed twice with PBS-T, and incubated with the protein lysate overnight at 4°C with gentle shaking. Unbound protein was removed by washing three times in PBS-T and streptavidin-conjugated HRP was added (1:1000 dilution in PBS-T 0.1% BSA) for 1 hour at 4°C with gently shaking. Plates were extensively washed, three times with PBS-T and three times with PBS. ELISA development reagent was added and the plate incubated at room temperature for approximately 15 minutes. The reaction was then stopped with 8M H₂SO₄ and the absorbance read at 490nm on a plate reader (Tecan).

2.2.15 Internalisation assays

1x10⁶ cells per 10cm² dish were incubated at 37°C/5%CO₂ for 48 hours. Maxisorp 96 well microtiter plates were incubated with 50µL/well of primary antibody diluted in ELISA coating buffer overnight at 4°C with gentle shaking. Cells were surface labelled with Sulfo-NHS-SS-Biotin by aspirating their media, placing them

on ice, washing them twice with ice-cold PBS, adding 0.13mg/mL Sulfo-NHS-SS-Biotin and rocking the cells gently for 45 minutes at 4°C. Cells were washed twice with ice-cold PBS to remove excess biotin. At this point, plates of cells required for total protein measurement were kept on ice until cell lysis, whilst plates of cells required for the blank measurement were kept on ice until MesNa treatment. The remaining plates were used to measure internalisation of surface proteins. Cells were incubated with pre-warmed growth media at 37°C for the described time, followed by media aspiration plates were incubated on ice as cells were washed once with ice-cold PBS and once with biotin reduction buffer. To remove cell surface biotin, cells were incubated with 20mM MesNa in biotin reduction buffer for 1 hour at 4°C with gentle rocking. The reaction was quenched by adding 20mM IAA and incubating the cells at 4°C with gentle rocking for 10 minutes. The cells were then lysed as described in 2.2.14 and the levels of internalised biotinylated proteins determined by capture-ELISA as described in 2.2.14.

2.2.16 Recycling assays

The internalisation assay described in 2.2.15 was repeated with the following modifications to enable measurement of the amount of internalised biotinylated surface protein recycled to the cell surface. Following the removal of cell surface biotin by MesNa treatment, cells were incubated on ice and washed twice with ice-cold PBS. Pre-warmed growth media was then added to the cells and plates incubated at 37°C for the described recycling time. Media was then aspirated, and plates returned to ice, the cell surface biotin reduction step was repeated and the protocol continues as described in 2.2.15.

2.2.17 Immunofluorescence

Glass bottomed 3cm² dishes were coated with 1µg/mL fibronectin at 37°C/5%CO₂ for 4 hours, washed once with PBS, and 7.5x10⁴ cells were seeded into the dishes in full growth media and incubated overnight at 37°C/5%CO₂. Media was removed, and cells fixed with 4% PFA at RT for 15 minutes. Cells were permeabilised in PBS + 0.2% Triton-X100 at RT for 5 minutes, washed twice with PBS, and blocked in PBS + 1% BSA for 1 hour at RT. Following one PBS wash, primary antibody was added in blocking solution for 1 hour at RT. Following

three PBS washes, secondary antibody was added in blocking solution for 1 hour at RT. After two PBS washes, the cells were incubated with phalloidin stain, 1:200 dilution in PBS, for 10 minutes at RT, then washed twice with PBS and mounted using Vectashield + DAPI. Cells were visualised by confocal microscopy using an Olympus FV-1000 microscope.

2.2.18 Metabolic labelling

Cells were grown to 80 - 90% confluence, washed twice with PBS and incubated for 30 minutes at 37°C/5% CO₂ with DMEM minus methionine and cysteine, but supplemented with 10% dialysed FBS and 200µM L-Glutamine. Cells were trypsinised as described in 2.2.4.1, resuspended in the media described above supplemented with 0.07mCi EasyTag Express Protein Labelling Max ³⁵S, and then incubated for 2 hours at 37°C/5% CO₂. Cells were washed with, and scraped into, ice-cold PBS. 25µL of cell suspension was aliquoted for total label measurement, and 25µL of cell suspension was then added to BSA/NaN₃ (1mg/mL BSA in 0.02% sodium azide) and precipitated by adding ice-cold 10% TCA solution, vortexing and then incubating the samples on ice for 30 minutes. The precipitated material was filtered onto Whatman GF/C 2.5cm filter paper, and the filters washed twice in ice-cold 10% TCA, twice in ice-cold 100% ethanol, and air dried for 30 minutes. The total count cell suspension was also spotted onto filter paper and dried. Scintillation fluid was added and filters analysed using a Microbeta Trilux scintillation counter (PerkinElmer).

2.2.19 SILAC based mass spectrometry

iMEF.Vector and iMEF.tRNA_i^{Met} cells were labelled with light (Arg0/Lys0) and heavy amino acids (Arg10/Lys8). Briefly, cells were passaged (as described in 2.2.4.1) in SILAC DMEM containing light or heavy amino acids supplemented with 10% FBS for 3 passages, and then transferred to media containing light or heavy amino acids supplemented with 10% dialysed FBS for 3 passages. Following full SILAC amino acid incorporation (as tested by David Sumpton, Proteomics, CR-UK Beatson Institute, Glasgow), cells were used in SILAC based mass spectrometry to assess quantitative changes in the secretome and cellular proteome.

2.2.19.1 Secretome

1×10^6 cells were plated into a 10cm^2 dish and cultured for 48 hours at $37^\circ \text{C}/5\% \text{CO}_2$, washed twice in PBS and transferred into serum-free media for 6 hours at $37^\circ \text{C}/5\% \text{CO}_2$. Media was then collected and combined. In the case of the forward experiment iMEF.Vector cells labelled with light amino acids were combined with iMEF.tRNA_i^{Met} cells labelled with heavy amino acids, and in the reverse experiment iMEF.Vector cells labelled with heavy amino acids were combined with iMEF.tRNA_i^{Met} cells labelled with light amino acids. Media was centrifuged at 300g for 10 minutes at 4°C , supernatant was collected and centrifuged at 2000g for 10 minutes at 4°C , the supernatant was collected again and centrifuged at 10,000g for 30 minutes at 4°C . The collected media was then acidified to pH5 with 10% TFA and 10uL strataclean beads added per 1mL media. The media/bead slurry was then vortexed for 1 minute and incubated overnight on a rotor wheel at 4°C . Beads were collected by brief centrifugation and resuspended in NuPAGE loading buffer + 0.1M DTT, and boiled for 5 minutes at 95°C . The supernatant was then loaded onto a 10% NuPAGE Bis-Tris gel and proteins separated by electrophoresis. The gel was coomassie stained and proteins analysed by quantitative mass spectrometry. Mass spectrometry was conducted by David Sumpton, Proteomics, CR-UK Beatson Institute, Glasgow. In short, gel slices were excised and destained before digestion. Proteins were reduced in 10mM DTT and alkylated with 50mM IAA, washed with 50% ACN/50mM ABC, dried in speedvac and digested with $0.05 \mu\text{g}/\text{mL}$ trypsin in 50mM ABC overnight. Extracted digests were stage tipped and analysed on Orbitrap Elite. Data was searched and quantified against swissprot MOUSE using MaxQuant.

2.2.19.2 Cellular proteome

1×10^6 of each of the SILAC labelled cell lines described above were plated into 10cm^2 dishes and cultured for 48 hours at $37^\circ \text{C}/5\% \text{CO}_2$. Cells were then washed twice in PBS and lysed into 4% SDS lysis buffer. Samples were sonicated and centrifuged at 13,000rpm for 5 minutes at RT. Protein supernatant was collected and the concentration measured using Qubit fluorometric quantitation (Life Technologies). Protein samples were then subjected to quantitative mass spectrometry by David Sumpton, Proteomics, CR-UK Beatson Institute, Glasgow. Briefly, lysates from heavy and light SILAC labelled cells were mixed 1:1. In the

case of the forward experiment iMEF.Vector cells labelled with light amino acids were combined with iMEF.tRNA_i^{Met} cells labelled with heavy amino acids, and in the reverse experiment iMEF.Vector cells labelled with heavy amino acids were combined with iMEF.tRNA_i^{Met} cells labelled with light amino acids. A total of 500µg of protein per experiment was reduced, alkylated and digested using the small FASP method. The digests were separated on a high pH reverse phase column and 22 fractions were collected. Each fraction was dried down, re-dissolved in 5% acetonitrile/0.25% formic acid and analysed on Orbitrap Velos (LC-MS). Data was searched and Quantified against swissprot MOUSE using MaxQuant.

2.2.20 ECM generation

2.2.20.1 ECM derived from control and tRNA_i^{Met} overexpressing cells

Cell derived matrix was generated from primary MEFs and iMEFs. For timelapse microscopy and immunostaining experiments ECM was derived in 6-well tissue culture plastic plates, and for AFM measurements ECM was generated in glass bottom 3cm² dishes. In each case, plates/dishes were coated in 0.2% gelatin and incubated at 37°C/5% CO₂ for 1 hour. Following two PBS washes, they were then cross-linked with 1% glutaraldehyde at RT for 30 minutes. After two PBS washes, plates were quenched in 1M glycine at RT for 20 minutes, washed twice with PBS, and incubated in full growth media at 37°C/5%CO₂ for 30 minutes. 2x10⁵ cells per well were seeded and cells incubated at 37°C/5%CO₂ overnight (or until cells fully confluent). Once cells reached confluence, the media was changed to full growth media containing 50µg/mL ascorbic acid, and the ascorbate containing media refreshed every other day for seven days. Media was then aspirated, cells washed once with PBS containing calcium and magnesium (D-PBS), and then incubated with extraction buffer for 2 minutes at RT. Following two D-PBS washes, residual DNA was digested with 10µg/mL DNase I in D-PBS at 37°C/5%CO₂ for 30 minutes. Following two D-PBS washes, cell derived matrices were stored at 4°C in D-PBS containing 100U/mL penicillin streptomycin and 0.25µg/mL fungizone. Prior to use, cell derived matrices were washed twice with D-PBS and incubated in full growth media for 30 minutes at 37°C/5%CO₂.

2.2.20.2 ECM derived from conditioned media treated cells

In cases where conditioned media from control or tRNA_i^{Met} overexpressing cells was used to generate the ECM, the above protocol was used on iMEF.Vector cells, but the media used to refresh the cells upon confluence, and every other day thereafter, was conditioned media. The conditioned media was obtained from 1x10⁶ cells per 10cm² dish that were plated for 48hrs, filtered through a 0.45µm filter, diluted 1:1 with fresh growth media and supplemented with 50µg/mL ascorbic acid. In each case, the cells providing the conditioned media were also cultured in the presence of 50µg/mL ascorbic acid for 48 hours.

2.2.20.3 ECM derived from microvesicle free conditioned media

In cases where microvesicle depleted conditioned media was used to generate ECM, cell derived matrices were made as described in 2.2.20.2, however the conditioned media used was depleted of microvesicles by sequential centrifugation as follows: conditioned media collected and centrifuged at 300g for 10 minutes at 4°C, supernatant collected and centrifuged at 2000g for 10 minutes at 4°C, supernatant collected and centrifuged at 10,000g for 30 minutes at 4°C, supernatant collected and centrifuged at 100,000g for 70 minutes at 4°C. The supernatant collected from the final centrifugation step corresponded to microvesicle free conditioned media.

2.2.20.4 ECM derived from conditioned media from siRNA treated cells

In cases where conditioned media collected from siRNA treated cells was used to generate ECM, cell derived matrices were made as described in 2.2.20.2, however the conditioned media was collected from cells 48 hours post-nucleofection with siRNA as described in 2.2.4.4, with 50µg/mL ascorbic acid included in the post-transfection growth media.

2.2.21 Immunostaining

ECM was generated as described in 2.2.20 and washed twice with D-PBS. Matrices were then fixed with 4% PFA for 15 minutes at RT and then washed five times in PBS + 0.1% Tween-20 for 5 minutes at RT with gentle shaking. The ECM was blocked with Odyssey blocking buffer for 90 minutes at RT with gentle

shaking, and then incubated overnight with primary antibody diluted in blocking buffer at 4°C with gentle shaking. The matrices were then washed five times in PBS + 0.1% Tween-20 for 5 minutes at RT with gentle shaking, and incubated with a fluorescently labelled secondary antibody, 1:10,000 dilution in blocking buffer for 1 hour at RT with gentle shaking and protected from light. The ECM was washed five times in PBS + 0.1% Tween-20 for 5 minutes at RT with gentle shaking. The final wash was aspirated and fluorescence quantified using the Aeries infrared imaging system (LI-COR).

2.2.22 Atomic force microscopy

ECM was generated as described in 2.2.20, and atomic force microscopy (AFM) conducted by Ellie Pulleine, School of Engineering, University of Glasgow. Briefly, to measure the thickness of ECMs following a wound scratch, AFM force spectroscopy and contact imaging were performed using a JPK NanoWizard II Bio AFM in combination with a Bruker MLCT cantilever. A Nanoworld Arrow TL-1 cantilever with bead attached was used for force spectroscopy.

2.2.23 Migration assays

2.2.23.1 Directional migration

2×10^5 cells were plated in 6 well tissue culture plates and incubated at 37°C/5%CO₂ until they reached confluence. A vertical wound was then scratched down the centre of each well using a 200µL pipette tip. Cells were washed twice with full growth media, and incubated with 4mL media per well. Cell migration was visualised by timelapse microscopy (Nikon microscope), images were taken at 10 minute intervals for 17 hours, at 4 different positions per well. Single cell tracking was used to quantify the speed of cell migration using the manual tracking plugin of Image J.

2.2.23.2 Random migration

Cells were plated at a density of 1×10^5 cells per well in 6 well tissue culture plates and incubated at 37°C/5%CO₂ for a minimum of 2 hours to adhere. Cell migration was visualised by timelapse microscopy (Nikon microscope), images were taken at 10 minute intervals for 17 hours, at a minimum of 4 different

positions per well. Single cell tracking was used to quantify the speed of cell migration using the manual tracking plugin of Image J.

2.2.24 Breast cancer tissue microarray & immunohistochemistry

The breast cancer TMA was produced by Clare Orange (TMA and Image Analysis Unit Manager, University Department of Pathology, Southern General Hospital), from a cohort of 544 breast cancer patients presenting with invasive breast cancer in the West of Scotland between 1995 and 1998. Full clinico-pathological analysis and 10 year follow-up data was available for the TMA. The slides were stained for collagen II by Colin Nixon and the histology service, CR-UK Beatson Institute, Glasgow. Briefly, slides were dewaxed in xylene and passed through ethanol for rehydration (2 × 100% ethanol and 1 × 70% ethanol). Heat-induced epitope retrieval was conducted in pH6 sodium citrate retrieval buffer. Endogenous peroxidases were blocked, and a collagen II specific antibody was applied at a 1:300 dilution for 35 minutes at RT. Slides were then incubated with Mouse EnVision for 30 minutes, and the staining was visualized with DAB and counterstained with Haematoxylin. Slides were scanned at 20x magnification using NanoZoomer NDP scanner (Hamamatsu) and were then stored on a dedicated server and available for viewing using Slidepath Digital Image Hub.

Collagen II expression was scored as low, medium or high depending on the predominant intensity of stromal staining. 10% of the TMA was double scored by Iain MacPherson, CR-UK Beatson Institute, Glasgow. Kaplan Meier survival analysis was performed to estimate differences in disease-free survival according to collagen II expression levels. Statistical analysis was performed using SPSS statistical package (version 19 for Windows), with assistance from Joanne Edwards, University of Glasgow, and Liane McGlynn and Iain MacPherson, CR-UK Beatson Institute, Glasgow.

2.2.25 Statistics

Statistical analysis was performed on all relevant experiments. To compare two data-sets unpaired t-tests were performed if the data was normally distributed, or a Mann-Whitney test if the data was not normally distributed. To compare

more than two data sets, ANOVA tests were used if the data was normally distributed, and a Kruskal-Wallis test if the data was not normally distributed. In the case of survival data a Log-rank Mantel-Cox test was used. Statistical significance is annotated within the figures and the associated p-values are indicated in each figure legend, with $p < 0.05$ considered as significant.

Chapter 3 The influence of tRNA_i^{Met} levels on fibroblast behaviour

3.1 Introduction

Fibroblasts play a key role in the progression of malignant disease, and understanding how CAFs differ from their normal counterparts could provide new opportunities to target the tumour stroma and develop cancer therapies. Compared to normal fibroblasts (NFs), CAFs have a higher capacity for cell proliferation, migration and invasion, and a number of studies have used gene expression analysis to investigate the mechanisms behind these functional differences (Finak et al., 2008, Singer et al., 2008, Bauer et al., 2010). Increased CAF proliferation can be ascribed to activation of signalling pathways that converge to regulate expression of oncogenes, such as c-Myc (Peng et al., 2013, Tang et al., 2015a). c-Myc has been widely implicated in tumourigenesis through its pathological activation in cancer cells (reviewed recently in (Gabay et al., 2014)), but the impact of c-Myc overexpression on fibroblast behaviour, and how that can influence tumour growth, tends to be overlooked. Indeed, oncogene and tumour suppressor pathways, including c-Myc, directly regulate Pol III transcription and can increase tRNA expression levels (Felton-Edkins et al., 2003). Changes in a cells tRNAome can influence its proliferation or differentiation state and this property can be exploited by cancer cells (Gingold et al., 2014), and so it is possible that altered tRNA expression in stromal cells could also provide a mechanism to enable CAFs to support tumour progression.

We therefore sought to characterise the effects of tRNA_i^{Met} overexpression on fibroblast behaviour, and understand whether any differences that we identified could be ascribed to the canonical or non-canonical functions of tRNAs. The primary role of tRNA_i^{Met} is in the initiation of protein synthesis, where it associates with eIF2·GTP to form the ternary complex (TC). Upon binding to the 40S ribosomal subunit to form the 43S pre-initiation complex, it can then associate with additional initiation factors and scan through the 5' UTR to find the correct start codon and initiate translation (Kapp and Lorsch, 2004). However, numerous non-canonical functions of tRNAs have also been described, raising the possibility that phenotypic effects of tRNA overexpression may not be due to direct influences on the protein synthesis machinery. tRNAs have been

implicated in apoptosis through their ability to associate directly with cytochrome c to inhibit caspase activation (Mei et al., 2010b), and the discovery of functional tRNA derived fragments (tRFs) also provides additional mechanisms by which tRNAs can affect cell function. Processing of tRNAs can generate tRFs, resulting in one of the most abundant categories of small RNAs. Interestingly, these tRFs also have increased expression in a variety of cancer cell lines (Lee et al., 2009a). Moreover, overexpression of tRF-1001, a tRF derived from the 3' end of Ser-TGA pre-tRNA was shown to induce proliferation in prostate cancer cells, while other work has shown that tRNA fragments can modulate the DNA damage response and cell proliferation in lymphoma (Lee et al., 2009a, Maute et al., 2013).

This chapter will therefore characterise the cellular effects of $\text{tRNA}_i^{\text{Met}}$ overexpression, and specifically describe how increased $\text{tRNA}_i^{\text{Met}}$ levels can affect the motile behaviour of fibroblasts, addressing some aspects of the cellular mechanisms through which $\text{tRNA}_i^{\text{Met}}$ may exert these effects.

3.2 Results

3.2.1 Generation of $\text{tRNA}_i^{\text{Met}}$ overexpressing immortalised fibroblast cell lines

To characterise the influence of $\text{tRNA}_i^{\text{Met}}$ expression on fibroblast behaviour we generated pools of immortalised mouse embryonic fibroblasts (iMEFs) which overexpressed $\text{tRNA}_i^{\text{Met}}$ (iMEF. $\text{tRNA}_i^{\text{Met}}$) or an empty vector as control (iMEF.Vector), and used qPCR to quantify the level of $\text{tRNA}_i^{\text{Met}}$ overexpression (Figure 3-1). Two pairs of iMEF pools were used throughout the subsequent experiments, with pools 1 and 2 having approximately 15 and 5-fold increases in $\text{tRNA}_i^{\text{Met}}$ expression respectively, corresponding to the range of increased tRNA expression seen in human breast tumours compared to normal tissue (Pavon-Eternod et al., 2009).

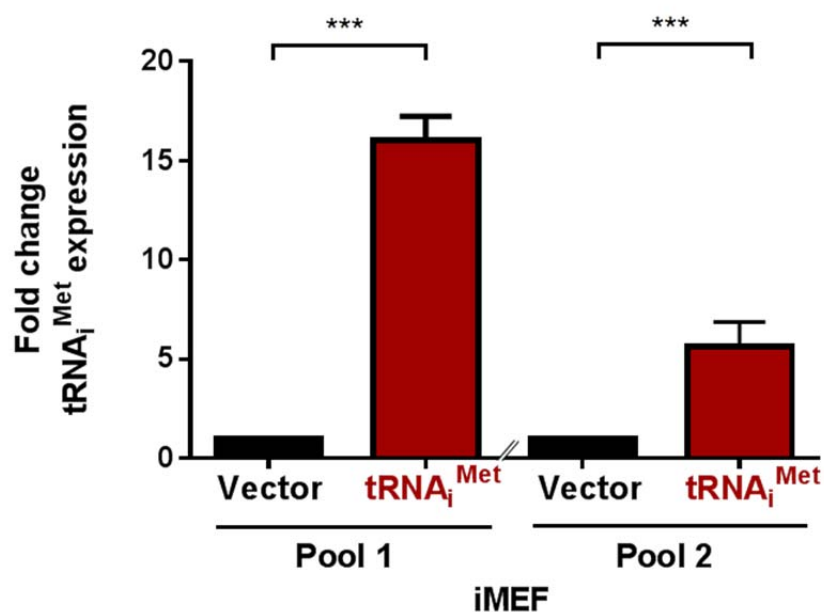


Figure 3-1- Overexpression of $\text{tRNA}_i^{\text{Met}}$ in immortalised mouse embryonic fibroblasts. qPCR of $\text{tRNA}_i^{\text{Met}}$ expression in pools of iMEFs, all samples are normalised to ARPP P0 and are presented relative to iMEF.Vector control, n=3, +/- SEM, unpaired t-test, *** p < 0.0005.

3.2.2 Overexpression of $\text{tRNA}_i^{\text{Met}}$ does not affect cellular protein synthesis

Owing to the essential role of $\text{tRNA}_i^{\text{Met}}$ in initiating translation, we sought to understand how increasing the levels of $\text{tRNA}_i^{\text{Met}}$ might affect the rate of cellular protein synthesis. ^{35}S -methionine incorporation was used to compare the

biosynthesis of proteins between iMEF.tRNA_i^{Met} and iMEF.Vector cells, and showed that increased levels of tRNA_i^{Met} did not significantly change the amount of radiolabel incorporated into newly synthesised TCA-precipitable proteins (Figure 3-2). Increasing the amount of tRNA_i^{Met} available for TC formation is therefore not sufficient to affect the overall rate of cellular protein synthesis in immortalised fibroblast cell lines.

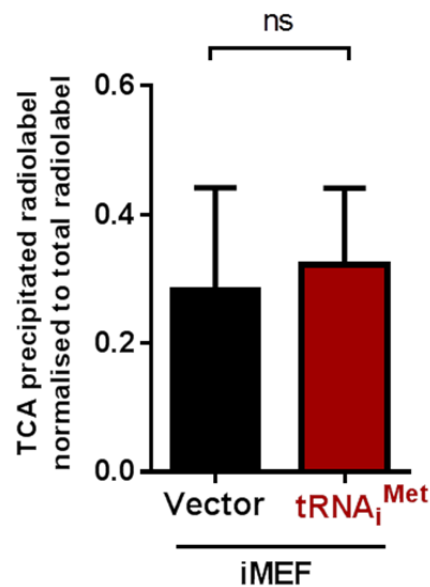


Figure 3-2- tRNA_i^{Met} does not affect the rate of cellular protein synthesis.

³⁵S-methionine incorporation was used to assess changes in the synthesis of new proteins. Cells were depleted of methionine and cysteine for 30 minutes at 37°C/5% CO₂, then trypsinised and resuspended in media containing 0.07mCi EasyTag Express Protein Labelling Max ³⁵S and incubated at 37°C/5% CO₂ for 2 hours. TCA precipitation was used to stop and concentrate the reaction, and the ratio of TCA precipitated radiolabel to total radiolabel calculated, n=5, +/- SEM, unpaired t-test, ns = not significant.

3.2.3 Overexpression of tRNA_i^{Met} does not affect cell proliferation

Previous publications have not only highlighted the ability of CAFs to proliferate faster than NFs (Peng et al., 2013, Tang et al., 2015a), but have also shown that increased levels of tRFs can drive increased cancer cell proliferation (Lee et al., 2009a). Furthermore, others have found that increased levels of tRNA_i^{Met} itself is able to drive an increase in proliferation of human epithelial cells (Pavon-Eternod et al., 2013). We therefore assessed the effects of tRNA_i^{Met} overexpression on the proliferation of iMEFs, and found that overexpression of tRNA_i^{Met} did not affect the rate at which they proliferated (Figure 3-3).

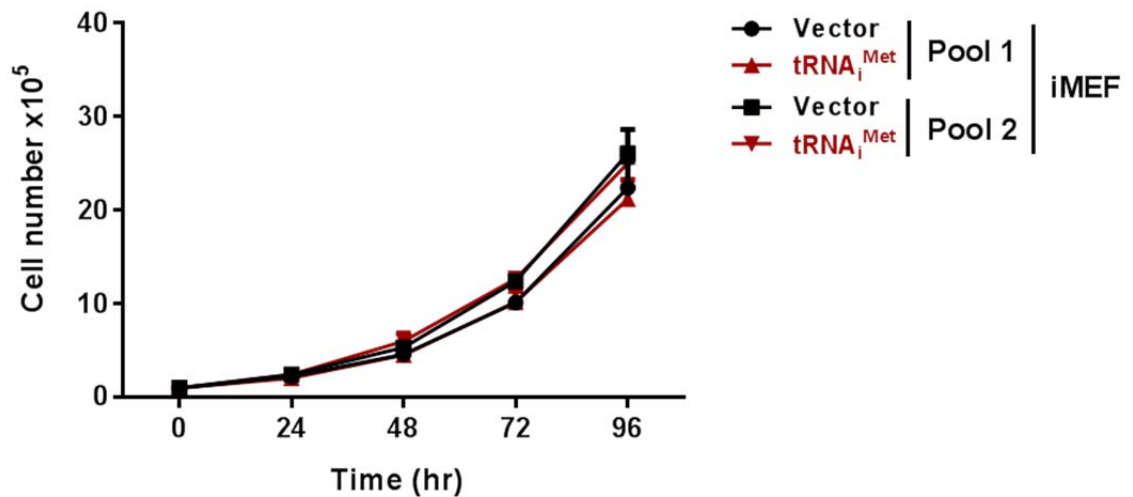


Figure 3-3- tRNA_i^{Met} does not affect the rate of cell proliferation.

1x10⁵ iMEF.Vector and iMEF.tRNA_i^{Met} cells were plated in 6 well tissue culture plates and cell number counted every day for 4 days, corresponding to the cells reaching 80 – 90% confluence, n=3, +/- SEM.

In addition to counting total cell number, we also used FACS analysis to visualise propidium iodide (PI) uptake to ensure that tRNA_i^{Met} overexpression was not affecting cell viability. PI is a membrane impermeant dye that binds double stranded DNA and so is excluded from viable cells. FACS analysis showed that tRNA_i^{Met} overexpression did not affect the viability of iMEFs (Figure 3-4). These FACS-based analyses also indicated that side scatter from iMEF.tRNA_i^{Met} and iMEF.Vector cells was not significantly different, suggesting no difference in ribosome content between the two cell lines and reinforcing the lack of effect on total protein synthesis. This analysis also showed no differences in forward scatter between iMEF.tRNA_i^{Met} and iMEF.Vector cells, indicating that tRNA_i^{Met} levels do not necessarily influence cell size (Figure 3-4). Cell size is intrinsically linked to growth and proliferation, and so these data again reinforce the view that tRNA_i^{Met} levels do not influence these processes.

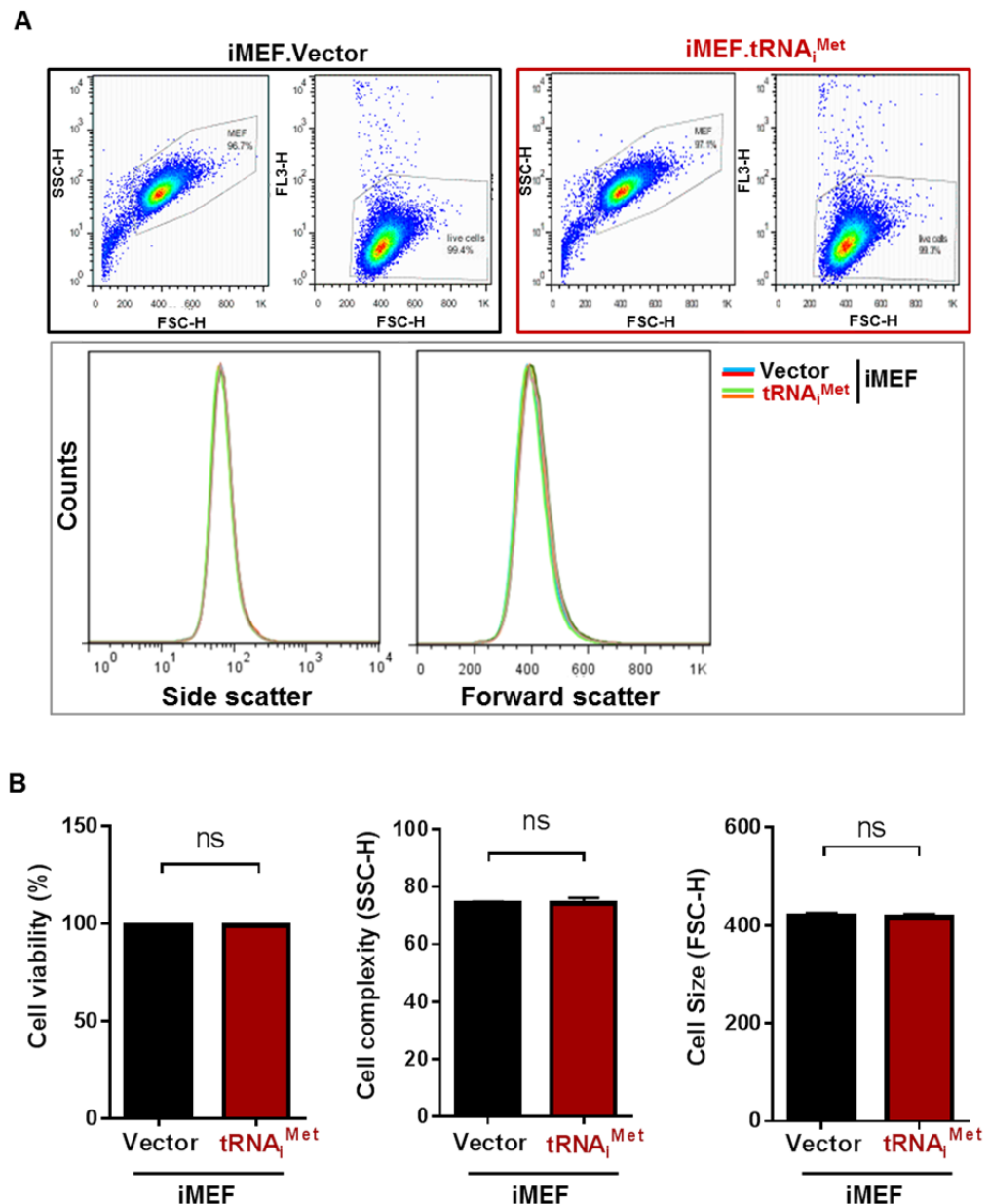


Figure 3-4- tRNA_i^{Met} does not affect cell viability, granularity or size.

(A) Representative FACS plots. Duplicate suspensions of 1×10^6 iMEF.Vector and iMEF.tRNA_i^{Met} pool 1 cells were prepared in FACS buffer (PBS + 1% BSA + 0.5 μ g/mL propidium iodide) and FACS used to assess cell viability via PI uptake, cell granularity by side scatter reading, and cell size by forward scatter reading. (B) Quantification of FACS analysis, $n=3$, \pm SEM, unpaired t-test, ns = not significant.

3.2.4 Overexpression of tRNA_i^{Met} does not affect energy metabolism

Published data have shown that tRNAs are able to regulate apoptosis by binding to cytochrome c and inhibiting caspase activation (Mei et al., 2010b). Cytochrome c, however, is also a component of the mitochondrial electron transport chain, and so plays an important role in generating mitochondrial membrane potential to drive ATP formation. It is therefore possible that tRNAs

may play a role in regulating electron transport and oxidative phosphorylation (Mei et al., 2010a). We used the XFp Extracellular Flux Analyser (Seahorse Bioscience) to determine whether $\text{tRNA}_i^{\text{Met}}$ overexpression had any effect on energy metabolism in iMEFs. An XF Cell Mitochondrial Stress Test was conducted on iMEF.Vector and iMEF. $\text{tRNA}_i^{\text{Met}}$ cells using modulators of respiration to target electron transport chain components to test for differences in metabolic capacity following $\text{tRNA}_i^{\text{Met}}$ overexpression. Oligomycin inhibits the ATP synthase (Complex V) to decrease oxygen consumption rate (OCR), FCCP affects the inner mitochondrial membrane to disrupt the electron gradient and increase the OCR, and Rotenone and Antimycin A target Complex I and III respectively to inhibit electron transport and electron transfer (Figure 3-5A). Sequential addition of these compounds to iMEF.Vector and iMEF. $\text{tRNA}_i^{\text{Met}}$ cells, and measurement of the resulting changes in OCR, showed that across multiple pools of cells there was no significant difference in the levels of basal respiration, ATP production, proton leak, maximal respiration, spare respiration capacity or non-mitochondrial respiration following $\text{tRNA}_i^{\text{Met}}$ overexpression (Figure 3-5B), and so increased levels of this one particular tRNA in fibroblasts did not detectably affect their capacity for energy metabolism.

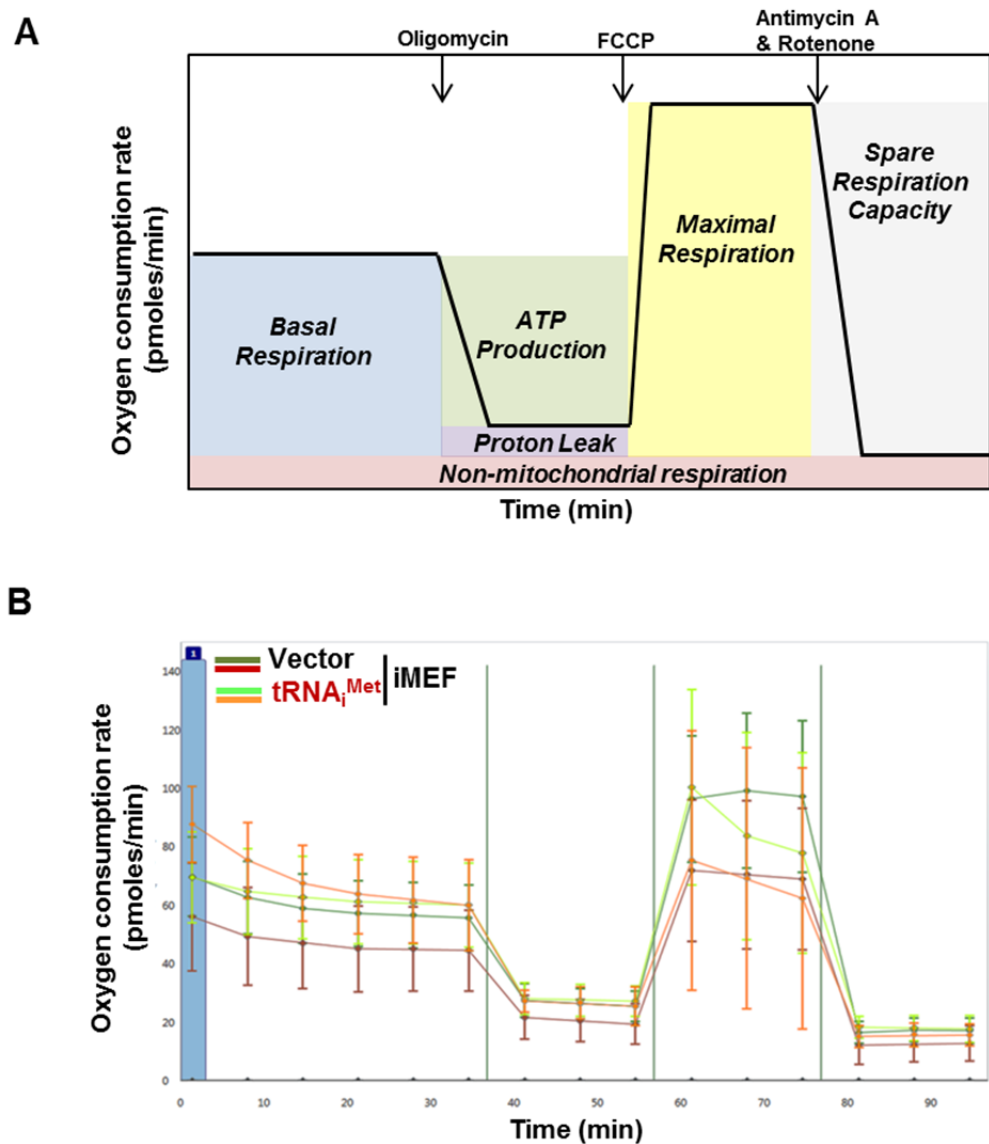


Figure 3-5- tRNA^{Met} does not affect energy metabolism.

(A) A schematic representation of the parameters measured by the XFp Extracellular Flux Analyser (Schematic adapted from www.seahorsebio.com). The XF Cell Mitochondrial Stress Test uses Oligomycin to inhibit ATP synthase, FCCP to disrupt the electron gradient, and Rotenone and Animycin A to inhibit electron transport and electron transfer. The measured oxygen consumption rate then indicates the parameters described in the figure. (B) Graphical representation of the results of the XF Mitochondrial Stress Test in iMEF.Vector and iMEF.tRNA^{Met} pool 1 and 2 cells, no significant difference consistent with tRNA^{Met} overexpression, n=1, +/- standard deviation of technical replicates.

3.2.5 Overexpression of tRNA^{Met} does not affect cell spreading

Secretion and remodelling of ECM proteins by fibroblasts plays a key role in defining the tumour microenvironment. However, the adhesive and migratory properties of fibroblasts also contribute to the establishment of a microenvironment that supports tumour growth. The way in which a cell is able to adhere and spread on a substrate is an important property, and in the case of cancer cells it can reflect their metastatic potential. With respect to stromal

cells, the adherence of fibroblasts can influence their ability to establish a niche to promote tumour growth, and so with this in mind we assessed the ability of the iMEFs to adhere and spread following $\text{tRNA}_i^{\text{Met}}$ overexpression. By measuring the cell area at various times following adherence to plastic, we found that there was no significant difference in the rate of cell spreading, or the final area of fully spread cells, between iMEF.Vector and iMEF. $\text{tRNA}_i^{\text{Met}}$ cells (Figure 3-6) suggesting that $\text{tRNA}_i^{\text{Met}}$ overexpression did not exert any influence on the adhesive properties of fibroblasts.

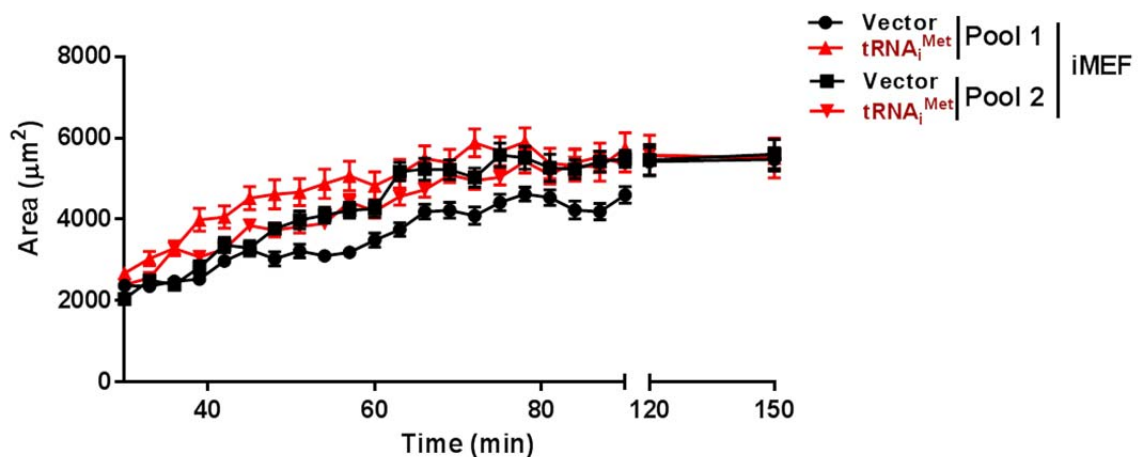


Figure 3-6- $\text{tRNA}_i^{\text{Met}}$ does not affect cell spreading.

1×10^5 iMEF.Vector and iMEF. $\text{tRNA}_i^{\text{Met}}$ cells were plated on plastic and imaged immediately for 2 minute intervals over the course of 2 hours by timelapse microscopy. Area of cell spreading was measured in Image J, data represents area of 40 cells over $n=3$ independent experiments, \pm SEM.

3.2.6 Overexpression of $\text{tRNA}_i^{\text{Met}}$ increases cell migration

Cell migration plays a pivotal role in tumour progression, and although a key determinant of metastatic dissemination is the increased migration of cancer cells themselves, an increase in the migratory ability of associated stromal cells is also essential to overcome a number of rate-limiting factors in tumour progression (Joyce and Pollard, 2009). We therefore used timelapse microscopy to study migration of iMEF.Vector and iMEF. $\text{tRNA}_i^{\text{Met}}$ cells to determine whether increasing the expression of $\text{tRNA}_i^{\text{Met}}$ could influence fibroblast migration. Wound-scratch assays of cells directionally migrating into a wound on plastic showed that iMEF. $\text{tRNA}_i^{\text{Met}}$ cells had an increased cell speed compared to iMEF.Vector control cells (Figure 3-7A). This $\text{tRNA}_i^{\text{Met}}$ -driven increase in cell

migration was also observed when sub-confluent cells were migrating randomly on plastic (Figure 3-7B).

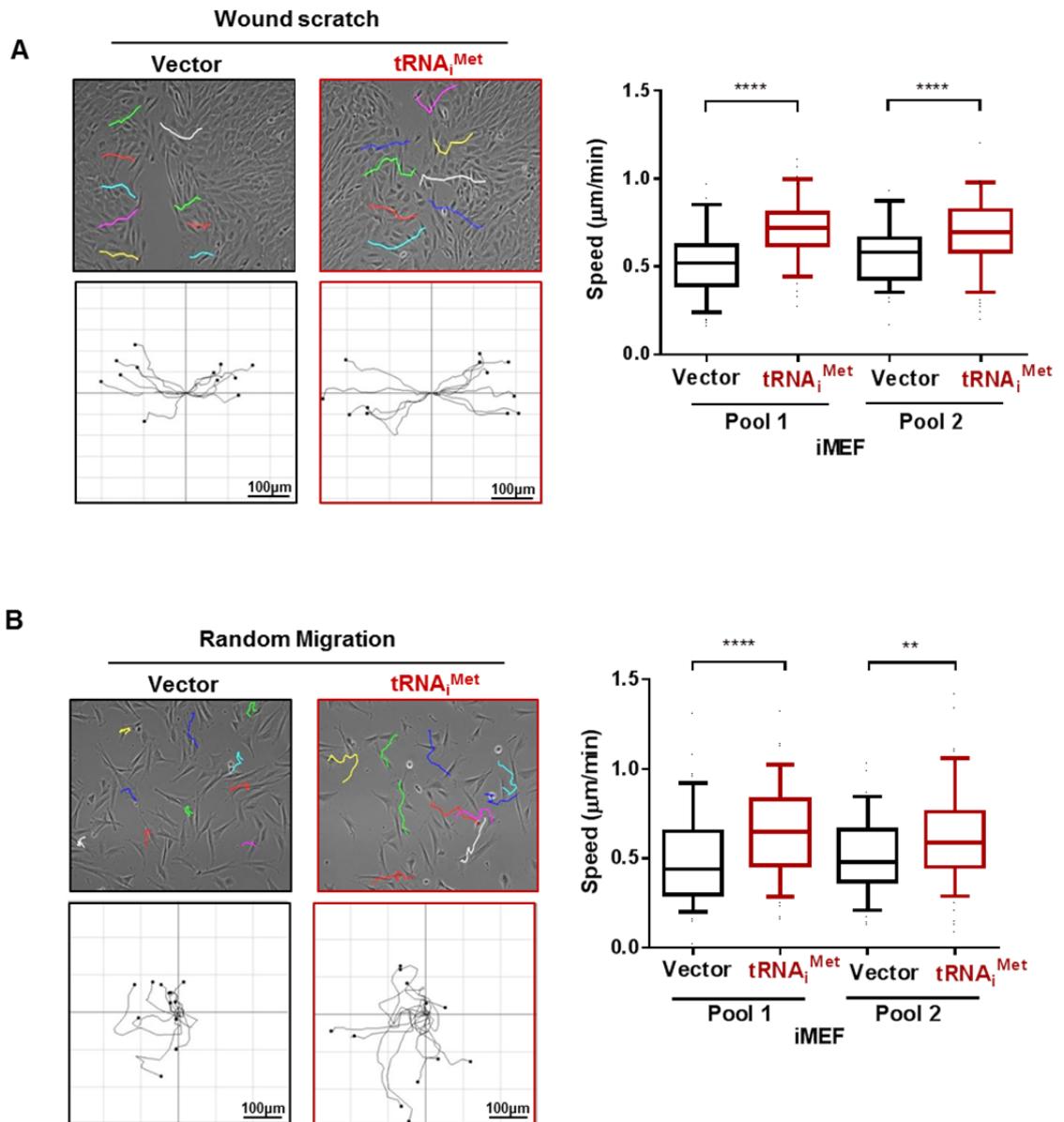


Figure 3-7- Overexpression of tRNA_i^{Met} increases speed of cell migration.

Cell migration was recorded by timelapse microscopy over a 17 hour time course for (A) confluent iMEF.Vector and iMEF.tRNA_i^{Met} cells migrating into a wound on plastic, and (B) subconfluent iMEF.Vector and iMEF.tRNA_i^{Met} cells randomly migrating on plastic. In each case the data represent the speed of 30 – 40 cells per experiment calculated using manual tracking in Image J over the first 200 minutes period (were 200 minutes corresponds to the time taken for the wound to close in iMEF.tRNA_i^{Met} cells), n=3, box and whisker plot represents 5-95 percentile, Kruskal-Wallis test, **** p < 0.0001, **p<0.01.

3.2.7 Overexpression of $\text{tRNA}_i^{\text{Met}}$ increases cell migration through a mechanism that does not involve synthesis of collagen II

In the following chapter the ability of $\text{tRNA}_i^{\text{Met}}$ to influence cell migration through non-cell autonomous mechanisms will be discussed. This work found that overexpression of $\text{tRNA}_i^{\text{Met}}$ influences the ECM secreted by fibroblasts, specifically through generation of a collagen II-rich matrix that supports increased cell migration. Because we found that $\text{tRNA}_i^{\text{Met}}$ overexpressing cells were able to increase secretion of soluble ECM components to produce a matrix that supports increased cell migration, we tested the ability of conditioned media from $\text{tRNA}_i^{\text{Met}}$ overexpressing cells to influence the migration of control iMEFs on plastic. Pre-treatment and continued incubation of iMEF.Vector cells with conditioned media from iMEF. $\text{tRNA}_i^{\text{Met}}$ cells did not increase the speed of cells migrating on plastic (Figure 3-8).

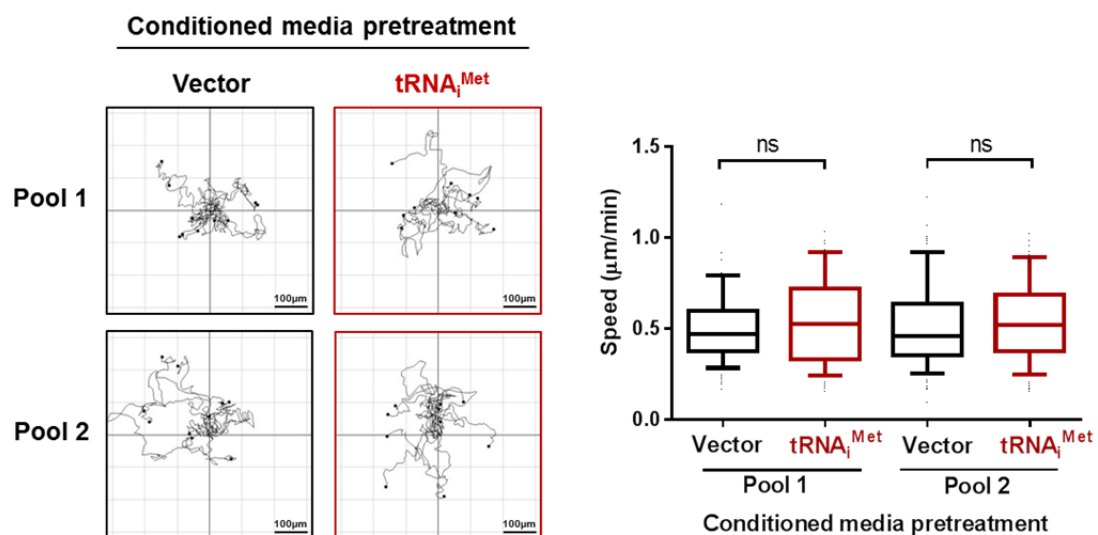


Figure 3-8- Conditioned media from $\text{tRNA}_i^{\text{Met}}$ overexpressing cells does not affect cell migration.

iMEF.Vector cells were plated at 1×10^5 cells/well and incubated at $37^\circ\text{C}/5\% \text{CO}_2$ for 2 hours to adhere on plastic. Cells were then incubated with conditioned media from iMEF.Vector and iMEF. $\text{tRNA}_i^{\text{Met}}$ cells for a further two hours, and random migration in the presence of the conditioned media recorded by timelapse microscopy over a 17 hour time course and analysed in ImageJ. Data represents the speed of 30 – 40 cells per experiment calculated using manual tracking in Image J over the 17 hour time course, $n=3$, box and whisker plot represents 5-95 percentile, Kruskal-Wallis test, ns = not significant.

As data presented in Chapter 4 specifically suggests that increased collagen II secretion is responsible for the $\text{tRNA}_i^{\text{Met}}$ -driven non-cell autonomous effects on cell migration, we also proceeded to use siRNA to knockdown collagen II expression in iMEF. $\text{tRNA}_i^{\text{Met}}$ cells and assessed its effect on their migration.

Knockdown of collagen II in iMEF.tRNA_i^{Met} cells had no effect on their migration speed (Figure 3-9), indicating that the way in which tRNA_i^{Met} levels influence fibroblast migration is mechanistically distinct from the non-cell autonomous control of cell migration described in the next chapter.

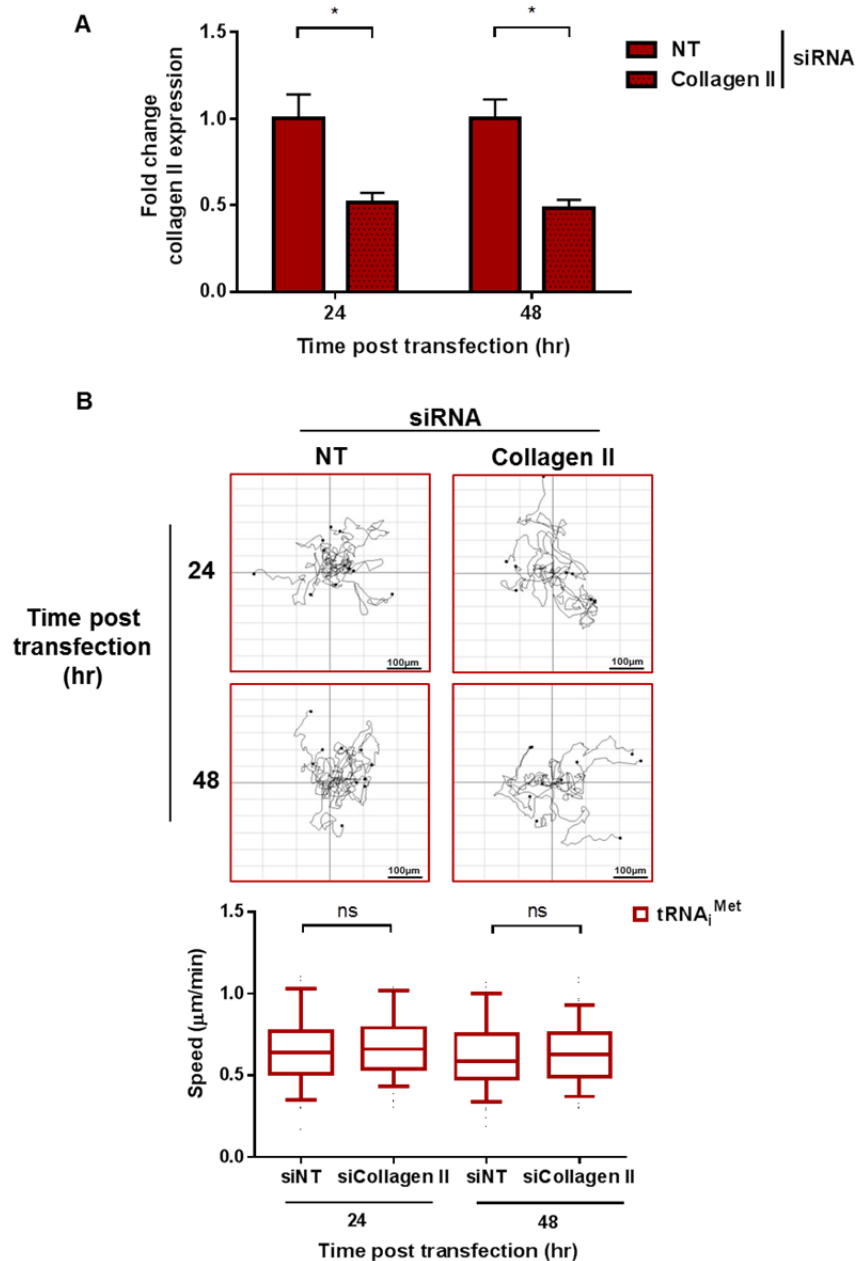


Figure 3-9- siRNA of collagen II does not affect tRNA_i^{Met}-driven fibroblast migration.

(A) qPCR was used to quantify collagen II levels in iMEF.tRNA_i^{Met} cells transfected with a NT or collagen II specific siRNA, all data normalised to ARPP P0 and presented relative to expression in the NT siRNA iMEF.tRNA_i^{Met} treated cells. Data presented is representative of one of the n=3 biological repeats, +/- standard deviation of technical replicates, 2 way ANOVA, *p<0.05. (B) iMEF.tRNA_i^{Met} cells transfected with NT or collagen II specific siRNA were trypsinised 24 and 48 hours post transfection, plated at 1x10⁵ cells/well and incubated at 37°C/5% CO₂ for 2 hours to adhere on plastic. Random migration was recorded by timelapse microscopy over a 17 hour time course and analysed in ImageJ. Data represents the speed of 30 – 40 cells per experiment calculated using manual tracking over the 17 hour time course, n=3, box and whisker plot represents 5-95 percentile, Kruskal-Wallis test, ns = not significant.

3.2.8 tRNA_i^{Met}-driven fibroblast migration is dependent on ternary complex formation

We wanted to consider whether the mechanism which enables tRNA_i^{Met} to drive increased cell migration is associated with its canonical function in protein synthesis. The role of tRNA_i^{Met} in translation initiation is dependent on its ability to associate with eIF2 and GTP to form the ternary complex (TC) (Sonenberg and Hinnebusch, 2009). Regulation of translation initiation can be controlled by the phosphorylation status of initiation factors. Phosphorylation of eIF2 α reduces TC formation and inhibits global translation initiation, and this phosphorylation event can be activated by exposure to cell stresses. Whilst reduced TC formation decreases levels of global protein synthesis, it increases the translation of specific mRNAs including stress-related mRNAs and other transcripts that have upstream open reading frames (uORFs). To determine whether differential TC formation was involved in tRNA_i^{Met}-driven cell migration we assessed the levels of phospho-eIF2 α in the iMEF.Vector and iMEF.tRNA_i^{Met} cell lines. Western blots showed no significant difference in phospho-eIF2 α levels following tRNA_i^{Met} overexpression, indicating that the increase in migration driven by tRNA_i^{Met} was not dependent on absolute differences in phospho-eIF2 α expression (Figure 3-10).

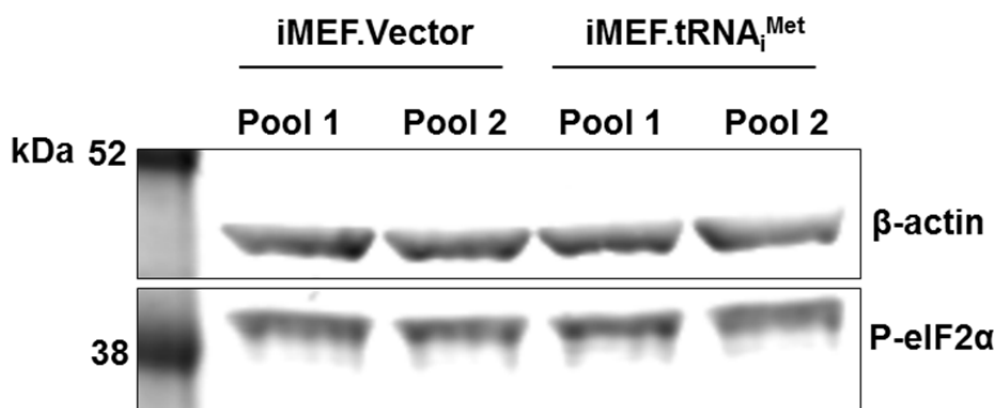


Figure 3-10- Endogenous levels of phospho-eIF2 α are unchanged by overexpression of tRNA_i^{Met}. iMEF.Vector and iMEF.tRNA_i^{Met} cells were plated at 1×10^5 cells/well overnight at 37°C/5% CO₂, lysed into 1% SDS lysis buffer and levels of phospho-eIF2 α determined by western blot.

Despite detecting no difference in the endogenous levels of phospho-eIF2 α following tRNA_i^{Met} overexpression, it is possible that cells may have different phospho-eIF2 α requirements following shifts in TC availability. Therefore, to

further investigate the dependency of $\text{tRNA}_i^{\text{Met}}$ -driven cell migration on TC levels, two additional methods were used to manipulate eIF2 α phosphorylation. The phosphatase inhibitor, salubrinal, can increase the levels of phospho-eIF2 α (by inhibiting phospho-eIF2 α dephosphorylation). Conversely, overexpression of the protein phosphatase regulatory subunit, GADD34, can decrease the levels of phospho-eIF2 α (by recruiting protein phosphatase 1 to dephosphorylate phospho-eIF2 α). We found that salubrinal treatment specifically increased the migration speed of iMEF.Vector cells, but did not influence migration of $\text{tRNA}_i^{\text{Met}}$ overexpressing cells (Figure 3-11), while transient transfection of a GADD34-expressing construct into fibroblasts decreased the ability of $\text{tRNA}_i^{\text{Met}}$ to promote the migration of iMEF. $\text{tRNA}_i^{\text{Met}}$ cells (Figure 3-12). Taken together these data indicate that the TC influences cell migration, and that overexpression of $\text{tRNA}_i^{\text{Met}}$ modifies the way in which the migratory machinery responds to alterations in TC levels.

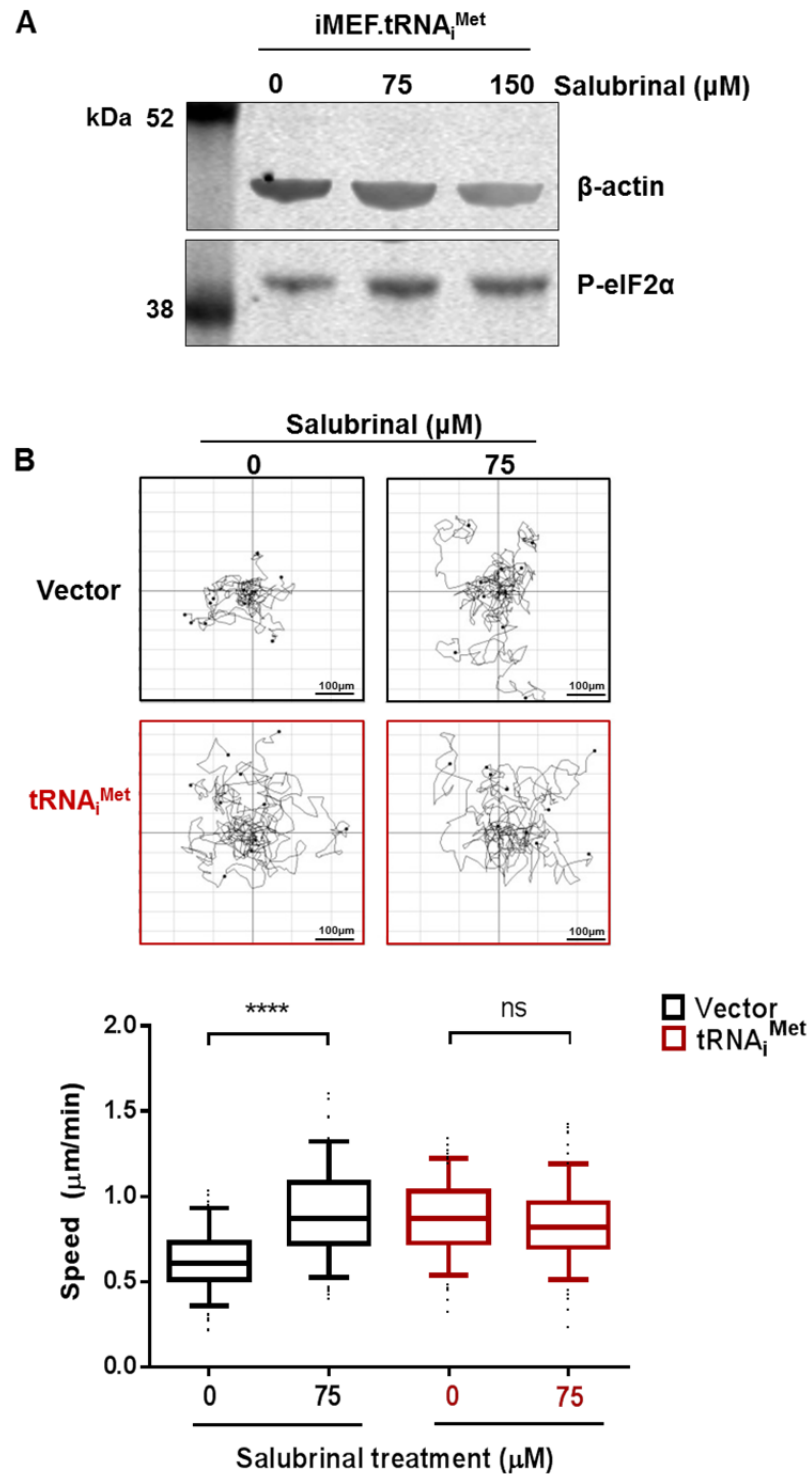


Figure 3-11- The tRNA_i^{Met} driven increase in cell speed can be recapitulated by increasing levels of phospho-eIF2α in control cells.

(A) Western blot to determine the concentration of salubrinal that increases phospho-eIF2α levels. iMEF.tRNA_i^{Met} cells were plated at 1×10^5 cells/well and incubated at $37^\circ\text{C}/5\% \text{CO}_2$ for 2 hours to adhere to plastic. Media was then replaced to contain salubrinal or corresponding DMSO control, and cells incubated overnight. Lysates were made using 1% SDS lysis buffer, and levels of phospho-eIF2α determined by western blot. (B) iMEF.Vector cells and iMEF.tRNA_i^{Met} were plated at 1×10^5 cells/well and incubated at $37^\circ\text{C}/5\% \text{CO}_2$ for 2 hours to adhere to plastic. Cells were then incubated with media containing $75 \mu\text{M}$ salubrinal, or corresponding DMSO control for 2 hours before using timelapse microscopy to record random migration over a 17 hour time course in media containing salubrinal or corresponding DMSO control. Data represents the speed of 30 – 40 cells per experiment calculated using manual tracking over the 17 hour time course, $n=3$, box and whisker plot represents 5-95 percentile, Kruskal-Wallis test, **** $p < 0.0001$, ns = not significant.

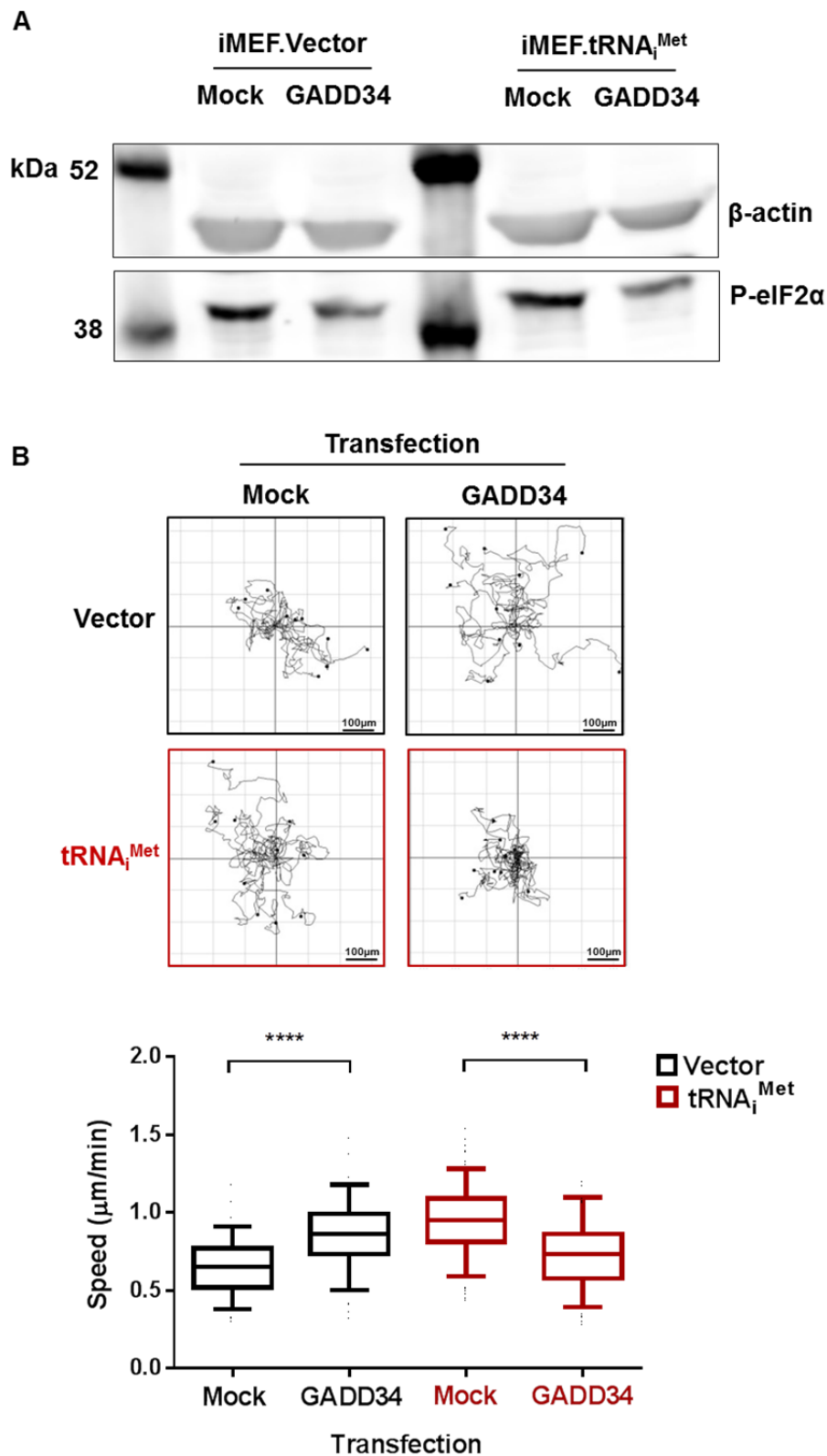


Figure 3-12- The tRNA_i^{Met}-driven increase in cell speed is influenced by manipulating levels of the ternary complex.

iMEF.Vector and iMEF.tRNA_i^{Met} cells were transfected with a GADD34 containing construct 48 hours prior to (A) lysis into 1% SDS lysis buffer, were levels of phospho-eIF2 α were then determined by western blot. (B) 1×10^5 cells/well were incubated at 37°C/5% CO₂ for 2 hours to adhere to plastic and random migration then recorded by timelapse microscopy over a 17 hour time course. Data represents the speed of 30 – 40 cells per experiment calculated using manual tracking over the 17 hour time course, n=3, box and whisker plot represents 5-95 percentile, Kruskal-Wallis test, **** p < 0.0001.

Although total levels of protein synthesis are not increased following $\text{tRNA}_i^{\text{Met}}$ overexpression (Figure 3-2) the results of the salubrinal and GADD34 experiments indicate that the effects of $\text{tRNA}_i^{\text{Met}}$ on cell migration may be due to the role of the TC in translation of a small subset of mRNAs. To investigate this we used cycloheximide, an inhibitor of protein synthesis, to determine whether synthesis of new protein was required for the increase in migration driven by $\text{tRNA}_i^{\text{Met}}$. Although addition of cycloheximide inhibited protein biosynthesis (Figure 3-13A), it was unable to inhibit the increase in migration induced by $\text{tRNA}_i^{\text{Met}}$ overexpression (Figure 3-13B&C). Cycloheximide exerts its effects through blocking the translocation step of elongation, and so does not affect the actual formation of the TC. Collectively this data therefore indicates that the effect of $\text{tRNA}_i^{\text{Met}}$ on cell migration is influenced by the TC, but is not dependent on translational elongation and the synthesis of new proteins.

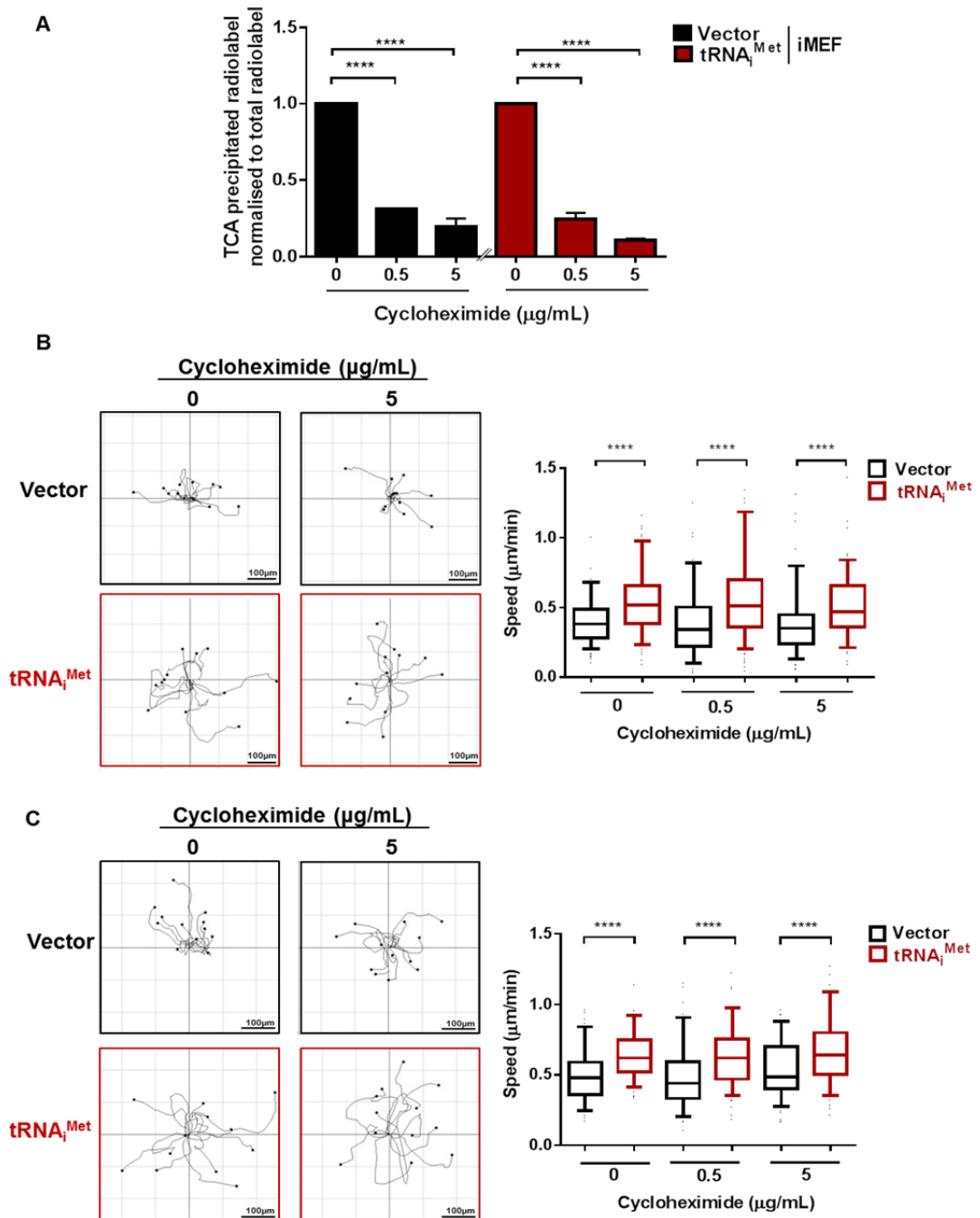


Figure 3-13- Cycloheximide does not inhibit tRNA^{Met}-driven cell migration.

(A) ³⁵S-methionine incorporation was used to ensure the cycloheximide concentrations used were inhibiting the synthesis of new proteins. Cells were pretreated with 0, 0.5 and 5 $\mu\text{g/mL}$ cycloheximide for 1 hour and then depleted of methionine and cysteine for 30 minutes at 37°C/5% CO₂ in media containing the described cycloheximide concentrations. Cells were then trypsinised and resuspended in media containing 0.07mCi EasyTag Express Protein Labelling Max ³⁵S including the described cycloheximide concentrations and incubated at 37°C/5% CO₂ for 2 hours. TCA precipitation was used to stop and concentrate the reaction, and the ratio of TCA precipitated radiolabel to total radiolabel calculated, n=2, +/- SEM of biological replicates, ANOVA, **** p < 0.0001. (B) iMEF pool 1 cells were pretreated with 0, 0.5 and 5 $\mu\text{g/mL}$ cycloheximide for 1 hour and then trypsinised, replated at 1x10⁵ cells/well in media containing the cycloheximide concentrations described and incubated at 37°C/5%CO₂ for 2 hours to adhere to plastic. Random migration was then recorded by timelapse microscopy over a 17 hour time course. The data represents the speed of 30 – 40 cells per experiment, calculated using manual tracking in Image J over the first 200 minute period, n=3, box and whisker plot represents 5-95 percentile, Kruskal-Wallis test, **** p < 0.0001. (C) iMEF pool 2 cell migration as described in (B).

3.2.9 tRNA_i^{Met}-driven cell migration is dependent on integrin $\alpha_5\beta_1$ -fibronectin association

To provide further insight into the mechanism by which tRNA_i^{Met} promotes increased cell migration, we determined the integrin-dependence of tRNA_i^{Met}-driven cell motility. We assessed the ability of iMEF.Vector and iMEF.tRNA_i^{Met} cells to migrate on surfaces coated with increasing concentrations of fibronectin. From this it was clear that the difference in migration speed between control and tRNA_i^{Met} overexpressing fibroblasts was abrogated when cells were plated onto fibronectin-coated surfaces (Figure 3-14). At a low coating concentration (0.25 μ g/mL) this was owing to the ability of this ECM protein to increase the migration speed of control cells, whereas higher fibronectin concentrations tended to inhibit cell movement so that there was no discernible difference between the migration speed of iMEF.Vector and iMEF.tRNA_i^{Met} cells.

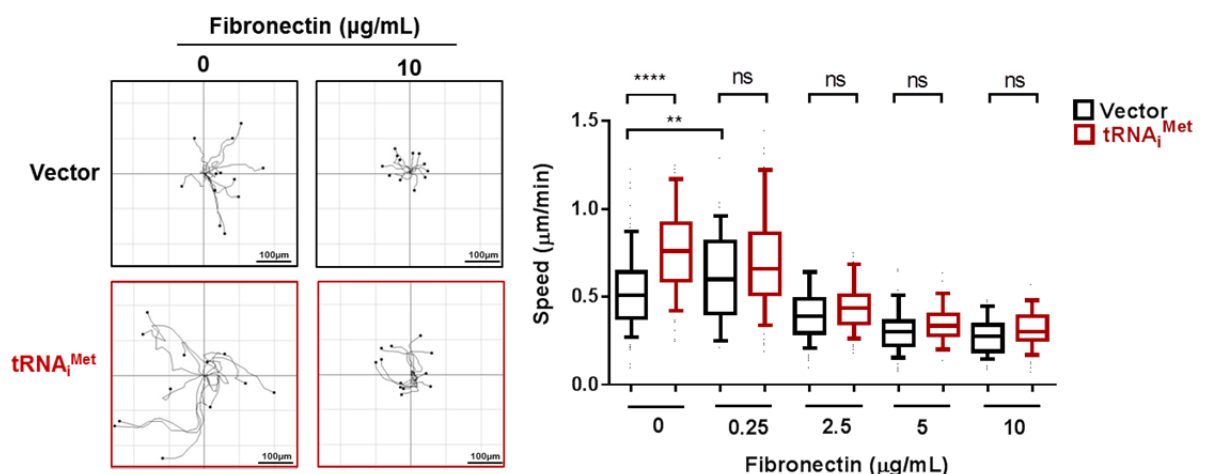


Figure 3-14- Fibronectin negates the increase in cell migration driven by tRNA_i^{Met}.

Plates were coated with the described concentration of fibronectin for 2 hours prior to cell plating. iMEF.Vector and iMEF.tRNA_i^{Met} cells were plated at 1×10^5 cells/well and incubated at 37°C/5%CO₂ for 2 hours to adhere. Timelapse microscopy was used to record random migration over a 17 hour time course. The speed of 30 – 40 cells was calculated using manual tracking in Image J over the first 200 minute period, n=3, box and whisker plot represents 5-95 percentile, Kruskal-Wallis test, **** p < 0.0001, ns = not significant.

Integrin $\alpha_5\beta_1$ is the primary receptor for fibronectin, and so we assessed the ability of integrin $\alpha_5\beta_1$ to influence tRNA_i^{Met}-driven cell migration. An antibody that binds and blocks the fibronectin binding site of integrin $\alpha_5\beta_1$ (mAb16) inhibited the migration of tRNA_i^{Met} overexpressing fibroblasts while not affecting the movement of iMEF.Vector cells (Figure 3-15). The involvement of $\alpha_5\beta_1$ in

tRNA_i^{Met}-driven cell migration was further investigated by using siRNA to knockdown integrin α_5 levels, and also by using an antibody (16G3) which binds to the RGD sequence in fibronectin to oppose its interaction with the $\alpha_5\beta_1$ receptor. siRNA of integrin α_5 (Figure 3-16) and addition of 16G3 (Figure 3-17) both inhibited migration of tRNA_i^{Met} overexpressing cells, but had no effect on the movement of control fibroblasts. Taken together, these data indicate that association of integrin $\alpha_5\beta_1$ with fibronectin is a prerequisite for tRNA_i^{Met}-driven cell migration.

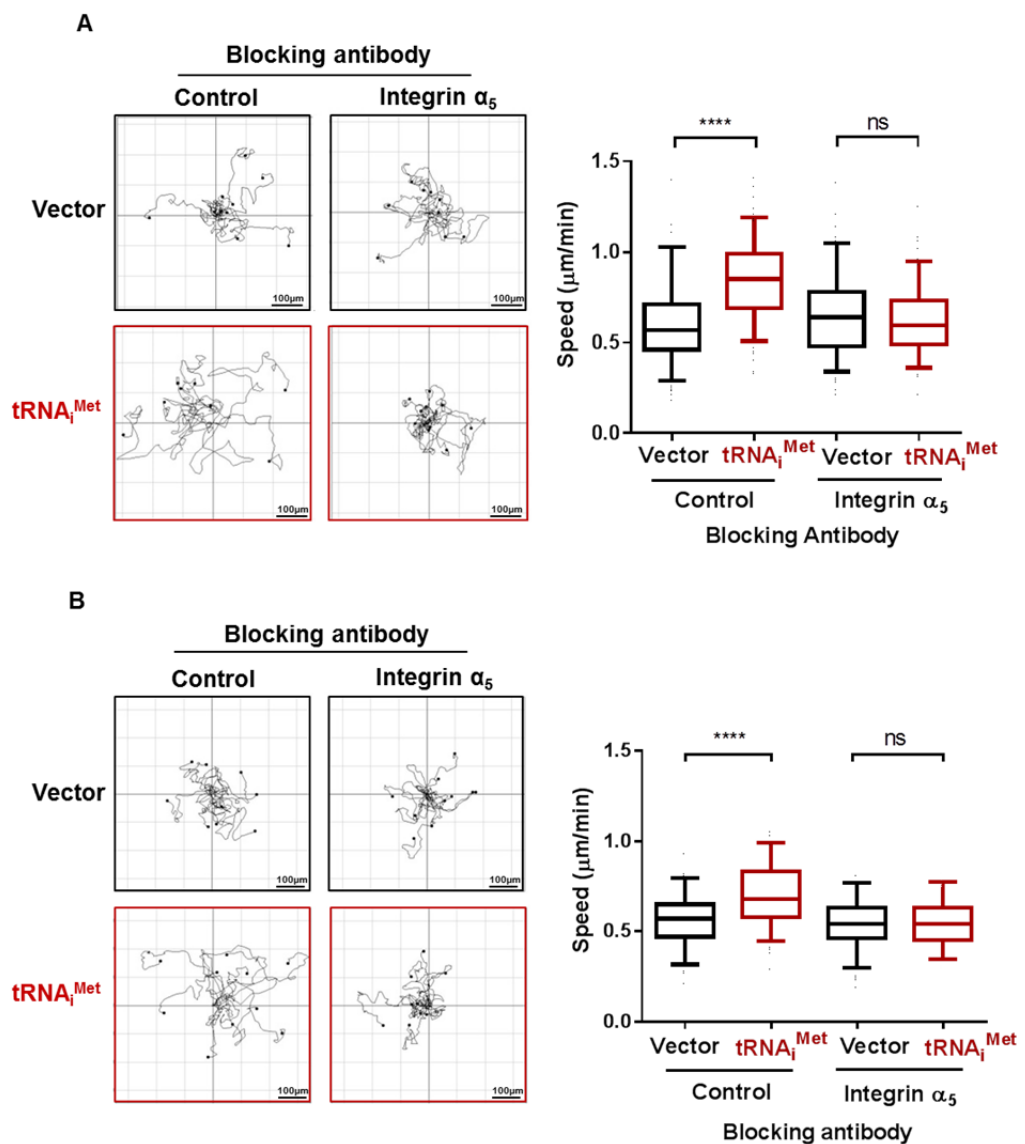


Figure 3-15- tRNA_i^{Met}-driven cell migration is opposed by an integrin α_5 blocking antibody. iMEF.Vector and iMEF.tRNA_i^{Met} cells were plated at 1×10^5 cells/well and incubated at $37^\circ\text{C}/5\%\text{CO}_2$ for 2 hours to adhere to plastic. Cells were then incubated for a further 2 hours with either $2\mu\text{g}/\text{mL}$ control IgG antibody, or $2\mu\text{g}/\text{mL}$ mAb16 antibody. Random migration of cells was then recorded by timelapse microscopy for 17 hours. In each case the velocity of 30 – 40 cells per experiment was calculated using manual tracking in Image J over the 17 hour time course for (A) Pool 1 cells, $n=3$, box and whisker plot represents 5-95 percentile, (B) Pool 2 cells, $n=2$, box and whisker plot represents 5-95 percentile, Kruskal-Wallis test, **** $p < 0.0001$, ns = not significant.

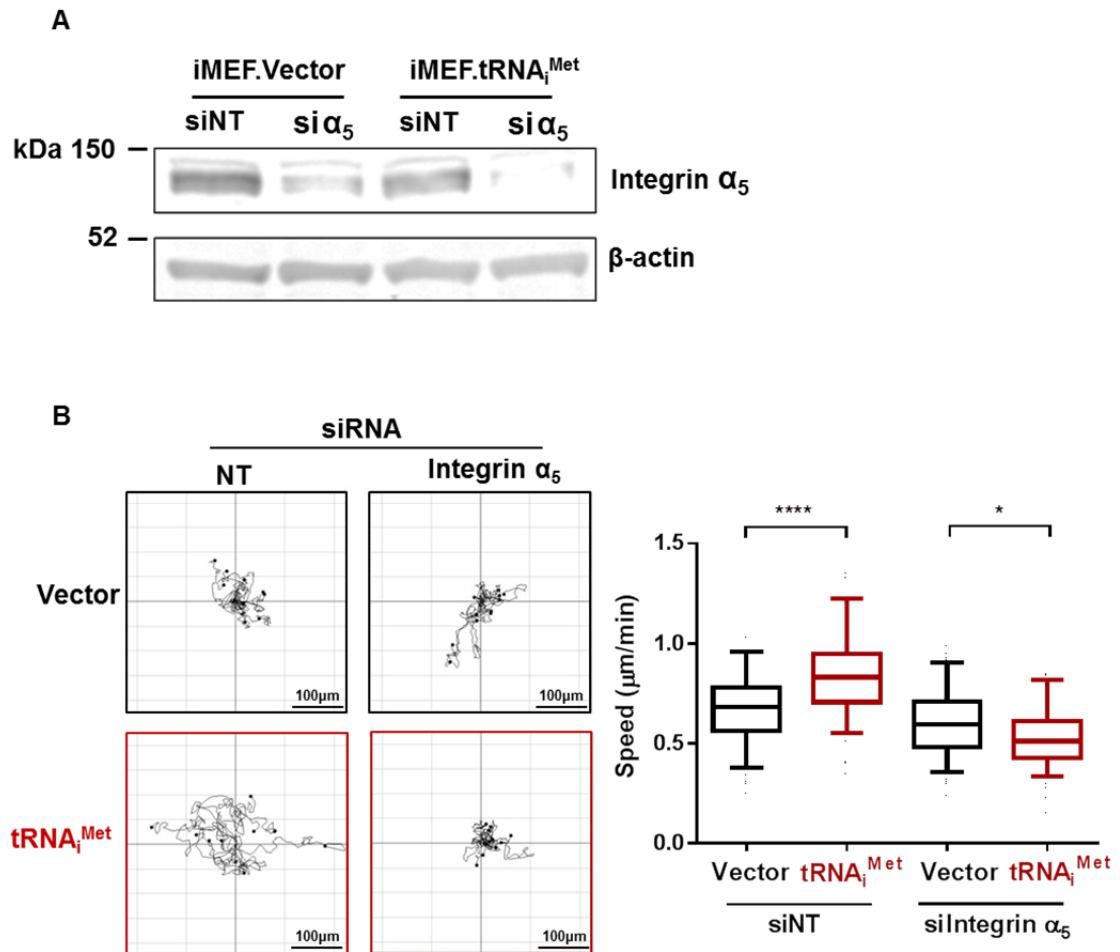


Figure 3-16- tRNA_i^{Met}-driven cell migration is opposed by siRNA of integrin α_5 .

(A) iMEF.Vector and iMEF.tRNA_i^{Met} cells were transfected with a NT or an integrin α_5 specific siRNA. Cells were lysed 24 hours post transfection into NDLB, and subjected to western blot to determine knockdown of integrin α_5 levels. (B) iMEF.Vector and iMEF.tRNA_i^{Met} cells treated with NT and integrin α_5 siRNA were trypsinised 24 hours post transfection and plated at 1×10^5 cells/well. After a 2 hour incubation at $37^\circ\text{C}/5\%\text{CO}_2$ to adhere to plastic, the random migration of cells was recorded for 17 hours by timelapse microscopy. In each case the velocity of 30 – 40 cells per experiment was calculated using manual tracking in Image J over the 17 hour time course, n=3, box and whisker plot represents 5-95 percentile, Kruskal-Wallis test, **** p < 0.0001, *p<0.05.

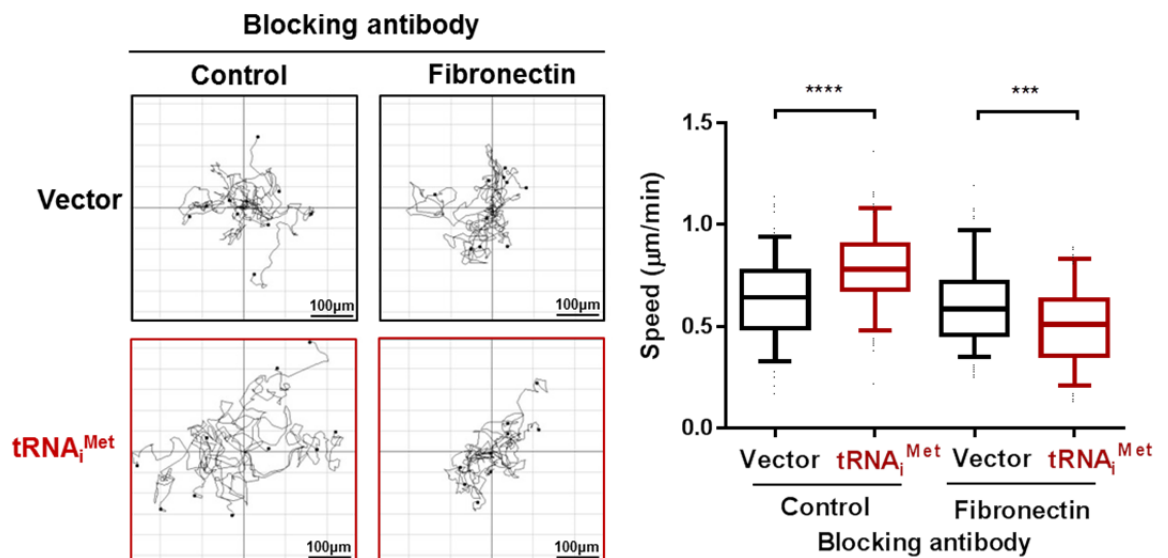


Figure 3-17- $tRNA_{i}^{Met}$ -driven cell migration is opposed by blockade of the RGD site in fibronectin.

iMEF.Vector and iMEF. $tRNA_{i}^{Met}$ cells were plated at 1×10^5 cells/well and incubated at $37^{\circ}\text{C}/5\%\text{CO}_2$ for 2 hours to adhere to plastic. Cells were then incubated for a further 2 hours with either $2\mu\text{g}/\text{mL}$ control IgG antibody, or $2\mu\text{g}/\text{mL}$ 16G3 antibody. Random migration of cells was then recorded by timelapse microscopy for 17 hours. In each case the velocity of 30 – 40 cells per experiment was calculated using manual tracking in Image J over the 17 hour time course, $n=3$, box and whisker plot represents 5-95 percentile, Kruskal-Wallis test, **** $p < 0.0001$, *** $p < 0.001$.

The dependency of $tRNA_{i}^{Met}$ -driven cell migration on the integrin $\alpha_5\beta_1$ -fibronectin interaction led us to examine the expression and localisation of $\alpha_5\beta_1$ in iMEFs. qPCR showed that there was no significant difference in the levels of mRNA encoding integrin $\alpha_5\beta_1$ following $tRNA_{i}^{Met}$ overexpression (Figure 3-18A), and Western blot showed no consistent differences in total α_5 protein levels between iMEF. $tRNA_{i}^{Met}$ and iMEF.Vector cells (Figure 3-18B). Surface expression of integrin α_5 was also measured, and while immunoprecipitation and ELISA showed that there was slightly less integrin α_5 at the surface of iMEF. $tRNA_{i}^{Met}$ pool 1 cells compared to control (Figure 3-18C&D), analysis in iMEF. $tRNA_{i}^{Met}$ pool 2 cells showed no significant difference in integrin α_5 surface expression (Figure 3-18E), suggesting that this was not a consistent consequence of $tRNA_{i}^{Met}$ overexpression.

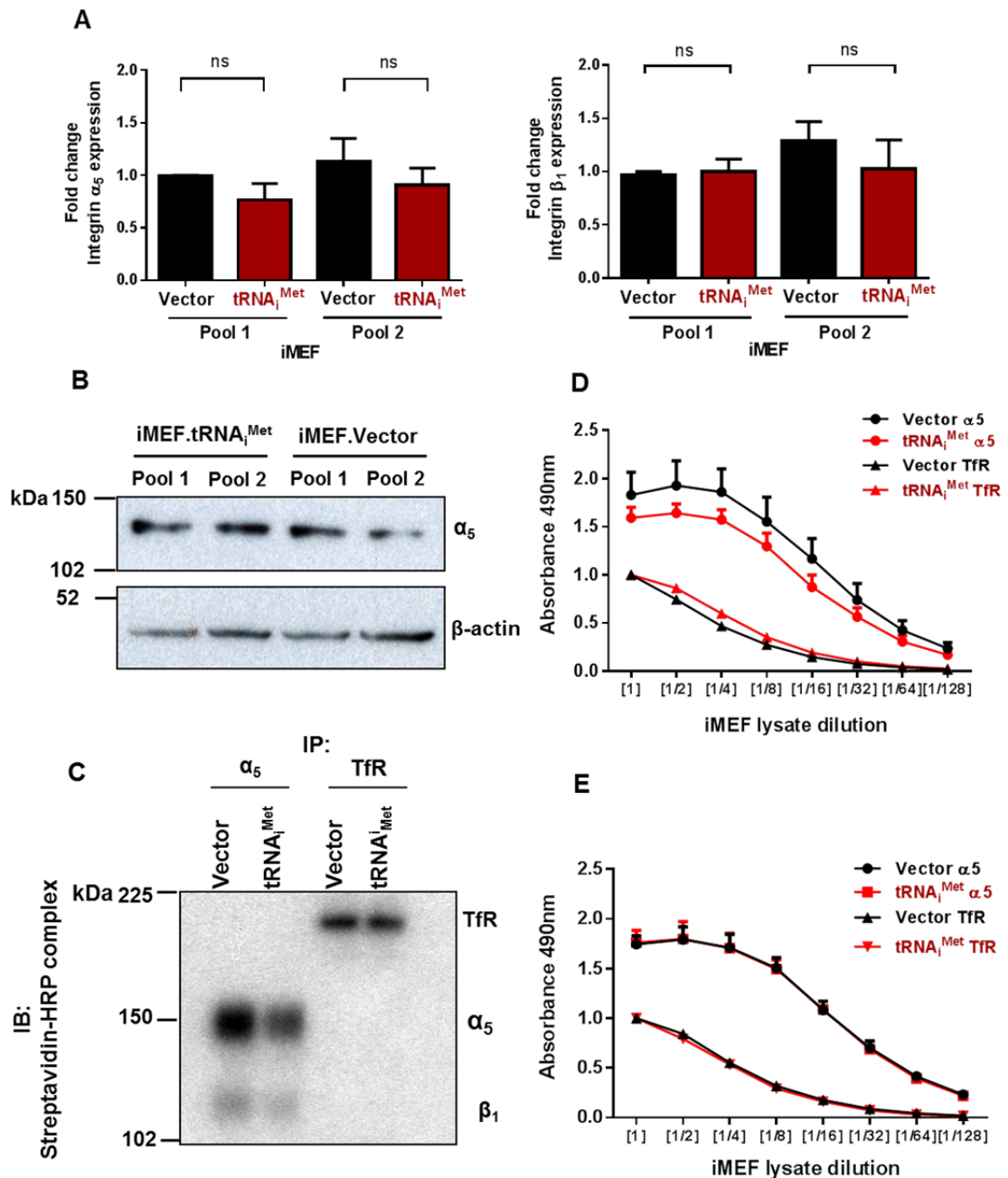


Figure 3-18- $tRNA_i^{Met}$ overexpression does not influence integrin $\alpha_5\beta_1$ expression.

(A) qPCR was used to quantify expression of integrin $\alpha_5\beta_1$ in iMEF.Vector and iMEF. $tRNA_i^{Met}$ cells. All data are normalised to ARPP P0 and are presented relative to expression in iMEF.Vector pool 1, n=3, +/- SEM, ANOVA, ns = not significant. (B) iMEF.Vector and iMEF. $tRNA_i^{Met}$ cells were plated to 80 – 90 % confluence, lysed into NDLB, and subjected to western blot to determine total protein integrin α_5 levels. (C) Surface expression of integrin α_5 , and transferrin receptor (Tfr) as a control, were assessed in pool 1 iMEF.Vector and iMEF. $tRNA_i^{Met}$ cells by immunoprecipitation. Cells were surface-labelled with NHS-S-S-Biotin at 4°C, then lysed and incubated with beads coated in monoclonal antibodies specific for integrin α_5 or Tfr. Lysates were separated by gel electrophoresis and surface expression of integrin α_5 or Tfr determined by binding and detection of streptavidin-HRP complex. (D) Surface expression of integrin α_5 , and Tfr were assessed in pool 1 iMEF.Vector and iMEF. $tRNA_i^{Met}$ cells by ELISA. Briefly, cells were surface-labelled with NHS-S-S-Biotin at 4°C, lysed and levels of biotinylated integrin α_5 determined by ELISA, using microtiter plates coated with monoclonal antibodies specific for integrin α_5 or Tfr and a dilution of iMEF lysate to ensure the detection was within the linear dynamic range of the assay, n=3, +/- SEM. (E) Surface expression of integrin α_5 in pool 2 iMEF.Vector and iMEF. $tRNA_i^{Met}$ cells was assessed by ELISA as described in (C).

Although there was no significant difference in mRNA, protein levels, or surface expression of integrin α_5 , we wanted to determine whether overexpression of $\text{tRNA}_i^{\text{Met}}$ could influence integrin α_5 distribution and function. We used immunofluorescence to examine the localisation of integrin α_5 , and were unable to detect any discernible difference in distribution of α_5 following $\text{tRNA}_i^{\text{Met}}$ overexpression (Figure 3-19).

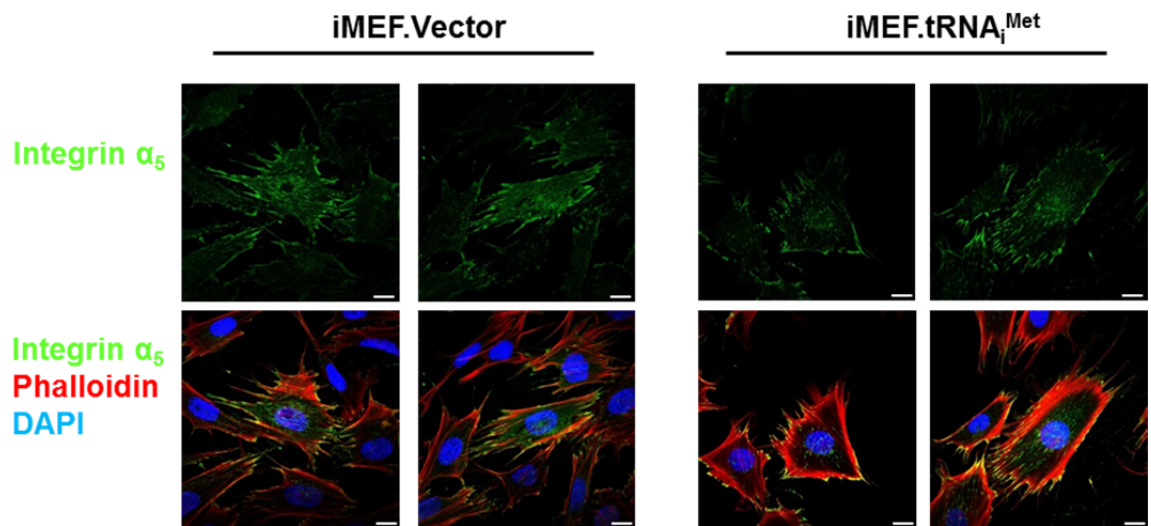


Figure 3-19- No significant difference in integrin $\alpha_5\beta_1$ localisation following $\text{tRNA}_i^{\text{Met}}$ overexpression.

Immunofluorescence was used to assess the localisation of integrin α_5 . iMEF.Vector and iMEF.tRNA_i^{Met} pool 1 cells were plated onto glass coated with 1 $\mu\text{g}/\text{mL}$ fibronectin for 24 hours and then fixed and stained for integrin α_5 , and counterstained with phalloidin and DAPI to visualise F-actin and nuclei respectively, scale bar represents 20 μm .

The internalisation and recycling of integrins is an important process that can influence cell migration, and the Rab GTPase dependent recycling of integrin $\alpha_5\beta_1$ to cell protrusions is a mechanism that can increase migration of cancer cells (Muller et al., 2009, Rainero et al., 2012). We therefore investigated rates of integrin $\alpha_5\beta_1$ internalisation and recycling in iMEF.Vector and iMEF.tRNA_i^{Met} cells. The rate of internalisation of integrin α_5 was unchanged between iMEF.Vector and iMEF.tRNA_i^{Met} cells, and an antibody to active integrin β_1 (9EG7) showed that there was also no difference in internalisation of the active conformation of the integrin (Figure 3-20A). There was no significant difference in recycling of internalised integrin α_5 back to the cell membrane, however there was less active integrin β_1 recycled back to the cell surface in tRNA_i^{Met} overexpressing cells (Figure 3-20B). Whilst keeping ligand engaged integrins within the cell may be a mechanism to promote increased cell migration, these internalisation and recycling experiments were conducted on pool 1 of tRNA_i^{Met}

overexpressing iMEFs, and are therefore most likely a reflection of the lower surface expression of integrin α_5 in pool 1 iMEFs detected by both ELISA and IP that was not reflected in pool 2 (Figure 3-18). And so, although the consistent increase in cell migration driven by $\text{tRNA}_i^{\text{Met}}$ is dependent on the ability of integrin $\alpha_5\beta_1$ to bind fibronectin, the actual mechanism by which it exerts its effects, and the link to its role in the TC, still remains to be identified.

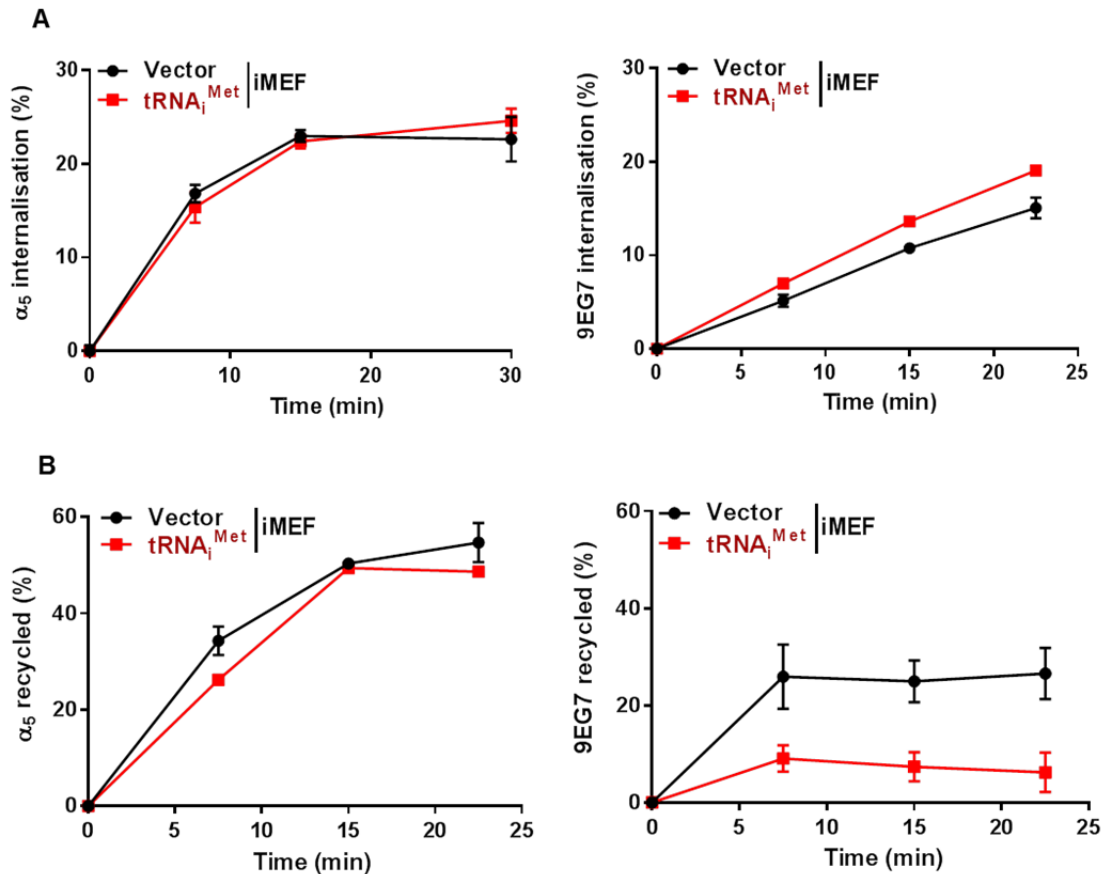


Figure 3-20- Investigation of integrin α_5 internalisation and recycling following $\text{tRNA}_i^{\text{Met}}$ overexpression.

(A) iMEF.Vector and iMEF. $\text{tRNA}_i^{\text{Met}}$ pool 1 cells were surface labelled with NHS-S-S-Biotin at 4°C, warmed to 37°C for indicated times, and the proportion of integrin α_5 and active β_1 (9EG7) internalisation determined by ELISA, n=1, +/- standard deviation of technical replicates. (B) iMEF.Vector and iMEF. $\text{tRNA}_i^{\text{Met}}$ pool 1 cells were surface labelled with NHS-S-S-Biotin at 4°C, warmed to 37°C for 30 minutes to allow internalisation of cell surface receptor, and the remaining label at the cell surface reduced. Cells were then warmed to 37°C for the indicated times and the proportion of integrin α_5 and active β_1 (9EG7) recycled to the cell surface determined by ELISA n=1, +/- standard deviation of technical replicates.

3.3 Discussion

The canonical function of tRNAs is their role in protein synthesis, and increased translation is necessary to implement many of the steps that are considered to be the hallmarks of cancer (Hanahan and Weinberg, 2000). High levels of tRNAs are seen across a variety of cancer types (Pavon-Eternod et al., 2009, Zhou et al., 2009, Mahlab et al., 2012). In malignant myeloma, increased tRNA abundance is associated with high translational activity, and treatment with a proteasome inhibitor decreases the charging of tRNAs, consequently increasing the accumulation of misfolded proteins, leading to apoptosis of myeloma cells (Zhou et al., 2009). The specificity of these effects have been attributed to tRNAs charged with hydrophobic amino acids, of which methionine is one, and so again provides evidence that specific tRNAs can be altered in cancer to accommodate the increased need for protein translation.

Translation initiation is generally considered to be the rate limiting step in eukaryotic protein synthesis (Sonenberg and Hinnebusch, 2009), however we found that increased levels of the initiator methionine tRNA did not affect the overall rate of cellular protein synthesis in fibroblasts (Figure 3-2). Thus, despite the fact that increased $\text{tRNA}_i^{\text{Met}}$ has a profound influence on cell migration, this tRNA is not likely to be a limiting factor in translation initiation in general. Furthermore, $\text{tRNA}_i^{\text{Met}}$ levels do not seem to be linked to cell size, energy metabolism, cell spreading, or rate of proliferation.

The contribution of tRNA expression to cell proliferation is a contested phenomenon, with opposing opinions in the literature. Distinct changes in the repertoires of tRNAs expressed in proliferating and differentiating cells results in increased translational efficiency of proliferative genes in actively dividing cells (Gingold et al., 2014). Thus, these workers classified $\text{tRNA}_i^{\text{Met}}$ as a “proliferative tRNA” owing to the fact that its transcription was increased in proliferating cells compared to differentiating cells. However, a causal link between $\text{tRNA}_i^{\text{Met}}$ levels and increased cell proliferation was not demonstrated. Other studies have claimed that overexpression of $\text{tRNA}_i^{\text{Met}}$ may increase the proliferation of human epithelial cells (Pavon-Eternod et al., 2013). However, this work used the intensity of Hoechst staining to quantify the increase in cell proliferation and it is worth noting that although Hoechst stain binds to all nucleic acids, its

fluorescence is dramatically increased upon binding to AT-rich double stranded DNA (Portugal and Waring, 1988). The work of Gingold and colleagues showed that changes in tRNA expression profiles correlate with an increase in activating epigenetic modifications, consequently changing the chromatin landscape in such cells. Analysis of codon usage in genes highly expressed in proliferative cells also described a tendency for proliferative-associated genes to be AT rich (Gingold et al., 2014). It is therefore possible that the $\text{tRNA}_i^{\text{Met}}$ induced increase in cell proliferation detected in human epithelial cells was owing to an increase in the accessibility of AT rich genes, and genes that are annotated as proliferative may also have other functions, including roles in cell migration. Indeed other publications have shown that although overexpression of components of the Pol III machinery can drive transformation, this effect is uncoupled from cellular proliferation (Johnson et al., 2008), and so our data sits in line with this view, as we find that increased expression of a single Pol III product, $\text{tRNA}_i^{\text{Met}}$, cannot drive an increase in cell proliferation. Furthermore, recent studies have also shown that the level of tRNA modification regulates cell growth, and not altered total tRNA expression levels (Rojas-Benitez et al., 2015). Therefore, although initial studies suggested that additional copies of the $\text{tRNA}_i^{\text{Met}}$ gene in *Drosophila* larvae could increase their growth rate (Rideout et al., 2012), this recent study showed that extra copies of $\text{tRNA}_i^{\text{Met}}$ alone do not influence growth, and it is an increase in levels of an N⁶-threonylcarbamoyl-adenosine modification of $\text{tRNA}_i^{\text{Met}}$ that is limiting for *Drosophila* growth *in vivo* (Rojas-Benitez et al., 2015). It would therefore be interesting to investigate differences in modification of $\text{tRNA}_i^{\text{Met}}$ within our fibroblast model, to understand whether the effects we see are a consequence of absolute increased $\text{tRNA}_i^{\text{Met}}$ expression or are related changes in $\text{tRNA}_i^{\text{Met}}$ modification.

Increased expression of $\text{tRNA}_i^{\text{Met}}$ increased the migration speed of fibroblasts (Figure 3-7). The opposing effects of salubrinal and GADD34 on cell migration suggest that TC levels are critical, and to some extent drive, the $\text{tRNA}_i^{\text{Met}}$ induced increase in cell speed (Figure 3-11 & Figure 3-12). If phospho-eIF2 α levels were increased by $\text{tRNA}_i^{\text{Met}}$ overexpression, the explanation for this phenomenon would be simple. However, this is not the case as phospho-eIF2 α levels are identical in iMEF. $\text{tRNA}_i^{\text{Met}}$ and iMEF.Vector cells (Figure 3-10). However, it may also be possible for local phosphorylation of eIF2 α to be

changed in the cell without affecting total phospho-protein levels, and so it would be interesting to use immunofluorescence to visualise the distribution of phospho-eIF2 α in the iMEF.tRNA_i^{Met} overexpressing cells and thus determine whether there are any changes in localisation of the protein synthesis machinery which could contribute to the increased cell migration driven by tRNA_i^{Met} levels.

Observations that cycloheximide treatment did not inhibit tRNA_i^{Met}-driven cell migration indicate that although increased cell speed is dependent on the formation of the TC, it is not necessarily reliant on active synthesis of new proteins (Figure 3-13). That is not to say that these effects could not be owing to expression of a highly stable protein whose levels would not be affected by these relatively brief cycloheximide treatments. Furthermore, although the concentrations of cycloheximide that we have used are effective in reducing protein synthesis, they do not completely abrogate it, and so it may still be possible for the cell to translate specific proteins at the sacrifice of others. However, it is also important to consider the possibility that the role of tRNA_i^{Met} and the TC in driving cell migration may not be owing to a direct role of the TC in selective translation. A well-established consequence of increased phosphorylation of eIF2 α is the inhibition of global translation and increase in selective protein synthesis. This causes an increase in the accumulation of untranslated mRNAs (Srivastava et al., 1998). Untranslated mRNAs are recruited to stress granules (SGs) which in addition to being in a dynamic equilibrium with polysomes, also contain many components of the cap-dependent pre-initiation complex (Kedersha et al., 2002). The formation of SGs re-localises cellular proteins and untranslated RNAs, and it has been shown that scaffold proteins such as Vinexin can be re-distributed from focal adhesions (FAs) to SG through association with CPEB4 (Chang and Huang, 2014). Promotion of the CPEB4-Vinexin interaction, and consequent Vinexin-Vinculin disassociation, through phospho-eIF2 α induced SG formation could affect cell migration through alterations in the dynamics of FAs. Therefore, although the tRNA_i^{Met} effect on cell migration is dependent on the TC, whether it exerts its effects directly, or indirectly, is yet to be determined.

In addition to its dependency on TC formation, iMEF.tRNA_i^{Met}-driven cell migration was also dependent on the ability of integrin $\alpha_5\beta_1$ to bind fibronectin (Figure 3-15, Figure 3-16 & Figure 3-17). When iMEF.Vector cells were plated

onto substrates containing fibronectin it rendered their migration more iMEF.tRNA_i^{Met}-like (Figure 3-14), while blocking the ability of integrin $\alpha_5\beta_1$ to bind fibronectin inhibited the increase in migration induced by tRNA_i^{Met} expression (Figure 3-15, Figure 3-16, Figure 3-17). Previous work has shown that cells are able to endocytose fibronectin and re-secrete it from a late endosomal/lysosomal compartment (LE/Lys) to provide an autocrine ECM to promote increased cell migration (Sung et al., 2011, Sung and Weaver, 2011). However, there was no consistent significant difference detected in transcript, total protein level, surface expression, rate of internalisation or recycling of the fibronectin receptor integrin $\alpha_5\beta_1$ (Figure 3-18, Figure 3-19 & Figure 3-20), nor was there any difference in the secretion of fibronectin from the fibroblasts themselves (as will be discussed in the next chapter). Nevertheless, tRNA_i^{Met} overexpressing cells are more dependent on integrin $\alpha_5\beta_1$ -fibronectin interaction than iMEF.Vector control cells for their cell movement. It could therefore be possible that there are differences in intracellular signalling downstream of ligand activation of the integrin, and so despite the integrin $\alpha_5\beta_1$ expression being similar, if subsequent connections to the actin cytoskeleton are altered, or there are differences in the downstream interactome, then changes in these pathways could affect cell migration. Indeed, integrin $\alpha_5\beta_1$ can signal to Rho subfamily GTPases, such as RacGAP1, to control the levels of Rac and RhoA activity to drive invasion into fibronectin-containing matrices (Timpson et al., 2011, Jacquemet et al., 2013, Machacek et al., 2009). Furthermore, local degradation and translation of RhoA has also been shown to have important roles in Sema3A-induced growth cone collapse during axonal outgrowth (Deglincerti et al., 2015), thus connecting translational control with regulation of cell protrusions through RhoA-mediated signalling pathways. It would therefore be interesting to consider whether there are changes in localisation and/or switches in activation of such molecules following tRNA_i^{Met} overexpression.

In this chapter we have described how increased levels of tRNA_i^{Met} can have profound impacts on fibroblast behaviour. Despite not affecting the total level of protein synthesis, cell size, metabolism, proliferation, or rate of spreading, overexpression of tRNA_i^{Met} increases the migration speed of fibroblasts, and this increase in cell speed is dependent on TC formation and on the ability of integrin $\alpha_5\beta_1$ to bind fibronectin (Figure 3-21).

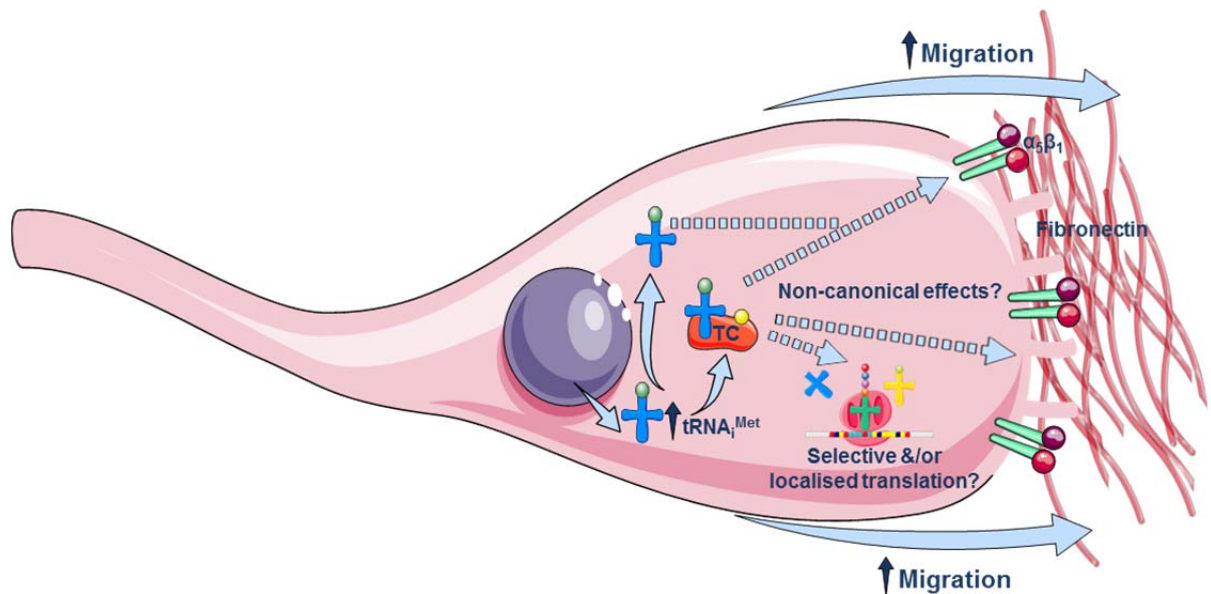


Figure 3-21- Model of the effect of $tRNA_i^{Met}$ overexpression on fibroblast behaviour.

Increased levels of $tRNA_i^{Met}$ increase the migration of fibroblasts through a mechanism that is dependent on the association of $tRNA_i^{Met}$ with the ternary complex, and the ability of integrin $\alpha_5\beta_1$ to bind fibronectin. It is currently unknown whether this is due to the effects of the ternary complex on protein synthesis, and/or whether this is directly related to integrin $\alpha_5\beta_1$ binding and responding to fibronectin. Image made using items from Image Bank in Servier Medical Art.

Although the mechanistic link between these two processes and increased $tRNA_i^{Met}$ expression still remains to be determined, taken together these data show that increased levels of specific tRNAs can influence fibroblast behaviour. These effects on cell migration are reminiscent of phenotypic effects seen in CAFs, and whilst CAFs can influence carcinogenesis through a number of mechanisms, their major influence is attributed to generation of a microenvironment that facilitates increased tumour growth. The next chapter will therefore explore the non-cell autonomous effects of $tRNA_i^{Met}$ overexpression, to understand whether small changes in the stromal cell tRNAome can influence the ECM secreted by fibroblasts to produce an environment that can support an increase in tumourigenicity.

Chapter 4 Increased tRNA_i^{Met} drives cell migration and tumour growth via non-cell autonomous mechanisms

4.1 Introduction

The microenvironment which surrounds tumour cells plays a key role in determining how they are able to grow and develop, and a key component of the tumour microenvironment (TME) is the fibroblasts and the ECM they secrete. Whilst the initial work of the Tlsty and Cunha groups highlighted the role of CAFs in cancer progression (Olumi et al., 1999), subsequent work has started to characterise how CAFs differ from their normal counterparts, and how these differences can account for the ability of CAFs to drive an increase in tumourigenicity (Orimo et al., 2005, Mitra et al., 2012).

In the previous chapter we found that increased expression of one particular tRNA, tRNA_i^{Met}, could influence distinct aspects of fibroblast behaviour. Published work has also described tissue-specific differences in tRNA expression across a variety of human tissues, with changes in relative expression levels correlating to the codon use of highly expressed genes in those tissues (Dittmar et al., 2006). Recent data has highlighted the coordination between tRNA supply and demand, demonstrating that cells can overexpress defined cohorts of tRNAs to increase the efficiency of translation of particular pathways (Gingold et al., 2014). In this study, proliferating cells were found to actively increase the transcription of tRNAs specific for codons overrepresented in pathways required for proliferation, essentially locking themselves into a proliferative state by optimising the translation of the components of these particular pathways. Additional work has also shown differential requirements for other components of the translation initiation machinery in normal development and cancer (Truitt et al., 2015), demonstrating that cancer cells can hijack excess levels of eIF4E to drive translation of oncogenic pathways. This dependency on components of the protein synthesis machinery is an effective mechanism to control translational efficiency in health, but can be exploited by cancer cells to drive specific gene expression programmes to support increased tumourigenicity in disease.

A number of publications have demonstrated that tRNAs are increased in different cancer types (Pavon-Eternod et al., 2009, Zhou et al., 2009, Mahlab et al., 2012). Although it was previously unknown whether this was a cause or consequence of carcinogenesis, understanding that expression of the components of the translation machinery can affect the efficiency of specific pathways highlights the possibility that tRNA levels could indeed play a role in cancer progression.

By focussing on the roles of specific tRNAs, a previous publication indicated that overexpression of tRNA_i^{Met} was able to essentially reprogramme global tRNA expression levels and increase proliferation of human epithelial cells (Pavon-Eternod et al., 2013). Other work also showed that increased levels of tRNA_i^{Met} could increase *Drosophila* larval growth owing to indirect effects involving increased mRNA translation and secretion of insulin-related peptides (Rideout et al., 2012). This *in vivo* effect on translation and protein secretion is particularly interesting, and again alludes to the fact that tRNA levels could function in regulating gene expression. Control of the CAF secretome through the mTOR/4E-BP1 pathway has been found to increase tumour growth and promote the chemoresistance of tumour cells, and selective inhibition of this pathway within CAFs can increase the sensitivity of cancer cells to chemotherapy (Duluc et al., 2015). Translational regulation therefore has a key role in cancer progression, not only within cancer cells themselves, but also in the stromal cells that support carcinogenesis (Gao and Roux, 2014, Loreni et al., 2014).

In this chapter we therefore sought to understand whether expression of tRNA_i^{Met} was differentially regulated in CAFs compared to NFs, and whether modulating the expression of tRNA_i^{Met} in fibroblasts could affect their role in the tumour microenvironment.

4.2 Results

4.2.1 Expression of tRNA_i^{Met} in cancer-associated fibroblasts

With an interest in understanding whether tRNA expression could help drive the pro-carcinogenic properties of CAFs, we used qPCR to quantify expression of tRNAs in immortalised human mammary cancer-associated fibroblasts (iCAFs) compared to immortalised patient-matched normal fibroblast controls (iNFs). These iCAFs have a greater capacity than iNFs to promote tumour growth and angiogenesis when co-injected with Ras transformed MCF7 cells as subcutaneous allografts, and are established to maintain their phenotype when grown in culture (Orimo et al., 2005). Increased expression of tRNA_i^{Met} and tRNA^{lle} was seen in iCAFs compared to iNFs, whilst no change was detected in the expression of 5S rRNA, another non-coding RNA transcribed by RNA Polymerase III (Pol III) (Figure 4-1A). The expression of tRNAs in primary fibroblasts isolated from tumour-associated or surrounding tissue in breast cancer patients was also assessed. From the 4 matched pairs of tumour-associated and ‘normal’ fibroblasts that were available, one displayed increased tRNA_i^{Met} expression in tumour-associated fibroblasts compared to those isolated from surrounding tissue (Figure 4-1B). Unfortunately no further clinical information was available on these particular patients, and so any correlation of increased tRNA_i^{Met} expression with breast cancer vascularity, subtype or stage could not be determined.

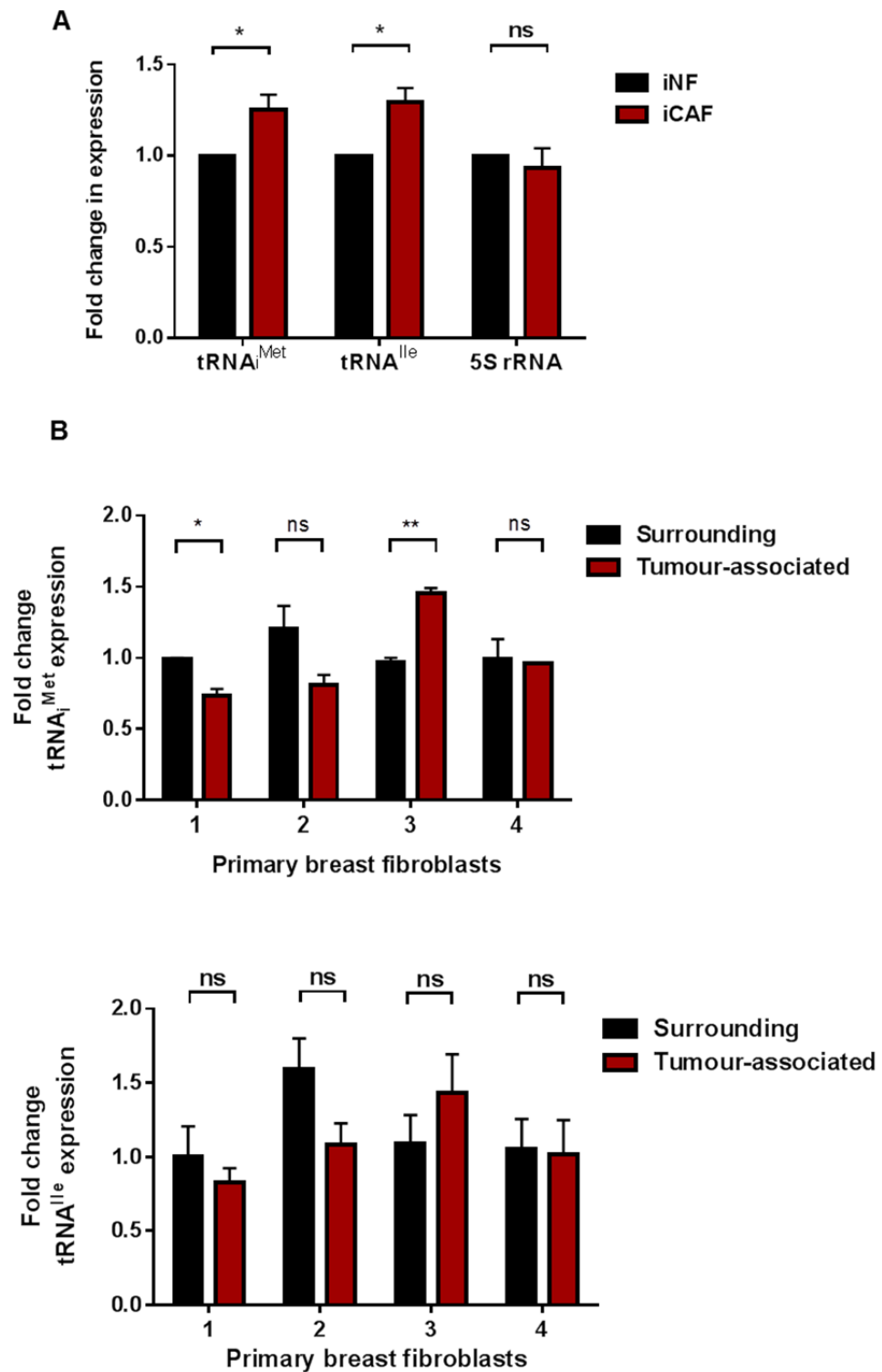


Figure 4-1- Changes in expression of specific tRNAs in cancer-associated fibroblasts and normal fibroblasts.

(A) qPCR was used to quantify the expression of tRNA_i^{Met}, tRNA^{Ile}, and 5S rRNA in immortalised normal fibroblasts (iNF) and immortalised cancer associated fibroblasts (iCAF). All samples are normalised to ARPP P0 and are presented relative to iNF, n=minimum of 3, +/- SEM, ANOVA, * p < 0.05. (B) qPCR was used to quantify the expression of tRNA_i^{Met} and tRNA^{Ile} in fibroblasts derived from breast tumour, or surrounding tissue, in four different breast cancer patients. All samples are normalised to ARPP P0 and are presented relative to expression of tRNA_i^{Met} in patient 1 surrounding fibroblasts, where 1 corresponds to patient number 1255, 2 is patient number 1764, 3 is patient number 1902 and 4 is patient number 1997, n=2, +/- SEM of the 2 biological replicates, ANOVA, * p < 0.05, ** p < 0.005, ns = not significant.

4.2.2 Increased expression of tRNA_i^{Met} in the host animal promotes growth and angiogenesis of allografted tumours

To further investigate the consequences of tRNA_i^{Met} overexpression in the stroma, we utilised a transgenic mouse expressing two additional copies of the tRNA_i^{Met} gene (2+tRNA_i^{Met} mouse) (Figure 4-2A). This resulted in a ubiquitous increase in tRNA_i^{Met} expression throughout the animal, including a 1.3 - 1.5 fold increase in expression in fibroblasts isolated from both the lungs and embryos of 2+tRNA_i^{Met} mice (Figure 4-2B), which was similar to increases previously seen in immortalised human CAFs (Figure 4-1A&B). To determine whether increased levels of tRNA_i^{Met} in the host animal could influence tumour progression, we introduced tumour cells into the 2+tRNA_i^{Met} mice as syngeneic subcutaneous allografts and recorded their growth. We initially used transformed melanoblasts derived from mice that were null for INK4a, and which expressed mutant NRas under a melanoblast specific promoter (Tyr:NrasQ61K;INK4a^{-/-}). These transformed melanoblasts grew more rapidly and reached their clinical end-point significantly faster in 2+tRNA_i^{Met} mice than they did in wild-type littermate controls (Figure 4-3A). To pursue this observation, we then introduced lewis lung carcinoma (LLC) or B16 F0 melanoma cells as subcutaneous syngeneic allografts into 2+tRNA_i^{Met} mice. When introduced into 2+tRNA_i^{Met} mice, both LLC (Figure 4-3B) and B16 F0 (Figure 4-3C) cells formed significantly larger and more vascularised tumours than when grown in wild-type littermate control animals, indicating that increased tRNA_i^{Met} expression in the host animal can promote increased angiogenesis and tumour growth.

A



B

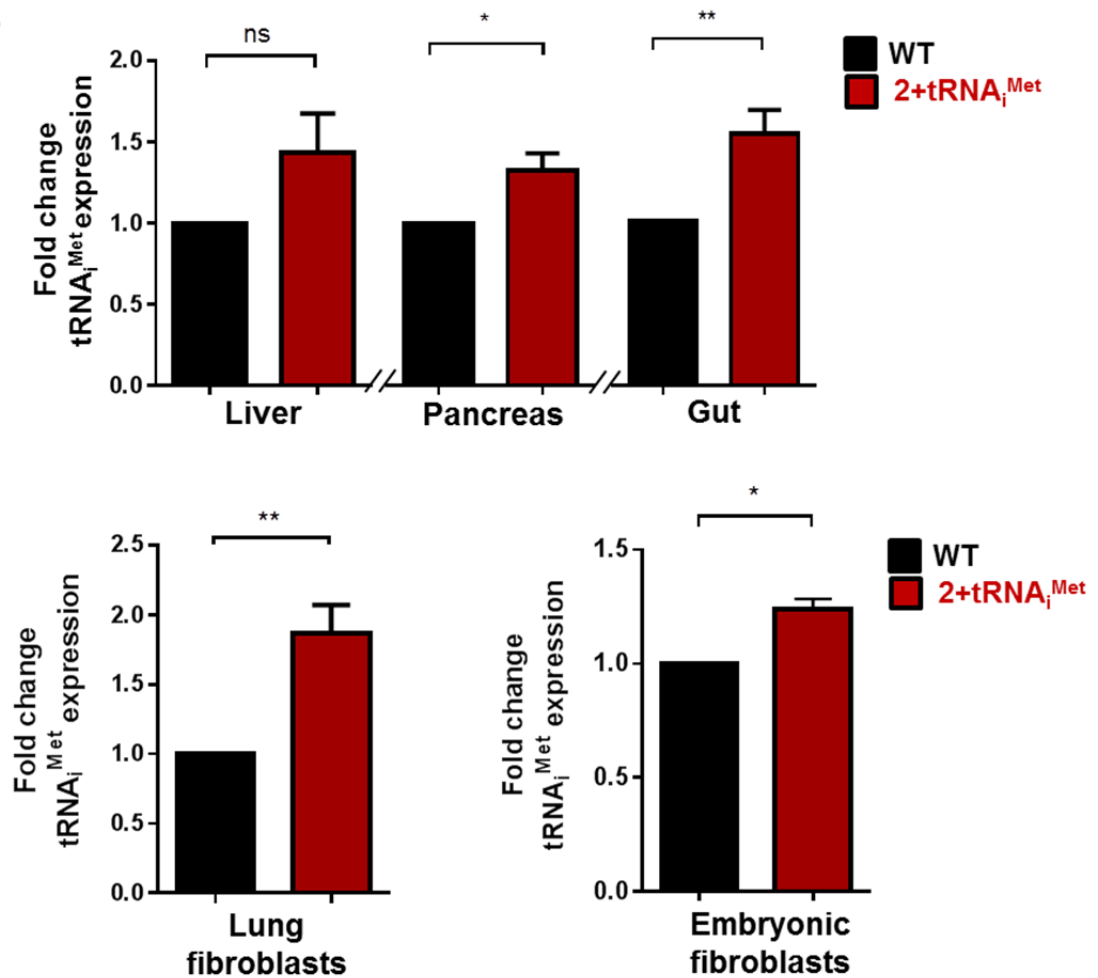


Figure 4-2- The 2+tRNA^{Met} transgenic mouse model.

(A) The HPRT-tRNA^{Met} targeted allele used to generate the 2+tRNA^{Met} transgenic mouse. Two additional copies of the tRNA^{Met} transgene were targeted to the HPRT locus on the X chromosome, with the targeted allele containing the human HPRT promoter sequence and exon 1 (box 1), and mouse HPRT exon 2 and 3 (box 2 and 3) (B) qPCR of tRNA^{Met} expression in various tissues and primary fibroblasts isolated from the lungs and embryos of the 2+tRNA^{Met} mouse, all samples normalised to ARPP P0, n=4 lung and n=2 embryonic fibroblasts, +/- SEM of biological replicates, unpaired t-test, ** p < 0.005, * p < 0.05. Tissue data provided by Dritan Liko, Kirsteen Campbell & Louise Mitchell, CR-UK Beatson Institute, Glasgow. Lung fibroblast data provided by Tracy Berg, Institute of Cancer Research, London.

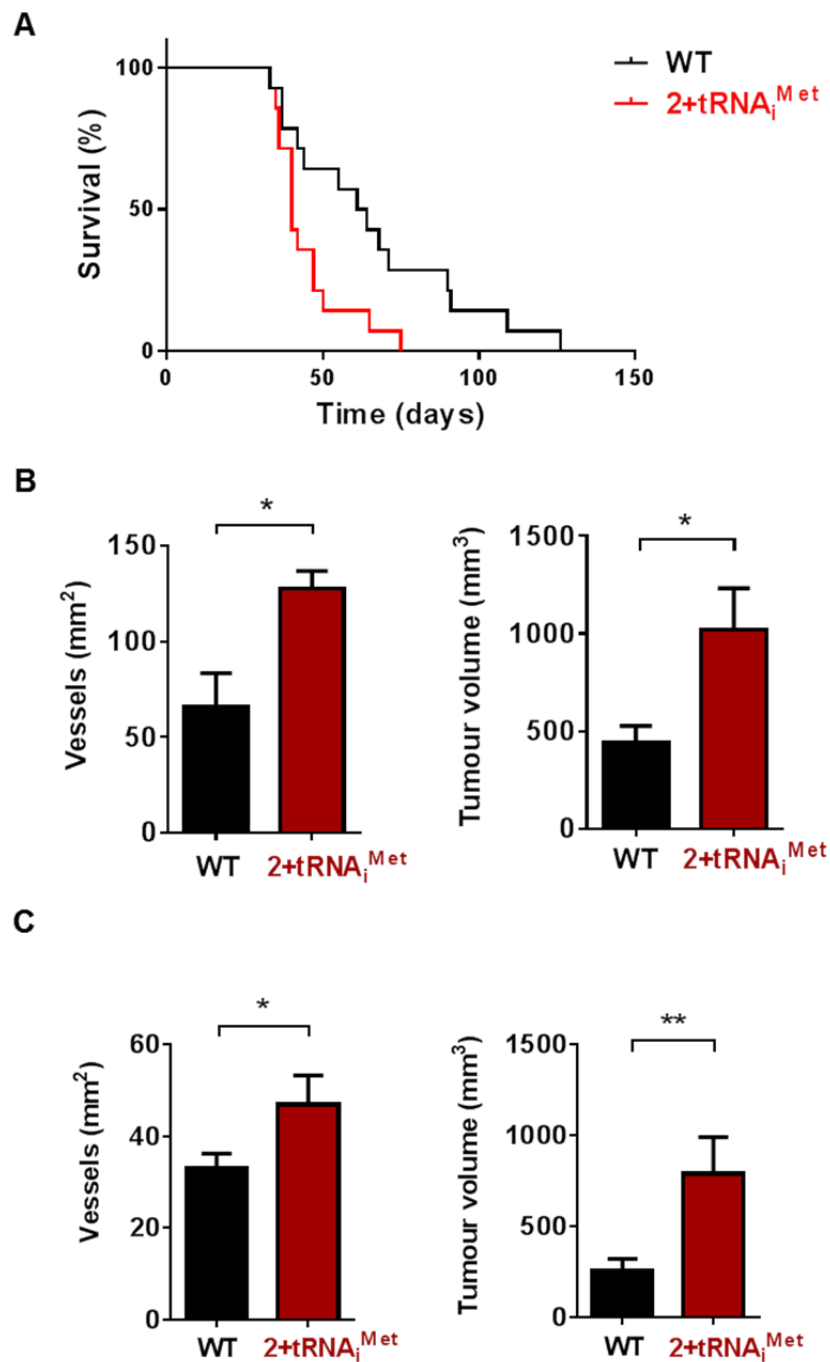


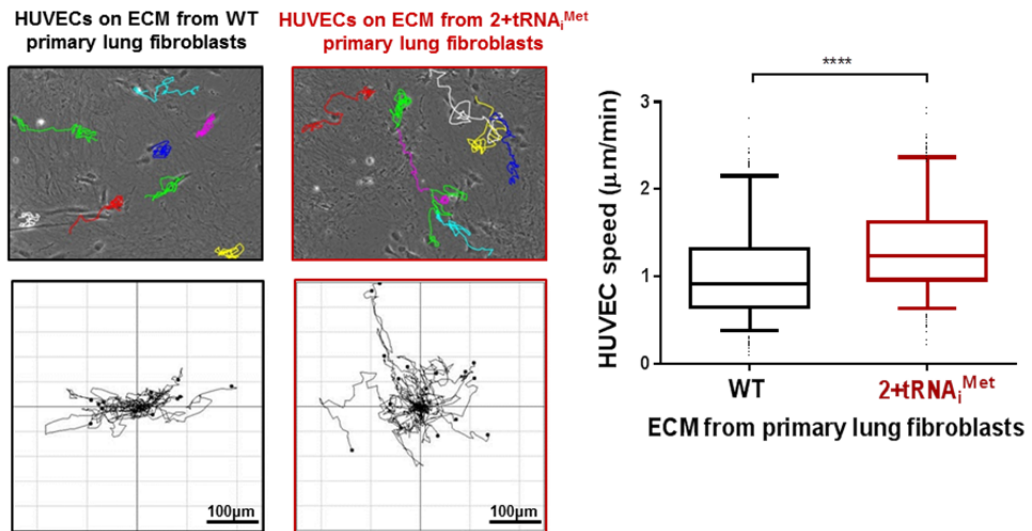
Figure 4-3- Increased expression of tRNA^{Met} in the host animal promotes angiogenesis and growth of allografted tumours.

(A) 1×10^6 transformed melanocytes (Tyr:NRasQ61K;Ink4a^{-/-}) were injected subcutaneously into littermatched WT or 2+tRNA^{Met} transgenic male mice and tumour size monitored. Mice were culled once tumours reached 15x15mm, and survival plotted by Kaplan-Meier, n = 14 WT mice, n = 14 2+tRNA^{Met} transgenic mice, Log-rank (Mantel-Cox) test, * p < 0.05. (B) 1×10^6 Lewis Lung Carcinoma cells were injected subcutaneously into littermatched WT or 2+tRNA^{Met} transgenic male mice. Tumours were harvested at 21 days and final tumour volume measured. Tumours were PFA fixed, stained with endomucin for blood vessel identification, and vessels counted across the entire tumour section, n = 10 WT mice, n = 9 2+tRNA^{Met} transgenic mice, +/- SEM, unpaired t-test, * p < 0.05. Experiment conducted by the Reynolds Lab, Institute of Cancer Research, London. (C) 0.5×10^6 B16 F0 mouse melanoma cells were injected subcutaneously into littermatched WT or 2+tRNA^{Met} transgenic male mice. Tumours were harvested 22 days from tumour establishment (classed as minimum 3x3mm measurable tumour), n = 20 WT mice, n = 14 2+tRNA^{Met} transgenic mice, +/- SEM, unpaired t-test, * p < 0.05, ** p < 0.005. Experiment conducted by the Reynolds Lab, Institute of Cancer Research, London.

4.2.3 Fibroblasts isolated from 2+tRNA_i^{Met} transgenic mice deposit a pro-migratory ECM

A key component of the tumour microenvironment that can influence cancer cell behaviour is the ECM deposited by stromal fibroblasts. To determine whether tRNA levels influence the characteristics of fibroblast-derived ECM we isolated fibroblasts from the lungs and embryos of 2+tRNA_i^{Met} mice, used them to prepare cell-derived matrices by previously established methods (Caswell et al., 2008, Cukierman et al., 2001, Vlodavsky, 1999), and assessed the ability of this cell-free ECM to support the migration of other cells. When used as a substrate for cell migration, the ECM derived from primary cells from 2+tRNA_i^{Met} mice was able to promote an increase in the migration speed of both endothelial cells and fibroblasts (Figure 4-4A&B). This suggested a role for tRNA_i^{Met} in driving changes in the ECM secreted by fibroblasts to promote endothelial cell migration that could contribute to angiogenesis and increase the migration of fibroblasts to further remodel the ECM.

A



B

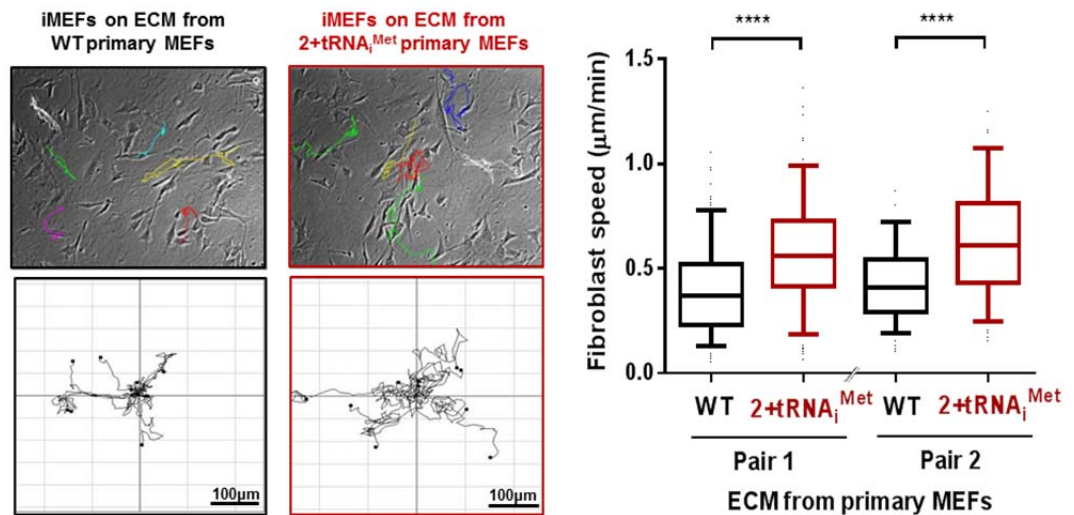


Figure 4-4- Fibroblasts isolated from 2+tRNA^{Met} transgenic mice deposit a pro-migratory ECM.

(A) ECM was generated from primary lung fibroblasts isolated from either WT or 2+tRNA^{Met} transgenic mice. Migration of human umbilical vein endothelial cells (HUVEC) on the ECM was recorded by timelapse microscopy and analysed in ImageJ. Data represents ECM generated from 7 independent isolations of primary fibroblasts from pools of 3 x WT and 3 x 2+tRNA^{Met} transgenic mice, tracking the migration of at least 28 HUVECs in each replicate. Box and whisker plot represents 5-95 percentile, Mann-Whitney test, **** $p < 0.0001$. Data provided by Tracy Berg, Institute of Cancer Research, London. (B) ECM was generated from primary fibroblasts isolated from littermatched WT or 2+tRNA^{Met} primary mouse embryonic fibroblasts (MEFs). Migration of immortalised MEFs (iMEFs) on the ECM was recorded by timelapse microscopy over a 17 hour time course, and analysed in ImageJ. Data represents ECM generated from 1 independent isolation of primary fibroblasts from two pairs of littermatched WT and 2+tRNA^{Met} transgenic mice, tracking the migration of at least 60 iMEFs in each replicate, $n=3$ for pair 1, $n=2$ for pair 2. Box and whisker plot represents 5-95 percentile, Mann-Whitney test, **** $p < 0.0001$.

4.2.4 tRNA_i^{Met} supports deposition of pro-migratory ECM via release of secreted factors

Many ECM components are secreted from fibroblasts as soluble proteins, and are then subsequently incorporated into the insoluble ECM. To determine the stage at which increased tRNA_i^{Met} expression influenced ECM deposition we went on to generate cell derived matrices from iMEF.tRNA_i^{Met} and iMEF.Vector cell lines. ECM generated from iMEF.tRNA_i^{Met} cells was also able to support increased migration speed of fibroblasts compared to ECM derived from iMEF.Vector control cells (Figure 4-5A). Furthermore, conditioned media from iMEF.tRNA_i^{Met} cells, when incubated with control fibroblasts, also enabled iMEFs to generate an ECM that could support increased cell migration (Figure 4-5B&C), indicating that tRNA expression levels can influence the synthesis and secretion of soluble ECM components.

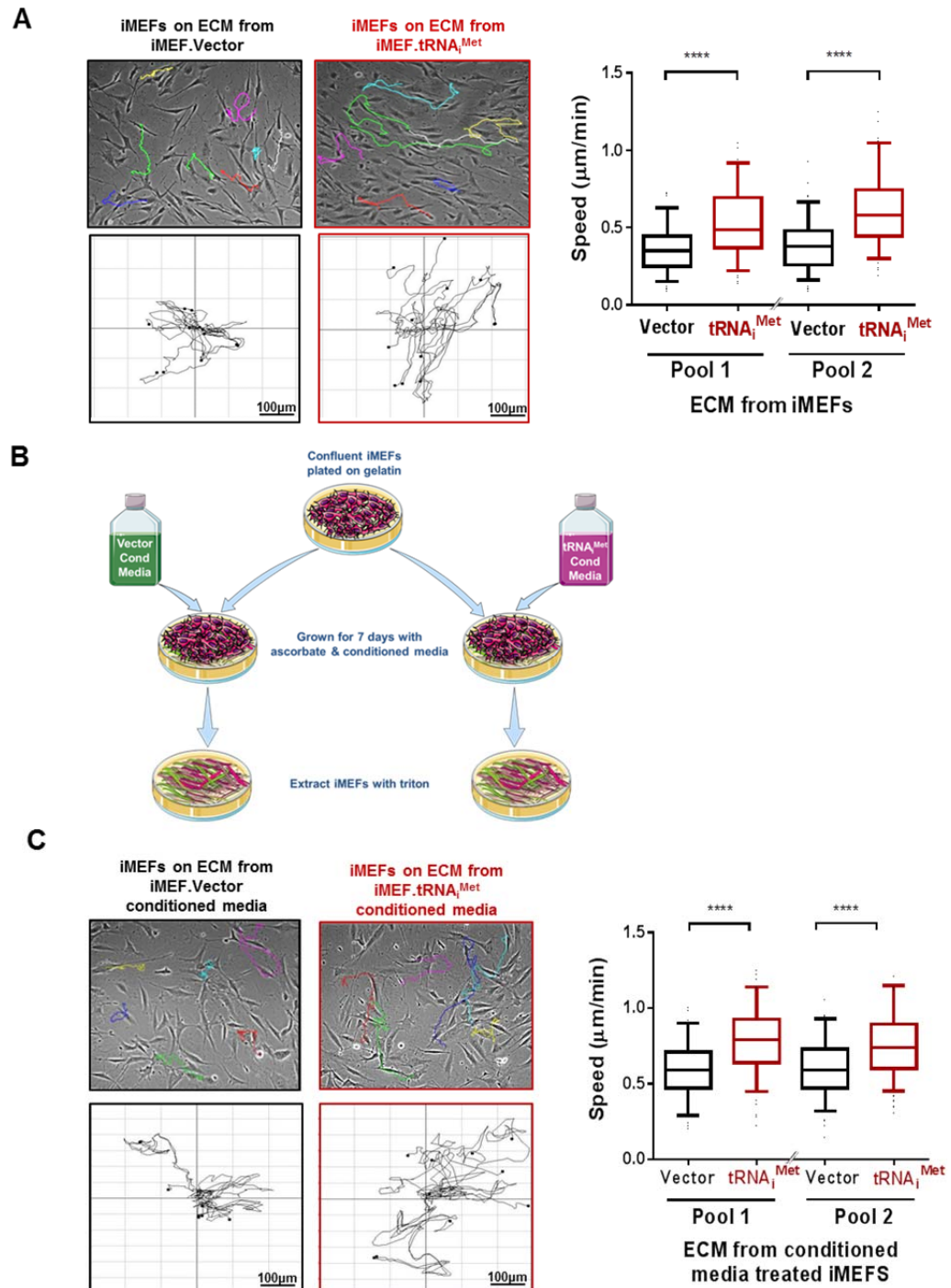


Figure 4-5- $tRNA_i^{Met}$ supports deposition of pro-migratory ECM via release of secreted factor(s).

(A) Migration of iMEFs on ECM was recorded by timelapse microscopy over a 17 hour time course and analysed in ImageJ for ECM generated from immortalised fibroblasts (iMEFs) stably overexpressing either empty vector (iMEF.Vector) or $tRNA_i^{Met}$ (iMEF. $tRNA_i^{Met}$). (B) Schematic representation of ECM derived from conditioned media treated cells. iMEF vector cells were plated to confluence on gelatin coated plates, and then cultured for 7 days in the presence of filter-sterilised conditioned media from iMEF.Vector or iMEF. $tRNA_i^{Met}$ cells, which was diluted 1:1 with fresh media and refreshed every other day for 7 days. Cells were then removed using a triton containing buffer, and the ECM used as a substrate for cell migration (C) Migration of iMEFs on ECM generated from iMEFs in the presence of conditioned media from iMEF.Vector or iMEF. $tRNA_i^{Met}$ cells was recorded by timelapse microscopy over a 17 hour time course and analysed in ImageJ. All data represents ECM generated from at least 3 independent ECM isolations, tracking the migration of at least 40 iMEFs in each replicate. Box and whisker plot represents 5-95 percentile, Mann-Whitney test, **** $p < 0.0001$.

Cell migration can be influenced by the mechanical properties of the ECM, and secreted enzymes such as lysyl oxidases and transglutaminases, have been shown to increase ECM stiffness to promote cell migration (Baker et al., 2013). Importantly, atomic force microscopy (AFM) showed that the ECM generated in the presence of conditioned media from iMEF.tRNA_i^{Met} cells was not thicker, nor was it consistently different in stiffness, than the ECM deposited in the presence of conditioned media from iMEF.Vector control cells (Figure 4-6). This therefore indicates that tRNA_i^{Met} overexpression supports deposition of a pro-migratory ECM via release of a secreted factor(s), and is not due to any physical changes in stiffness of the matrix.

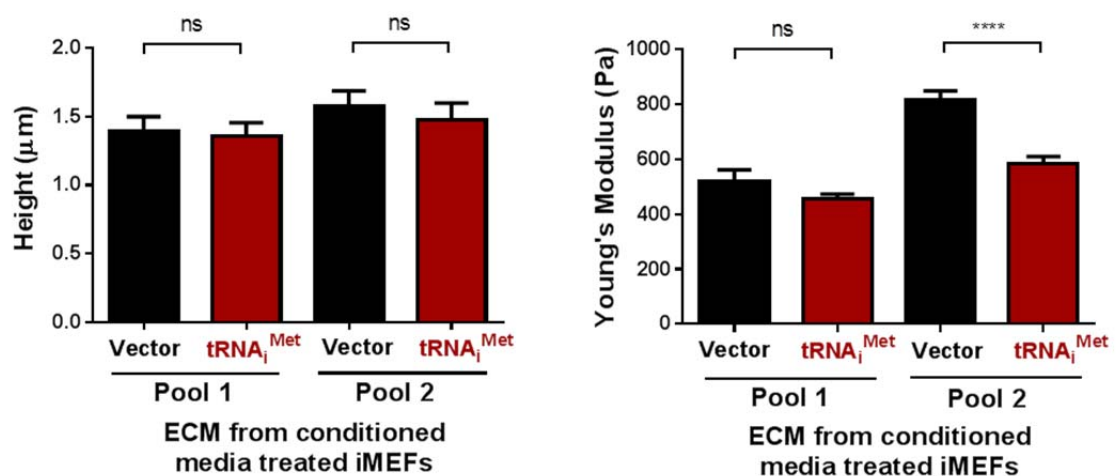


Figure 4-6- No consistent difference in the thickness or stiffness of the pro-migratory ECM generated in the presence of conditioned media from tRNA_i^{Met} overexpressing cells.

Atomic force microscopy and contact imaging were performed using a JPK NanoWizard II Bio AFM in combination with a Bruker MLCT cantilever and to measure the thickness the ECMs following wound scratch, or a Nanoworld Arrow TL-1 cantilever with bead attached for force spectroscopy, n=3 independent ECM generations, +/- SEM, **** p < 0.0001, ns = not significant, ANOVA test. Experiment conducted in collaboration with Ellie Pulleine, University of Glasgow.

Previously published work has highlighted the ability of microvesicles (MVs) released by fibroblasts to mediate tumour-stroma communication and influence cancer cell motility (Luga and Wrana, 2013). To assess whether any of the secreted factors that mediate tRNA_i^{Met}'s ability to generate pro-migratory ECM might be MV-associated, we centrifuged the conditioned media collected from iMEF.Vector and iMEF.tRNA_i^{Met} cells to deplete it of MVs and assessed its subsequent ability to influence the ECM deposited by iMEFs. Centrifugation of iMEF.tRNA_i^{Met} conditioned media did not affect its ability to support the deposition of a pro-migratory ECM (Figure 4-7), indicating that tRNA_i^{Met}-driven

MV release is not a key mediator of this tRNA's ability to influence ECM generation.

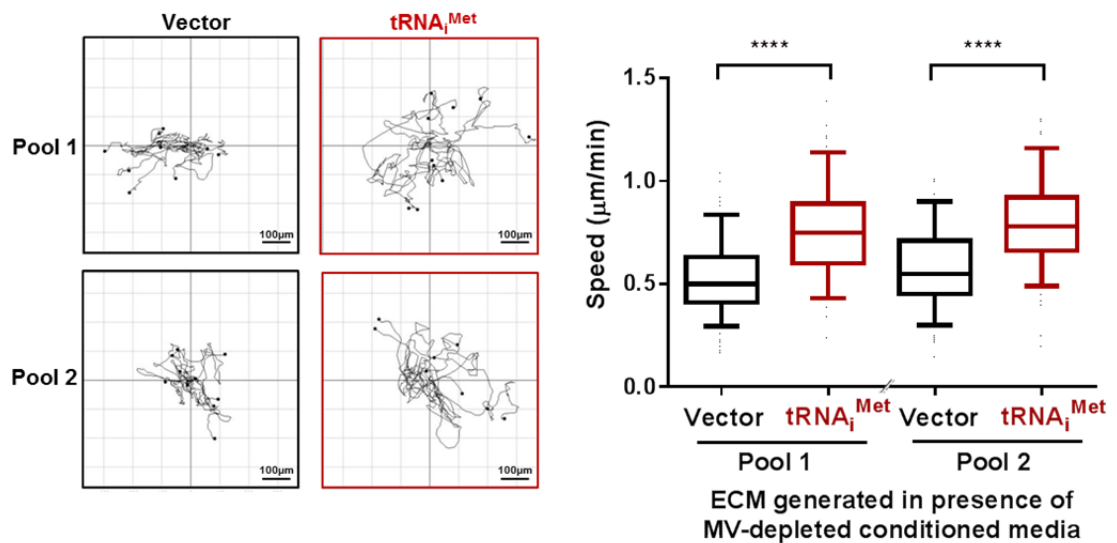


Figure 4-7- Microvesicles are not the secreted factor required for tRNA^{Met} to support deposition of pro-migratory ECM.

ECM was generated from iMEFs in the presence of microvesicle depleted conditioned media from iMEF.Vector or iMEF.tRNA^{Met} cell lines. Migration of iMEFs on the ECM was recorded by timelapse microscopy over a 17 hour time course and analysed in ImageJ. Data represents ECM generated from at least 3 independent ECM isolations, tracking the migration of at least 40 iMEFs in each replicate. Box and whisker plot represents 5-95 percentile, Mann-Whitney test, **** p < 0.0001.

Other published work has shown that secreted factors can modify the ECM in a way that does not necessarily depend on the presence of the matrix-depositing cells. For example, enzymes such as lysyl oxidase and tissue transglutaminase are capable of catalysing the formation of inter-chain cross-bridges and this can occur after matrix deposition (Cox et al., 2013, Forsprecher et al., 2009). Furthermore, if the conditioned media from tRNA^{Met} overexpressing cells were to be particularly rich in motogens possessing heparin-binding domains (such as fibroblast growth factors), these could potentially associate with the heparin sulphate groups of a pre-assembled ECM. We were therefore interested in understanding whether conditioned media from tRNA^{Met} overexpressing cells required the presence of cells to generate a pro-migratory ECM, or whether addition of conditioned media to cell-free ECM was sufficient to influence the matrix and increase cell migration. When conditioned media from either iMEF.Vector or iMEF.tRNA^{Met} cells was incubated with control, cell-free ECM for 24hr, and fibroblasts were then plated onto these matrices, no consistent difference in cell speed was observed between the two conditions. These data

indicate that factors released from $\text{tRNA}_i^{\text{Met}}$ overexpressing cells influence the way in which matrix proteins are deposited by fibroblasts, but they are not able to modify a pre-assembled ECM (Figure 4-8).

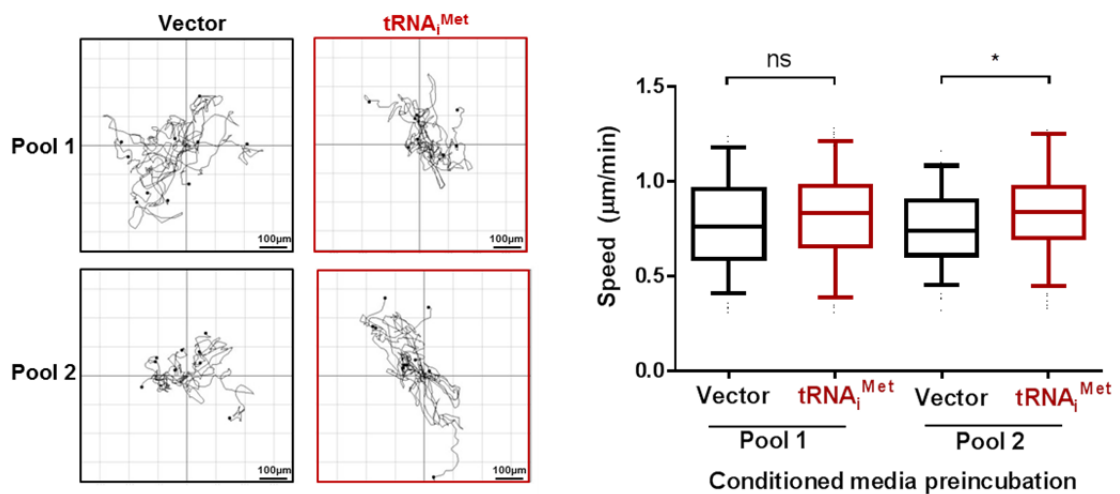


Figure 4-8- Conditioned media from $\text{tRNA}_i^{\text{Met}}$ overexpressing cells is not able to influence the migratory characteristics of pre-assembled ECM.

ECM was generated from iMEF.Vector cells and the cell free ECM was then incubated with conditioned media from iMEF.Vector or iMEF. $\text{tRNA}_i^{\text{Met}}$ cell lines for 24 hours. Migration of iMEFs on the ECM was recorded by timelapse microscopy over a 17 hour time course and analysed in ImageJ. Data represents ECM generated from 2 independent ECM isolations, tracking the migration of at least 40 iMEFs in each replicate. Box and whisker plot represents 5-95 percentile, Kruskal-Wallis test, * $p < 0.05$, ns = not significant.

Cell migration can be affected by a number of different parameters, and our previous data indicated that the $\text{tRNA}_i^{\text{Met}}$ effect on generation of a pro-migratory ECM was not owing to a change in the physical properties of the matrix, nor was it recapitulated by simply incubating the secreted factors with ECM alone. It therefore seemed likely to be due to a change in the composition of the ECM secreted by the $\text{tRNA}_i^{\text{Met}}$ overexpressing cells. A major component of the ECM secreted by fibroblasts is fibronectin, and initial fibronectin deposition and fibrillogenesis by integrin $\alpha_5\beta_1$ is an early and integral part of ECM generation. Data presented in the previous chapter indicate that when cells are plated onto plastic surfaces iMEF. $\text{tRNA}_i^{\text{Met}}$ -driven migration is dependent on the integrin $\alpha_5\beta_1$ -fibronectin interaction. We therefore proceeded to assess the migration of iMEF.Vector and iMEF. $\text{tRNA}_i^{\text{Met}}$ cells using their own pre-derived matrices as ECM substrates. When iMEF.Vector and iMEF. $\text{tRNA}_i^{\text{Met}}$ cells were plated onto their own cell-derived matrices, the ECM derived from iMEF. $\text{tRNA}_i^{\text{Met}}$ cells was able to promote increased cell migration, however the difference in migration speed between iMEF.Vector and iMEF. $\text{tRNA}_i^{\text{Met}}$ cell lines evident when these cells

migrate on plastic surfaces (as described in the previous chapter) was no longer apparent (Figure 4-9). Next, we determined the $\alpha_5\beta_1$ and fibronectin-dependence of $\text{tRNA}_i^{\text{Met}}$ -driven cell migration using the blocking antibodies described in the previous chapter. Blockade of integrin $\alpha_5\beta_1$ (using mAb16) or fibronectin's RGD site (with the 16G3 antibody) did not influence the migration speed of fibroblasts on ECM deposited by either iMEF.Vector or iMEF. $\text{tRNA}_i^{\text{Met}}$ overexpressing cells (Figure 4-10). These data indicate that the integrin $\alpha_5\beta_1$ -fibronectin interaction is not required for cell movement on cell-derived matrix, nor is $\alpha_5\beta_1$ required for fibroblasts to sense the pro-migratory properties of ECM derived from $\text{tRNA}_i^{\text{Met}}$ overexpressing cells.

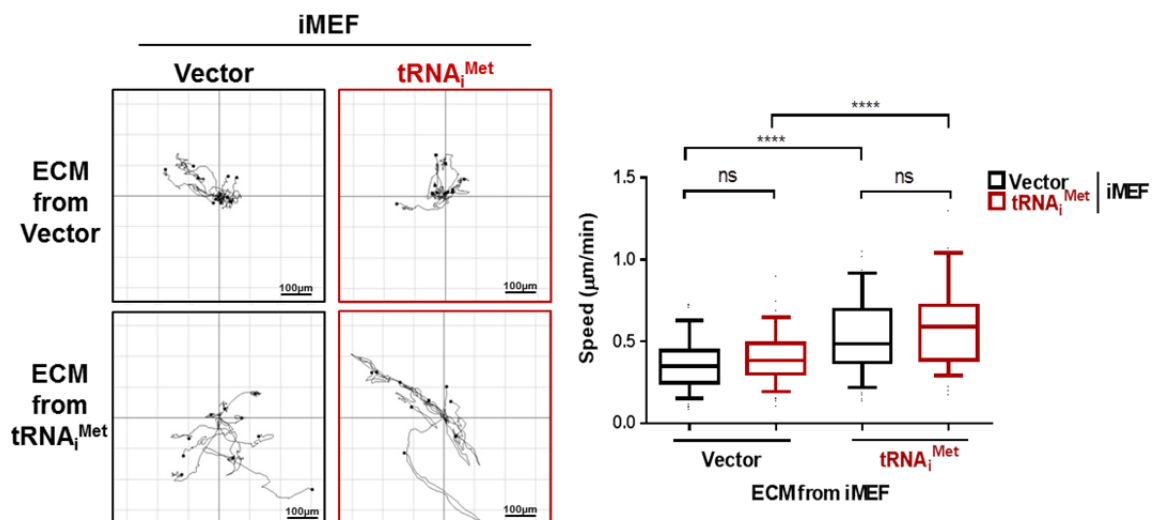


Figure 4-9- ECM derived from $\text{tRNA}_i^{\text{Met}}$ -overexpressing cells promotes increased migration of fibroblasts but negates the difference in migration between iMEF.Vector and iMEF. $\text{tRNA}_i^{\text{Met}}$.

iMEF.Vector and iMEF. $\text{tRNA}_i^{\text{Met}}$ cells were plated at 1×10^5 cells/well on ECM derived from iMEF.Vector or iMEF. $\text{tRNA}_i^{\text{Met}}$ cells and incubated at $37^\circ\text{C}/5\%\text{CO}_2$ for 2 hours to adhere. Random migration was then recorded by timelapse microscopy over a 17 hour time course. The data represents the speed of 30 – 40 cells per experiment, calculated using manual tracking in Image J over the 17 hour time course, $n=3$, box and whisker plot represents 5-95 percentile, Kruskal-Wallis test, **** $p < 0.0001$, ns = not significant.

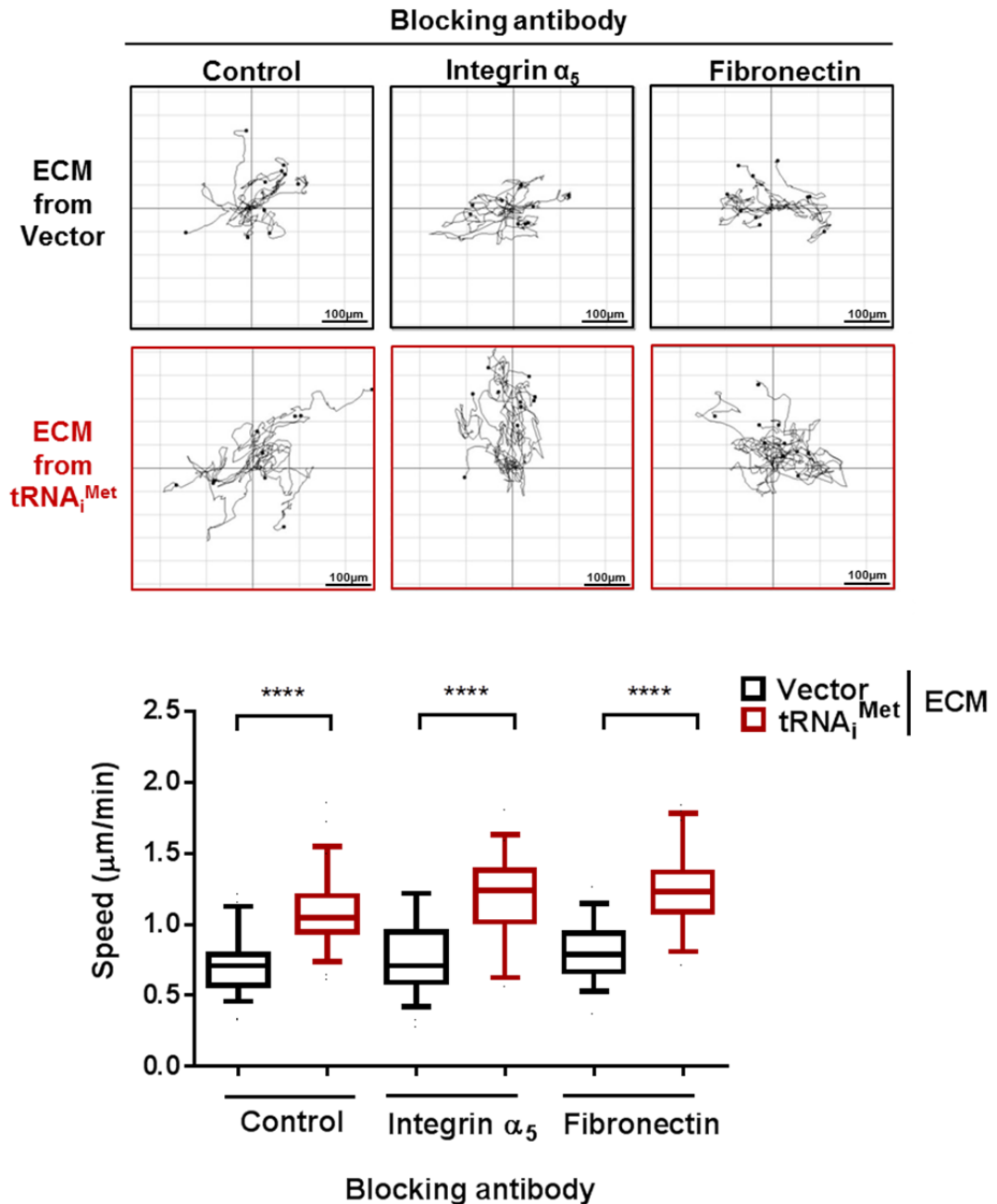


Figure 4-10- Integrin $\alpha_5\beta_1$ -fibronectin interaction does not influence fibroblast migration on ECM derived from control or tRNA_i^{Met} overexpressing cells.

ECM was generated from iMEF.Vector and iMEF.tRNA_i^{Met} cell lines, and iMEFs then incubated at 37°C/5%CO₂ on the ECM for 2 hours to adhere. Media was changed to contain 2µg/mL blocking antibody and incubated for a further 2 hours. Migration of iMEFs on the ECM was then recorded by timelapse microscopy over a 17 hour time course and analysed in ImageJ. Data represents ECM generated from 2 independent ECM isolations, tracking the migration of at least 40 iMEFs in each replicate. Box and whisker plot represents 5-95 percentile, Kruskal-Wallis test, **** p < 0.0001.

4.2.5 tRNA_i^{Met} drives a secretome that is enriched in collagen II and collagen-modifying enzymes

We used SILAC based mass spectrometry to quantitatively analyse the complement of soluble proteins secreted from control and tRNA_i^{Met}

overexpressing iMEFs (pool 1). Briefly, iMEF.tRNA_i^{Met} and iMEF.Vector cells were labelled with light and heavy amino acids respectively and combined for the forward experiment (FWD), with corresponding heavy and light amino acid labelling in the reverse experiment (REV). We used an affinity bead-based approach to extract the proteins secreted into serum-free conditioned media, and also prepared cell extracts for cellular proteome analysis. Analysis of the secretome showed that the most upregulated protein secreted following tRNA_i^{Met} overexpression was collagen II, while there was also an increase in secretion of additional collagens and collagen processing enzymes in the iMEF.tRNA_i^{Met} cell-exposed media (Figure 4-11A&C and Appendix I). The increase in secretion of ECM components was particularly striking, as over half of the significant changes in proteins secreted following tRNA_i^{Met} overexpression were associated with the ECM (highlighted in red, Figure 4-11A&C). Proteomic analysis on the cells themselves indicated that tRNA_i^{Met} expression also disproportionately increased cellular synthesis of secretory proteins, with 88% of the proteomic hits following tRNA_i^{Met} overexpression being secretory, while the production of other cellular components was not greatly affected (Figure 4-11B and Appendix II). Furthermore, specificity towards increased secretion of particular proteins was also apparent. Despite fibronectin being one of the most abundant proteins in the iMEF secretome, its levels were not changed following tRNA_i^{Met} overexpression, while expression of the normally less abundant collagen II was increased almost 70 fold (Figure 4-11D). Immunostaining of the ECM derived from iMEF.Vector and iMEF.tRNA_i^{Met} cells further confirmed that the collagen II secreted into the media was also incorporated into the ECM itself, with the level of collagen II incorporation correlating to the extent of tRNA_i^{Met} overexpression in the iMEF cell lines (Figure 4-11E and Figure 3-1).

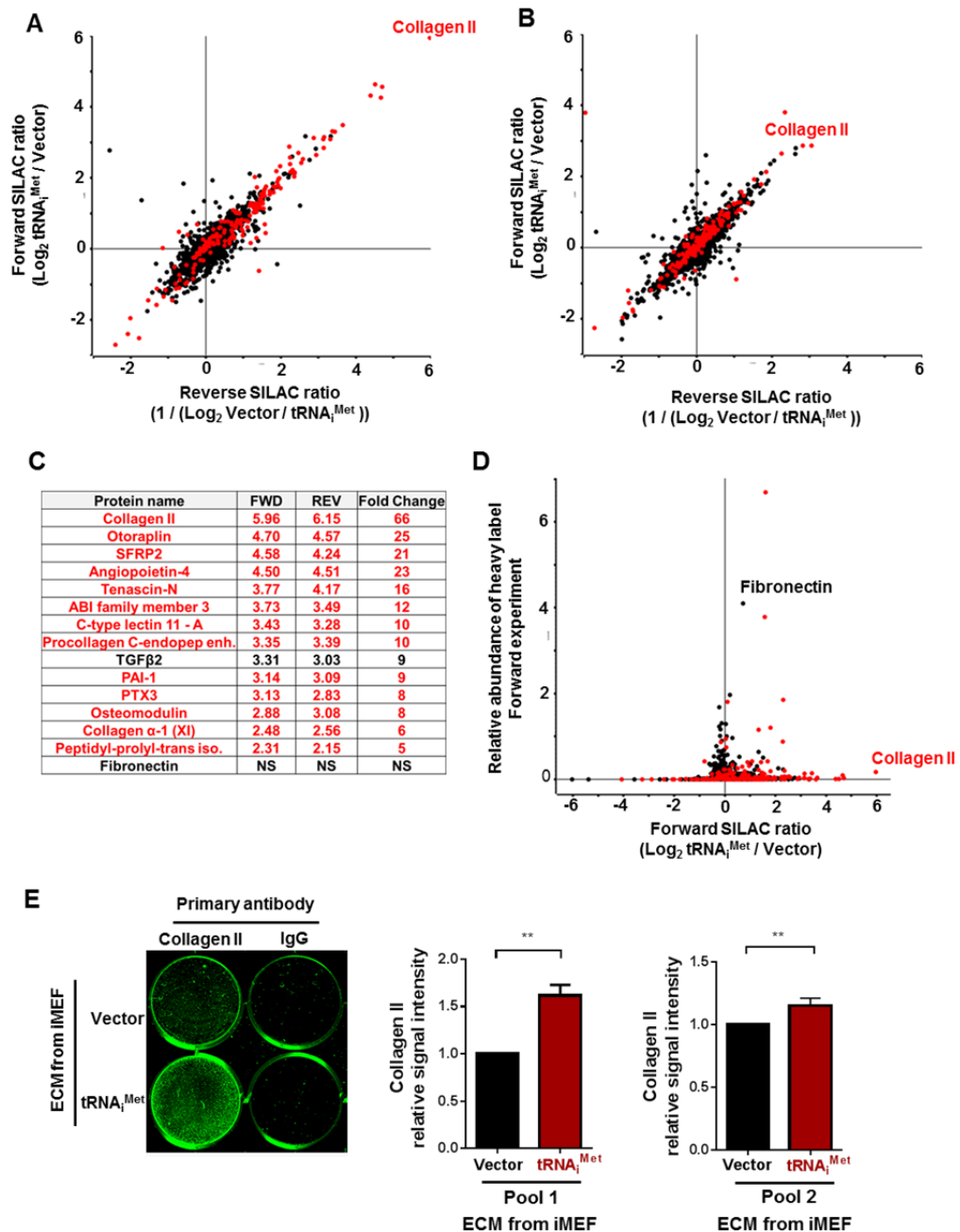


Figure 4-11- $tRNA_i^{Met}$ drives a secretome that is enriched in collagen II and collagen-modifying enzymes.

(A) The secretome was analysed following $tRNA_i^{Met}$ overexpression using quantitative SILAC mass spectrometry. iMEF.Vector and iMEF. $tRNA_i^{Met}$ cells were labelled with heavy and light amino acids, secreted proteins isolated from the conditioned media, separated by gel electrophoresis, and then analysed by mass spectrometry. Forward experiment (FWD) corresponds to iMEF. $tRNA_i^{Met}$ cells labelled with heavy amino acids combined with iMEF.Vector cells labelled with light amino acids, and the reverse experiment (REV) corresponds to iMEF.Vector cells labelled with heavy amino acids combined with iMEF. $tRNA_i^{Met}$ cells labelled with light amino acids. ECM associated proteins are highlighted in red. (B) The total cellular proteome of iMEF.Vector and iMEF. $tRNA_i^{Met}$ cells, ECM proteins are highlighted in red. (C) A table of some of the top upregulated secreted proteins identified in the media in the secretome following $tRNA_i^{Met}$ overexpression. (D) Data from (A) replotted to show the total abundance of proteins identified in the media of iMEF. $tRNA_i^{Met}$ cells against the fold change in expression of proteins in the iMEF. $tRNA_i^{Met}$ cells compared to iMEF.Vector. (E) ECM was generated from iMEF.Vector and iMEF. $tRNA_i^{Met}$ cells. Incorporation of collagen II into the ECM was assessed by immunostaining using collagen II specific antibodies, and quantified using the Aeries infrared imaging system (LI-COR® Biosciences), unpaired t-test, $**p < 0.005$ (A-D data generated in collaboration with David Sumpton, CR-UK Beatson Institute, Glasgow).

After discovering the striking effects of $\text{tRNA}_i^{\text{Met}}$ on the synthesis and secretion of collagen II and ECM components at the proteomic level, we were also interested in understanding whether these effects were reflected at the level of transcription. We used RNA sequencing (RNA-Seq) to analyse the transcriptome of iMEF.Vector and iMEF. $\text{tRNA}_i^{\text{Met}}$ (pool 1) cells. Distance heatmaps by biological sample showed that iMEF. $\text{tRNA}_i^{\text{Met}}$ cells did indeed cluster separately from iMEF.Vector cells on the basis of their transcriptome (N.B., the third biological repeat of iMEF. $\text{tRNA}_i^{\text{Met}}$ clustered with control cells, the reason for this experimental variability was unknown, and so the data set was still included in all analysis) (Figure 4-12A and Appendix III). Pathway enrichment analysis of genes differentially expressed following $\text{tRNA}_i^{\text{Met}}$ overexpression showed that stellate cell activation, liver fibrosis, and ECM remodelling were among the top pathways enriched at the transcriptomic level following $\text{tRNA}_i^{\text{Met}}$ overexpression (Figure 4-12B). Whilst our previous data had already highlighted the role of $\text{tRNA}_i^{\text{Met}}$ in ECM remodelling, the pathway enrichment analysis provided additional support for this, as activated stellate cells are also responsible for secreting collagen scar tissue and inducing fibrogenic activity (Mannaerts et al., 2013). Moreover, it also raised the possibility that $\text{tRNA}_i^{\text{Met}}$ overexpression may also be affecting cellular differentiation and so could essentially be acting to reprogramme fibroblast cell fates.

A large proportion of the most upregulated proteins previously identified following $\text{tRNA}_i^{\text{Met}}$ overexpression were also upregulated in this RNA-Seq analysis of the transcriptome, including collagen II (Figure 4-12C). We used qPCR to validate the increase in collagen II mRNA levels identified following $\text{tRNA}_i^{\text{Met}}$ overexpression, and found that this was indeed the case for iMEF pool 1 (the same pool used for the RNA-Seq experiments). However, there was no change in collagen II mRNA levels in iMEF pool 2 following $\text{tRNA}_i^{\text{Met}}$ overexpression (Figure 4-12D) despite these cells still increasing the incorporation of collagen II protein into the ECM and being able to deposit a highly pro-migratory matrix (Figure 4-11E & Figure 4-5A&B). As previously shown in Figure 3-1, the increase in $\text{tRNA}_i^{\text{Met}}$ expression in pool 1 is much greater than that of pool 2. It may therefore be possible for there to be a threshold required to see the effects of $\text{tRNA}_i^{\text{Met}}$ overexpression, and larger increases in $\text{tRNA}_i^{\text{Met}}$ are able to drive changes

at the level of both transcription and translation, whereas smaller increases in $\text{tRNA}_i^{\text{Met}}$ expression result only in regulation at the post-transcriptional level.

As conditioned media from $\text{tRNA}_i^{\text{Met}}$ overexpressing cells was sufficient to enable fibroblasts to generate a pro-migratory ECM, we wanted to understand whether factors in the media were affecting gene expression pathways in the cells forming the ECM, or whether the conditioned media was simply providing extra soluble components to be incorporated into the matrix by the cells. We therefore treated iMEF.Vector cells with conditioned media from either iMEF. $\text{tRNA}_i^{\text{Met}}$ or iMEF.Vector cells and used RNA-Seq to analyse any changes in gene expression. The transcriptome of iMEF.Vector cells remained largely unchanged regardless of whether they were treated with conditioned media from control or $\text{tRNA}_i^{\text{Met}}$ overexpressing cells (N.B., the third biological repeat of cells treated with iMEF. $\text{tRNA}_i^{\text{Met}}$ conditioned media clustered separately from all the other samples, but the data set was still included in all analysis) (Figure 4-12E). In fact, only five genes in the iMEF.Vector cells were significantly differentially regulated following treatment with iMEF. $\text{tRNA}_i^{\text{Met}}$ or iMEF.Vector cell conditioned media (Figure 4-12F). Considering over 400 genes were differentially regulated between iMEF. $\text{tRNA}_i^{\text{Met}}$ and iMEF.Vector cells, it seems that alterations to the secretome following $\text{tRNA}_i^{\text{Met}}$ overexpression do not affect gene expression in neighbouring cells, but simply provide increased levels of soluble ECM components which these cells can then incorporate into the surrounding microenvironment.

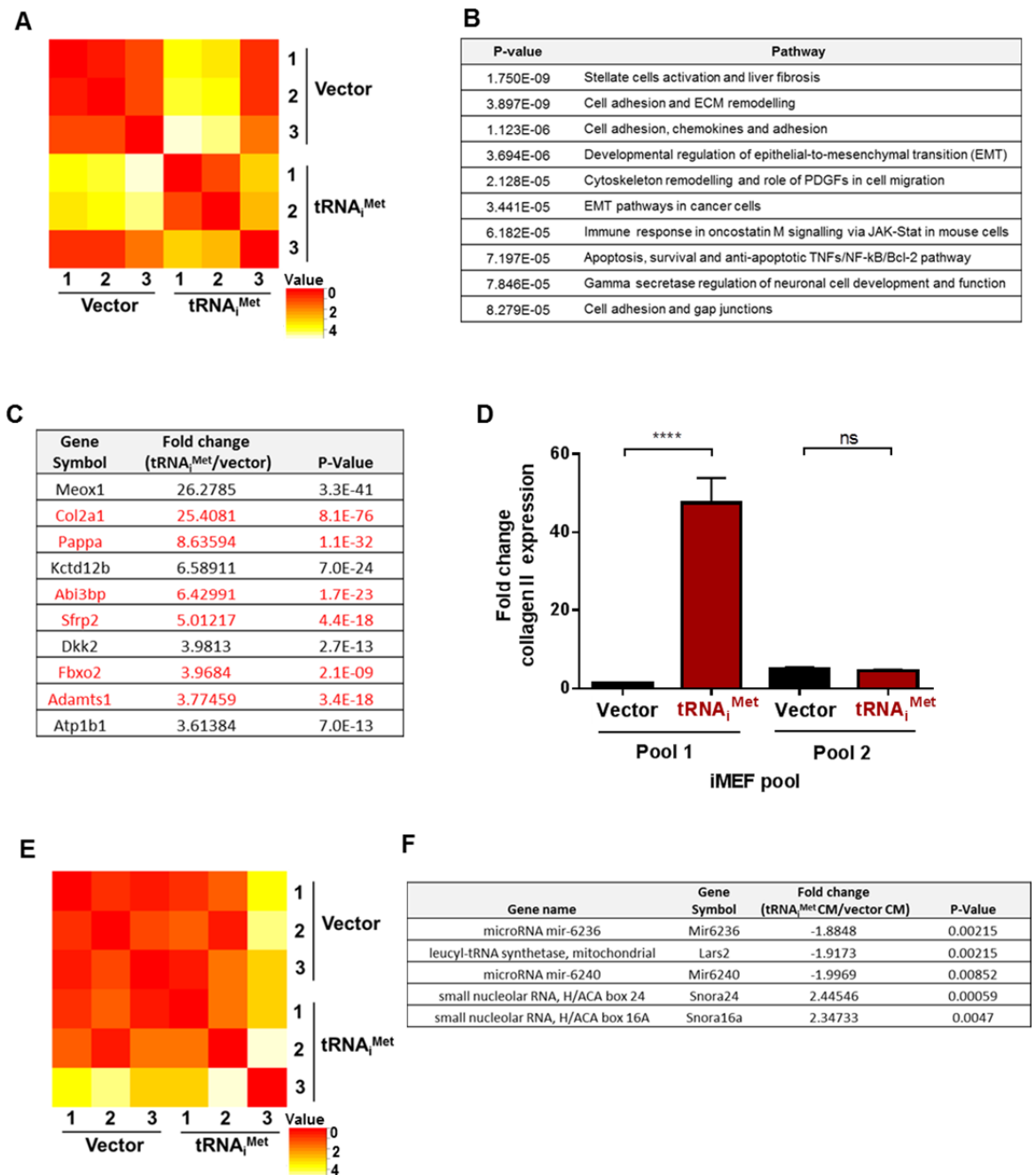


Figure 4-12- RNA sequencing following tRNA_i^{Met} overexpression.

(A) Heatmap cluster analysis representing differences in gene expression between iMEF.tRNA_i^{Met} and iMEF.Vector cells. Red represents similarity, with progression to yellow representing increasing differences. Number represents the number of biological replicate. (B) Pathway enrichment analysis of genes differentially expressed in iMEF.tRNA_i^{Met} compared to iMEF.Vector cells. (C) The top 10 upregulated genes expressed in iMEF.tRNA_i^{Met} compared to iMEF.Vector cells, with red text highlighting those genes that were also upregulated at the level of the secretome. (D) qPCR to quantify the levels of collagen II expression in pools of iMEF.tRNA_i^{Met} and iMEF.Vector cells, presented relative to iMEF.Vector pool 1, and normalised to ARPP P0, n=3, +/- SEM, ANOVA, **** p < 0.0001, ns = not significant. (E) Heatmap cluster analysis representing differences in gene expression between iMEF.Vector cells treated with conditioned media from iMEF.tRNA_i^{Met} or iMEF.Vector cells. Red represents similarity, with progression to yellow representing increasing differences. (F) The only differentially expressed genes in iMEF.Vector cells following treatment with iMEF.tRNA_i^{Met} conditioned media compared to iMEF.Vector conditioned media.

4.2.6 Collagen II secretion is required for tRNA_i^{Met} to drive production of pro-tumourigenic ECM

To assess whether collagen II secretion was responsible for the ability of tRNA_i^{Met} overexpression to drive deposition of pro-migratory ECM, cell-derived matrices were generated from iMEFs cultured with conditioned media from iMEF.tRNA_i^{Met} cells which had previously been transfected with non-targeting (NT) or collagen II specific siRNA (Figure 4-13A). Knockdown of collagen II in iMEF.tRNA_i^{Met} cells resulted in conditioned media that had a decreased ability to enable iMEFs to generate an ECM that supported increased fibroblast migration (Figure 4-13B-D). Furthermore, knockdown of collagen II in primary lung fibroblasts isolated from 2+tRNA_i^{Met} mice also compromised the ability of the ECM derived from these cells to support increased migration of endothelial cells (Figure 4-13E).

We also studied ECM that had been deposited by iMEFs in which we had used a CRISPR gene editing approach to stably knockdown collagen II levels (MEF.tRNA_i^{Met} Collagen II CRISPR) (Figure 4-14A&B). Immunostaining of the ECM showed that CRISPR-mediated collagen II knockdown led to a significant decrease in the incorporation of collagen II into the matrix (Figure 4-14C), and this correlated with a decreased ability of this ECM to support increased cell migration (Figure 4-14D&E), reinforcing the conclusion that increased collagen II secretion following tRNA_i^{Met} overexpression is responsible for generation of a pro-migratory ECM.

To investigate the role of collagen deposition supporting tumourigenicity *in vivo*, we introduced lewis lung carcinoma cells as syngeneic allografts into WT and 2+tRNA_i^{Met} mice in the presence and absence of ethyl-3,4-dihydroxybenzoate (DHB), a prolyl hydroxylase inhibitor that is well established to compromise collagen synthesis *in vivo* (Gilkes et al., 2013). While DHB administration did not affect the vascularity or growth of tumours in WT mice, it did inhibit increased vascularity and growth of tumours in 2+tRNA_i^{Met} mice, indicating that collagen secretion is also required for tRNA_i^{Met} to drive production of a pro-tumourigenic ECM *in vivo* (Figure 4-15).

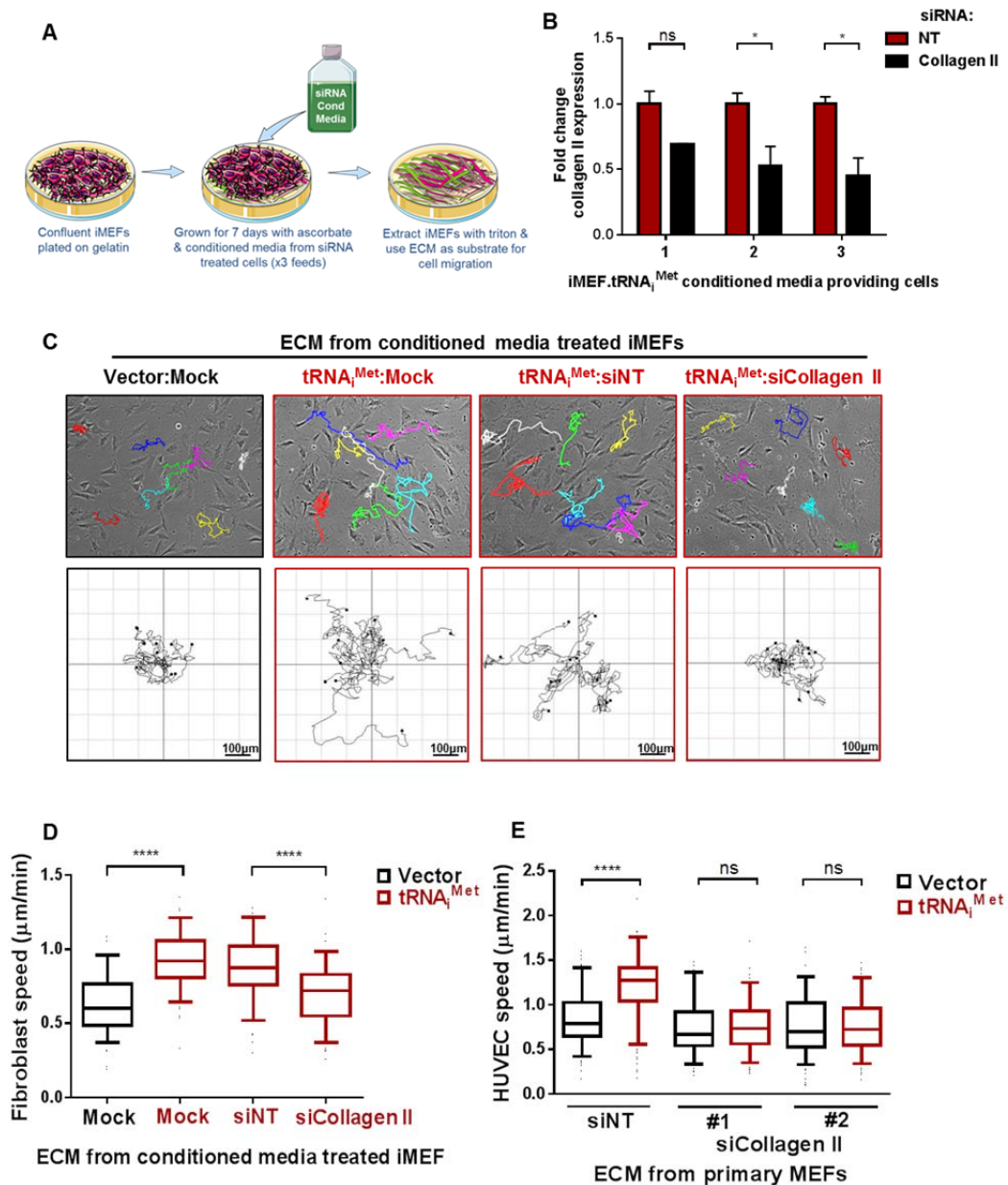


Figure 4-13- Collagen II secretion is required for tRNA^{Met} to drive production of a pro-migratory ECM.

(A) Schematic representation of method used to generate siRNA conditioned media derived ECM. iMEF cells were plated to confluence on gelatin coated plates, and then grown for a further 7 days in ascorbate containing media that was diluted 1:1 with filter sterilised conditioned media from iMEF.tRNA^{Met} cells treated with either NT or collagen II specific siRNA. The ascorbate media/conditioned media mix was refreshed and replaced every 2 days over the 7 day time course. Cells were then removed using a triton containing buffer, leaving the ECM of interest coating the culture dish. (B) qPCR was used to quantify collagen II knockdown in the cells providing conditioned media to generate the iMEF siRNA conditioned media derived ECM, all data normalised to ARPP P0 and presented relative to expression in the iMEF.tRNA^{Met} non-targeting siRNA treated cells. Data presented is representative of n=3 independent experiments, +/- standard deviation of technical replicates, ANOVA, *p<0.05. (C) Single cell traces and spiderplots representative of the data quantified in (D). Migration of iMEFs, or HUVECs were indicated, on ECM was recorded by timelapse microscopy over a 17 hour time course and analysed in ImageJ for (D) ECM generated from iMEFs in the presence of conditioned media from iMEF.tRNA^{Met} cells treated with NT or collagen II specific siRNA. (E) ECM generated from primary lung fibroblasts treated with NT or collagen II specific siRNA. HUVEC data provided by Tracy Berg, Institute of Cancer Research, London. Data represents ECM generated from at least 3 independent ECM isolations, tracking the migration of at least 40 iMEFs in each replicate. Box and whisker plot represents 5-95 percentile, Kruskal-Wallis test, **** p < 0.0001, ns = not significant.

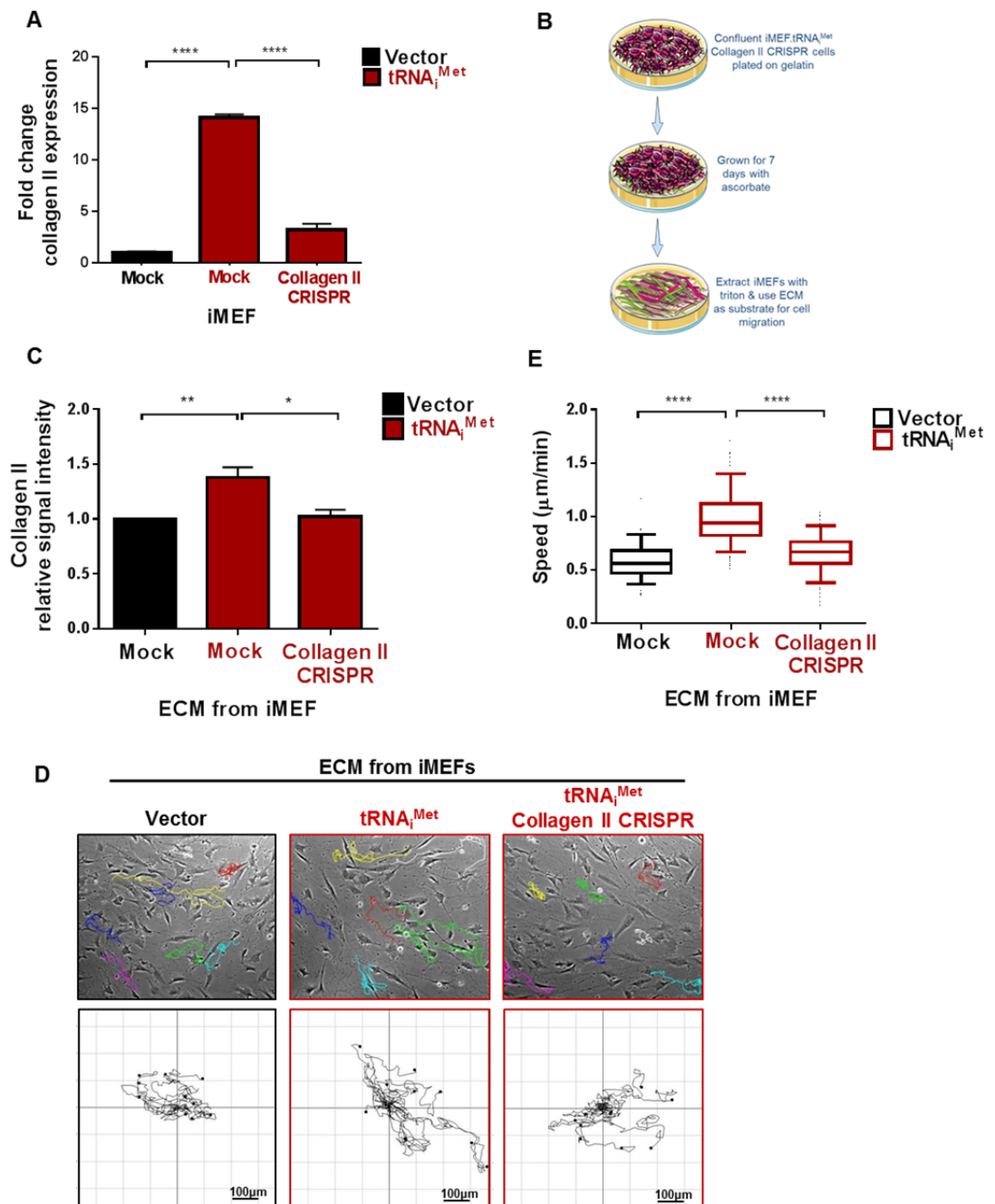


Figure 4-14- CRISPR gene editing methods indicate that collagen II secretion is required for tRNA_i^{Met} to drive production of a pro-migratory ECM.

(A) qPCR was used to quantify collagen II levels in iMEF.Vector and iMEF.tRNA_i^{Met} cells transfected with an empty CRISPR vector, and in iMEF.tRNA_i^{Met} cells transfected with a CRISPR vector specific for collagen II, all data normalised to ARPP P0 and presented relative to expression in the iMEF.Vector cells, n=3, +/- SEM, ANOVA, ****p<0.0001 (B) Schematic representation of method used to generate ECM from iMEF pools. iMEF cells were plated to confluence on gelatin coated plates, and then grown for a further 7 days in ascorbate containing media. The ascorbate containing media was refreshed and replaced every 2 days over the 7 day time course. Cells were then removed using a triton containing buffer, leaving the ECM of interest coating the culture dish. (C) ECM generated from iMEF.Vector, iMEF.tRNA_i^{Met} and iMEF.tRNA_i^{Met} Collagen II CRISPR cells. Incorporation of collagen II into the ECM was assessed by immunostaining using collagen II specific antibodies, quantified using the Aeries infrared imaging system (LI-COR® Biosciences), ANOVA, ** p < 0.005. (D) Single cell traces and spiderplots representative of the data quantified in (E). (E) Migration of iMEFs was recorded by timelapse microscopy over a 17 hour time course and analysed in ImageJ. Data represents ECM generated from at least 3 independent ECM isolations, tracking the migration of at least 40 iMEFs in each replicate. Box and whisker plot represents 5-95 percentile, Kruskal-Wallis test, **** p < 0.0001.

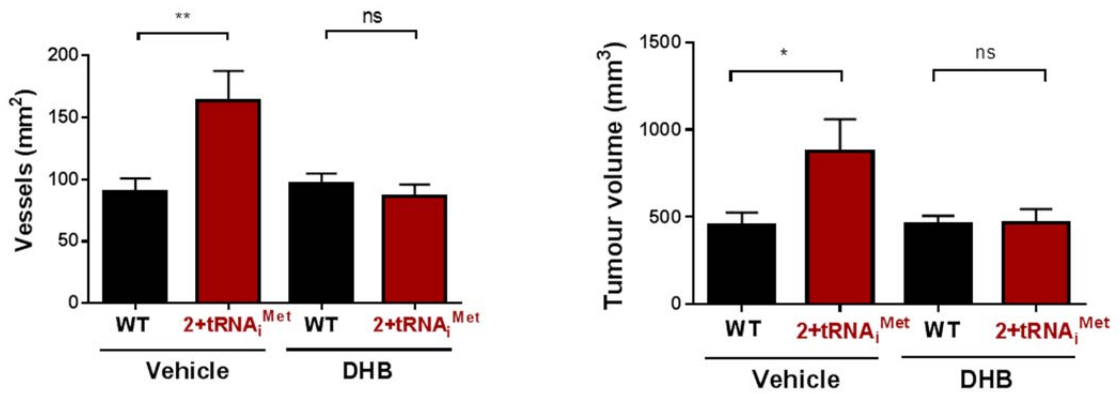


Figure 4-15- The prolyl hydroxylase inhibitor, DHB, opposes the ability of tRNA^{Met} to drive production of a pro-tumourigenic ECM.

1×10^6 lewis lung carcinoma cells were injected subcutaneously into littermatched WT or 2+tRNA^{Met} transgenic male mice, followed by daily dosing 40mg/kg DHB. Tumours were harvested at 21 days and final tumour volume measured. Tumours were PFA fixed and subjected to IHC against endomucin for vessel counts across the entire tumour section, ANOVA, ** $p < 0.005$, * $p < 0.05$, ns = not significant. Experiment conducted by the Reynolds Lab, Institute of Cancer Research, London.

4.2.7 Collagen II expression in human cancer

After establishing the role of collagen II in supporting increased tumourigenicity following tRNA^{Met} overexpression in mouse models, we were interested in understanding how this might relate to tumour progression in human disease. A tissue microarray (TMA) of primary operable breast cancer was available to us, established from a cohort of 544 breast cancer patients diagnosed with invasive breast cancer in the West of Scotland from 1995 to 1998, containing three replicate tumour cores from each patient (1800-Bre-TMA, Dr Joanne Edwards, University of Glasgow). This TMA was associated with a full clinico-pathological characterisation of the patients involved and a 10 year follow-up of breast cancer specific survival, and so provided a powerful tool to determine whether increased collagen II expression correlated with decreased survival in human breast cancer patients.

The TMA was stained for collagen II and scored based on the intensity of collagen II staining in the tumour stroma. We categorised the tumour cores into those that had predominantly low, medium or high collagen II expression (Figure 4-16A), separating the samples into estrogen receptor (ER) positive and negative breast cancers in-case of hormone dependency, and compared these with overall patient survival. Data collected was specific to breast cancer survival, which tends to have a clinical association with death due to metastases from a primary

breast cancer source. It should be noted however that scoring of TMAs for stromal staining can be complicated by the heterogeneity of staining and differences in stromal percentage, but in this instance the TMA cores had also been pre-selected for tumour rich areas, and so were not necessarily representative of the total tumour stroma.

When considering the whole dataset, low collagen II expression correlated with decreased survival, with the effects being more pronounced in ER negative breast cancer (Figure 4-16B). It is therefore possible that whilst increased stromal expression of collagen II can increase the tumorigenicity of lung cancer and melanoma cell lines in mouse models, it may not necessarily be responsible for progression in human breast cancer patients. However, because collagen II expression was scored regardless of tumour stroma percentage (TSP), we also separately analysed the datasets comparing patient survival and collagen II expression in patients with high TSP and low TSP (which had been previously determined by scoring TSP on full sections of the patient derived material, Fadia Gujam, University of Glasgow, unpublished data). In ER negative breast cancer, patients with high TSP did seem to have a trend of decreased survival with increased collagen II expression up to the 40 month mark, however this did not extend beyond this time point, nor did it reach statistical significance (Figure 4-16B). However, it should be noted that as the survival described is time from diagnosis to death due to breast cancer, the number of events plotted (N of events) is actually much lower than the number of patients monitored (Total N), especially when the patient population is separated on TSP and ER status. The reduced N numbers are not only due to survival, but also due to censored patients that died from causes other than breast cancer. There was therefore little statistical power in the analysis of ER negative breast cancer patients with high TSP, which was unfortunate as this may have been the most appropriate population to study within this patient cohort with respect to stromal collagen II expression and its contribution to tumour progression.

When considering all patients with high TSP, having either low or high collagen II expression correlated with decreased survival and this did reach statistical significance due to the improved patient number (p value = 0.046 using a Log Rank (Mantel-Cox) testing equality of survival distributions for the different levels of collagen II score). This suggests a bell-shaped association of collagen II

expression with survival, and so having an optimum medium amount of stromal collagen II could be protective from breast cancer progression, whilst having either low or high amounts are detrimental. Low concentrations of collagen II could result in the organisation of a stroma with larger pore sizes and an architecture that is easily amenable to cell invasion and metastases, whilst high concentrations of collagen could also be supportive of increased cell migration and metastases, but through different mechanisms, including engagement of transmembrane receptors on the surface of cancer cells and consequent activation of signalling pathways that support increased dissemination.

The relationship between increased collagen II expression and cancer progression in human disease is therefore a complex one. Going forward it would be interesting to stain the same TMA for $\text{tRNA}_i^{\text{Met}}$ expression to understand whether tumours with high TSP and high collagen II expression also correlate with increased $\text{tRNA}_i^{\text{Met}}$ levels, to enable us to fully understand whether levels of $\text{tRNA}_i^{\text{Met}}$ can modulate ECM secretion to facilitate increased tumourigenesis in human cancer patients.

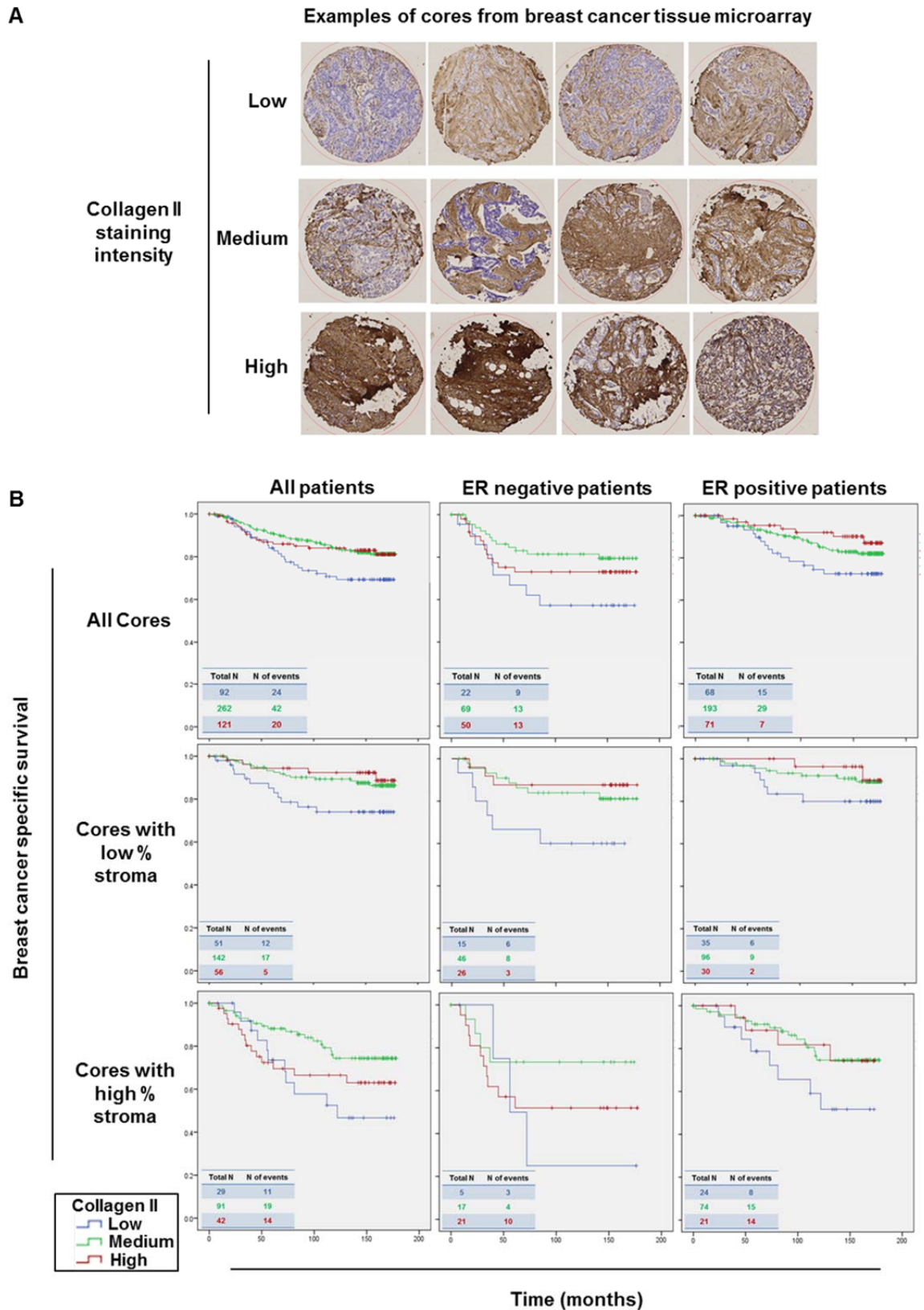


Figure 4-16- Collagen II expression in a breast cancer tissue microarray.

(A) Representative cores from collagen II IHC of breast cancer TMA, scored for low, medium or high collagen II expression based on the intensity of the predominant stromal stain. (B) Patient survival assessed according to low, medium or high collagen II staining intensity, including all patients together, and then separating patients with low TSP compared to high TSP, and those with a ER negative and positive status. Total N indicates initial patient numbers included. Vertical dash indicates censored patients, indicative of survival or cause of death other than breast cancer. N of events indicates breast cancer related death.

4.3 Discussion

As our understanding of tRNA biology grows we are beginning to appreciate that these small non-coding RNAs are much more than just housekeepers that translate mRNA to protein, and recognise that controlling the expression of tRNAs adds a complexity to protein synthesis in health and disease. The data described in this chapter demonstrate that expression of tRNAs is differentially regulated in immortalised cancer-associated fibroblasts compared to normal fibroblasts, and a stromal environment that has increased levels of tRNA_i^{Met} can promote an increase in the vascularity and growth of tumours. Indeed, the ability of iCAFs to constitute a drive to tumour growth *in vivo* is well established (Orimo et al., 2005), and here we show that tRNA_i^{Met} overexpressing fibroblasts can generate an ECM that supports increased migration of endothelial cells for vascularisation, and of fibroblasts themselves for further ECM remodelling. Our results indicate that this effect is due to increased secretion of extracellular proteins, with striking differences in the synthesis and secretion of various collagens and collagen related peptides. Specifically, we find that increased secretion of collagen II is responsible for the pro-migratory effects of the ECM derived from tRNA_i^{Met}-overexpressing fibroblasts, whilst we also show that compromising the secretion of collagens *in vivo* opposes the ability of tRNA_i^{Met} to promote increased tumour vascularity and growth. These findings are of great interest for three reasons: firstly, because they show that the relative levels of tRNA expression play an essential role in the tumour promoting abilities of CAFs; secondly, they indicate that tRNA_i^{Met} levels are closely linked to the cellular secretome and to ECM synthesis in particular; and thirdly, they provide the first pro-tumorigenic link to collagen II expression.

Fibroblasts are one of the most abundant cell types in the stromal compartment, and much work has been done to understand their role in promoting carcinogenesis. This pro-tumorigenic ability has been attributed to secretion of a number of pro-angiogenic factors, including SDF-1 (Orimo et al., 2005). Using qPCR we were able to show that tRNA expression was differentially regulated in iCAFs compared to iNFs, including increased expression of our tRNA of interest, tRNA_i^{Met} (Figure 4-1). However, as may be expected, tRNA_i^{Met} was not the only tRNA differentially regulated in CAFs compared to controls. It would therefore be interesting to use custom arrays to compare the whole tRNAome of cancer-

associated and normal fibroblasts to understand whether there are global changes in tRNA expression in these stromal cells, and to investigate whether overexpression of other specific tRNAs could also influence the ECM and its ability to promote tumourigenicity.

We have shown *in vivo* that mice with increased expression of $\text{tRNA}_i^{\text{Met}}$ can generate a microenvironment that facilitates increased tumour cell growth, and this could be attributed in part to the increased vascularity of those tumours (Figure 4-3). This has been mechanistically dissected using an *in vitro* approach which demonstrates the ability of $\text{tRNA}_i^{\text{Met}}$ -overexpressing fibroblasts to generate an ECM that supports increased migration velocity of both fibroblasts and endothelial cells (Figure 4-4 & Figure 4-5). As tumours can essentially be described as “wounds that do not heal” (Dvorak, 1986), these effects on tumour growth *in vivo* and cell migration *in vitro* highlight the role of the $\text{tRNA}_i^{\text{Met}}$ -derived ECM in the desmoplastic response of tumour progression. Increased migration of fibroblasts is a characteristic of the CAF response seen in carcinogenesis (Ishii et al., 2010) while the ECM-induced increase in migration of endothelial cells provides a link to the increased vascularity of tumours in the $2+\text{tRNA}_i^{\text{Met}}$ mice. Endothelial cell migration is an essential process in angiogenesis, and involves three major mechanisms - chemotaxis, haptotaxis, and mechanotaxis. Chemotaxis refers to cell movement in response to soluble chemoattractants, haptotaxis describes directed migration towards immobilised ligand(s), and mechanotaxis is migration in response to mechanical stimuli (Lamallice et al., 2007). As we were unable to demonstrate any significant difference in thickness or stiffness of the ECM following $\text{tRNA}_i^{\text{Met}}$ overexpression (Figure 4-6), it seems unlikely that increased endothelial cell migration is due to difference in mechanotaxis. The pro-migratory effects of the ECM from $\text{tRNA}_i^{\text{Met}}$ -overexpressing cells are therefore most probably owing to chemotaxis and/or haptotaxis. Although the *in vitro* ECM experiments performed are not capable of distinguishing between the contribution of chemotaxis and haptotaxis, they do suggest that both processes may be involved in the ability of ECM from $\text{tRNA}_i^{\text{Met}}$ -overexpressing cells to support increased endothelial cell migration. Characterisation of the fibroblast secretome revealed that overexpression of $\text{tRNA}_i^{\text{Met}}$ led to increased secretion of molecules such as angiotensin-4 (Figure 4-11B). Angiotensins have essential roles in angiogenic chemotaxis (Fagiani and

Christofori, 2013). Published data on the role of angiopoietin-4 in angiogenesis is however conflicting; with some studies suggesting a pro-angiogenic role (Brunckhorst et al., 2010) and others reporting inhibitory effects (Olsen et al., 2006). However, the results of the collagen II knockdown experiments and the ability of the prolyl-hydroxylase inhibitor DHB to block the increase in vascularity and growth of tumours in the $2+tRNA_i^{Met}$ mice suggest that the main driver of the increased tumourigenicity is most probably via haptotaxis; with $tRNA_i^{Met}$'s ability to increase collagen deposition into the ECM directly influencing the migration of endothelial cells in a pro-angiogenic manner. Cell surface collagen receptors are therefore likely to play a role in this process. While angiogenesis can be coordinated by a number of different integrin receptors (reviewed in (Silva et al., 2008)), integrin $\alpha_2\beta_1$ preferentially binds fibrillar collagens and is expressed on the surface of both endothelial cells and fibroblasts. This receptor could therefore be important in both facilitating endothelial migration in angiogenesis and in fibroblast-mediated remodelling of the collagen-rich TME (Hu et al., 2011). Receptor tyrosine kinases from the discoidin domain receptor (DDR) family that recognise and respond to collagen could also influence tumour progression, including DDR2 which preferentially binds collagen II (Leitinger et al., 2004), and whose activity has been associated with tumour progression in squamous cell carcinoma of the lung (Hammerman et al., 2011) and cancers of the head and neck (Chua et al., 2008). The collagen rich matrix generated following $tRNA_i^{Met}$ overexpression could therefore be promoting an increase in tumour growth through a number of different but complementary processes.

Our SILAC characterisation of protein secretion following $tRNA_i^{Met}$ overexpression was key to beginning to understand the mechanism by which $tRNA_i^{Met}$ could promote generation of a pro-tumourigenic ECM. The role of other translation factors, associated ribosomal proteins, and their contribution to tumour progression, has already been well established (Loreni et al., 2014, Rubio et al., 2014, Wolfe et al., 2014, Ruggero, 2013). Oncogenic and tumour suppressor signals are known to converge on pathways that promote protein synthesis, and control of translation is regarded as an essential requirement in cancer progression. Moreover, this control is performed with an element of specificity, and translation of particular mRNAs can be achieved through a number of

mechanisms, including the presence of secondary structure in the 5' UTR, in addition to IRES sites and uORFs (Wolfe et al., 2014, Hsieh et al., 2012, Thoreen et al., 2012). The importance of the translation initiation machinery in driving translational selectivity is also now apparent. The RNA-cap binding protein, eIF4E, is commonly overexpressed in cancer, and its ability to drive an increase in tumourigenicity has been attributed to its selective effects on the translation of the anti-apoptotic protein, MCL1 (Wendel et al., 2007). More recently eIF4A, an RNA helicase, has also been shown to favour translation of oncoproteins such as Myc, Notch and BCL2, all of which possess G-quadruplex structures in their 5'-UTRs (Wolfe et al., 2014). Furthermore, TORC1, the mTOR-containing kinase complex which phosphorylates the eIF4E-binding protein (4E-BP1) leading to activation of eIF4E, has also been shown to contribute to metastasis by favouring translation of a cohort of mRNAs with pyrimidine-rich translational elements (PRTEs) or terminal oligopyrimidine tracts (TOPs) in their 5'-UTRs (Hsieh et al., 2012). Amongst these transcripts are the gene products of YB1, vimentin and CD44, which are all thought to cooperate to generate an invasive cancer phenotype. Moreover, we also now know that changes in the cellular tRNA repertoire can further dictate the efficiency of translational programmes to define cell fates (Gingold et al., 2014). A positive correlation between tRNA expression and codon usage for ECM genes has been previously observed in breast cancer cells (Pavon-Eternod et al., 2009), and so a dose dependency between tRNA expression and translational efficiency could therefore influence gene expression. Whilst knockdown of tRNAs is technically difficult with standard siRNA methods, the advent of CRISPR gene editing technologies now provides a strategy to knockout specific tRNA genes, and so use of these methods could further contribute to this work and advance our understanding of the influence of tRNA expression in translational control.

Gene expression studies have identified distinct subtypes of CAFs with differing tumour promoting abilities. Furthermore, many of these gene expression analyses have shown that expression levels of collagen XV, collagen XI and biglycan, a cartilage proteoglycan with a role in assembling collagen fibrils including collagen II, are commonly upregulated in CAFs (Costea et al., 2013). Whilst the RNA-Seq data we have generated here indicates that the level of gene expression is increased for some of the differentially regulated ECM proteins

following $\text{tRNA}_i^{\text{Met}}$ overexpression, such as collagen II, this is not consistent across all iMEF pools tested. The increase in $\text{tRNA}_i^{\text{Met}}$ expression is much larger in iMEF pool 1 compared to iMEF pool 2, and as a consequence drives a much larger increase in collagen II protein secretion. It is therefore possible that this larger increase in protein synthesis may consequently feed forward into the cells transcriptional cycle, either increasing the level of transcription of collagen II itself, or stabilising expression of the collagen II transcript. However, not all $\text{tRNA}_i^{\text{Met}}$ regulated proteins are upregulated at the level of transcription. Collagen I and collagen XI are both secreted proteins that have increased total protein levels and increased protein secretion following $\text{tRNA}_i^{\text{Met}}$ overexpression, but have no corresponding change in the levels of their mRNAs, indicating that $\text{tRNA}_i^{\text{Met}}$ can influence gene expression at the level of translational control.

Future work to investigate the effect of $\text{tRNA}_i^{\text{Met}}$ on translational efficiency would further complement the transcriptome and proteomic changes that we have already described, and provide a more detailed understanding of how $\text{tRNA}_i^{\text{Met}}$ can control the expression of specific ECM proteins. The use of techniques such as ribosome profiling and ribosome footprinting would help capture more information regarding which transcripts are being actively transcribed following $\text{tRNA}_i^{\text{Met}}$ overexpression, whilst detailed bioinformatic analysis of hits would also enable us to understand whether particular sequence elements are responsible for $\text{tRNA}_i^{\text{Met}}$'s specificity. ECM production constitutes a significant commitment to the cell, both in terms of load on the endoplasmic reticulum (ER) and the biosynthetic machinery, highlighting the need for special mechanisms to control the translation of ECM proteins and other abundant components of the fibroblast secretome. For example, it is already known that expression of collagen I, a fibril-forming collagen, can be controlled at the level of mRNA stability and translation, due to unique stem loops in its 5' UTR (Manojlovic and Stefanovic, 2012), and a role for collagen I in cancer progression has been previously shown (Cheng and Leung, 2011, Zou et al., 2013). It may therefore be possible that $\text{tRNA}_i^{\text{Met}}$ is selectively increasing translation of proteins that have specific structures, or sequences, in their flanking regions, and control of this selectivity may play an important role in maintaining cellular fitness.

Collagen II, the most upregulated secreted protein following $\text{tRNA}_i^{\text{Met}}$ overexpression, is a fibril-forming collagen, composed of three $\alpha 1(\text{II})$ chains, with alternative splicing contributing to two different isoforms of the $\alpha 1(\text{II})$ chains, type IIA and type IIB (Ricard-Blum, 2011). Collagen II is an abundant component of cartilage and is produced in large quantities by chondrocytes. By contrast, normal fibroblasts are not thought to secrete collagen II and, consistently, our SILAC data show that this collagen is a minor component of the fibroblast secretome. Thus, acquisition of type II collagen secretion when $\text{tRNA}_i^{\text{Met}}$ levels are increased may represent a shift to a more chondrocyte-like phenotype, and this may be consistent with a role for the tRNA repertoire in influencing cellular differentiation states (Gingold et al., 2014).

Chondrocytes synthesise cartilage ECM, and this matrix is predominantly composed of type IIB collagen II. Synthesised as procollagens, NH_2 - and COOH -terminal extension peptides are cleaved and removed prior to type IIB collagen II incorporation into the ECM, however in the case of type IIA collagen II the NH_2 -propeptide is not removed, and the entire procollagen is deposited into the ECM (Wang et al., 2010). The cleaved NH_2 - propeptide of collagen type IIB has been shown to induce tumour cell death, however the intact NH_2 - domain of type IA collagen II, although able to bind tumour cells through $\alpha_v\beta_3$ and $\alpha_v\beta_5$ integrins, does not induce tumour cell death (Wang et al., 2010). Type IIA collagen II is also able to bind growth factors, such as BMP-2 and TGF- β , and so it is possible that this isoform could promote tumour cell proliferation and migration via these growth factors. Indeed, type IIA collagen II is the collagen that is most upregulated following $\text{tRNA}_i^{\text{Met}}$ overexpression, and so the desmoplastic response in cancer and increased tumour growth seen in our transgenic mouse models could be due to a dynamic interplay between tRNA controlled translation and the consequent upregulation of a type IIA collagen II-rich ECM.

With regard to relevance in human disease, we found that high levels of collagen II expression in tumour stroma from breast cancer patients correlated with increased survival when analysing the patient cohort as a whole. Whilst this result initially seemed contradictory to our *in vitro* and *in vivo* findings, it may simply mean that the $\text{tRNA}_i^{\text{Met}}$ driven effects on collagen II secretion do not contribute to tumour progression in breast cancer, but may still have effects in other human cancer types. However, in light of the differential activity of the

alternative splice forms of collagen II it is also possible that it is type IIB collagen II expression that is differentially regulated in the stroma of breast cancer patients. The antibody used to stain the breast cancer TMA is unable to differentiate between type IIA and type IIB collagen II splice variants, and so if type IIB collagen II expression is specifically increased in breast cancer patients then this could indeed correlate with anti-tumour effects and increased survival. Thus, it may be that expression of type IIA (but not type IIB) collagen II is pro-tumourigenic and responsible for the increase in vascularity and tumour cell growth in the 2+tRNA_i^{Met} mice. It would therefore be interesting to use CRISPR gene editing approaches to knock-out the specific splice variants of collagen II in fibroblasts and assess the ability of ECM deposited by these cells to support migration *ex vivo*, while a more detailed *in vivo* analysis could include using fibroblast specific knockouts of type IIA collagen II in 2+tRNA_i^{Met} mice and consequent assessment of syngeneic tumour growth. Alternatively, if we consider only tumour cores that were judged to have high TSP, then we could also conclude that having a moderate amount of collagen II promotes increased survival whilst having an extreme amount, be it either low or high, can generate a stroma that promotes disease progression. Whilst this may initially seem like a paradox, it is reflective of the many opposing mechanisms that can contribute to tumour progression and highlights the fine balance between them.

Collagens are large, bulky proteins, whose synthesis and secretion requires dedicated vesicular transport pathways, including the use of modified COPII protein vesicles to encapsulate the large procollagen molecules for transport from the ER to the Golgi complex (Jin et al., 2012) and the implementation of a specialised budding process to allow the formation of post-Golgi vesicles of sufficient size to carry collagens (Nogueira et al., 2014). Thus general upregulation of secretory capacity and secretory protein vesicular transport suggests the possibility that the pro-tumourigenic effects of tRNA_i^{Met} are not solely owing to direct effects of collagen II, but to other molecule(s) that are co-secreted with it. To investigate this possibility it would be interesting to use SILAC mass spectrometry to characterise the fibroblast secretome in tRNA_i^{Met} overexpressing cells in which collagen II expression is stably knocked-out using CRISPR, and compare this to the secretome previously obtained for tRNA_i^{Met} overexpressing cells. This would help us understand whether the effects of

tRNA_i^{Met} on generation of a pro-migratory ECM are specifically due to collagen II expression, or due to a collagen II-dependent secretome that impacts the tumour microenvironment.

In conclusion, we have found compelling evidence indicating that increased expression of tRNA_i^{Met} in fibroblasts has profound non-cell autonomous effects on tumour progression. Through increasing the synthesis and secretion of particular ECM components, specifically collagen II, the ECM generated from fibroblasts overexpressing tRNA_i^{Met} is able to promote increased cell migration, increased angiogenesis and increased tumour growth (Figure 4-17). Combined with data presented in the previous chapter, the work presented in this thesis collectively shows that increased expression of tRNA_i^{Met} in fibroblasts can influence their behaviour to promote an increase in cell migration and an increase in tumourigenicity.

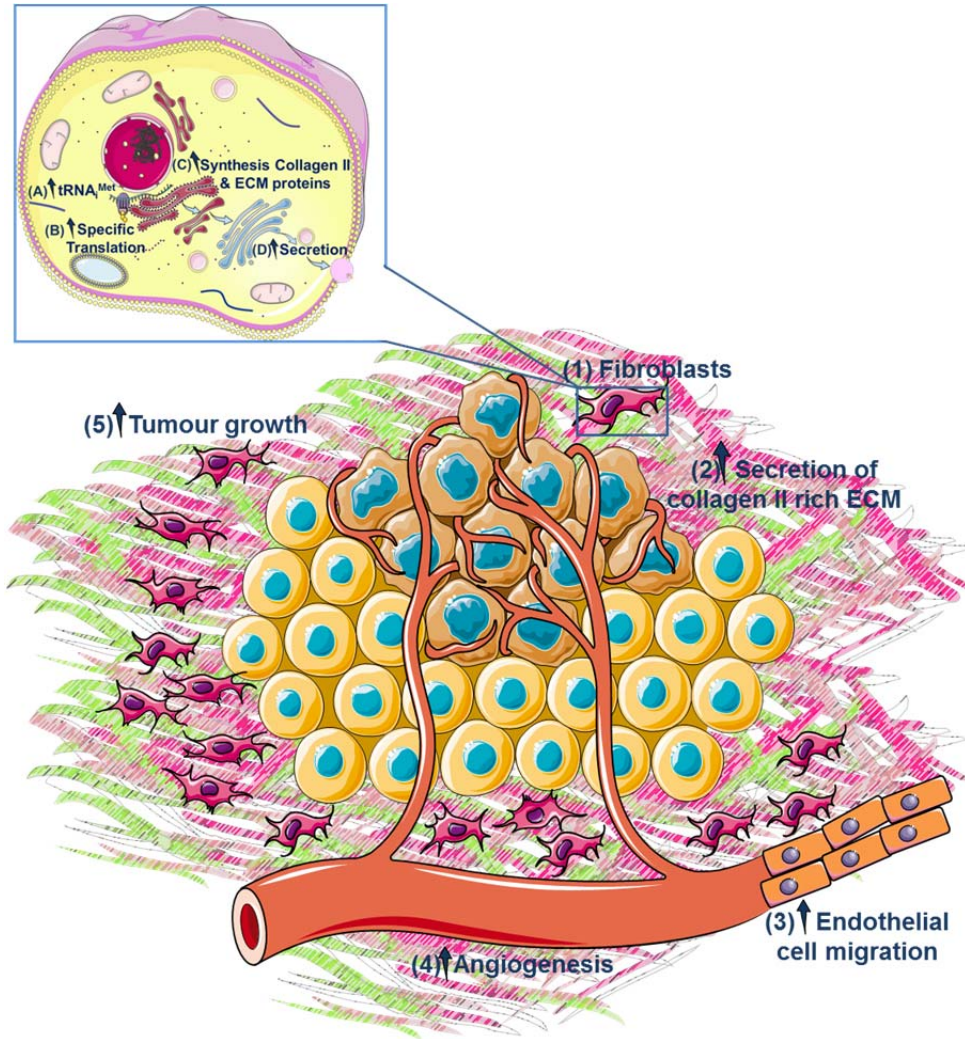


Figure 4-17- Schematic representation of the non-cell autonomous effects of $tRNA_i^{Met}$ overexpression.

(1) Fibroblasts with increased expression of $tRNA_i^{Met}$ increase the translation and secretion of specific proteins such as collagen II. (2) This collagen II-rich ECM increases the migration of (3) fibroblasts and endothelial cells contributing to the (4) increased vascularity and (5) growth of tumours. Image made using items from Image Bank in Servier Medical Art.

Chapter 5 Final Discussion

Misregulation of translational control is one mechanism that enables cancer cells to evade normal cellular homeostasis and drive an increase in their tumourigenicity. We show here that overexpression of $tRNA_i^{\text{Met}}$, an integral component of the translation initiation machinery, can drive increases in cell migration and can selectively influence the fibroblast secretome. This leads to production of an ECM that is rich in collagen II, a normally minor component of the fibroblast-derived ECM, which then provides a microenvironment that supports increased migration of endothelial cells, increased angiogenesis, and increased fibroblast migration, which can all collectively increase the rate of tumour progression (Figure 5-1).

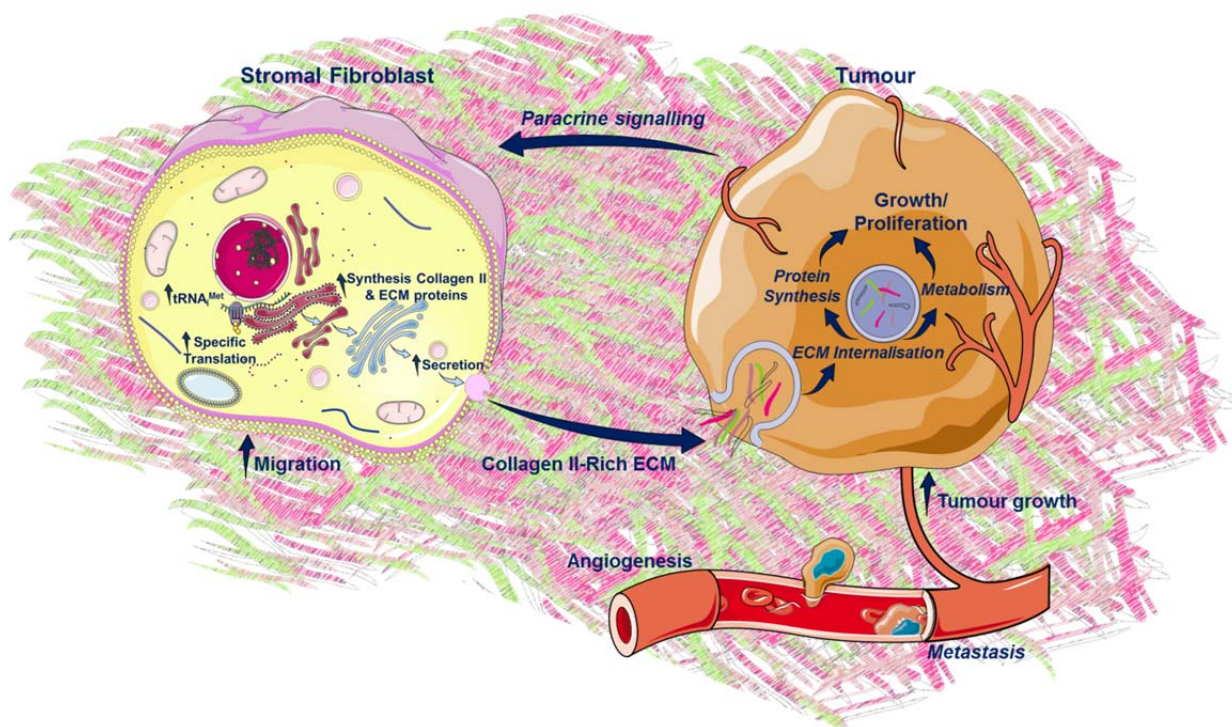


Figure 5-1- Proposed model of the $tRNA_i^{\text{Met}}$ effect on tumour progression.

Stromal fibroblasts with increased $tRNA_i^{\text{Met}}$ levels can increase the synthesis and secretion of specific ECM proteins, including collagen II. The collagen II-rich ECM can then facilitate increased tumour growth through increased endothelial cell migration and angiogenesis. Further speculative effects of the ECM on tumour growth are suggested in italic font, including the possibility that the ECM could be internalised and used as substrate for increased protein synthesis and cancer cell metabolism. The cancer cells could also stimulate a paracrine signalling pathway to the adjacent fibroblasts for continual remodelling of the matrix, whilst the increase in vascularity could also result in an increase in metastasis at distant sites. Image made using items from Image Bank in Servier Medical Art.

A recent publication revealed that there are differential requirements for the level of eIF4E, the major cap-binding protein in translation initiation, in normal development compared to cancer (Truitt et al., 2015). This study showed that eIF4E is expressed in excess throughout normal development, and only becomes limiting under the specific conditions of oncogene-induced transformation. Cancer cells consequently utilise this excess eIF4E to drive their transformation by directing the translation of specific subsets of mRNAs which can support tumour cell growth and survival. It is well-established that reactive oxygen species (ROS) can influence many aspects of tumour development (reviewed in (Liou and Storz, 2010)). This study identified that a number of transcripts for proteins functioning as ROS scavengers are characterised by specific motifs in their 5' UTRs, and increased translation of these transcripts was supported by high levels of eIF4E. Our study has marked analogies to the study by Truitt et al. in that we also find a dose-dependent effect of a translation initiation component that seems to be particularly important to cancer progression, but that has less relevance to normal growth and development. Indeed, we find that excess $\text{tRNA}_i^{\text{Met}}$ in the $2+\text{tRNA}_i^{\text{Met}}$ mouse also does not affect normal mouse development or the overall rates of protein synthesis in normal cells. However, the increased $\text{tRNA}_i^{\text{Met}}$ levels in stromal cells increases secretion of specific ECM proteins, and whilst this does not exert an overt phenotypic effect in the normal animal, when exposed to a specific insult, such as the introduction of transformed cells as a syngeneic allograft, the altered matrix secreted by the $\text{tRNA}_i^{\text{Met}}$ -overexpressing fibroblasts then facilitates more rapid tumour progression.

Deregulated translational control can contribute to each step of cellular transformation, from the initial expression of specific oncogenes owing to structures in their untranslated regions, to the increase in ribosome biogenesis and global protein synthesis required for increased cell growth and cell division (Ruggero, 2013). By facilitating protein enrichment at its site of function, the spatial location of translation is another important mechanism that enables protein synthesis to influence cell behaviour. Eukaryotic initiation factors have been shown to localise to the leading edge of migrating fibroblasts, with eIF4E and eIF4G associating with Golgi apparatus at membrane microdomains that also co-localise with sites of active translation (Willett et al., 2011). Translation of

intracellular proteins, such as β -actin, at the leading edge of migrating cells could promote increased cell migration through the local synthesis of new β -actin which is thought to be more efficiently polymerised than older, more modified, actin molecules (Liao et al., 2015), and local synthesis of proteins required for new membrane formation could also be important in generating new cell protrusions. Translation of secretory proteins at such sites could also facilitate their efficient secretion from the cell, especially considering the large size of matrix proteins such as collagen, thus promoting cell motility in a manner that is energetically favourable to the cell, and supporting generation of a microenvironment that can promote tumour growth.

The increase in migration that we have characterised in fibroblasts following $\text{tRNA}_i^{\text{Met}}$ overexpression is dependent on the role of $\text{tRNA}_i^{\text{Met}}$ in the TC and the ability of integrin $\alpha_5\beta_1$ to bind fibronectin. As initial fibronectin deposition and fibrillogenesis are important in subsequent fibrillar collagen assembly (Egeblad et al., 2010), and cells are able to secrete their own matrix to promote motility (Sung et al., 2011), the integrin $\alpha_5\beta_1$ -fibronectin dependent effects on cell migration are likely to play an important role in the early stages of ECM remodelling, and so may also be a pre-requisite for the non-cell autonomous pro-tumourigenic effects of the $\text{tRNA}_i^{\text{Met}}$ -driven collagen II-rich ECM.

With regard to relevance in human cancer, it seems that the relationship between collagen II expression and disease progression is likely to be complex. Previous studies have found that modifications in collagen metabolism in breast cancer can result in decreased collagen content in breast tumour tissue (Cechowska-Pasko et al., 2006) and collagen α_1 (XI) has been found to be downregulated in the immediate stroma surrounding breast tumours (Halsted et al., 2008). Similar to collagen II, collagen α_1 (XI) is also mainly expressed in chondrocytes under normal conditions, however recent work has shown that it becomes highly expressed in stromal cells associated with other aggressive cancers such as glioblastoma, and has consequently been proposed to be a biomarker for carcinoma-associated stromal cells and aggressive cancer progression (Vazquez-Villa et al., 2015). Although this work was not specifically focused on collagen II, collagen α_3 (XI) is the same gene product as collagen II and differs only by hyperglycosylation (Burgeson and Hollister, 1979, Morris and Bachinger, 1987), and so it is likely that collagen II could also follow a similar

expression pattern to collagen $\alpha 3$ (XI). Studies in prostate cancer, lung cancer and colorectal cancer have found increased expression of collagens in cancerous compared to normal tissues (Fischer et al., 2001, Chang et al., 2004, Banyard et al., 2007), and so investigating the contribution of a collagen II-rich stroma to tumour progression in these cancer types may also be appropriate. In the future it would be interesting to understand exactly how a collagen II-rich tumour microenvironment affects cancer cells, and whether the increase in tumour growth that we see in our *in vivo* models is simply due to the increase in vascularity of the tumours, or whether there are also other processes that contribute to this. Changes in collagen metabolism associated with the Gleason grade of tumour have been identified in prostate cancer (Burns-Cox et al., 2001). Thus, in addition to increasing the migration of stromal and endothelial cells, endocytosis of the altered matrix could also fuel cellular metabolism, protein synthesis and cell growth. The increased collagen content of the ECM could essentially act as a proline reservoir for cancer cells, and consequent proline metabolism may serve not only as an energy source but can also increase formation of signalling ROS (Phang et al., 2015). Increased rates of ROS have been found across a variety of different cancer types, and have been shown to influence a number of signalling pathways associated with cell proliferation, motility and metastasis (reviewed in (Liou and Storz, 2010)). The metabolism of proline from a collagen-rich tumour microenvironment could therefore provide additional mechanisms to fuel an increase in tumourigenicity.

Tumour cells are also known to secrete cytokines and chemokines (Zheng et al., 2015, Maxwell et al., 2014), and these molecules can signal to stromal cells in a paracrine fashion to further promote a reactive microenvironment. Whilst the inflammatory response to tumour growth is well established, recent data has also shown how NF- κ B, a transcription factor known to mediate inflammatory signals, can also directly regulate the Pol III mediated transcription of tRNAs in macrophages to influence their cytokine secretion and phagocytic response (Graczyk et al., 2015). The NF- κ B mediated increase in Pol III transcription described in macrophages could therefore also be a potential mechanism exploited by cancer cells, not only in driving immune activity in the tumour microenvironment, but if cytokine release from cancer cells could also mediate NF- κ B-stimulated transcription of tRNAs in stromal cells, then it would provide a

means for cancer cells to co-opt their neighbours into increasing expression of tRNAs to ignite a positive feedback loop and further promote increased tumour growth.

Throughout the course of this work we have only discussed the effects of $\text{tRNA}_i^{\text{Met}}$ overexpression with regard to absolute tRNA expression levels, and although the increases in expression of $\text{tRNA}_i^{\text{Met}}$ in both our *in vivo* and *in vitro* models are analogous to those increases found in human cancer populations (Pavon-Eternod et al., 2009), we are unable to comment on what influence the modification of $\text{tRNA}_i^{\text{Met}}$ may be having in these systems. The nucleobases and ribose sugars of tRNAs are highly modified by various enzymes to form chemically different tRNA structures, and changes in expression of these enzymes and consequent shifts in the levels of tRNA modification have been associated with a variety of cancer types (Shimada et al., 2009, Begley et al., 2013). Furthermore, tRNA modifications can be dynamically controlled in association with the cell's stress response (Chan et al., 2010), and these modifications can shift translational efficiency through codon bias to consequently effect the expression of specific genes (Chan et al., 2012). The ability of cells to modify their tRNAs in response to external stimuli has been likened to the regulatory networks that influence epigenetic changes (Dedon and Begley, 2014), and so the regulatory function of tRNA modification may provide another mechanism that enables tRNA expression to influence disease states.

The data presented in this thesis is also specific to the effects of $\text{tRNA}_i^{\text{Met}}$ in fibroblasts. However, increased Pol III transcription is also a common feature of cancer cells themselves. Using fibroblasts as a model, it is likely that increased expression of specific Pol III products, such as $\text{tRNA}_i^{\text{Met}}$, could also contribute to increased migration and invasion of cancer cells. Any cellular functions that are sensitive to small changes in $\text{tRNA}_i^{\text{Met}}$ levels could not only provide an effective route to target the tumour stroma, but could also be useful in treating more metastatic and invasive cancers that may rely on $\text{tRNA}_i^{\text{Met}}$ to support their own cell migration. Targeting the tumour stroma has become an attractive strategy in cancer therapy (Zhou et al., 2015, Lunardi et al., 2014, Teichgraber et al., 2015) and if the pro-tumourigenic effects of $\text{tRNA}_i^{\text{Met}}$ are indeed common to both stromal fibroblasts and cancer cells, then therapeutics aimed at suppressing levels of $\text{tRNA}_i^{\text{Met}}$ could have dual effectiveness in halting tumour progression.

Whilst initial proposals to target the translational machinery for therapeutic use were dismissed owing to a lack of specificity, it has since been demonstrated that targeting initiation factors *in vivo* can be efficacious (Loreni et al., 2014, Bhat et al., 2015). Translation plays an essential role in mediating dysregulated signalling across a variety of different cancer types, and a number of inhibitors of the TC have already been developed as potential anti-cancer therapies, including drugs that prevent binding of tRNA_i^{Met} to eIF2 (Robert et al., 2006). Whilst efficacy of the latter is yet to be reported, a small molecule inhibitor of RNA polymerase I (Pol I) has been effective in preventing tumour growth in mouse allograft models (Drygin et al., 2011). Pol I is also responsible for the transcription of non-coding RNAs, and so *in vivo* success with Pol I inhibitors may provide future promise for targeting Pol III and its transcripts.

Collectively, the data presented throughout this thesis highlights how increased levels of specific tRNAs are not merely a consequence of tumourigenesis, but are important in driving increased tumour progression. Translation is a process that is tightly controlled via a number of different mechanisms, and elegant adaptations have evolved to increase translational efficiency, including changes in the cells tRNA_{ome}. Whilst in health this can essentially increase cellular fitness, in disease it may be hijacked to detrimental effect. Cancer provides a prime example of this, and we show here how overexpression of tRNA_i^{Met} in stromal fibroblasts can significantly influence the tumour microenvironment to promote increased tumour growth. Continuing to develop a more detailed understanding of tRNA functionality may therefore not only uncover new layers of complexity in cell biology, but could also potentially highlight new targets for future cancer therapies.

Appendices

Appendix I: Secretome dataset

Protein name	Gene Symbol	MW kDa	Forward SILAC ratio	Reverse SILAC ratio	Unique peptides
Collagen alpha-1(II)	Col2a1	135	5.96	6.15	37
Otoraplin	Otor	14	4.70	4.57	4
Secreted frizzled-related protein 2	Sfrp2	33	4.58	4.24	11
Angiopoietin-4	Angpt4	58	4.50	4.51	9
Tenascin-N	Tnn	173	3.77	4.17	18
ABI family member 3 NESH binding protein	Abi3bp	130	3.73	3.49	21
C-type lectin domain family 11 member A	Clec11a	36	3.43	3.28	12
Procollagen C-endopeptidase enhancer 2	Pcolce2	45	3.35	3.39	6
Pappalysin 2	Pappa2	199	3.32	2.83	4
Transforming growth factor beta-2	Tgfb2	48	3.31	3.03	8
Plasminogen activator inhibitor 1	Serpine1	45	3.14	3.09	15
Pentraxin-related protein PTX3	Ptx3	42	3.13	2.83	17
Immunoglobulin superfamily containing leucine-rich repeat protein	Islr	46	3.10	3.15	7
Semaphorin-3A	Sema3a	89	3.03	2.60	19
Atrial natriuretic peptide receptor 3	Npr3	60	2.89	2.88	11
Osteomodulin	Omd	50	2.88	3.08	5
Heat shock protein beta-1	Hspb1	22	2.66	3.02	8
Dickkopf-related protein 3	Dkk3	38	2.59	2.53	6
Phospholipid transfer protein	Pltp	54	2.51	2.42	13
Collagen alpha-1(XI) chain	Col11a1	171	2.48	2.56	26
Fibromodulin	Fmod	43	2.44	2.71	7
Follistatin-related protein	Fstl1	35	2.35	2.15	15
A disintegrin and metalloproteinase with thrombospondin motifs 1	Adamts1	106	2.34	2.10	6
Protein NOV homolog	Nov	39	2.33	2.37	7
SPARC-like protein 1	Sparcl1	72	2.31	2.04	12
Peptidyl-prolyl cis-trans isomerase	Fkbp10	65	2.31	2.15	28
Collagen alpha-1(XII) chain	Col12a1	340	2.30	2.13	199
Mimecan	Ogn	34	2.29	2.11	22
Clusterin	Clu	52	2.29	2.23	5
Fibulin-5	Fbln5	50	2.25	2.03	12
Periostin	Postn	93	2.24	2.58	19
Procollagen-lysine,2-oxo	Plod3	85	2.23	2.04	20

glutarate 5-dioxygenase 3					
Twisted gastrulation protein homolog 1	Twsg1	25	2.23	2.84	2
DnaJ homolog subfamily B member 11	Dnajb11	41	2.20	2.02	4
Complement C1q tumor necrosis factor-related protein 5	C1qtnf5	23	2.17	2.60	4
Platelet-derived growth factor D	Pdgfd	42	2.15	2.11	3
Amyloid beta A4 protein	App	87	2.07	2.09	10
Nidogen-2	Nid2	154	2.06	2.02	39
EGF-containing fibulin-like extracellular matrix protein 2	Efemp2	49	1.90	1.97	12
Vitamin K-dependent protein S	Pros1	75	1.90	1.75	10
Acyl-coenzyme A thioesterase 2	Acot2; Acot1	50	1.90	1.84	9
Immunoglobulin superfamily member 10	Igsf10	286	1.89	1.67	37
Latent-transforming growth factor beta-binding protein 3	Ltbp3	134	1.88	2.19	8
Thrombospondin-1	Thbs1	130	1.88	1.96	15
Coiled-coil domain-containing protein 80	Ccdc80	108	1.82	1.73	18
Platelet-derived growth factor receptor-like protein	Pdgfrl	42	1.80	1.63	16
Lysyl oxidase homolog 4	Loxl4	85	1.79	1.89	11
SPARC	Sparc	34	1.77	1.74	18
Peptidyl-prolyl cis-trans isomerase C	Ppic	23	1.76	1.67	11
Peptidyl-prolyl cis-trans isomerase FKBP9	Fkbp9	63	1.73	1.59	10
Calumenin	Calu	37	1.69	1.53	3
Membrane-bound transcription factor site-1 protease	Mbtps1	117	1.66	1.42	9
Carboxypeptidase E	Cpe	53	1.64	1.43	25
Protein FAM3C	Fam3c	21	1.56	1.48	11
EMILIN-1	Emilin1	108	1.53	1.54	45
Thrombospondin-3	Thbs3	100	1.52	1.47	8
Sulfated glycoprotein 1	Psap	61	1.52	1.63	10
Calreticulin	Calr	48	1.49	1.34	25
Protein canopy homolog 2	Cnpy2	21	1.49	1.44	10
Thioredoxin domain-containing protein 12	Txndc12	19	1.48	1.46	4
Serpin H1	Serpinh1	47	1.48	1.39	28
Granulins	Grn	63	1.48	1.54	3
Metalloproteinase inhibitor 2	Timp2	24	1.47	1.45	17
Collagen alpha-2(I) chain	Col1a2	130	1.46	1.50	110

Peroxidasin homolog	Pxdn	165	1.46	1.35	50
Vasorin	Vasn	72	1.44	1.50	12
F-box only protein 2	Fbxo2	34	1.44	1.56	2
Guanine nucleotide-binding protein G(o) subunit alpha	Gnao1	40	1.43	1.61	8
Roundabout homolog 1	Robo1	176	1.43	2.06	7
Collagen alpha-1(I) chain	Col1a1	138	1.40	1.50	92
Protein-lysine 6-oxidase	Lox	47	1.35	1.31	19
78 kDa glucose-regulated protein	Hspa5	72	1.29	1.23	46
Collagen, type VI, alpha 3	Col6a3	354	-0.80	-1.06	191
Carbonic anhydrase 13	Ca13	30	-0.96	-1.10	8
DnaJ (Hsp40) homolog, subfamily C, member 13	Dnajc13	254	-1.01	-1.02	53
Glutathione S-transferase A4	Gsta4	26	-1.01	-1.14	16
Aldo-Keto Reductase Family 1, Member B10	Akr1b10	36	-1.07	-1.16	7
Laminin subunit alpha-5	Lama5	404	-1.10	-1.38	40
Aldose reductase-related protein 2	Akr1b8	36	-1.11	-1.11	9
Serine/threonine-protein kinase SMG1	Smg1	402	-1.13	-1.34	4
Cadherin-11	Cdh11	88	-1.14	-1.18	27
5'-Nucleotidase Domain Containing 2	Nt5dc2	46	-1.27	-1.22	6
Cellular retinoic acid-binding protein 2	Crabp2	16	-1.28	-1.62	4
Matrix Gla protein	Mgp	12	-1.31	-1.58	3
Glypican-1;Secreted glypican-1	Gpc1	61	-1.47	-1.10	17
Apolipoprotein B-100;Apolipoprotein B-48	Apob	504	-1.88	2.99	3
Versican core protein	Vcan	367	-2.00	-1.95	5
Serine protease inhibitor A3G	Serpina3g	49	-2.07	-2.39	10
Ubiquitin-like protein ISG15	Isg15	18	-2.13	-2.51	4
Interleukin-1 receptor antagonist protein	Il1rn	18	-2.40	-2.72	6
Osteopontin	Spp1	32	-2.81	-3.13	3
Stromelysin-1	Mmp3	54	-3.01	-2.13	18

Appendix I – Secreted proteins significantly changed in the conditioned media of iMEF.tRNA_i^{Met} cells versus iMEF.Vector cells (pool 1).

The secretome was analysed following tRNA_i^{Met} overexpression using quantitative SILAC mass spectrometry. iMEF.Vector and iMEF.tRNA_i^{Met} cells were labelled with heavy and light amino acids, secreted proteins isolated from the conditioned media, separated by gel electrophoresis, and then analysed by mass spectrometry. Forward experiment corresponds to iMEF.tRNA_i^{Met} cells labelled with heavy amino acids combined with iMEF.Vector cells labelled with light amino acids, and the reverse experiment corresponds to iMEF.Vector cells labelled with heavy amino acids combined with iMEF.tRNA_i^{Met} cells labelled with light amino acids. Forward SILAC ratio is calculated as (Log₂ tRNA_i^{Met} / Vector), and reverse SILAC ratio as (1/(Log₂ tRNA_i^{Met} / Vector)), MW = molecular weight, and unique peptides refers to the number of peptides identified that exist only in that one protein of interest. Data generated in collaboration with David Sumpton, CR-UK Beatson Institute, Glasgow.

Appendix II: Cellular proteome dataset

Protein name	Gene Symbol	MW kDa	Forward SILAC ratio	Reverse SILAC ratio	Unique peptides
ABI family member 3 NESH binding protein	Abi3bp	118	3.70	2.91	9
Immunoglobulin superfamily containing leucine-rich repeat protein	Islr	46	2.90	2.87	6
Collagen alpha-1(II)	Col2a1	132	2.82	2.39	12
Cytochrome P450 26B1	Cyp26b1	57	2.63	2.80	3
Atrial natriuretic peptide receptor 3	Npr3	60	2.61	2.62	16
Angiopietin-4	Angpt4	58	2.59	3.63	8
Transforming growth factor beta-2	Tgfb2	48	2.26	2.61	4
Collagen alpha-1(XI) chain	Col11a1	171	2.04	2.35	14
Heat shock protein beta-1	Hspb1	23	1.96	2.33	8
Cytokine receptor-like factor 1	Crlf1	47	1.91	1.82	6
Dickkopf-related protein 3	Dkk3	38	1.86	2.13	3
Aryl hydrocarbon receptor	Ahr	95	1.82	1.76	12
Guanine nucleotide-binding protein G(o) subunit alpha	Gnao1	40	1.77	1.56	12
Collagen alpha-1(XII) chain	Col12a1	334	1.70	1.77	97
Prolyl 3-hydroxylase 2	Leprel1	80	1.67	1.55	17
Acyl-coenzyme A thioesterase 2	Acot2; Acot1	50	1.67	1.71	10
Core histone macro-H2A.2	H2afy2	40	1.62	1.76	13
F-box only protein 2	Fbxo2	34	1.62	1.72	5
Midline-1	Mid1	75	1.61	1.77	14
Membrane primary amine oxidase	Aoc3	85	1.61	2.10	10
Sulfate transporter	Slc26a2	82	1.54	1.91	4
C-type lectin domain family 11 member A	Clec11a	36	1.53	2.12	2
Galactocerebrosidase	Galc	77	1.49	1.27	5
Protein bicaudal C homolog 1	Bicc1	105	1.45	1.25	11
Sodium/potassium-transporting ATPase subunit beta-1	Atp1b1	35	1.43	1.48	7
Pentraxin-related protein PTX3	Ptx3	42	1.39	1.25	7
Protocadherin Fat 4	Fat4	540	1.39	1.56	39
TSC22 Domain Family, Member 2	Tsc22d2	78	1.36	1.87	4
Transmembrane protein 2	Tmem2	154	1.33	1.49	22

Alpha-1-syntrophin	Snta1	53	1.33	1.21	8
Interferon-induced helicase C domain-containing protein 1	Ifih1	116	1.29	1.29	20
Calponin-1	Cnn1	33	1.28	1.25	15
Solute carrier family 12 member 2	Slc12a2	131	1.28	1.45	29
Eukaryotic initiation factor 4A-II	Eif4a2	46	1.23	1.45	9
Netrin receptor UNC5B	Unc5b	102	1.23	1.29	13
Protein FAM115A	Fam115a	103	1.23	1.34	14
Alpha-(1,3)-fucosyltransferase 11	Fut11	56	1.21	1.52	2
MAGUK p55 subfamily member 2	Mpp2	62	1.21	1.59	7
Thrombospondin-1	Thbs1	130	1.21	1.44	24
Eukaryotic translation initiation factor 2A	Eif2a	64	1.19	1.22	19
Semaphorin-3A	Sema3a	79	1.19	1.07	8
Mimecan	Ogn	34	1.18	1.56	10
Methylmalonate-semialdehyde dehydrogenase	Aldh6a1	58	1.17	1.55	5
Nucleobindin-2	Nucb2	50	1.15	1.23	11
Fibronectin type-III domain-containing protein 3A	Fndc3a	127	1.15	1.40	10
Absent In Melanoma 1	Aim1	185	1.14	1.38	28
Immunoglobulin superfamily member 10	Igsf10	286	1.10	1.09	33
Probable ATP-dependent RNA helicase DHX36	Dhx36	114	1.08	1.15	26
FAT Atypical Cadherin 1	Fat1	506	1.06	1.08	85
Selenoprotein T	Selt	22	1.06	0.97	5
Uncharacterized protein KIAA1671	Kiaa1671	35	1.05	1.19	6
Coiled-coil domain-containing protein 80	Ccdc80	108	1.01	1.23	10
Peptidyl-prolyl cis-trans isomerase C	Ppic	23	1.00	1.15	6
Ubiquitin carboxyl-terminal hydrolase 15	Usp15	112	1.00	1.01	28
Collagen alpha-1(I) chain	Col1a1	138	0.99	1.19	45
Palladin	Palld	108	0.89	0.86	28
Collagen alpha-1(V) chain	Col5a1	184	0.87	1.07	23
Collagen alpha-2(I) chain	Col1a2	130	0.86	1.12	50
Utrophin	Utrn	393	0.77	0.84	116
UTP-glucose-1-phosphate uridylyltransferase	Ugp2	57	0.74	0.80	24
Serpin H1	Serpinh1	47	0.73	0.74	22
Myosin-10	Myh10	229	0.69	0.76	69
Alanine--tRNA ligase, cytoplasmic	Aars	107	0.57	0.68	45
Glucose-6-phosphate	Gpi;Gm18	63	-0.67	-0.66	17

isomerase	40				
Protein S100-A4	S100a4	12	-0.69	-0.66	4
Serpin B6	Serpinb6	43	-0.78	-0.79	18
Heat shock 70 kDa protein 4L	Hspa4l	94	-0.82	-0.90	26
Prostaglandin F2 receptor negative regulator	Ptgfrn	99	-0.91	-1.01	13
Apolipoprotein B-100;Apolipoprotein B-48	Apob	504	-0.91	2.11	4
Serine hydroxymethyltransferase cytosolic	Shmt1	53	-0.91	-0.93	22
Thymidine kinase, cytosolic	Tk1	26	-0.95	-0.98	7
Calcium-binding mitochondrial carrier protein SCaMC-1	Slc25a24	53	-0.97	-1.07	17
Hematopoietic progenitor cell antigen CD34	Cd34	35	-0.97	-1.00	5
Voltage-dependent calcium channel subunit alpha-2/delta-1	Cacna2d1	123	-0.98	-1.19	13
Latexin	Lxn	25	-0.99	-1.03	6
ATPase WRNIP1	Wrnip1	72	-1.00	-1.04	13
Serine/threonine-protein phosphatase 6 regulatory ankyrin repeat subunit A	Ankrd28	113	-1.00	-0.96	13
Coiled-coil domain-containing protein 109B	Ccdc109b	40	-1.00	-0.99	4
Protocadherin-19	Pcdh19	121	-1.00	-2.02	3
Peptidyl-prolyl cis-trans isomerase FKBP5	Fkbp5	51	-1.01	-1.12	11
Plakophilin 2	Pkp2	52	-1.04	-0.97	5
Microtubule-associated protein 1B	Map1b	270	-1.09	-1.09	51
N-acylglucosamine 2-epimerase	Renbp	48	-1.11	-1.08	8
Ras Association And Pleckstrin Homology Domains 1	Raph1	67	-1.11	-1.01	9
Lymphocyte antigen 6C1	Ly6c1;Ly6c2	14	-1.11	-1.14	2
Argininosuccinate synthase	Ass1;Gm5424	47	-1.13	-1.09	18
Caspase-12	Casp12	48	-1.14	-1.07	7
High mobility group protein HMG-I/HMG-Y	Hmga1	12	-1.15	-1.09	2
Leukocyte elastase inhibitor A	Serpinb1a	43	-1.17	-1.18	12
Integrin alpha-6	Itga6	120	-1.18	-1.16	6
Testin	Tes	47	-1.19	-0.93	16
KH domain-containing, RNA-binding, signal transduction-associated protein 3	Khdrbs3	39	-1.21	-1.31	5

Carbonic anhydrase 13	Ca13	30	-1.23	-1.15	7
Interferon-activable protein 204	Ifi204	69	-1.26	-1.20	6
DEP domain-containing mTOR-interacting protein	Deptor	46	-1.26	-0.93	9
Ectonucleotide pyrophosphatase/ phosphodiesterase family member 1	Enpp1	103	-1.29	-1.73	11
Interferon-activable protein 202	Ifi202	50	-1.31	-1.51	10
Pirin	Pir	28	-1.33	-1.40	4
UDP-glucuronosyl transferase 1-6	Ugt1a6	60	-1.34	-1.23	7
Aldo-Keto Reductase Family 1, Member B10	Akr1b10	36	-1.42	-1.29	6
Glutathione S-transferase A4	Gsta4	26	-1.44	-1.49	8
Receptor-interacting serine/threonine-protein kinase 3	Ripk3	53	-1.45	-1.32	8
Aldose reductase-related protein 2	Akr1b8	36	-1.53	-1.56	5
Nestin	Nes	202	-1.55	-1.46	35
Tight junction protein ZO-2	Tjp2	131	-1.58	-1.29	14
Collectin-12	Colec12	81	-1.63	-1.87	14
Collagen, Type VI, Alpha 3	Col6a3	354	-1.68	-1.76	78
Neuropilin-1	Nrp1	103	-1.73	-1.28	3
Matrix Gla protein	Mgp	12	-1.78	-1.56	2
Protein-glutamine gamma-glutamyltransferase 2	Tgm2	77	-1.82	-1.19	8
Stimulator of interferon genes protein	Tmem173	43	-1.84	-1.90	7
Cadherin-11	Cdh11	88	-1.87	-1.96	11
Fos-related antigen 1	Fosl1	30	-1.88	-1.29	3
Ceruloplasmin	Cp	121	-1.94	-1.51	3
Epidermal growth factor receptor kinase substrate 8	Eps8	92	-1.94	-1.84	17
Histone H1.1	Hist1h1a	22	-1.96	-2.02	4
Stromal cell-derived factor 1	Cxcl12	10	-1.97	-1.96	2
Cellular retinoic acid-binding protein 2	Crabp2	16	-2.01	-1.87	4
Tudor and KH domain-containing protein	Tdrkh	62	-2.16	-2.57	2
Versican core protein	Vcan	263	-2.25	-1.81	8
Interleukin-1 receptor antagonist protein	Il1rn	18	-2.51	-3.10	4
Serine protease inhibitor A3G	Serpina3g	49	-2.86	-3.22	7
Ubiquitin-like protein	Isg15	18	-3.06	-2.25	5

ISG15					
Interferon-induced protein with tetratricopeptide repeats 1	Ifit1	54	-3.13	-2.95	12
Collagen triple helix repeat-containing protein 1	Cthrc1	26	-3.27	-1.92	4
Osteopontin	Spp1	32	-3.83	-1.88	3

Appendix II – Cellular proteins significantly changed in iMEF.tRNA_i^{Met} cells versus iMEF.Vector cells (pool 1).

The cellular proteome was analysed following tRNA_i^{Met} overexpression using quantitative SILAC mass spectrometry. iMEF.Vector and iMEF.tRNA_i^{Met} cells were labelled with heavy and light amino acids, protein lysates were prepared in 4% SDS lysis buffer, samples combined and analysed by liquid chromatography-mass spectrometry. Forward experiment corresponds to iMEF.tRNA_i^{Met} cells labelled with heavy amino acids combined with iMEF.Vector cells labelled with light amino acids, and the reverse experiment corresponds to iMEF.Vector cells labelled with heavy amino acids combined with iMEF.tRNA_i^{Met} cells labelled with light amino acids. Forward SILAC ratio is calculated as (Log₂ tRNA_i^{Met} / Vector), and reverse SILAC ratio as (1/(Log₂ tRNA_i^{Met} / Vector)), MW = molecular weight, and unique peptides refers to the number of peptides identified that exist only in that one protein of interest. Data generated in collaboration with David Sumpton, CR-UK Beatson Institute, Glasgow.

Appendix II: RNA-Sequencing dataset

Gene Name	Gene symbol	Fold change	P-value
mesenchyme homeobox 1	Meox1	26.28	3.28E-41
collagen, type II, alpha 1	Col2a1	25.41	8.12E-76
pregnancy-associated plasma protein A	Pappa	8.64	1.13E-32
potassium channel tetramerisation domain containing 12b	Kctd12b	6.59	7.03E-24
ABI gene family, member 3 (NESH) binding protein	Abi3bp	6.43	1.74E-23
secreted frizzled-related protein 2	Sfrp2	5.01	4.43E-18
dickkopf homolog 2	Dkk2	3.98	2.66E-13
F-box protein 2	Fbxo2	3.97	2.12E-09
a disintegrin-like and metallopeptidase with thrombospondin type 1 motif, 1	Adamts1	3.77	3.35E-18
ATPase, Na ⁺ /K ⁺ transporting, beta 1 polypeptide	Atp1b1	3.61	7.05E-13
H2A histone family, member Y2	H2afy2	3.44	3.38E-11
nephroblastoma overexpressed gene	Nov	3.22	5.62E-14
homeobox D13	Hoxd13	3.19	3.61E-10
absent in melanoma 1	Aim1	2.88	2.71E-10
platelet-derived growth factor, D polypeptide	Pdgfd	2.82	1.29E-09
carbohydrate (N-acetylglucosamino) sulfotransferase 7	Chst7	2.82	3.72E-08
aryl-hydrocarbon receptor	Ahr	2.81	3.23E-10
family with sequence similarity 198, member B	Fam198b	2.80	9.97E-09
SUN domain containing ossification factor	Suco	2.69	2.06E-09
heat shock protein 1	Hspb1	2.68	6.21E-06
coxsackie virus and adenovirus receptor	Cxadr	2.55	1.44E-08
MDS1 and EVI1 complex locus	Mecom	2.52	2.29E-08
DEAH (Asp-Glu-Ala-His) box polypeptide 36	Dhx36	2.46	5.27E-08
eukaryotic translation initiation factor 2A	Eif2a	2.44	1.82E-07
natriuretic peptide receptor 3	Npr3	2.43	3.73E-08
deleted in liver cancer 1	Dlc1	2.42	3.36E-08
selenoprotein T	Selt	2.41	2.67E-08
GLIS family zinc finger 3	Glis3	2.40	1.99E-07
family with sequence similarity 188, member A	Fam188a	2.38	1.24E-06
lysophosphatidic acid receptor 6	Lpar6	2.38	6.08E-05
unc-5 homolog B	Unc5b	2.37	1.99E-07
fibronectin type 3 and SPRY domain-containing protein	Fsd1	2.37	5.17E-04
ankyrin repeat domain 1 (cardiac muscle)	Ankrd1	2.33	3.37E-07
semaphorin 3A	Sema3a	2.31	7.73E-08
C-type lectin domain family 11, member a	Clec11a	2.30	3.59E-04
transforming, acidic coiled-coil containing protein 1	Tacc1	2.25	1.42E-06
TSC22 domain family, member 2	Tsc22d2	2.25	3.53E-07
UDP-glucose pyrophosphorylase 2	Ugp2	2.18	3.43E-06
sorting nexin 7	Snx7	2.16	5.05E-06
solute carrier family 5 (inositol transporters), member 3	Slc5a3	2.15	5.43E-06
ecotropic viral integration site 2a	Evi2a	2.15	2.91E-03
GULP, engulfment adaptor PTB domain	Gulp1	2.12	1.55E-05

containing 1			
apelin	Apln	2.11	9.55E-05
ezrin	Ezr	2.09	1.56E-05
epithelial membrane protein 1	Emp1	2.08	1.18E-05
serine palmitoyltransferase, small subunit A	Sptssa	2.06	3.48E-05
melanoma cell adhesion molecule	Mcam	2.06	6.15E-04
4-nitrophenylphosphatase domain and non-neuronal SNAP25-like protein homolog 1 (C. elegans)	Nipsnap1	2.05	6.78E-04
serine (or cysteine) peptidase inhibitor, clade E, member 1	Serpine1	2.05	1.15E-05
dickkopf homolog 3 (Xenopus laevis)	Dkk3	2.04	5.27E-05
GTP cyclohydrolase I feedback regulator	Gchfr	2.04	2.86E-03
nidogen 2	Nid2	2.02	2.08E-04
eyes absent 4 homolog	Eya4	2.02	7.19E-05
a disintegrin-like and metallopeptidase with thrombospondin type 1 motif 5	Adamts5	2.02	7.39E-06
semaphorin 3E	Sema3e	1.98	8.66E-05
follistatin-like 1	Fstl1	1.98	5.46E-05
paternally expressed 10	Peg10	1.97	9.37E-05
FAT tumor suppressor homolog 4	Fat4	1.96	8.74E-05
stress-associated endoplasmic reticulum protein 1	Serp1	1.96	8.41E-05
WW domain binding protein 4	Wbp4	1.93	1.77E-03
RIKEN cDNA 4921524J17 gene	4921524J17Rik	1.92	5.54E-03
integrin alpha 3	Itga3	1.92	2.37E-04
procollagen C-endopeptidase enhancer 2	Pcolce2	1.91	9.84E-04
T-box18	Tbx18	1.91	1.33E-03
fibronectin type III domain containing 3A	Fndc3a	1.90	3.48E-04
high mobility group AT-hook 2	Hmga2	1.89	8.68E-04
zinc finger protein 938	Zfp938	1.88	1.51E-02
ubiquitin-conjugating enzyme E2 variant 2	Ube2v2	1.86	1.79E-03
cytokine receptor-like factor 1	Crlf1	1.86	3.10E-02
fucokinase	Fuk	1.86	9.57E-03
E2F transcription factor 6	E2f6	1.86	1.40E-02
ubiquitin specific peptidase 15	Usp15	1.86	4.93E-04
osteoglycin	Ogn	1.86	1.88E-04
component of oligomeric golgi complex 6	Cog6	1.85	9.41E-03
protein kinase C, iota	Prkci	1.84	5.42E-04
membrane protein, palmitoylated 5	Mpp5	1.84	1.96E-03
heparan sulfate 6-O-sulfotransferase 2	Hs6st2	1.83	2.61E-03
sirtuin 1	Sirt1	1.83	4.12E-03
phosphatidylinositol 3-kinase, C2 domain containing, alpha	Pik3c2a	1.83	8.53E-04
suppressor of G2 allele of SKP1	Sugt1	1.83	2.42E-03
polymerase (DNA directed), beta	Polb	1.82	8.12E-03
amyloid beta (A4) precursor protein	App	1.81	6.83E-04
low density lipoprotein receptor-related protein associated protein 1	Lrpap1	1.80	6.92E-03
RIKEN cDNA 2610008E11 gene	2610008E11Rik	1.80	1.82E-03
Fgfr1op N-terminal like	Fopnl	1.80	8.64E-03
ADP-ribosylation factor 2	Arf2	1.79	7.94E-03
charged multivesicular body protein 2B	Chmp2b	1.79	1.25E-02
adenosine kinase	Adk	1.79	3.38E-03
forty-two-three domain containing 1	Fydd1	1.78	1.74E-03
deltex 3 homolog	Dtx3	1.77	2.51E-02

ATP-binding cassette, sub-family B (MDR/TAP), member 10	Abcb10	1.77	3.26E-03
NADH dehydrogenase (ubiquinone) 1, subcomplex unknown, 1	Ndufc1	1.76	2.92E-02
testis-specific protein, Y-encoded-like 1	Tspyl1	1.76	3.36E-03
fibroblast growth factor 7	Fgf7	1.75	1.22E-03
glutathione S-transferase, mu 5	Gstm5	1.74	3.12E-02
TATA box binding protein (Tbp)-associated factor, RNA polymerase I, B	Taf1b	1.74	3.81E-02
kinesin family member 16B	Kif16b	1.74	1.03E-02
E2F-associated phosphoprotein	Eapp	1.74	1.19E-02
Cnksr family member 3	Cnksr3	1.74	1.98E-02
F-box protein 30	Fbxo30	1.74	5.09E-03
vestigial like 3	Vgll3	1.73	6.46E-03
protocadherin 18	Pcdh18	1.73	3.26E-03
UFM1-specific peptidase 2	Ufsp2	1.73	1.35E-02
cytochrome b-245, alpha polypeptide	Cyba	1.72	4.02E-02
LEM domain containing 3	Lemd3	1.72	1.74E-02
stathmin-like 2	Stmn2	1.72	4.83E-03
transmembrane protein 30A	Tmem30a	1.71	6.06E-03
stannin	Snn	1.71	2.41E-02
SMAD specific E3 ubiquitin protein ligase 2	Smurf2	1.70	5.82E-03
ring finger protein 13	Rnf13	1.70	2.11E-02
TGF-beta activated kinase 1/MAP3K7 binding protein 2	Tab2	1.70	6.50E-03
formin homology 2 domain containing 1	Fhod1	1.70	2.58E-02
twist basic helix-loop-helix transcription factor 1	Twist1	1.69	4.56E-02
zinc finger, DHHC domain containing 17	Zdhhc17	1.69	2.88E-02
frizzled homolog 1	Fzd1	1.69	1.64E-02
muscleblind-like 1	Mbnl1	1.68	4.43E-03
signal peptidase complex subunit 3 homolog	Spcs3	1.67	4.08E-03
fibulin 5	Fbln5	1.67	2.51E-02
transmembrane protein 62	Tmem62	1.67	3.75E-02
annexin A3	Anxa3	1.67	4.83E-03
dynein light chain Tctex-type 3	Dynlt3	1.67	1.68E-02
interferon induced with helicase C domain 1	Ifih1	1.67	2.00E-02
tRNA methyltransferase 11	Trmt11	1.66	4.21E-02
cysteine rich protein 61	Cyr61	1.66	3.57E-03
zinc finger protein 617	Zfp617	1.66	3.03E-02
RIKEN cDNA 1700021K19 gene	1700021K19Rik	1.66	2.07E-02
family with sequence similarity 107, member B	Fam107b	1.66	1.32E-02
CD151 antigen	Cd151	1.66	1.56E-02
transmembrane protein 2	Tmem2	1.65	1.28E-02
phosducin-like	Pdcl	1.65	2.04E-02
kinase D-interacting substrate 220	Kidins220	1.65	2.16E-02
host cell factor C2	Hcfc2	1.64	3.80E-02
microtubule associated monooxygenase, calponin and LIM domain containing 1	Mical1	1.64	3.31E-02
LSM4 homolog, U6 small nuclear RNA associated	Lsm4	1.64	3.08E-02
Rho family GTPase 3	Rnd3	1.64	4.92E-03
phosphorylase kinase alpha 2	Phka2	1.64	4.29E-02
exocyst complex component 5	Exoc5	1.63	8.65E-03

high mobility group box transcription factor 1	Hbp1	1.63	2.60E-02
transmembrane 4 superfamily member 1	Tm4sf1	1.63	1.24E-02
disabled 2, mitogen-responsive phosphoprotein	Dab2	1.63	2.47E-02
FK506 binding protein 3	Fkbp3	1.63	3.96E-02
proteasome (prosome, macropain) 26S subunit, ATPase, 6	Psmc6	1.62	1.19E-02
striatin, calmodulin binding protein 3	Strn3	1.62	1.46E-02
G protein-coupled receptor 126	Gpr126	1.62	2.47E-02
REV3-like, catalytic subunit of DNA polymerase zeta RAD54 like	Rev3l	1.62	2.10E-02
store-operated calcium entry-associated regulatory factor	Saraf	1.62	3.19E-02
microfibrillar-associated protein 3-like	Mfap3l	1.62	4.51E-02
C1D nuclear receptor co-repressor	C1d	1.61	3.31E-02
scavenger receptor class F, member 2	Scarf2	1.61	4.10E-02
procollagen lysine, 2-oxoglutarate 5-dioxygenase 2	Plod2	1.61	4.73E-02
serine incorporator 1	Serinc1	1.61	1.59E-02
dermatan sulfate epimerase	Dse	1.60	1.70E-02
pyridoxal-dependent decarboxylase domain containing 1	Pdxdc1	1.60	2.35E-02
Rho guanine nucleotide exchange factor (GEF) 25	Arhgef25	1.60	3.05E-02
regulator of chromosome condensation (RCC1) and BTB (POZ) domain containing protein 2	Rcbtb2	1.60	3.32E-02
peptidylprolyl isomerase (cyclophilin)-like 4	Ppil4	1.59	4.02E-02
heat shock protein 70 family, member 13	Hspa13	1.59	3.14E-02
NUAK family, SNF1-like kinase, 1	Nuak1	1.59	4.54E-02
vacuolar protein sorting 26 homolog A	Vps26a	1.58	3.83E-02
RB1-inducible coiled-coil 1	Rb1cc1	1.58	1.71E-02
succinate-Coenzyme A ligase, ADP-forming, beta subunit	Sucla2	1.58	4.28E-02
family with sequence similarity 115, member A	Fam115a	1.58	3.33E-02
lin-7 homolog C	Lin7c	1.57	1.75E-02
semaphorin 3F	Sema3f	1.57	4.48E-02
LIM and senescent cell antigen-like domains 1	Lims1	1.57	2.17E-02
pleckstrin homology-like domain, family B, member 2	Phldb2	1.57	2.70E-02
caldesmon 1	Cald1	1.56	2.60E-02
myosin, light polypeptide 6, alkali, smooth muscle and non-muscle	Myl6	1.56	2.87E-02
myosin light polypeptide 6 alkali smooth muscle and non-muscle protein, pseudogene	Gm8894	1.56	2.87E-02
proteasome (prosome, macropain) 26S subunit, non-ATPase, 6	Psm6	1.56	4.07E-02
A kinase (PRKA) anchor protein 11	Akap11	1.56	4.52E-02
collagen, type XII, alpha 1	Col12a1	1.55	2.65E-02
methionine sulfoxide reductase B3	Msr3	1.54	3.92E-02
transmembrane emp24 protein transport domain containing 5	Tmed5	1.53	4.22E-02

CD24a antigen	Cd24a	1.52	4.53E-02
G protein-coupled receptor 124	Gpr124	-1.51	4.55E-02
glyceraldehyde-3-phosphate dehydrogenase	Gapdh	-1.52	3.80E-02
predicted gene, 20899	Gm20899	-1.52	3.80E-02
ubiquitin specific peptidase 9, X chromosome	Usp9x	-1.52	4.66E-02
lysosomal-associated membrane protein 2	Lamp2	-1.52	4.03E-02
H1 histone family, member 0	H1f0	-1.53	4.66E-02
parathymosin	Ptms	-1.53	3.83E-02
nucleolin	Ncl	-1.54	4.70E-02
CD34 antigen	Cd34	-1.54	3.57E-02
moesin	Msn	-1.54	3.01E-02
LIM domain and actin binding 1	Lima1	-1.55	2.75E-02
predicted gene 2444	Gm2444	-1.55	3.77E-02
DAZ associated protein 2	Dazap2	-1.55	3.77E-02
golgi transport 1 homolog B	Golt1b	-1.55	4.90E-02
HEAT repeat containing 1	Heatr1	-1.55	3.88E-02
forkhead box P1	Foxp1	-1.56	3.56E-02
NOP2 nucleolar protein	Nop2	-1.56	2.29E-02
antizyme inhibitor 1	Azin1	-1.57	2.39E-02
NADH dehydrogenase subunit 1	ND1	-1.57	2.65E-02
glucose-6-phosphate dehydrogenase X-linked	G6pdx	-1.57	4.19E-02
transducer of ERBB2, 2	Tob2	-1.57	4.96E-02
collagen, type V, alpha 1	Col5a1	-1.58	1.63E-02
integrin alpha 6	Itga6	-1.58	4.57E-02
block of proliferation 1	Bop1	-1.58	2.43E-02
NHP2 ribonucleoprotein	Nhp2	-1.58	4.22E-02
mannosidase 2, alpha 1	Man2a1	-1.59	1.63E-02
solute carrier family 7 (cationic amino acid transporter, y+ system), member 1	Slc7a1	-1.59	3.75E-02
eukaryotic translation initiation factor 4E binding protein 1	Eif4ebp1	-1.59	2.15E-02
UTP15, U3 small nucleolar ribonucleoprotein, homolog	Utp15	-1.59	4.48E-02
cysteinyl-tRNA synthetase	Cars	-1.59	4.02E-02
discoidin domain receptor family, member 2	Ddr2	-1.59	1.69E-02
glutamate receptor, ionotropic, N-methyl D-aspartate-associated protein 1 (glutamate binding)	Grina	-1.59	1.49E-02
four and a half LIM domains 3	Fhl3	-1.59	3.88E-02
protein kinase C, delta	Prkcd	-1.60	2.63E-02
PHD finger protein 10	Phf10	-1.60	2.92E-02
tight junction protein 1	Tjp1	-1.60	1.65E-02
interleukin-1 receptor-associated kinase 1	Irak1	-1.60	3.88E-02
serine (or cysteine) peptidase inhibitor, clade B, member 6a	Serpinb6a	-1.60	1.85E-02
zinc finger CCCH type, antiviral 1	Zc3hav1	-1.61	1.48E-02
RAS p21 protein activator 1	Rasa1	-1.61	2.24E-02
sideroflexin 1	Sfxn1	-1.61	2.65E-02
platelet derived growth factor receptor, beta polypeptide	Pdgfrb	-1.61	1.16E-02
ribosomal RNA processing 1 homolog B	Rrp1b	-1.62	3.34E-02
mitochondrial ribosomal protein L12	Mrpl12	-1.62	4.29E-02
ZPR1 zinc finger	Zpr1	-1.63	4.35E-02

threonyl-tRNA synthetase	Tars	-1.63	9.93E-03
ring finger protein 150	Rnf150	-1.64	1.82E-02
clustered mitochondria (cluA/CLU1) homolog	Cluh	-1.64	1.48E-02
RUN and FYVE domain containing 1	Rufy1	-1.64	4.37E-02
eukaryotic translation initiation factor 3, subunit B	Eif3b	-1.64	9.89E-03
ArfGAP with SH3 domain, ankyrin repeat and PH domain1	Asap1	-1.64	7.91E-03
aldo-keto reductase family 1, member B3 (aldose reductase)	Akr1b3	-1.65	3.31E-02
NA	NA	-1.65	3.42E-02
suppressor of variegation 3-9 homolog 1	Suv39h1	-1.65	2.22E-02
docking protein 1	Dok1	-1.66	1.88E-02
mediator of DNA damage checkpoint 1	Mdc1	-1.66	2.07E-02
tubulin tyrosine ligase-like family, member 12	Ttll12	-1.66	1.52E-02
interferon induced transmembrane protein 3	Ifitm3	-1.66	8.16E-03
NADH dehydrogenase subunit 2	ND2	-1.66	5.74E-03
tumor necrosis factor receptor superfamily, member 1a	Tnfrsf1a	-1.67	1.63E-02
pleckstrin homology domain containing, family O member 1	Plekho1	-1.67	2.59E-02
cerebellar degeneration-related protein 2-like	Cdr2l	-1.67	2.05E-02
PAP associated domain containing 7	Papd7	-1.68	3.08E-02
calcium channel, voltage-dependent, beta 3 subunit	Cacnb3	-1.68	1.56E-02
angiopoietin 1	Angpt1	-1.68	3.05E-02
septin 9	Sept9	-1.69	3.56E-03
gem (nuclear organelle) associated protein 5	Gemin5	-1.69	7.89E-03
plectin	Plec	-1.69	4.92E-03
solute carrier family 11 (proton-coupled divalent metal ion transporters), member 2	Slc11a2	-1.70	1.26E-02
four and a half LIM domains 2	Fhl2	-1.70	1.09E-02
fibrillin 1	Fbn1	-1.70	2.61E-03
methylenetetrahydrofolate dehydrogenase (NADP+ dependent) 1-like	Mthfd1l	-1.71	7.34E-03
mitochondrial ribosomal protein S27	Mrps27	-1.71	4.55E-02
adaptor-related protein complex 3, sigma 1 subunit	Ap3s1	-1.71	2.97E-02
glucose phosphate isomerase 1	Gpi1	-1.71	4.06E-03
KDEL (Lys-Asp-Glu-Leu) endoplasmic reticulum protein retention receptor 3	Kdelr3	-1.71	1.91E-02
transmembrane protein 173	Tmem173	-1.72	3.63E-02
serine hydroxymethyltransferase 1 (soluble)	Shmt1	-1.72	1.12E-02
protein tyrosine phosphatase, receptor type, S	Ptprs	-1.73	1.40E-03
high mobility group AT-hook 1	Hmga1	-1.73	7.27E-03
high mobility group AT-hook I, related sequence 1	Hmga1-rs1	-1.73	7.27E-03
processing of precursor 1, ribonuclease P/MRP family	Pop1	-1.73	5.76E-03

AFG3-like AAA ATPase 2	Afg3l2	-1.73	1.69E-02
interferon-induced protein 35	Ifi35	-1.74	2.95E-02
NOL1/NOP2/Sun domain family member 2	Nsun2	-1.74	2.23E-03
poly(A) binding protein, cytoplasmic 1	Pabpc1	-1.74	2.54E-03
myosin X	Myo10	-1.74	1.92E-03
hexokinase 2	Hk2	-1.75	8.35E-03
sterile alpha motif domain containing 9-like	Samd9l	-1.75	8.57E-03
glypican 1	Gpc1	-1.75	2.11E-03
tubulin, beta 2A class IIA	Tubb2a	-1.75	5.09E-03
erythrocyte protein band 4.1-like 1	Epb4.1l1	-1.76	2.88E-03
family with sequence similarity 102, member B	Fam102b	-1.76	3.10E-03
receptor (TNFRSF)-interacting serine-threonine kinase 1	Ripk1	-1.76	6.45E-03
translocator protein	Tspo	-1.77	1.87E-03
CNDP dipeptidase 2 (metallopeptidase M20 family)	Cndp2	-1.77	4.08E-02
forkhead box M1	Foxm1	-1.77	7.66E-03
Ras and Rab interactor 1	Rin1	-1.77	2.35E-03
coagulation factor II (thrombin) receptor	F2r	-1.77	2.56E-03
phosphoserine aminotransferase 1	Psat1	-1.77	1.47E-03
rho/rac guanine nucleotide exchange factor (GEF) 2	Arhgef2	-1.78	3.98E-03
biglycan	Bgn	-1.78	1.10E-03
5'-nucleotidase domain containing 2	Nt5dc2	-1.78	2.12E-03
branched chain aminotransferase 1, cytosolic	Bcat1	-1.78	1.63E-03
copine VIII	Cpne8	-1.78	5.89E-03
40S ribosomal protein S16-like	LOC100862433	-1.79	1.34E-03
ribosomal protein S16	Rps16	-1.79	1.34E-03
integrin alpha 5 (fibronectin receptor alpha)	Itga5	-1.79	1.34E-03
prostaglandin F2 receptor negative regulator	Ptgfrn	-1.80	2.67E-03
dihydropyrimidinase-like 3	Dpysl3	-1.80	8.68E-04
high mobility group AT-hook I, related sequence 1	Hmga1-rs1	-1.81	6.45E-03
high mobility group AT-hook 1	Hmga1	-1.81	6.45E-03
spermidine synthase	Srm	-1.82	2.50E-03
mannose receptor, C type 2	Mrc2	-1.82	9.97E-04
ral guanine nucleotide dissociation stimulator	Ralgds	-1.82	2.76E-03
interactor of little elongation complex ELL subunit 1	Ice1	-1.82	1.54E-03
nuclear receptor subfamily 3, group C, member 1	Nr3c1	-1.83	2.69E-03
coiled-coil domain containing 109B	Ccdc109b	-1.83	1.20E-02
methylenetetrahydrofolate dehydrogenase (NAD ⁺ dependent)	Mthfd2	-1.84	2.56E-03
renin binding protein	Renbp	-1.84	2.76E-03
neuropilin 1	Nrp1	-1.84	9.56E-04
layilin	Layn	-1.85	1.98E-02
active BCR-related gene	Abr	-1.85	9.49E-04
plasminogen activator, urokinase	Plau	-1.86	6.24E-03
centromere protein H	Cenph	-1.86	1.71E-02
inverted formin, FH2 and WH2 domain	Inf2	-1.86	4.16E-03

containing			
dpy-19-like 1	Dpy19l1	-1.86	1.61E-03
nischarin	Nisch	-1.87	1.17E-04
sperm antigen with calponin homology and coiled-coil domains 1	Specc1	-1.87	3.78E-04
growth arrest specific 1	Gas1	-1.88	2.23E-04
vacuole membrane protein 1	Vmp1	-1.88	2.76E-04
enolase 3, beta muscle	Eno3	-1.89	8.06E-04
glutamate dehydrogenase 1	Glud1	-1.89	1.86E-04
oncostatin M receptor	Osmr	-1.89	6.83E-04
MYB binding protein (P160) 1a	Mybbp1a	-1.89	1.14E-04
strawberry notch homolog 2	Sbno2	-1.89	1.34E-03
heparan sulfate 6-O-sulfotransferase 1	Hs6st1	-1.89	3.47E-03
aldehyde dehydrogenase 18 family, member A1	Aldh18a1	-1.89	3.16E-04
AXL receptor tyrosine kinase	Axl	-1.90	1.11E-04
glutathione S-transferase, theta 1	Gstt1	-1.90	3.27E-03
tubulin, beta 6 class V	Tubb6	-1.90	2.26E-04
glycophorin C	Gypc	-1.90	2.59E-03
Treacher Collins Franceschetti syndrome 1, homolog	Tcof1	-1.91	3.66E-04
glutathione S-transferase, mu 1	Gstm1	-1.91	1.80E-03
Ngfi-A binding protein 1	Nab1	-1.92	1.39E-03
poly (ADP-ribose) polymerase family, member 8	Parp8	-1.93	2.96E-03
cathepsin L	Ctsl	-1.93	8.65E-05
glutamic pyruvate transaminase (alanine aminotransferase) 2	Gpt2	-1.93	2.69E-04
fibronectin 1	<td>-1.94</td> <td>5.98E-05</td>	-1.94	5.98E-05
matrix metalloproteinase 2	Mmp2	-1.94	9.21E-05
sterol O-acyltransferase 1	Soat1	-1.94	1.24E-04
plasminogen activator, tissue	Plat	-1.94	9.07E-05
early growth response 1	Egr1	-1.96	7.14E-03
WNT1 inducible signaling pathway protein 1	Wisp1	-1.96	8.56E-05
histocompatibility 2, K1, K region	H2-K1	-1.97	1.15E-03
cathepsin Z	Ctsz	-1.99	5.44E-04
extracellular matrix protein 1	Ecm1	-2.00	1.92E-03
inhibitor of DNA binding 2	Id2	-2.00	6.50E-03
tensin 3	Tns3	-2.00	1.04E-04
interferon, alpha-inducible protein 27	Ifi27	-2.00	2.09E-04
KH domain containing, RNA binding, signal transduction associated 3	Khdrbs3	-2.01	5.62E-04
abhydrolase domain containing 17C	Abhd17c	-2.02	8.31E-04
tissue inhibitor of metalloproteinase 1	Timp1	-2.02	8.74E-05
fibulin 1	Fbln1	-2.03	1.12E-04
desumoylating isopeptidase 1	Desi1	-2.03	8.46E-04
caspase 12	Casp12	-2.06	6.39E-04
NA	NA	-2.08	6.06E-03
predicted gene 2115	Gm2115	-2.09	1.47E-04
solute carrier family 25 (mitochondrial carrier, phosphate carrier), member 24	Slc25a24	-2.10	1.42E-05
tubulin, alpha 4A	Tuba4a	-2.12	4.01E-04
nestin	Nes	-2.12	3.14E-06
UDP-Gal:betaGlcNAc beta 1,4-galactosyltransferase, polypeptide 5	B4galt5	-2.13	1.02E-04
DEP domain containing MTOR-interacting	Deptor	-2.13	8.84E-06

protein			
suppressor of cytokine signaling 5	Socs5	-2.14	8.50E-05
lysocardiolipin acyltransferase 1	Lclat1	-2.14	3.09E-05
nuclear factor of kappa light polypeptide gene enhancer in B cells 2, p49/p100	Nfkb2	-2.15	9.17E-06
TAP binding protein	Tapbp	-2.17	1.83E-06
exostoses (multiple) 1	Ext1	-2.19	1.61E-06
ribosomal protein S6 kinase, polypeptide 2	Rps6ka2	-2.20	2.91E-05
ankyrin repeat domain 28	Ankrd28	-2.21	2.48E-06
signal-induced proliferation-associated 1 like 2	Sipa1l2	-2.22	1.24E-05
suppressor of cytokine signaling 3	Socs3	-2.23	1.49E-04
death-associated protein	Dap	-2.25	5.79E-07
solute carrier family 1 (neutral amino acid transporter), member 5	Slc1a5	-2.25	4.98E-06
asparagine synthetase	Asns	-2.25	6.57E-07
matrix Gla protein	Mgp	-2.26	4.80E-08
E26 avian leukemia oncogene 2, 3' domain	Ets2	-2.26	9.48E-06
schlafen 9	Slfn9	-2.26	1.38E-05
endoplasmic reticulum metalloproteinase 1	Ermp1	-2.29	3.88E-07
thioredoxin 2	Txn2	-2.29	7.27E-06
epidermal growth factor receptor pathway substrate 8	Eps8	-2.29	4.66E-07
tripartite motif-containing 44	Trim44	-2.30	1.68E-06
serine (or cysteine) peptidase inhibitor, clade F, member 1	Serpinf1	-2.30	9.84E-08
NA	NA	-2.36	3.98E-05
CCAAT/enhancer binding protein (C/EBP), beta	Cebpb	-2.41	1.06E-06
phosphatidic acid phosphatase type 2B	Ppap2b	-2.44	2.47E-06
ChaC, cation transport regulator 1	Chac1	-2.45	6.41E-06
SH3-domain kinase binding protein 1	Sh3kbp1	-2.46	8.09E-08
AE binding protein 1	Aebp1	-2.50	5.02E-09
small nucleolar RNA host gene 9	Snhg9	-2.50	4.64E-02
signal transducer and activator of transcription 2	Stat2	-2.51	7.71E-07
solute carrier family 48 (heme transporter), member 1	Slc48a1	-2.52	1.10E-07
prune homolog 2 (Drosophila)	Prune2	-2.54	1.25E-08
transmembrane protein 119	Tmem119	-2.54	3.98E-07
microtubule-associated protein 1B	Map1b	-2.55	5.11E-09
paired related homeobox 1	Prrx1	-2.56	1.00E-08
phosphatidylinositol 3-kinase, regulatory subunit, polypeptide 1 (p85 alpha)	Pik3r1	-2.64	3.42E-08
chemokine (C-X3-C motif) ligand 1	Cx3cl1	-2.65	1.49E-08
ring finger protein 213	Rnf213	-2.66	8.23E-11
carbonic anhydrase 13	Car13	-2.67	2.22E-07
chemokine (C-X-C motif) ligand 5	Cxcl5	-2.68	8.08E-07
tripartite motif-containing 25	Trim25	-2.69	3.39E-08
latexin	Lxn	-2.73	4.07E-08
vascular endothelial growth factor A	Vegfa	-2.73	1.58E-08
lymphocyte antigen 6 complex, locus E	Ly6e	-2.76	5.49E-08
neuroepithelial cell transforming gene 1	Net1	-2.80	7.99E-10
twist basic helix-loop-helix transcription factor 2	Twist2	-2.85	3.53E-08
cystathionase (cystathionine gamma-lyase)	Cth	-2.86	2.47E-07
protocadherin 19	Pcdh19	-2.91	1.21E-11

OAF homolog (<i>Drosophila</i>)	Oaf	-2.93	7.87E-10
aldehyde dehydrogenase 1 family, member L2	Aldh1l2	-2.94	2.35E-11
CD14 antigen	Cd14	-2.95	1.09E-06
jade family PHD finger 1	Jade1	-2.98	1.14E-09
interferon regulatory factor 1	Irf1	-3.00	3.40E-10
musculoskeletal, embryonic nuclear protein 1	Mustn1	-3.00	2.98E-07
elastin microfibril interfacier 2	Emilin2	-3.04	5.09E-09
collagen, type III, alpha 1	Col3a1	-3.05	6.67E-14
aldo-keto reductase family 1, member B8	Akr1b8	-3.08	2.71E-10
tumor necrosis factor receptor superfamily, member 1b	Tnfrsf1b	-3.11	5.89E-11
cellular retinoic acid binding protein II	Crabp2	-3.12	3.34E-07
CD47 antigen (Rh-related antigen, integrin-associated signal transducer)	Cd47	-3.14	1.50E-10
six transmembrane epithelial antigen of the prostate 1	Steap1	-3.18	1.26E-08
olfactomedin-like 3	Olfml3	-3.24	1.22E-12
LIM and cysteine-rich domains 1	Lmcd1	-3.26	3.17E-09
actin, gamma 2, smooth muscle, enteric	Actg2	-3.37	1.19E-14
glutathione S-transferase, alpha 4	Gsta4	-3.43	9.50E-12
C-type lectin domain family 2, member d	Clec2d	-3.45	6.11E-10
histone cluster 1, H1a	Hist1h1a	-3.55	1.29E-12
platelet derived growth factor receptor, alpha polypeptide	Pdgfra	-3.75	2.65E-14
interferon-activable protein 202-like	LOC100044068	-3.75	1.29E-12
interferon activated gene 202B	Ifi202b	-3.75	1.29E-12
neuregulin 1	Nrg1	-3.83	2.46E-13
leucine-rich repeats and immunoglobulin-like domains 1	Lrig1	-3.84	8.86E-16
activating transcription factor 5	Atf5	-3.88	6.71E-14
collagen, type V, alpha 3	Col5a3	-3.94	1.28E-16
lymphocyte antigen 6 complex, locus C1	Ly6c1	-4.19	3.98E-13
myristoylated alanine rich protein kinase C substrate	Marcks	-4.25	1.58E-21
serine (or cysteine) peptidase inhibitor, clade B, member 1a	Serp1n1a	-4.26	8.52E-11
lymphocyte antigen 6 complex, locus A	Ly6a	-4.49	1.25E-22
Iroquois related homeobox 1	Irx1	-4.64	7.24E-15
corneodesmosin	Cdsn	-4.92	8.10E-16
collectin sub-family member 12	Colec12	-5.13	1.49E-25
bone marrow stromal cell antigen 2	Bst2	-5.63	1.53E-11
pleiotrophin	Ptn	-5.70	3.86E-18
chemokine (C-X-C motif) ligand 12	Cxcl12	-6.16	2.44E-32
interleukin 13 receptor, alpha 1	Il13ra1	-6.68	7.04E-29
insulin-like growth factor binding protein 7	Igfbp7	-6.85	1.72E-23
progressive ankylosis	Ank	-6.94	3.93E-35
interleukin 1 receptor-like 1	Il1rl1	-6.95	3.75E-39
apolipoprotein L 10B	Apol10b	-9.00	3.36E-26
versican	Vcan	-9.14	1.05E-44
interferon-induced protein with tetratricopeptide repeats 1	Ifit1	-9.60	1.92E-38
ISG15 ubiquitin-like modifier	Isg15	-10.55	4.65E-23
chemokine (C-X-C motif) ligand 10	Cxcl10	-10.94	4.42E-33
chemokine (C-C motif) ligand 7	Ccl7	-11.25	1.07E-35
chemokine (C-C motif) ligand 2	Ccl2	-11.89	1.04E-41

collagen, type VI, alpha 3	Col6a3	-12.42	9.39E-60
metallothionein 1	Mt1	-13.00	1.97E-37
secreted phosphoprotein 1	Spp1	-13.54	6.16E-63
cadherin 11	Cdh11	-14.04	9.48E-59
metallothionein 2	Mt2	-14.13	1.23E-26
embigin	Emb	-14.68	1.93E-33
transmembrane protein 176B	Tmem176b	-16.34	1.13E-52
transforming growth factor, beta induced	Tgfb1	-16.76	1.02E-39
chemokine (C-C motif) ligand 5	Ccl5	-19.41	4.47E-40
transmembrane protein 176A	Tmem176a	-20.58	1.22E-45
tetraspanin 11	Tspan11	-25.68	5.21E-62
matrix metalloproteinase 3	Mmp3	-54.25	2.12E-56

Appendix III - Transcripts significantly changed in iMEF.tRNA_i^{Met} cells versus iMEF.Vector cells (pool 1).

The transcriptome was analysed following tRNA_i^{Met} overexpression. RNA was extracted and ribodepleted from three biological replicates of iMEF.tRNA_i^{Met} and iMEF.Vector cell preparations. The RNA-Seq library was prepared with an Illumina TruSeq RNA Sample Prep Kit, with sequencing being performed on the NextSeq500 platform using a High Output 75 cycle kit. The number of reads was normalised for library size, and the mean calculated from the three biological replicates. Fold change represents the ratio of iMEF.tRNA_i^{Met} / iMEF.Vector, with the corresponding adjusted P-value. Only transcripts with a FPKM (fragments per kilobase of exon per million reads) greater than 10 are presented. RNA-Seq conducted by Billy Clark and data analysed by Ann Hedley, CR-UK Beatson Institute, Glasgow.

References

- AARONSON, S. A. 1991. Growth factors and cancer. *Science*, 254, 1146-53.
- ABBOTT, J. A., FRANCKLYN, C. S. & ROBEY-BOND, S. M. 2014. Transfer RNA and human disease. *Front Genet*, 5, 158.
- ABELL, B. M., POOL, M. R., SCHLENKER, O., SINNING, I. & HIGH, S. 2004. Signal recognition particle mediates post-translational targeting in eukaryotes. *EMBO J*, 23, 2755-64.
- ABRAHAM, N., STOJDL, D. F., DUNCAN, P. I., METHOT, N., ISHII, T., DUBE, M., VANDERHYDEN, B. C., ATKINS, H. L., GRAY, D. A., MCBURNEY, M. W., KOROMILAS, A. E., BROWN, E. G., SONENBERG, N. & BELL, J. C. 1999. Characterization of transgenic mice with targeted disruption of the catalytic domain of the double-stranded RNA-dependent protein kinase, PKR. *J Biol Chem*, 274, 5953-62.
- AGRIS, P. F., VENDEIX, F. A. & GRAHAM, W. D. 2007. tRNA's wobble decoding of the genome: 40 years of modification. *J Mol Biol*, 366, 1-13.
- ANDERBERG, C., LI, H., FREDRIKSSON, L., ANDRAE, J., BETSHOLTZ, C., LI, X., ERIKSSON, U. & PIETRAS, K. 2009. Paracrine signaling by platelet-derived growth factor-CC promotes tumor growth by recruitment of cancer-associated fibroblasts. *Cancer Res*, 69, 369-78.
- ANTONELLIS, A., ELLSWORTH, R. E., SAMBUUGHIN, N., PULS, I., ABEL, A., LEE-LIN, S. Q., JORDANOVA, A., KREMENSKY, I., CHRISTODOULOU, K., MIDDLETON, L. T., SIVAKUMAR, K., IONASESCU, V., FUNALOT, B., VANCE, J. M., GOLDFARB, L. G., FISCHBECK, K. H. & GREEN, E. D. 2003. Glycyl tRNA synthetase mutations in Charcot-Marie-Tooth disease type 2D and distal spinal muscular atrophy type V. *Am J Hum Genet*, 72, 1293-9.
- AO, M., FRANCO, O. E., PARK, D., RAMAN, D., WILLIAMS, K. & HAYWARD, S. W. 2007. Cross-talk between paracrine-acting cytokine and chemokine pathways promotes malignancy in benign human prostatic epithelium. *Cancer Res*, 67, 4244-53.
- ARES, M., JR., GRATE, L. & PAULING, M. H. 1999. A handful of intron-containing genes produces the lion's share of yeast mRNA. *RNA*, 5, 1138-9.
- ARNOLD, J. J., SMIDANSKY, E. D., MOUSTAFA, I. M. & CAMERON, C. E. 2012. Human mitochondrial RNA polymerase: structure-function, mechanism and inhibition. *Biochim Biophys Acta*, 1819, 948-60.
- ARTS, G. J., FORNEROD, M. & MATTAJ, I. W. 1998. Identification of a nuclear export receptor for tRNA. *Curr Biol*, 8, 305-14.
- ASTROM, S. U. & BYSTROM, A. S. 1994. Rit1, a tRNA backbone-modifying enzyme that mediates initiator and elongator tRNA discrimination. *Cell*, 79, 535-46.
- B'CHIR, W., MAURIN, A. C., CARRARO, V., AVEROUS, J., JOUSSE, C., MURANISHI, Y., PARRY, L., STEPIEN, G., FAFOURNOUX, P. & BRUHAT, A. 2013. The eIF2alpha/ATF4 pathway is essential for stress-induced autophagy gene expression. *Nucleic Acids Res*, 41, 7683-99.
- BAKER, A. M., BIRD, D., LANG, G., COX, T. R. & ERLER, J. T. 2013. Lysyl oxidase enzymatic function increases stiffness to drive colorectal cancer progression through FAK. *Oncogene*, 32, 1863-8.
- BANDTLOW, C. E. & ZIMMERMANN, D. R. 2000. Proteoglycans in the developing brain: new conceptual insights for old proteins. *Physiol Rev*, 80, 1267-90.
- BANYARD, J., BAO, L., HOFER, M. D., ZURAKOWSKI, D., SPIVEY, K. A., FELDMAN, A. S., HUTCHINSON, L. M., KUEFER, R., RUBIN, M. A. & ZETTER, B. R.

2007. Collagen XXIII expression is associated with prostate cancer recurrence and distant metastases. *Clin Cancer Res*, 13, 2634-42.
- BASS, M. D., MORGAN, M. R. & HUMPHRIES, M. J. 2007a. Integrins and syndecan-4 make distinct, but critical, contributions to adhesion contact formation. *Soft Matter*, 3, 372-376.
- BASS, M. D., MORGAN, M. R., ROACH, K. A., SETTLEMAN, J., GORYACHEV, A. B. & HUMPHRIES, M. J. 2008. p190RhoGAP is the convergence point of adhesion signals from alpha 5 beta 1 integrin and syndecan-4. *J Cell Biol*, 181, 1013-26.
- BASS, M. D., ROACH, K. A., MORGAN, M. R., MOSTAFAVI-POUR, Z., SCHOEN, T., MURAMATSU, T., MAYER, U., BALLESTREM, C., SPATZ, J. P. & HUMPHRIES, M. J. 2007b. Syndecan-4-dependent Rac1 regulation determines directional migration in response to the extracellular matrix. *J Cell Biol*, 177, 527-38.
- BASS, M. D., WILLIAMSON, R. C., NUNAN, R. D., HUMPHRIES, J. D., BYRON, A., MORGAN, M. R., MARTIN, P. & HUMPHRIES, M. J. 2011. A syndecan-4 hair trigger initiates wound healing through caveolin- and RhoG-regulated integrin endocytosis. *Dev Cell*, 21, 681-93.
- BAUER, M., SU, G., CASPER, C., HE, R., REHRAUER, W. & FRIEDL, A. 2010. Heterogeneity of gene expression in stromal fibroblasts of human breast carcinomas and normal breast. *Oncogene*, 29, 1732-40.
- BEGLEY, U., SOSA, M. S., AVIVAR-VALDERAS, A., PATIL, A., ENDRES, L., ESTRADA, Y., CHAN, C. T., SU, D., DEDON, P. C., AGUIRRE-GHISO, J. A. & BEGLEY, T. 2013. A human tRNA methyltransferase 9-like protein prevents tumour growth by regulating LIN9 and HIF1-alpha. *EMBO Mol Med*, 5, 366-83.
- BEUNING, P. J. & MUSIER-FORSYTH, K. 1999. Transfer RNA recognition by aminoacyl-tRNA synthetases. *Biopolymers*, 52, 1-28.
- BHAT, M., ROBICHAUD, N., HULEA, L., SONENBERG, N., PELLETIER, J. & TOPISIROVIC, I. 2015. Targeting the translation machinery in cancer. *Nat Rev Drug Discov*, 14, 261-78.
- BI, M., NACZKI, C., KORITZINSKY, M., FELS, D., BLAIS, J., HU, N., HARDING, H., NOVOA, I., VARIA, M., RALEIGH, J., SCHEUNER, D., KAUFMAN, R. J., BELL, J., RON, D., WOUTERS, B. G. & KOUMENIS, C. 2005. ER stress-regulated translation increases tolerance to extreme hypoxia and promotes tumor growth. *EMBO J*, 24, 3470-81.
- BLAIS, J. D., FILIPENKO, V., BI, M., HARDING, H. P., RON, D., KOUMENIS, C., WOUTERS, B. G. & BELL, J. C. 2004. Activating transcription factor 4 is translationally regulated by hypoxic stress. *Mol Cell Biol*, 24, 7469-82.
- BOGUTA, M. 2013. Maf1, a general negative regulator of RNA polymerase III in yeast. *Biochim Biophys Acta*, 1829, 376-84.
- BRODSKY, B. & PERSIKOV, A. V. 2005. Molecular structure of the collagen triple helix. *Adv Protein Chem*, 70, 301-39.
- BROWN, L. F., BERSE, B., VAN DE WATER, L., PAPADOPOULOS-SERGIU, A., PERRUZZI, C. A., MANSEAU, E. J., DVORAK, H. F. & SENGER, D. R. 1992. Expression and distribution of osteopontin in human tissues: widespread association with luminal epithelial surfaces. *Mol Biol Cell*, 3, 1169-80.
- BROWN, L. F., VAN DE WATER, L., HARVEY, V. S. & DVORAK, H. F. 1988. Fibrinogen influx and accumulation of cross-linked fibrin in healing wounds and in tumor stroma. *Am J Pathol*, 130, 455-65.
- BRUNCKHORST, M. K., WANG, H., LU, R. & YU, Q. 2010. Angiopoietin-4 promotes glioblastoma progression by enhancing tumor cell viability and angiogenesis. *Cancer Res*, 70, 7283-93.

- BUDDE, B. S., NAMAVAR, Y., BARTH, P. G., POLL-THE, B. T., NURNBERG, G., BECKER, C., VAN RUISSEN, F., WETERMAN, M. A., FLUITER, K., TE BEEK, E. T., ARONICA, E., VAN DER KNAAP, M. S., HOHNE, W., TOLIAT, M. R., CROW, Y. J., STEINLING, M., VOIT, T., ROELSEN, F., BRUSSEL, W., BROCKMANN, K., KYLLERMAN, M., BOLTSHAUSER, E., HAMMERSEN, G., WILLEMSSEN, M., BASEL-VANAGAITE, L., KRAGELOH-MANN, I., DE VRIES, L. S., SZTRIHA, L., MUNTONI, F., FERRIE, C. D., BATTINI, R., HENNEKAM, R. C., GRILLO, E., BEEMER, F. A., STOETS, L. M., WOLLNIK, B., NURNBERG, P. & BAAS, F. 2008. tRNA splicing endonuclease mutations cause pontocerebellar hypoplasia. *Nat Genet*, 40, 1113-8.
- BURGESSON, R. E. & HOLLISTER, D. W. 1979. Collagen heterogeneity in human cartilage: identification of several new collagen chains. *Biochem Biophys Res Commun*, 87, 1124-31.
- BURNS-COX, N., AVERY, N. C., GINGELL, J. C. & BAILEY, A. J. 2001. Changes in collagen metabolism in prostate cancer: a host response that may alter progression. *J Urol*, 166, 1698-701.
- CAIRNS, C. A. & WHITE, R. J. 1998. p53 is a general repressor of RNA polymerase III transcription. *EMBO J*, 17, 3112-23.
- CANELLA, D., PRAZ, V., REINA, J. H., COUSIN, P. & HERNANDEZ, N. 2010. Defining the RNA polymerase III transcriptome: Genome-wide localization of the RNA polymerase III transcription machinery in human cells. *Genome Res*, 20, 710-21.
- CASWELL, P. T., CHAN, M., LINDSAY, A. J., MCCAFFREY, M. W., BOETTIGER, D. & NORMAN, J. C. 2008. Rab-coupling protein coordinates recycling of alpha5beta1 integrin and EGFR1 to promote cell migration in 3D microenvironments. *J Cell Biol*, 183, 143-55.
- CASWELL, P. T. & NORMAN, J. C. 2006. Integrin trafficking and the control of cell migration. *Traffic*, 7, 14-21.
- CAWSTON, T. E. & YOUNG, D. A. 2010. Proteinases involved in matrix turnover during cartilage and bone breakdown. *Cell Tissue Res*, 339, 221-35.
- CEBALLOS, M. & VIOQUE, A. 2007. tRNase Z. *Protein Pept Lett*, 14, 137-45.
- CECHOWSKA-PASKO, M., PALKA, J. & WOJTUKIEWICZ, M. Z. 2006. Enhanced prolidase activity and decreased collagen content in breast cancer tissue. *Int J Exp Pathol*, 87, 289-96.
- CHAN, C. T., DYAVAIAH, M., DEMOTT, M. S., TAGHIZADEH, K., DEDON, P. C. & BEGLEY, T. J. 2010. A quantitative systems approach reveals dynamic control of tRNA modifications during cellular stress. *PLoS Genet*, 6, e1001247.
- CHAN, C. T., PANG, Y. L., DENG, W., BABU, I. R., DYAVAIAH, M., BEGLEY, T. J. & DEDON, P. C. 2012. Reprogramming of tRNA modifications controls the oxidative stress response by codon-biased translation of proteins. *Nat Commun*, 3, 937.
- CHANG, H., IIZASA, T., SHIBUYA, K., IYODA, A., SUZUKI, M., MORIYA, Y., LIU, T. L., HIWASA, T., HIROSHIMA, K. & FUJISAWA, T. 2004. Increased expression of collagen XVIII and its prognostic value in nonsmall cell lung carcinoma. *Cancer*, 100, 1665-72.
- CHANG, Y. W. & HUANG, Y. S. 2014. Arsenite-activated JNK signaling enhances CPEB4-Vinexin interaction to facilitate stress granule assembly and cell survival. *PLoS One*, 9, e107961.
- CHEN, W., BOCKER, W., BROSIUS, J. & TIEDGE, H. 1997. Expression of neural BC200 RNA in human tumours. *J Pathol*, 183, 345-51.
- CHENG, J. C. & LEUNG, P. C. 2011. Type I collagen down-regulates E-cadherin expression by increasing PI3KCA in cancer cells. *Cancer Lett*, 304, 107-16.

- CHERNYAKOV, I., WHIPPLE, J. M., KOTELAWALA, L., GRAYHACK, E. J. & PHIZICKY, E. M. 2008. Degradation of several hypomodified mature tRNA species in *Saccharomyces cerevisiae* is mediated by Met22 and the 5'-3' exonucleases Rat1 and Xrn1. *Genes Dev*, 22, 1369-80.
- CHOI, S. T., KIM, J. H., KANG, E. J., LEE, S. W., PARK, M. C., PARK, Y. B. & LEE, S. K. 2008. Osteopontin might be involved in bone remodelling rather than in inflammation in ankylosing spondylitis. *Rheumatology (Oxford)*, 47, 1775-9.
- CHUA, H. H., YEH, T. H., WANG, Y. P., HUANG, Y. T., SHEEN, T. S., LO, Y. C., CHOU, Y. C. & TSAI, C. H. 2008. Upregulation of discoidin domain receptor 2 in nasopharyngeal carcinoma. *Head Neck*, 30, 427-36.
- CIRRI, P. & CHIARUGI, P. 2012. Cancer-associated-fibroblasts and tumour cells: a diabolic liaison driving cancer progression. *Cancer Metastasis Rev*, 31, 195-208.
- CLARKE, E. M., PETERSON, C. L., BRAINARD, A. V. & RIGGS, D. L. 1996. Regulation of the RNA polymerase I and III transcription systems in response to growth conditions. *J Biol Chem*, 271, 22189-95.
- COLLEN, A., HANEMAAIJER, R., LUPU, F., QUAX, P. H., VAN LENT, N., GRIMBERGEN, J., PETERS, E., KOOLWIJK, P. & VAN HINSBERGH, V. W. 2003. Membrane-type matrix metalloproteinase-mediated angiogenesis in a fibrin-collagen matrix. *Blood*, 101, 1810-7.
- CONKLIN, M. W., EICKHOFF, J. C., RICHING, K. M., PEHLKE, C. A., ELICEIRI, K. W., PROVENZANO, P. P., FRIEDL, A. & KEELY, P. J. 2011. Aligned collagen is a prognostic signature for survival in human breast carcinoma. *Am J Pathol*, 178, 1221-32.
- COSTANTINI, V., ZACHARSKI, L. R., MEMOLI, V. A., KISIEL, W., KUDRYK, B. J. & ROUSSEAU, S. M. 1991. Fibrinogen deposition without thrombin generation in primary human breast cancer tissue. *Cancer Res*, 51, 349-53.
- COSTEA, D. E., HILLS, A., OSMAN, A. H., THURLOW, J., KALNA, G., HUANG, X., PENA MURILLO, C., PARAJULI, H., SULIMAN, S., KULASEKARA, K. K., JOHANNESSEN, A. C. & PARTRIDGE, M. 2013. Identification of two distinct carcinoma-associated fibroblast subtypes with differential tumor-promoting abilities in oral squamous cell carcinoma. *Cancer Res*, 73, 3888-901.
- COX, T. R., BIRD, D., BAKER, A. M., BARKER, H. E., HO, M. W., LANG, G. & ERLER, J. T. 2013. LOX-mediated collagen crosslinking is responsible for fibrosis-enhanced metastasis. *Cancer Res*, 73, 1721-32.
- CRICK, F. 1970. Central dogma of molecular biology. *Nature*, 227, 561-3.
- CUKIERMAN, E., PANKOV, R., STEVENS, D. R. & YAMADA, K. M. 2001. Taking cell-matrix adhesions to the third dimension. *Science*, 294, 1708-12.
- DALY, N. L., ARVANITIS, D. A., FAIRLEY, J. A., GOMEZ-ROMAN, N., MORTON, J. P., GRAHAM, S. V., SPANDIDOS, D. A. & WHITE, R. J. 2005. Deregulation of RNA polymerase III transcription in cervical epithelium in response to high-risk human papillomavirus. *Oncogene*, 24, 880-8.
- DANEN, E. H., VAN RHEENEN, J., FRANKEN, W., HUVENEERS, S., SONNEVELD, P., JALINK, K. & SONNENBERG, A. 2005. Integrins control motile strategy through a Rho-cofilin pathway. *J Cell Biol*, 169, 515-26.
- DAVIDSON, L. A. & KELLER, R. E. 1999. Neural tube closure in *Xenopus laevis* involves medial migration, directed protrusive activity, cell intercalation and convergent extension. *Development*, 126, 4547-56.
- DAVULURI, R. V., SUZUKI, Y., SUGANO, S. & ZHANG, M. Q. 2000. CART classification of human 5' UTR sequences. *Genome Res*, 10, 1807-16.

- DE FRANCESCHI, N., HAMIDI, H., ALANKO, J., SAHGAL, P. & IVASKA, J. 2015. Integrin traffic - the update. *J Cell Sci*, 128, 839-52.
- DE WEVER, O., NGUYEN, Q. D., VAN HOORDE, L., BRACKE, M., BRUYNEEL, E., GESPACH, C. & MAREEL, M. 2004. Tenascin-C and SF/HGF produced by myofibroblasts in vitro provide convergent pro-invasive signals to human colon cancer cells through RhoA and Rac. *FASEB J*, 18, 1016-8.
- DEDON, P. C. & BEGLEY, T. J. 2014. A system of RNA modifications and biased codon use controls cellular stress response at the level of translation. *Chem Res Toxicol*, 27, 330-7.
- DEGEN, M., BRELLIER, F., SCHENK, S., DRISCOLL, R., ZAMAN, K., STUPP, R., TORNILLO, L., TERRACCIANO, L., CHIQUET-EHRISMANN, R., RUEGG, C. & SEELENAG, W. 2008. Tenascin-W, a new marker of cancer stroma, is elevated in sera of colon and breast cancer patients. *Int J Cancer*, 122, 2454-61.
- DEGLINCERTI, A., LIU, Y., COLAK, D., HENGST, U., XU, G. & JAFFREY, S. R. 2015. Coupled local translation and degradation regulate growth cone collapse. *Nat Commun*, 6, 6888.
- DEL RIO, A., PEREZ-JIMENEZ, R., LIU, R., ROCA-CUSACHS, P., FERNANDEZ, J. M. & SHEETZ, M. P. 2009. Stretching single talin rod molecules activates vinculin binding. *Science*, 323, 638-41.
- DEVER, T. E., FENG, L., WEK, R. C., CIGAN, A. M., DONAHUE, T. F. & HINNEBUSCH, A. G. 1992. Phosphorylation of initiation factor 2 alpha by protein kinase GCN2 mediates gene-specific translational control of GCN4 in yeast. *Cell*, 68, 585-96.
- DIECI, G., FIORINO, G., CASTELNUOVO, M., TEICHMANN, M. & PAGANO, A. 2007. The expanding RNA polymerase III transcriptome. *Trends Genet*, 23, 614-22.
- DIREKZE, N. C., HODIVALA-DILKE, K., JEFFERY, R., HUNT, T., POULSON, R., OUKRIF, D., ALISON, M. R. & WRIGHT, N. A. 2004. Bone marrow contribution to tumor-associated myofibroblasts and fibroblasts. *Cancer Res*, 64, 8492-5.
- DITTMAR, K. A., GOODENBOUR, J. M. & PAN, T. 2006. Tissue-specific differences in human transfer RNA expression. *PLoS Genet*, 2, e221.
- DONG, J., QIU, H., GARCIA-BARRIO, M., ANDERSON, J. & HINNEBUSCH, A. G. 2000. Uncharged tRNA activates GCN2 by displacing the protein kinase moiety from a bipartite tRNA-binding domain. *Mol Cell*, 6, 269-79.
- DONZE, O., JAGUS, R., KOROMILAS, A. E., HERSHEY, J. W. & SONENBERG, N. 1995. Abrogation of translation initiation factor eIF-2 phosphorylation causes malignant transformation of NIH 3T3 cells. *EMBO J*, 14, 3828-34.
- DOZYNKIEWICZ, M. A., JAMIESON, N. B., MACPHERSON, I., GRINDLAY, J., VAN DEN BERGHE, P. V., VON THUN, A., MORTON, J. P., GOURLEY, C., TIMPSON, P., NIXON, C., MCKAY, C. J., CARTER, R., STRACHAN, D., ANDERSON, K., SANSOM, O. J., CASWELL, P. T. & NORMAN, J. C. 2012. Rab25 and CLIC3 collaborate to promote integrin recycling from late endosomes/lysosomes and drive cancer progression. *Dev Cell*, 22, 131-45.
- DRYGIN, D., LIN, A., BLIESATH, J., HO, C. B., O'BRIEN, S. E., PROFFITT, C., OMORI, M., HADDACH, M., SCHWAEBE, M. K., SIDDIQUI-JAIN, A., STREINER, N., QUIN, J. E., SANIJ, E., BYWATER, M. J., HANNAN, R. D., RYCKMAN, D., ANDERES, K. & RICE, W. G. 2011. Targeting RNA polymerase I with an oral small molecule CX-5461 inhibits ribosomal RNA synthesis and solid tumor growth. *Cancer Res*, 71, 1418-30.

- DULEH, S. N. & WELCH, M. D. 2012. Regulation of integrin trafficking, cell adhesion, and cell migration by WASH and the Arp2/3 complex. *Cytoskeleton (Hoboken)*, 69, 1047-58.
- DULUC, C., MOATASSIM-BILLAH, S., CHALABI-DCHAR, M., PERRAUD, A., SAMAIN, R., BREIBACH, F., GAYRAL, M., CORDELIER, P., DELISLE, M. B., BOUSQUET-DUBOUCH, M. P., TOMASINI, R., SCHMID, H., MATHONNET, M., PYRONNET, S., MARTINEAU, Y. & BOUSQUET, C. 2015. Pharmacological targeting of the protein synthesis mTOR/4E-BP1 pathway in cancer-associated fibroblasts abrogates pancreatic tumour chemoresistance. *EMBO Mol Med*, 7, 735-53.
- DVORAK, H. F. 1986. Tumors: wounds that do not heal. Similarities between tumor stroma generation and wound healing. *N Engl J Med*, 315, 1650-9.
- EGEBLAD, M., RASCH, M. G. & WEAVER, V. M. 2010. Dynamic interplay between the collagen scaffold and tumor evolution. *Curr Opin Cell Biol*, 22, 697-706.
- EL YACOUBI, B., BAILLY, M. & DE CRECY-LAGARD, V. 2012. Biosynthesis and function of posttranscriptional modifications of transfer RNAs. *Annu Rev Genet*, 46, 69-95.
- ELLISON, J. A., VELIER, J. J., SPERA, P., JONAK, Z. L., WANG, X., BARONE, F. C. & FEUERSTEIN, G. Z. 1998. Osteopontin and its integrin receptor alpha(v)beta3 are upregulated during formation of the glial scar after focal stroke. *Stroke*, 29, 1698-706; discussion 1707.
- ERLER, J. T., BENNEWITH, K. L., COX, T. R., LANG, G., BIRD, D., KOONG, A., LE, Q. T. & GIACCIA, A. J. 2009. Hypoxia-induced lysyl oxidase is a critical mediator of bone marrow cell recruitment to form the premetastatic niche. *Cancer Cell*, 15, 35-44.
- ERLER, J. T., BENNEWITH, K. L., NICOLAU, M., DORNHOFER, N., KONG, C., LE, Q. T., CHI, J. T., JEFFREY, S. S. & GIACCIA, A. J. 2006. Lysyl oxidase is essential for hypoxia-induced metastasis. *Nature*, 440, 1222-6.
- ERLER, J. T. & GIACCIA, A. J. 2006. Lysyl oxidase mediates hypoxic control of metastasis. *Cancer Res*, 66, 10238-41.
- FAGIANI, E. & CHRISTOFORI, G. 2013. Angiopoietins in angiogenesis. *Cancer Lett*, 328, 18-26.
- FAIRLEY, J. A., MITCHELL, L. E., BERG, T., KENNETH, N. S., VON SCHUBERT, C., SILLJE, H. H., MEDEMA, R. H., NIGG, E. A. & WHITE, R. J. 2012. Direct regulation of tRNA and 5S rRNA gene transcription by Polo-like kinase 1. *Mol Cell*, 45, 541-52.
- FANG, M., YUAN, J., PENG, C. & LI, Y. 2014. Collagen as a double-edged sword in tumor progression. *Tumour Biol*, 35, 2871-82.
- FELTON-EDKINS, Z. A., KENNETH, N. S., BROWN, T. R., DALY, N. L., GOMEZ-ROMAN, N., GRANDORI, C., EISENMAN, R. N. & WHITE, R. J. 2003. Direct regulation of RNA polymerase III transcription by RB, p53 and c-Myc. *Cell Cycle*, 2, 181-4.
- FEOKTISTOVA, K., TUVSHINTOGS, E., DO, A. & FRASER, C. S. 2013. Human eIF4E promotes mRNA restructuring by stimulating eIF4A helicase activity. *Proc Natl Acad Sci U S A*, 110, 13339-44.
- FINAK, G., BERTOS, N., PEPIN, F., SADEKOVA, S., SOULEIMANOVA, M., ZHAO, H., CHEN, H., OMEROGU, G., METERISSIAN, S., OMEROGU, A., HALLETT, M. & PARK, M. 2008. Stromal gene expression predicts clinical outcome in breast cancer. *Nat Med*, 14, 518-27.
- FISCHER, H., STENLING, R., RUBIO, C. & LINDBLOM, A. 2001. Colorectal carcinogenesis is associated with stromal expression of COL11A1 and COL5A2. *Carcinogenesis*, 22, 875-8.

- FORSPRECHER, J., WANG, Z., NELEA, V. & KAARTINEN, M. T. 2009. Enhanced osteoblast adhesion on transglutaminase 2-crosslinked fibronectin. *Amino Acids*, 36, 747-53.
- FRANK, D. N. & PACE, N. R. 1998. Ribonuclease P: unity and diversity in a tRNA processing ribozyme. *Annu Rev Biochem*, 67, 153-80.
- FRIEDL, P., NOBLE, P. B., WALTON, P. A., LAIRD, D. W., CHAUVIN, P. J., TABAH, R. J., BLACK, M. & ZANKER, K. S. 1995. Migration of coordinated cell clusters in mesenchymal and epithelial cancer explants in vitro. *Cancer Res*, 55, 4557-60.
- FRIEDL, P. & WOLF, K. 2003. Tumour-cell invasion and migration: diversity and escape mechanisms. *Nat Rev Cancer*, 3, 362-74.
- FUKUMURA, D., XAVIER, R., SUGIURA, T., CHEN, Y., PARK, E. C., LU, N., SELIG, M., NIELSEN, G., TAKSIR, T., JAIN, R. K. & SEED, B. 1998. Tumor induction of VEGF promoter activity in stromal cells. *Cell*, 94, 715-25.
- GABAY, M., LI, Y. & FELSHER, D. W. 2014. MYC activation is a hallmark of cancer initiation and maintenance. *Cold Spring Harb Perspect Med*, 4.
- GABBIANI, G., RYAN, G. B. & MAJNE, G. 1971. Presence of modified fibroblasts in granulation tissue and their possible role in wound contraction. *Experientia*, 27, 549-50.
- GALVEZ, B. G., MATIAS-ROMAN, S., YANEZ-MO, M., SANCHEZ-MADRID, F. & ARROYO, A. G. 2002. ECM regulates MT1-MMP localization with beta1 or alphavbeta3 integrins at distinct cell compartments modulating its internalization and activity on human endothelial cells. *J Cell Biol*, 159, 509-21.
- GANI, R. 1976. The nucleoli of cultured human lymphocytes. I. Nucleolar morphology in relation to transformation and the DNA cycle. *Exp Cell Res*, 97, 249-58.
- GAO, B. & ROUX, P. P. 2014. Translational control by oncogenic signaling pathways. *Biochim Biophys Acta*.
- GETZ, M. J., ELDER, P. K., BENZ, E. W., JR., STEPHENS, R. E. & MOSES, H. L. 1976. Effect of cell proliferation on levels and diversity of poly(A)-containing mRNA. *Cell*, 7, 255 -65.
- GHAJAR, C. M., PEINADO, H., MORI, H., MATEI, I. R., EVASON, K. J., BRAZIER, H., ALMEIDA, D., KOLLER, A., HAJJAR, K. A., STAINIER, D. Y., CHEN, E. I., LYDEN, D. & BISSELL, M. J. 2013. The perivascular niche regulates breast tumour dormancy. *Nat Cell Biol*, 15, 807-17.
- GIACHELLI, C. M. & STEITZ, S. 2000. Osteopontin: a versatile regulator of inflammation and biomineralization. *Matrix Biol*, 19, 615-22.
- GIAMPIERI, S., MANNING, C., HOOPER, S., JONES, L., HILL, C. S. & SAHAI, E. 2009. Localized and reversible TGFbeta signalling switches breast cancer cells from cohesive to single cell motility. *Nat Cell Biol*, 11, 1287-96.
- GILKES, D. M., CHATURVEDI, P., BAJPAI, S., WONG, C. C., WEI, H., PITCAIRN, S., HUBBI, M. E., WIRTZ, D. & SEMENZA, G. L. 2013. Collagen prolyl hydroxylases are essential for breast cancer metastasis. *Cancer Res*, 73, 3285-96.
- GINGOLD, H., TEHLER, D., CHRISTOFFERSEN, N. R., NIELSEN, M. M., ASMAR, F., KOOISTRA, S. M., CHRISTOPHERSEN, N. S., CHRISTENSEN, L. L., BORRE, M., SORENSEN, K. D., ANDERSEN, L. D., ANDERSEN, C. L., HULLEMAN, E., WURDINGER, T., RALFKIAER, E., HELIN, K., GRONBAEK, K., ORNTOFT, T., WASZAK, S. M., DAHAN, O., PEDERSEN, J. S., LUND, A. H. & PILPEL, Y. 2014. A dual program for translation regulation in cellular proliferation and differentiation. *Cell*, 158, 1281-92.

- GOMEZ-ROMAN, N., FELTON-EDKINS, Z. A., KENNETH, N. S., GOODFELLOW, S. J., ATHINEOS, D., ZHANG, J., RAMSBOTTOM, B. A., INNES, F., KANTIDAKIS, T., KERR, E. R., BRODIE, J., GRANDORI, C. & WHITE, R. J. 2006. Activation by c-Myc of transcription by RNA polymerases I, II and III. *Biochem Soc Symp*, 141-54.
- GOMEZ-ROMAN, N., GRANDORI, C., EISENMAN, R. N. & WHITE, R. J. 2003. Direct activation of RNA polymerase III transcription by c-Myc. *Nature*, 421, 290-4.
- GOODENBOUR, J. M. & PAN, T. 2006. Diversity of tRNA genes in eukaryotes. *Nucleic Acids Res*, 34, 6137-46.
- GRACZYK, D., WHITE, R. J. & RYAN, K. M. 2015. Involvement of RNA Polymerase III in Immune Responses. *Mol Cell Biol*, 35, 1848-59.
- GU, Z., NOSS, E. H., HSU, V. W. & BRENNER, M. B. 2011. Integrins traffic rapidly via circular dorsal ruffles and macropinocytosis during stimulated cell migration. *J Cell Biol*, 193, 61-70.
- HAAG, J. R. & PIKAARD, C. S. 2011. Multisubunit RNA polymerases IV and V: purveyors of non-coding RNA for plant gene silencing. *Nat Rev Mol Cell Biol*, 12, 483-92.
- HALSTED, K. C., BOWEN, K. B., BOND, L., LUMAN, S. E., JORCYK, C. L., FYFFE, W. E., KRONZ, J. D. & OXFORD, J. T. 2008. Collagen alpha1(XI) in normal and malignant breast tissue. *Mod Pathol*, 21, 1246-54.
- HAMMERMAN, P. S., SOS, M. L., RAMOS, A. H., XU, C., DUTT, A., ZHOU, W., BRACE, L. E., WOODS, B. A., LIN, W., ZHANG, J., DENG, X., LIM, S. M., HEYNCK, S., PEIFER, M., SIMARD, J. R., LAWRENCE, M. S., ONOFRIO, R. C., SALVESEN, H. B., SEIDEL, D., ZANDER, T., HEUCKMANN, J. M., SOLTERMANN, A., MOCH, H., KOKER, M., LEENDERS, F., GABLER, F., QUERINGS, S., ANSEN, S., BRAMBILLA, E., BRAMBILLA, C., LORIMIER, P., BRUSTUGUN, O. T., HELLAND, A., PETERSEN, I., CLEMENT, J. H., GROEN, H., TIMENS, W., SIETSMA, H., STOELBEN, E., WOLF, J., BEER, D. G., TSAO, M. S., HANNA, M., HATTON, C., ECK, M. J., JANNE, P. A., JOHNSON, B. E., WINCKLER, W., GREULICH, H., BASS, A. J., CHO, J., RAUH, D., GRAY, N. S., WONG, K. K., HAURA, E. B., THOMAS, R. K. & MEYERSON, M. 2011. Mutations in the DDR2 kinase gene identify a novel therapeutic target in squamous cell lung cancer. *Cancer Discov*, 1, 78-89.
- HANAHAH, D. & WEINBERG, R. A. 2000. The hallmarks of cancer. *Cell*, 100, 57-70.
- HANAHAH, D. & WEINBERG, R. A. 2011. Hallmarks of cancer: the next generation. *Cell*, 144, 646-74.
- HANGAI, M., KITAYA, N., XU, J., CHAN, C. K., KIM, J. J., WERB, Z., RYAN, S. J. & BROOKS, P. C. 2002. Matrix metalloproteinase-9-dependent exposure of a cryptic migratory control site in collagen is required before retinal angiogenesis. *Am J Pathol*, 161, 1429-37.
- HAO, S., SHARP, J. W., ROSS-INTA, C. M., MCDANIEL, B. J., ANTHONY, T. G., WEK, R. C., CAVENER, D. R., MCGRATH, B. C., RUDELL, J. B., KOEHNLE, T. J. & GIETZEN, D. W. 2005. Uncharged tRNA and sensing of amino acid deficiency in mammalian piriform cortex. *Science*, 307, 1776-8.
- HARPEL, J. G., SCHULTZ-CHERRY, S., MURPHY-ULLRICH, J. E. & RIFKIN, D. B. 2001. Tamoxifen and estrogen effects on TGF-beta formation: role of thrombospondin-1, alphavbeta3, and integrin-associated protein. *Biochem Biophys Res Commun*, 284, 11-4.
- HARPER, J. & SAINSON, R. C. 2014. Regulation of the anti-tumour immune response by cancer-associated fibroblasts. *Semin Cancer Biol*, 25, 69-77.

- HAUSSECKER, D., HUANG, Y., LAU, A., PARAMESWARAN, P., FIRE, A. Z. & KAY, M. A. 2010. Human tRNA-derived small RNAs in the global regulation of RNA silencing. *RNA*, 16, 673-95.
- HAUZENBERGER, D., OLIVIER, P., GUNDERSEN, D. & RUEGG, C. 1999. Tenascin-C inhibits beta1 integrin-dependent T lymphocyte adhesion to fibronectin through the binding of its fnIII 1-5 repeats to fibronectin. *Eur J Immunol*, 29, 1435-47.
- HEGERFELDT, Y., TUSCH, M., BROCKER, E. B. & FRIEDL, P. 2002. Collective cell movement in primary melanoma explants: plasticity of cell-cell interaction, beta1-integrin function, and migration strategies. *Cancer Res*, 62, 2125-30.
- HIRATSUKA, S., NAKAMURA, K., IWAI, S., MURAKAMI, M., ITOH, T., KIJIMA, H., SHIPLEY, J. M., SENIOR, R. M. & SHIBUYA, M. 2002. MMP9 induction by vascular endothelial growth factor receptor-1 is involved in lung-specific metastasis. *Cancer Cell*, 2, 289-300.
- HOAGLAND, M. B., STEPHENSON, M. L., SCOTT, J. F., HECHT, L. I. & ZAMECNIK, P. C. 1958. A soluble ribonucleic acid intermediate in protein synthesis. *J Biol Chem*, 231, 241-57.
- HOFMEISTER, V., SCHRAMA, D. & BECKER, J. C. 2008. Anti-cancer therapies targeting the tumor stroma. *Cancer Immunol Immunother*, 57, 1-17.
- HOLCIK, M. 2004. Targeting translation for treatment of cancer--a novel role for IRES? *Curr Cancer Drug Targets*, 4, 299-311.
- HOLLINGSWORTH, K. G., GORMAN, G. S., TRENELL, M. I., MCFARLAND, R., TAYLOR, R. W., TURNBULL, D. M., MACGOWAN, G. A., BLAMIRE, A. M. & CHINNERY, P. F. 2012. Cardiomyopathy is common in patients with the mitochondrial DNA m.3243A>G mutation and correlates with mutation load. *Neuromuscul Disord*, 22, 592-6.
- HOPPER, A. K. & SHAHEEN, H. H. 2008. A decade of surprises for tRNA nuclear-cytoplasmic dynamics. *Trends Cell Biol*, 18, 98-104.
- HSIEH, A. C., LIU, Y., EDLIND, M. P., INGOLIA, N. T., JANES, M. R., SHER, A., SHI, E. Y., STUMPF, C. R., CHRISTENSEN, C., BONHAM, M. J., WANG, S., REN, P., MARTIN, M., JESSEN, K., FELDMAN, M. E., WEISSMAN, J. S., SHOKAT, K. M., ROMMEL, C. & RUGGERO, D. 2012. The translational landscape of mTOR signalling steers cancer initiation and metastasis. *Nature*, 485, 55-61.
- HSIEH, Y. J., KUNDU, T. K., WANG, Z., KOVELMAN, R. & ROEDER, R. G. 1999a. The TFIIC90 subunit of TFIIC interacts with multiple components of the RNA polymerase III machinery and contains a histone-specific acetyltransferase activity. *Mol Cell Biol*, 19, 7697-704.
- HSIEH, Y. J., WANG, Z., KOVELMAN, R. & ROEDER, R. G. 1999b. Cloning and characterization of two evolutionarily conserved subunits (TFIIC102 and TFIIC63) of human TFIIC and their involvement in functional interactions with TFIIB and RNA polymerase III. *Mol Cell Biol*, 19, 4944-52.
- HU, S., CUI, D., YANG, X., HU, J., WAN, W. & ZENG, J. 2011. The crucial role of collagen-binding integrins in maintaining the mechanical properties of human scleral fibroblasts-seeded collagen matrix. *Mol Vis*, 17, 1334-42.
- HUIJBERS, I. J., IRAVANI, M., POPOV, S., ROBERTSON, D., AL-SARRAJ, S., JONES, C. & ISACKE, C. M. 2010. A role for fibrillar collagen deposition and the collagen internalization receptor endo180 in glioma invasion. *PLoS One*, 5, e9808.
- HUMPHRIES, J. D., BYRON, A. & HUMPHRIES, M. J. 2006. Integrin ligands at a glance. *J Cell Sci*, 119, 3901-3.

- HUVENEERS, S., TRUONG, H., FASSLER, R., SONNENBERG, A. & DANEN, E. H. 2008. Binding of soluble fibronectin to integrin alpha5 beta1 - link to focal adhesion redistribution and contractile shape. *J Cell Sci*, 121, 2452-62.
- HWANG, R. F., MOORE, T., ARUMUGAM, T., RAMACHANDRAN, V., AMOS, K. D., RIVERA, A., JI, B., EVANS, D. B. & LOGSDON, C. D. 2008. Cancer-associated stromal fibroblasts promote pancreatic tumor progression. *Cancer Res*, 68, 918-26.
- HYNES, R. O. 1987. Integrins: a family of cell surface receptors. *Cell*, 48, 549-54.
- HYNES, R. O. 2002. Integrins: bidirectional, allosteric signaling machines. *Cell*, 110, 673-87.
- IBEN, J. R. & MARAIA, R. J. 2012. tRNAomics: tRNA gene copy number variation and codon use provide bioinformatic evidence of a new anticodon:codon wobble pair in a eukaryote. *RNA*, 18, 1358-72.
- IIDA, J., WILHELMSON, K. L., NG, J., LEE, P., MORRISON, C., TAM, E., OVERALL, C. M. & MCCARTHY, J. B. 2007. Cell surface chondroitin sulfate glycosaminoglycan in melanoma: role in the activation of pro-MMP-2 (pro-gelatinase A). *Biochem J*, 403, 553-63.
- ILIC, D., KOVACIC, B., JOHKURA, K., SCHLAEPFER, D. D., TOMASEVIC, N., HAN, Q., KIM, J. B., HOWERTON, K., BAUMBUSCH, C., OGIWARA, N., STREBLOW, D. N., NELSON, J. A., DAZIN, P., SHINO, Y., SASAKI, K. & DAMSKY, C. H. 2004. FAK promotes organization of fibronectin matrix and fibrillar adhesions. *J Cell Sci*, 117, 177-87.
- ISHII, G., HASHIMOTO, H., ASADA, K., ITO, T., HOSHINO, A., FUJII, S., KOJIMA, M., KUWATA, T., HARIGAYA, K., NAGAI, K., USHIJIMA, T. & OCHIAI, A. 2010. Fibroblasts associated with cancer cells keep enhanced migration activity after separation from cancer cells: a novel character of tumor educated fibroblasts. *Int J Oncol*, 37, 317-25.
- IVANOV, P., EMARA, M. M., VILLEN, J., GYGI, S. P. & ANDERSON, P. 2011. Angiogenin-induced tRNA fragments inhibit translation initiation. *Mol Cell*, 43, 613-23.
- IVASKA, J., VUORILUOTO, K., HUOVINEN, T., IZAWA, I., INAGAKI, M. & PARKER, P. J. 2005. PKCepsilon-mediated phosphorylation of vimentin controls integrin recycling and motility. *EMBO J*, 24, 3834-45.
- JACQUEMET, G., GREEN, D. M., BRIDGEWATER, R. E., VON KRIEGSHEIM, A., HUMPHRIES, M. J., NORMAN, J. C. & CASWELL, P. T. 2013. RCP-driven alpha5beta1 recycling suppresses Rac and promotes RhoA activity via the RacGAP1-IQGAP1 complex. *J Cell Biol*, 202, 917-35.
- JIN, L., PAHUJA, K. B., WICKLIFFE, K. E., GORUR, A., BAUMGARTEL, C., SCHEKMAN, R. & RAPE, M. 2012. Ubiquitin-dependent regulation of COPII coat size and function. *Nature*, 482, 495-500.
- JOESTING, M. S., PERRIN, S., ELENBAAS, B., FAWELL, S. E., RUBIN, J. S., FRANCO, O. E., HAYWARD, S. W., CUNHA, G. R. & MARKER, P. C. 2005. Identification of SFRP1 as a candidate mediator of stromal-to-epithelial signaling in prostate cancer. *Cancer Res*, 65, 10423-30.
- JOHNSON, L. F., LEVIS, R., ABELSON, H. T., GREEN, H. & PENMAN, S. 1976. Changes in RNA in relation to growth of the fibroblast. IV. Alterations in the production and processing of mRNA and rRNA in resting and growing cells. *J Cell Biol*, 71, 933-8.
- JOHNSON, S. A., DUBEAU, L. & JOHNSON, D. L. 2008. Enhanced RNA polymerase III-dependent transcription is required for oncogenic transformation. *J Biol Chem*, 283, 19184-91.

- JONES, F. S. & JONES, P. L. 2000. The tenascin family of ECM glycoproteins: structure, function, and regulation during embryonic development and tissue remodeling. *Dev Dyn*, 218, 235-59.
- JOYCE, J. A. & POLLARD, J. W. 2009. Microenvironmental regulation of metastasis. *Nat Rev Cancer*, 9, 239-52.
- KADABA, S., KRUEGER, A., TRICE, T., KRECIC, A. M., HINNEBUSCH, A. G. & ANDERSON, J. 2004. Nuclear surveillance and degradation of hypomodified initiator tRNAMet in *S. cerevisiae*. *Genes Dev*, 18, 1227-40.
- KADLER, K. E., HILL, A. & CANTY-LAIRD, E. G. 2008. Collagen fibrillogenesis: fibronectin, integrins, and minor collagens as organizers and nucleators. *Curr Opin Cell Biol*, 20, 495-501.
- KALLURI, R. & ZEISBERG, M. 2006. Fibroblasts in cancer. *Nat Rev Cancer*, 6, 392-401.
- KANERVA, P. A. & MAENPAA, P. H. 1981. Codon-specific serine transfer ribonucleic acid degradation in avian liver during vitellogenin induction. *Acta Chem Scand B*, 35, 379-85.
- KANTIDAKIS, T., RAMSBOTTOM, B. A., BIRCH, J. L., DOWDING, S. N. & WHITE, R. J. 2010. mTOR associates with TFIIC, is found at tRNA and 5S rRNA genes, and targets their repressor Maf1. *Proc Natl Acad Sci U S A*, 107, 11823-8.
- KAPLAN, R. N., RIBA, R. D., ZACHAROULIS, S., BRAMLEY, A. H., VINCENT, L., COSTA, C., MACDONALD, D. D., JIN, D. K., SHIDO, K., KERNS, S. A., ZHU, Z., HICKLIN, D., WU, Y., PORT, J. L., ALTORKI, N., PORT, E. R., RUGGERO, D., SHMELKOV, S. V., JENSEN, K. K., RAFII, S. & LYDEN, D. 2005. VEGFR1-positive haematopoietic bone marrow progenitors initiate the pre-metastatic niche. *Nature*, 438, 820-7.
- KAPP, L. D. & LORSCH, J. R. 2004. The molecular mechanics of eukaryotic translation. *Annu Rev Biochem*, 73, 657-704.
- KASSAVETIS, G. A., BRAUN, B. R., NGUYEN, L. H. & GEIDUSCHEK, E. P. 1990. *S. cerevisiae* TFIIB is the transcription initiation factor proper of RNA polymerase III, while TFIIA and TFIIC are assembly factors. *Cell*, 60, 235-45.
- KEDERSHA, N., CHEN, S., GILKS, N., LI, W., MILLER, I. J., STAHL, J. & ANDERSON, P. 2002. Evidence that ternary complex (eIF2-GTP-tRNA(i)(Met))-deficient preinitiation complexes are core constituents of mammalian stress granules. *Mol Biol Cell*, 13, 195-210.
- KELWICK, R., DESANLIS, I., WHEELER, G. N. & EDWARDS, D. R. 2015. The ADAMTS (A Disintegrin and Metalloproteinase with Thrombospondin motifs) family. *Genome Biol*, 16, 113.
- KENNETH, N. S., RAMSBOTTOM, B. A., GOMEZ-ROMAN, N., MARSHALL, L., COLE, P. A. & WHITE, R. J. 2007. TRRAP and GCN5 are used by c-Myc to activate RNA polymerase III transcription. *Proc Natl Acad Sci U S A*, 104, 14917-22.
- KIM, J. H., SKATES, S. J., UEDE, T., WONG, K. K., SCHORGE, J. O., FELTMATE, C. M., BERKOWITZ, R. S., CRAMER, D. W. & MOK, S. C. 2002. Osteopontin as a potential diagnostic biomarker for ovarian cancer. *JAMA*, 287, 1671-9.
- KISLAUSKIS, E. H., ZHU, X. & SINGER, R. H. 1994. Sequences responsible for intracellular localization of beta-actin messenger RNA also affect cell phenotype. *J Cell Biol*, 127, 441-51.
- KLANN, E. & DEVER, T. E. 2004. Biochemical mechanisms for translational regulation in synaptic plasticity. *Nat Rev Neurosci*, 5, 931-42.
- KLASS, C. M., COUCHMAN, J. R. & WOODS, A. 2000. Control of extracellular matrix assembly by syndecan-2 proteoglycan. *J Cell Sci*, 113 (Pt 3), 493-506.

- KLEINMAN, H. K., MCGOODWIN, E. B., MARTIN, G. R., KLEBE, R. J., FIETZEK, P. P. & WOOLLEY, D. E. 1978. Localization of the binding site for cell attachment in the alpha1(I) chain of collagen. *J Biol Chem*, 253, 5642-6.
- KLINE, C. L., SCHRUFER, T. L., JEFFERSON, L. S. & KIMBALL, S. R. 2006. Glucosamine-induced phosphorylation of the alpha-subunit of eukaryotic initiation factor 2 is mediated by the protein kinase R-like endoplasmic-reticulum associated kinase. *Int J Biochem Cell Biol*, 38, 1004-14.
- KNUDSON, C. B. & KNUDSON, W. 2001. Cartilage proteoglycans. *Semin Cell Dev Biol*, 12, 69-78.
- KOBEL, M., WEIDENDORFER, D., REINKE, C., LEDERER, M., SCHMITT, W. D., ZENG, K., THOMSEN, C., HAUPTMANN, S. & HUTTELMAIER, S. 2007. Expression of the RNA-binding protein IMP1 correlates with poor prognosis in ovarian carcinoma. *Oncogene*, 26, 7584-9.
- KORITZINSKY, M., MAGAGNIN, M. G., VAN DEN BEUCKEN, T., SEIGNEURIC, R., SAVELKOULS, K., DOSTIE, J., PYRONNET, S., KAUFMAN, R. J., WEPPLER, S. A., VONCKEN, J. W., LAMBIN, P., KOUMENIS, C., SONENBERG, N. & WOUTERS, B. G. 2006. Gene expression during acute and prolonged hypoxia is regulated by distinct mechanisms of translational control. *EMBO J*, 25, 1114-25.
- KOROMILAS, A. E., LAZARIS-KARATZAS, A. & SONENBERG, N. 1992a. mRNAs containing extensive secondary structure in their 5' non-coding region translate efficiently in cells overexpressing initiation factor eIF-4E. *EMBO J*, 11, 4153-8.
- KOROMILAS, A. E., ROY, S., BARBER, G. N., KATZE, M. G. & SONENBERG, N. 1992b. Malignant transformation by a mutant of the IFN-inducible dsRNA-dependent protein kinase. *Science*, 257, 1685-9.
- KRISHNAMOORTHY, T., PAVITT, G. D., ZHANG, F., DEVER, T. E. & HINNEBUSCH, A. G. 2001. Tight binding of the phosphorylated alpha subunit of initiation factor 2 (eIF2alpha) to the regulatory subunits of guanine nucleotide exchange factor eIF2B is required for inhibition of translation initiation. *Mol Cell Biol*, 21, 5018-30.
- KULTTI, A., ZHAO, C., SINGHA, N. C., ZIMMERMAN, S., OSGOOD, R. J., SYMONS, R., JIANG, P., LI, X., THOMPSON, C. B., INFANTE, J. R., JACOBETZ, M. A., TUVESON, D. A., FROST, G. I., SHEPARD, H. M. & HUANG, Z. 2014. Accumulation of extracellular hyaluronan by hyaluronan synthase 3 promotes tumor growth and modulates the pancreatic cancer microenvironment. *Biomed Res Int*, 2014, 817613.
- KUNDU, T. K., WANG, Z. & ROEDER, R. G. 1999. Human TFIIC relieves chromatin-mediated repression of RNA polymerase III transcription and contains an intrinsic histone acetyltransferase activity. *Mol Cell Biol*, 19, 1605-15.
- KUTAY, U., LIPOWSKY, G., IZAURRALDE, E., BISCHOFF, F. R., SCHWARZMAIER, P., HARTMANN, E. & GORLICH, D. 1998. Identification of a tRNA-specific nuclear export receptor. *Mol Cell*, 1, 359-69.
- LAMALICE, L., LE BOEUF, F. & HUOT, J. 2007. Endothelial cell migration during angiogenesis. *Circ Res*, 100, 782-94.
- LATHAM, V. M., JR., KISLAUSKIS, E. H., SINGER, R. H. & ROSS, A. F. 1994. Beta-actin mRNA localization is regulated by signal transduction mechanisms. *J Cell Biol*, 126, 1211-9.
- LATHAM, V. M., YU, E. H., TULLIO, A. N., ADELSTEIN, R. S. & SINGER, R. H. 2001. A Rho-dependent signaling pathway operating through myosin localizes beta-actin mRNA in fibroblasts. *Curr Biol*, 11, 1010-6.

- LECUYER, E., YOSHIDA, H., PARTHASARATHY, N., ALM, C., BABAK, T., CEROVINA, T., HUGHES, T. R., TOMANCAK, P. & KRAUSE, H. M. 2007. Global analysis of mRNA localization reveals a prominent role in organizing cellular architecture and function. *Cell*, 131, 174-87.
- LEE, Y. S., SHIBATA, Y., MALHOTRA, A. & DUTTA, A. 2009a. A novel class of small RNAs: tRNA-derived RNA fragments (tRFs). *Genes Dev*, 23, 2639-49.
- LEE, Y. Y., CEVALLOS, R. C. & JAN, E. 2009b. An upstream open reading frame regulates translation of GADD34 during cellular stresses that induce eIF2alpha phosphorylation. *J Biol Chem*, 284, 6661-73.
- LEITINGER, B., STEPLEWSKI, A. & FERTALA, A. 2004. The D2 period of collagen II contains a specific binding site for the human discoidin domain receptor, DDR2. *J Mol Biol*, 344, 993-1003.
- LEUNG, K. M., VAN HORCK, F. P., LIN, A. C., ALLISON, R., STANDART, N. & HOLT, C. E. 2006. Asymmetrical beta-actin mRNA translation in growth cones mediates attractive turning to netrin-1. *Nat Neurosci*, 9, 1247-56.
- LI, X., MA, Q., XU, Q., DUAN, W., LEI, J. & WU, E. 2012. Targeting the cancer-stroma interaction: a potential approach for pancreatic cancer treatment. *Curr Pharm Des*, 18, 2404-15.
- LIAO, G., MINGLE, L., VAN DE WATER, L. & LIU, G. 2015. Control of cell migration through mRNA localization and local translation. *Wiley Interdiscip Rev RNA*, 6, 1-15.
- LIU, G. Y. & STORZ, P. 2010. Reactive oxygen species in cancer. *Free Radic Res*, 44, 479-96.
- LOIKE, J. D., CAO, L., BUDHU, S., HOFFMAN, S. & SILVERSTEIN, S. C. 2001. Blockade of alpha 5 beta 1 integrins reverses the inhibitory effect of tenascin on chemotaxis of human monocytes and polymorphonuclear leukocytes through three-dimensional gels of extracellular matrix proteins. *J Immunol*, 166, 7534-42.
- LORENI, F., MANCINO, M. & BIFFO, S. 2014. Translation factors and ribosomal proteins control tumor onset and progression: how? *Oncogene*, 33, 2145-56.
- LOWE, T. M. & EDDY, S. R. 1997. tRNAscan-SE: a program for improved detection of transfer RNA genes in genomic sequence. *Nucleic Acids Res*, 25, 955-64.
- LU, P., TAKAI, K., WEAVER, V. M. & WERB, Z. 2011. Extracellular matrix degradation and remodeling in development and disease. *Cold Spring Harb Perspect Biol*, 3.
- LUGA, V. & WRANA, J. L. 2013. Tumor-stroma interaction: Revealing fibroblast-secreted exosomes as potent regulators of Wnt-planar cell polarity signaling in cancer metastasis. *Cancer Res*, 73, 6843-7.
- LUNARDI, S., MUSCHEL, R. J. & BRUNNER, T. B. 2014. The stromal compartments in pancreatic cancer: are there any therapeutic targets? *Cancer Lett*, 343, 147-55.
- LUND, E. & DAHLBERG, J. E. 1998. Proofreading and aminoacylation of tRNAs before export from the nucleus. *Science*, 282, 2082-5.
- LUO, B. H., CARMAN, C. V. & SPRINGER, T. A. 2007. Structural basis of integrin regulation and signaling. *Annu Rev Immunol*, 25, 619-47.
- MACHACEK, M., HODGSON, L., WELCH, C., ELLIOTT, H., PERTZ, O., NALBANT, P., ABELL, A., JOHNSON, G. L., HAHN, K. M. & DANUSER, G. 2009. Coordination of Rho GTPase activities during cell protrusion. *Nature*, 461, 99-103.
- MAHLAB, S., TULLER, T. & LINIAL, M. 2012. Conservation of the relative tRNA composition in healthy and cancerous tissues. *RNA*, 18, 640-52.

- MANNAERTS, I., SCHROYEN, B., VERHULST, S., VAN LOMMEL, L., SCHUIT, F., NYSSSEN, M. & VAN GRUNSVEN, L. A. 2013. Gene expression profiling of early hepatic stellate cell activation reveals a role for Igfbp3 in cell migration. *PLoS One*, 8, e84071.
- MANOJLOVIC, Z. & STEFANOVIĆ, B. 2012. A novel role of RNA helicase A in regulation of translation of type I collagen mRNAs. *RNA*, 18, 321-34.
- MARSHALL, L., RIDEOUT, E. J. & GREWAL, S. S. 2012. Nutrient/TOR-dependent regulation of RNA polymerase III controls tissue and organismal growth in *Drosophila*. *EMBO J*, 31, 1916-30.
- MASAMUNE, A., KIKUTA, K., WATANABE, T., SATOH, K., HIROTA, M., HAMADA, S. & SHIMOSEGAWA, T. 2009. Fibrinogen induces cytokine and collagen production in pancreatic stellate cells. *Gut*, 58, 550-9.
- MAUCK, J. C. & GREEN, H. 1974. Regulation of pre-transfer RNA synthesis during transition from resting to growing state. *Cell*, 3, 171-7.
- MAULIK, G., KIJIMA, T., MA, P. C., GHOSH, S. K., LIN, J., SHAPIRO, G. I., SCHAEFER, E., TIBALDI, E., JOHNSON, B. E. & SALGIA, R. 2002. Modulation of the c-Met/hepatocyte growth factor pathway in small cell lung cancer. *Clin Cancer Res*, 8, 620-7.
- MAURIN, A. C., JOUSSE, C., AVEROUS, J., PARRY, L., BRUHAT, A., CHERASSE, Y., ZENG, H., ZHANG, Y., HARDING, H. P., RON, D. & FAFOURNOUX, P. 2005. The GCN2 kinase biases feeding behavior to maintain amino acid homeostasis in omnivores. *Cell Metab*, 1, 273-7.
- MAUTE, R. L., SCHNEIDER, C., SUMAZIN, P., HOLMES, A., CALIFANO, A., BASSO, K. & DALLA-FAVERA, R. 2013. tRNA-derived microRNA modulates proliferation and the DNA damage response and is down-regulated in B cell lymphoma. *Proc Natl Acad Sci U S A*, 110, 1404-9.
- MAXWELL, P. J., NEISEN, J., MESSENGER, J. & WAUGH, D. J. 2014. Tumor-derived CXCL8 signaling augments stroma-derived CCL2-promoted proliferation and CXCL12-mediated invasion of PTEN-deficient prostate cancer cells. *Oncotarget*, 5, 4895-908.
- MCDONALD, J. A., KELLEY, D. G. & BROEKELMANN, T. J. 1982. Role of fibronectin in collagen deposition: Fab' to the gelatin-binding domain of fibronectin inhibits both fibronectin and collagen organization in fibroblast extracellular matrix. *J Cell Biol*, 92, 485-92.
- MEI, Y., STONESTROM, A., HOU, Y. M. & YANG, X. 2010a. Apoptotic regulation and tRNA. *Protein Cell*, 1, 795-801.
- MEI, Y., YONG, J., LIU, H., SHI, Y., MEINKOTH, J., DREYFUSS, G. & YANG, X. 2010b. tRNA binds to cytochrome c and inhibits caspase activation. *Mol Cell*, 37, 668-78.
- MILI, S., MOISSOGLU, K. & MACARA, I. G. 2008. Genome-wide screen reveals APC-associated RNAs enriched in cell protrusions. *Nature*, 453, 115-9.
- MING, G. L., WONG, S. T., HENLEY, J., YUAN, X. B., SONG, H. J., SPITZER, N. C. & POO, M. M. 2002. Adaptation in the chemotactic guidance of nerve growth cones. *Nature*, 417, 411-8.
- MISHRA, P. J., MISHRA, P. J., HUMENIUK, R., MEDINA, D. J., ALEXE, G., MESIROV, J. P., GANESAN, S., GLOD, J. W. & BANERJEE, D. 2008. Carcinoma-associated fibroblast-like differentiation of human mesenchymal stem cells. *Cancer Res*, 68, 4331-9.
- MITCHELL, S. A., SPRIGGS, K. A., BUSHELL, M., EVANS, J. R., STONELEY, M., LE QUESNE, J. P., SPRIGGS, R. V. & WILLIS, A. E. 2005. Identification of a motif that mediates polypyrimidine tract-binding protein-dependent internal ribosome entry. *Genes Dev*, 19, 1556-71.

- MITRA, A. K., ZILLHARDT, M., HUA, Y., TIWARI, P., MURMANN, A. E., PETER, M. E. & LENGYEL, E. 2012. MicroRNAs reprogram normal fibroblasts into cancer-associated fibroblasts in ovarian cancer. *Cancer Discov*, 2, 1100-8.
- MOGK, A., SCHMIDT, R. & BUKAU, B. 2007. The N-end rule pathway for regulated proteolysis: prokaryotic and eukaryotic strategies. *Trends Cell Biol*, 17, 165-72.
- MOORE, P. B. & STEITZ, T. A. 2002. The involvement of RNA in ribosome function. *Nature*, 418, 229-35.
- MOQTADERI, Z. & STRUHL, K. 2004. Genome-wide occupancy profile of the RNA polymerase III machinery in *Saccharomyces cerevisiae* reveals loci with incomplete transcription complexes. *Mol Cell Biol*, 24, 4118-27.
- MORGAN, M. R., BYRON, A., HUMPHRIES, M. J. & BASS, M. D. 2009. Giving off mixed signals--distinct functions of alpha5beta1 and alphavbeta3 integrins in regulating cell behaviour. *IUBMB Life*, 61, 731-8.
- MORGAN, M. R., HAMIDI, H., BASS, M. D., WARWOOD, S., BALLESTREM, C. & HUMPHRIES, M. J. 2013. Syndecan-4 phosphorylation is a control point for integrin recycling. *Dev Cell*, 24, 472-85.
- MORRIS, N. P. & BACHINGER, H. P. 1987. Type XI collagen is a heterotrimer with the composition (1 alpha, 2 alpha, 3 alpha) retaining non-triple-helical domains. *J Biol Chem*, 262, 11345-50.
- MOSER, M., LEGATE, K. R., ZENT, R. & FASSLER, R. 2009. The tail of integrins, talin, and kindlins. *Science*, 324, 895-9.
- MOSS, T. & STEFANOVSKY, V. Y. 2002. At the center of eukaryotic life. *Cell*, 109, 545-8.
- MOUW, J. K., OU, G. & WEAVER, V. M. 2014. Extracellular matrix assembly: a multiscale deconstruction. *Nat Rev Mol Cell Biol*, 15, 771-85.
- MULLER, P. A., CASWELL, P. T., DOYLE, B., IWANICKI, M. P., TAN, E. H., KARIM, S., LUKASHCHUK, N., GILLESPIE, D. A., LUDWIG, R. L., GOSSELIN, P., CROMER, A., BRUGGE, J. S., SANSOM, O. J., NORMAN, J. C. & VOUSDEN, K. H. 2009. Mutant p53 drives invasion by promoting integrin recycling. *Cell*, 139, 1327-41.
- MULLER, P. A., TRINIDAD, A. G., TIMPSON, P., MORTON, J. P., ZANIVAN, S., VAN DEN BERGHE, P. V., NIXON, C., KARIM, S. A., CASWELL, P. T., NOLL, J. E., COFFILL, C. R., LANE, D. P., SANSOM, O. J., NEILSEN, P. M., NORMAN, J. C. & VOUSDEN, K. H. 2013. Mutant p53 enhances MET trafficking and signalling to drive cell scattering and invasion. *Oncogene*, 32, 1252-65.
- NAUMOV, G. N., AKSLEN, L. A. & FOLKMAN, J. 2006. Role of angiogenesis in human tumor dormancy: animal models of the angiogenic switch. *Cell Cycle*, 5, 1779-87.
- NIELSEN, S., YUZENKOVA, Y. & ZENKIN, N. 2013. Mechanism of eukaryotic RNA polymerase III transcription termination. *Science*, 340, 1577-80.
- NISHIMURA, K., MATSUMIYA, K., MIURA, H., TSUJIMURA, A., NONOMURA, N., MATSUMOTO, K., NAKAMURA, T. & OKUYAMA, A. 2003. Effects of hepatocyte growth factor on urokinase-type plasminogen activator (uPA) and uPA receptor in DU145 prostate cancer cells. *Int J Androl*, 26, 175-9.
- NIU, G. & CHEN, X. 2011. Why integrin as a primary target for imaging and therapy. *Theranostics*, 1, 30-47.
- NOGUEIRA, C., ERLMANN, P., VILLENEUVE, J., SANTOS, A. J., MARTINEZ-ALONSO, E., MARTINEZ-MENARGUEZ, J. A. & MALHOTRA, V. 2014. SLY1 and Syntaxin 18 specify a distinct pathway for procollagen VII export from the endoplasmic reticulum. *Elife*, 3, e02784.

- NOVOA, E. M., PAVON-ETERNOD, M., PAN, T. & RIBAS DE POUPLANA, L. 2012. A role for tRNA modifications in genome structure and codon usage. *Cell*, 149, 202-13.
- NWAGWU, M. & NANA, M. 1980. Ribonucleic acid synthesis in embryonic chick muscle, rates of synthesis and half-lives of transfer and ribosomal RNA species. *J Embryol Exp Morphol*, 56, 253-67.
- O'BRIEN, E. P., VENDRUSCOLO, M. & DOBSON, C. M. 2014. Kinetic modelling indicates that fast-translating codons can coordinate cotranslational protein folding by avoiding misfolded intermediates. *Nat Commun*, 5, 2988.
- OLER, A. J., ALLA, R. K., ROBERTS, D. N., WONG, A., HOLLENHORST, P. C., CHANDLER, K. J., CASSIDAY, P. A., NELSON, C. A., HAGEDORN, C. H., GRAVES, B. J. & CAIRNS, B. R. 2010. Human RNA polymerase III transcriptomes and relationships to Pol II promoter chromatin and enhancer-binding factors. *Nat Struct Mol Biol*, 17, 620-8.
- OLEYNIKOV, Y. & SINGER, R. H. 1998. RNA localization: different zipcodes, same postman? *Trends Cell Biol*, 8, 381-3.
- OLSEN, M. W., LEY, C. D., JUNKER, N., HANSEN, A. J., LUND, E. L. & KRISTJANSEN, P. E. 2006. Angiopoietin-4 inhibits angiogenesis and reduces interstitial fluid pressure. *Neoplasia*, 8, 364-72.
- OLUMI, A. F., GROSSFELD, G. D., HAYWARD, S. W., CARROLL, P. R., TLSTY, T. D. & CUNHA, G. R. 1999. Carcinoma-associated fibroblasts direct tumor progression of initiated human prostatic epithelium. *Cancer Res*, 59, 5002-11.
- ORIMO, A., GUPTA, P. B., SGROI, D. C., ARENZANA-SEISDEDOS, F., DELAUNAY, T., NAEEM, R., CAREY, V. J., RICHARDSON, A. L. & WEINBERG, R. A. 2005. Stromal fibroblasts present in invasive human breast carcinomas promote tumor growth and angiogenesis through elevated SDF-1/CXCL12 secretion. *Cell*, 121, 335-48.
- OSKARSSON, T., ACHARYYA, S., ZHANG, X. H., VANHARANTA, S., TAVAZOIE, S. F., MORRIS, P. G., DOWNEY, R. J., MANOVA-TODOROVA, K., BROGI, E. & MASSAGUE, J. 2011. Breast cancer cells produce tenascin C as a metastatic niche component to colonize the lungs. *Nat Med*, 17, 867-74.
- PAGE-MCCAW, A., EWALD, A. J. & WERB, Z. 2007. Matrix metalloproteinases and the regulation of tissue remodelling. *Nat Rev Mol Cell Biol*, 8, 221-33.
- PAL, S., MOULIK, S., DUTTA, A. & CHATTERJEE, A. 2014. Extracellular matrix protein laminin induces matrix metalloproteinase-9 in human breast cancer cell line mcf-7. *Cancer Microenviron*, 7, 71-8.
- PANG, Y. L., PORURI, K. & MARTINIS, S. A. 2014. tRNA synthetase: tRNA aminoacylation and beyond. *Wiley Interdiscip Rev RNA*, 5, 461-80.
- PARK, J. E., KELLER, G. A. & FERRARA, N. 1993. The vascular endothelial growth factor (VEGF) isoforms: differential deposition into the subepithelial extracellular matrix and bioactivity of extracellular matrix-bound VEGF. *Mol Biol Cell*, 4, 1317-26.
- PASZEK, M. J., ZAHIR, N., JOHNSON, K. R., LAKINS, J. N., ROZENBERG, G. I., GEFEN, A., REINHART-KING, C. A., MARGULIES, S. S., DEMBO, M., BOETTIGER, D., HAMMER, D. A. & WEAVER, V. M. 2005. Tensional homeostasis and the malignant phenotype. *Cancer Cell*, 8, 241-54.
- PATSIALOU, A., BRAVO-CORDERO, J. J., WANG, Y., ENTENBERG, D., LIU, H., CLARKE, M. & CONDEELIS, J. S. 2013. Intravital multiphoton imaging reveals multicellular streaming as a crucial component of in vivo cell migration in human breast tumors. *Intravital*, 2, e25294.

- PAVON-ETERNOD, M., GOMES, S., GESLAIN, R., DAI, Q., ROSNER, M. R. & PAN, T. 2009. tRNA over-expression in breast cancer and functional consequences. *Nucleic Acids Res*, 37, 7268-80.
- PAVON-ETERNOD, M., GOMES, S., ROSNER, M. R. & PAN, T. 2013. Overexpression of initiator methionine tRNA leads to global reprogramming of tRNA expression and increased proliferation in human epithelial cells. *RNA*, 19, 461-6.
- PENG, Q., ZHAO, L., HOU, Y., SUN, Y., WANG, L., LUO, H., PENG, H. & LIU, M. 2013. Biological characteristics and genetic heterogeneity between carcinoma-associated fibroblasts and their paired normal fibroblasts in human breast cancer. *PLoS One*, 8, e60321.
- PERCUDANI, R., PAVESI, A. & OTTONELLO, S. 1997. Transfer RNA gene redundancy and translational selection in *Saccharomyces cerevisiae*. *J Mol Biol*, 268, 322-30.
- PEREZ, W. B. & KINZY, T. G. 2014. Translation elongation factor 1A mutants with altered actin bundling activity show reduced aminoacyl-tRNA binding and alter initiation via eIF2alpha phosphorylation. *J Biol Chem*, 289, 20928-38.
- PESOLE, G., MIGNONE, F., GISSI, C., GRILLO, G., LICCIULLI, F. & LIUNI, S. 2001. Structural and functional features of eukaryotic mRNA untranslated regions. *Gene*, 276, 73-81.
- PETERSEN, O. W., NIELSEN, H. L., GUDJONSSON, T., VILLADSEN, R., RANK, F., NIEBUHR, E., BISSELL, M. J. & RONNOV-JESSEN, L. 2003. Epithelial to mesenchymal transition in human breast cancer can provide a nonmalignant stroma. *Am J Pathol*, 162, 391-402.
- PHANG, J. M., LIU, W., HANCOCK, C. N. & FISCHER, J. W. 2015. Proline metabolism and cancer: emerging links to glutamine and collagen. *Curr Opin Clin Nutr Metab Care*, 18, 71-7.
- PHIZICKY, E. M. & HOPPER, A. K. 2010. tRNA biology charges to the front. *Genes Dev*, 24, 1832-60.
- PIPER, M., SALIH, S., WEINL, C., HOLT, C. E. & HARRIS, W. A. 2005. Endocytosis-dependent desensitization and protein synthesis-dependent resensitization in retinal growth cone adaptation. *Nat Neurosci*, 8, 179-86.
- PLUTA, K., LEFEBVRE, O., MARTIN, N. C., SMAGOWICZ, W. J., STANFORD, D. R., ELLIS, S. R., HOPPER, A. K., SENTENAC, A. & BOGUTA, M. 2001. Maf1p, a negative effector of RNA polymerase III in *Saccharomyces cerevisiae*. *Mol Cell Biol*, 21, 5031-40.
- PORTUGAL, J. & WARING, M. J. 1988. Assignment of DNA binding sites for 4',6'-diamidine-2-phenylindole and bisbenzimidazole (Hoechst 33258). A comparative footprinting study. *Biochim Biophys Acta*, 949, 158-68.
- PROVENCAL, M., BERGER-THIBAUT, N., LABBE, D., VEITCH, R., BOIVIN, D., RIVARD, G. E., GINGRAS, D. & BELIVEAU, R. 2010. Tissue factor mediates the HGF/Met-induced anti-apoptotic pathway in DAOY medulloblastoma cells. *J Neurooncol*, 97, 365-72.
- RAINERO, E., CASWELL, P. T., MULLER, P. A., GRINDLAY, J., MCCAFFREY, M. W., ZHANG, Q., WAKELAM, M. J., VOUSDEN, K. H., GRAZIANI, A. & NORMAN, J. C. 2012. Diacylglycerol kinase alpha controls RCP-dependent integrin trafficking to promote invasive migration. *J Cell Biol*, 196, 277-95.
- RAINERO, E., HOWE, J. D., CASWELL, P. T., JAMIESON, N. B., ANDERSON, K., CRITCHLEY, D. R., MACHESKY, L. & NORMAN, J. C. 2015. Ligand-Occupied Integrin Internalization Links Nutrient Signaling to Invasive Migration. *Cell Rep*.
- REN, B., YEE, K. O., LAWLER, J. & KHOSRAVI-FAR, R. 2006. Regulation of tumor angiogenesis by thrombospondin-1. *Biochim Biophys Acta*, 1765, 178-88.

- RICARD-BLUM, S. 2011. The collagen family. *Cold Spring Harb Perspect Biol*, 3, a004978.
- RICCIARDELLI, C., FREWIN, K. M., TAN IDE, A., WILLIAMS, E. D., OPESKIN, K., PRITCHARD, M. A., INGMAN, W. V. & RUSSELL, D. L. 2011. The ADAMTS1 protease gene is required for mammary tumor growth and metastasis. *Am J Pathol*, 179, 3075-85.
- RIDEOUT, E. J., MARSHALL, L. & GREWAL, S. S. 2012. Drosophila RNA polymerase III repressor Maf1 controls body size and developmental timing by modulating tRNAⁱMet synthesis and systemic insulin signaling. *Proc Natl Acad Sci U S A*, 109, 1139-44.
- RIDLEY, A. J. 2006. Rho GTPases and actin dynamics in membrane protrusions and vesicle trafficking. *Trends Cell Biol*, 16, 522-9.
- RIEDL, S. J. & SALVESEN, G. S. 2007. The apoptosome: signalling platform of cell death. *Nat Rev Mol Cell Biol*, 8, 405-13.
- ROBERT, F., KAPP, L. D., KHAN, S. N., ACKER, M. G., KOLITZ, S., KAZEMI, S., KAUFMAN, R. J., MERRICK, W. C., KOROMILAS, A. E., LORSCH, J. R. & PELLETIER, J. 2006. Initiation of protein synthesis by hepatitis C virus is refractory to reduced eIF2.GTP.Met-tRNA(i)(Met) ternary complex availability. *Mol Biol Cell*, 17, 4632-44.
- ROBERTS, M., BARRY, S., WOODS, A., VAN DER SLUIJS, P. & NORMAN, J. 2001. PDGF-regulated rab4-dependent recycling of alphavbeta3 integrin from early endosomes is necessary for cell adhesion and spreading. *Curr Biol*, 11, 1392-402.
- ROBERTS, M. S., WOODS, A. J., DALE, T. C., VAN DER SLUIJS, P. & NORMAN, J. C. 2004. Protein kinase B/Akt acts via glycogen synthase kinase 3 to regulate recycling of alpha v beta 3 and alpha 5 beta 1 integrins. *Mol Cell Biol*, 24, 1505-15.
- ROJAS-BENITEZ, D., THIAVILLE, P. C., DE CRECY-LAGARD, V. & GLAVIC, A. 2015. The Levels of a Universally Conserved tRNA Modification Regulate Cell Growth. *J Biol Chem*.
- RONNOV-JESSEN, L. & PETERSEN, O. W. 1993. Induction of alpha-smooth muscle actin by transforming growth factor-beta 1 in quiescent human breast gland fibroblasts. Implications for myofibroblast generation in breast neoplasia. *Lab Invest*, 68, 696-707.
- ROSENTHAL, E., MCCRORY, A., TALBERT, M., YOUNG, G., MURPHY-ULLRICH, J. & GLADSON, C. 2004. Elevated expression of TGF-beta1 in head and neck cancer-associated fibroblasts. *Mol Carcinog*, 40, 116-21.
- ROSS, A. F., OLEJNIKOV, Y., KISLAUSKIS, E. H., TANEJA, K. L. & SINGER, R. H. 1997. Characterization of a beta-actin mRNA zipcode-binding protein. *Mol Cell Biol*, 17, 2158-65.
- ROUSSOS, E. T., BALSAMO, M., ALFORD, S. K., WYCKOFF, J. B., GLIGORIJEVIC, B., WANG, Y., POZZUTO, M., STOBEZKI, R., GOSWAMI, S., SEGALL, J. E., LAUFFENBURGER, D. A., BRESNICK, A. R., GERTLER, F. B. & CONDEELIS, J. S. 2011. Mena invasive (Mena^{INV}) promotes multicellular streaming motility and transendothelial migration in a mouse model of breast cancer. *J Cell Sci*, 124, 2120-31.
- ROZEN, F., EDERY, I., MEEROVITCH, K., DEVER, T. E., MERRICK, W. C. & SONENBERG, N. 1990. Bidirectional RNA helicase activity of eucaryotic translation initiation factors 4A and 4F. *Mol Cell Biol*, 10, 1134-44.
- RUBIO, C. A., WEISBURD, B., HOLDERFIELD, M., ARIAS, C., FANG, E., DERISI, J. L. & FANIDI, A. 2014. Transcriptome-wide characterization of the eIF4A signature highlights plasticity in translation regulation. *Genome Biol*, 15, 476.

- RUGGERO, D. 2013. Translational control in cancer etiology. *Cold Spring Harb Perspect Biol*, 5.
- RYBARCZYK, B. J. & SIMPSON-HAIDARIS, P. J. 2000. Fibrinogen assembly, secretion, and deposition into extracellular matrix by MCF-7 human breast carcinoma cells. *Cancer Res*, 60, 2033-9.
- SAITO, K., CHEN, M., BARD, F., CHEN, S., ZHOU, H., WOODLEY, D., POLISCHUK, R., SCHEKMAN, R. & MALHOTRA, V. 2009. TANGO1 facilitates cargo loading at endoplasmic reticulum exit sites. *Cell*, 136, 891-902.
- SAN FRANCISCO, I. F., DEWOLF, W. C., PEEHL, D. M. & OLUMI, A. F. 2004. Expression of transforming growth factor-beta 1 and growth in soft agar differentiate prostate carcinoma-associated fibroblasts from normal prostate fibroblasts. *Int J Cancer*, 112, 213-8.
- SAWADA, Y., TAMADA, M., DUBIN-THALER, B. J., CHERNIAVSKAYA, O., SAKAI, R., TANAKA, S. & SHEETZ, M. P. 2006. Force sensing by mechanical extension of the Src family kinase substrate p130Cas. *Cell*, 127, 1015-26.
- SCHERBERICH, A., TUCKER, R. P., DEGEN, M., BROWN-LUEDDI, M., ANDRES, A. C. & CHIQUET-EHRISMANN, R. 2005. Tenascin-W is found in malignant mammary tumors, promotes alpha8 integrin-dependent motility and requires p38MAPK activity for BMP-2 and TNF-alpha induced expression in vitro. *Oncogene*, 24, 1525-32.
- SCHRAMM, L. & HERNANDEZ, N. 2002. Recruitment of RNA polymerase III to its target promoters. *Genes Dev*, 16, 2593-620.
- SCHWARZBAUER, J. E. 1991. Identification of the fibronectin sequences required for assembly of a fibrillar matrix. *J Cell Biol*, 113, 1463-73.
- SCHWARZBAUER, J. E. & DESIMONE, D. W. 2011. Fibronectins, their fibrillogenesis, and in vivo functions. *Cold Spring Harb Perspect Biol*, 3.
- SCITA, G. & DI FIORE, P. P. 2010. The endocytic matrix. *Nature*, 463, 464-73.
- SEQUEIRA, S. J., RANGANATHAN, A. C., ADAM, A. P., IGLESIAS, B. V., FARIAS, E. F. & AGUIRRE-GHISO, J. A. 2007. Inhibition of proliferation by PERK regulates mammary acinar morphogenesis and tumor formation. *PLoS One*, 2, e615.
- SHAN, S. O. & WALTER, P. 2005. Co-translational protein targeting by the signal recognition particle. *FEBS Lett*, 579, 921-6.
- SHI, F., HARMAN, J., FUJIWARA, K. & SOTTILE, J. 2010. Collagen I matrix turnover is regulated by fibronectin polymerization. *Am J Physiol Cell Physiol*, 298, C1265-75.
- SHI, F. & SOTTILE, J. 2011. MT1-MMP regulates the turnover and endocytosis of extracellular matrix fibronectin. *J Cell Sci*, 124, 4039-50.
- SHI, Y., YANG, Y., HOANG, B., BARDELEBEN, C., HOLMES, B., GERA, J. & LICHTENSTEIN, A. 2015. Therapeutic potential of targeting IRES-dependent c-myc translation in multiple myeloma cells during ER stress. *Oncogene*.
- SHIMADA, K., NAKAMURA, M., ANAI, S., DE VELASCO, M., TANAKA, M., TSUJIKAWA, K., OUJI, Y. & KONISHI, N. 2009. A novel human AlkB homologue, ALKBH8, contributes to human bladder cancer progression. *Cancer Res*, 69, 3157-64.
- SHIMODA, M., MELLODY, K. T. & ORIMO, A. 2010. Carcinoma-associated fibroblasts are a rate-limiting determinant for tumour progression. *Semin Cell Dev Biol*, 21, 19-25.
- SHIN, W. S., TANAKA, M., SUZUKI, J., HEMMI, C. & TOYO-OKA, T. 2000. A novel homoplasmic mutation in mtDNA with a single evolutionary origin as a risk factor for cardiomyopathy. *Am J Hum Genet*, 67, 1617-20.

- SILVA, R., D'AMICO, G., HODIVALA-DILKE, K. M. & REYNOLDS, L. E. 2008. Integrins: the keys to unlocking angiogenesis. *Arterioscler Thromb Vasc Biol*, 28, 1703-13.
- SINGER, C. F., GSCHWANTLER-KAULICH, D., FINK-RETTNER, A., HAAS, C., HUDELIST, G., CZERWENKA, K. & KUBISTA, E. 2008. Differential gene expression profile in breast cancer-derived stromal fibroblasts. *Breast Cancer Res Treat*, 110, 273-81.
- SINGH, P., CARRAHER, C. & SCHWARZBAUER, J. E. 2010. Assembly of fibronectin extracellular matrix. *Annu Rev Cell Dev Biol*, 26, 397-419.
- SONENBERG, N. & HINNEBUSCH, A. G. 2009. Regulation of translation initiation in eukaryotes: mechanisms and biological targets. *Cell*, 136, 731-45.
- SOTTILE, J. & HOCKING, D. C. 2002. Fibronectin polymerization regulates the composition and stability of extracellular matrix fibrils and cell-matrix adhesions. *Mol Biol Cell*, 13, 3546-59.
- SPRIGGS, K. A., STONELEY, M., BUSHELL, M. & WILLIS, A. E. 2008. Re-programming of translation following cell stress allows IRES-mediated translation to predominate. *Biol Cell*, 100, 27-38.
- SRIVASTAVA, S. P., KUMAR, K. U. & KAUFMAN, R. J. 1998. Phosphorylation of eukaryotic translation initiation factor 2 mediates apoptosis in response to activation of the double-stranded RNA-dependent protein kinase. *J Biol Chem*, 273, 2416-23.
- STEPP, M. A., DALEY, W. P., BERNSTEIN, A. M., PAL-GHOSH, S., TADVALKAR, G., SHASHURIN, A., PALSEN, S., JURJUS, R. A. & LARSEN, M. 2010. Syndecan-1 regulates cell migration and fibronectin fibril assembly. *Exp Cell Res*, 316, 2322-39.
- STEWART, O. & LEVY, W. B. 1982. Preferential localization of polyribosomes under the base of dendritic spines in granule cells of the dentate gyrus. *J Neurosci*, 2, 284-91.
- STUART, H. C., JIA, Z., MESSENERG, A., JOSHI, B., UNDERHILL, T. M., MOUKHLES, H. & NABI, I. R. 2008. Localized Rho GTPase activation regulates RNA dynamics and compartmentalization in tumor cell protrusions. *J Biol Chem*, 283, 34785-95.
- SUNG, B. H. & WEAVER, A. M. 2011. Regulation of lysosomal secretion by cortactin drives fibronectin deposition and cell motility. *Bioarchitecture*, 1, 257-260.
- SUNG, B. H., ZHU, X., KAVERINA, I. & WEAVER, A. M. 2011. Cortactin controls cell motility and lamellipodial dynamics by regulating ECM secretion. *Curr Biol*, 21, 1460-9.
- SUZUKI, T., NAGAO, A. & SUZUKI, T. 2011. Human mitochondrial tRNAs: biogenesis, function, structural aspects, and diseases. *Annu Rev Genet*, 45, 299-329.
- TAKAHASHI, Y., SAWADA, G., KURASHIGE, J., MATSUMURA, T., UCHI, R., UEO, H., ISHIBASHI, M., TAKANO, Y., AKIYOSHI, S., IWAYA, T., EGUCHI, H., SUDO, T., SUGIMACHI, K., YAMAMOTO, H., DOKI, Y., MORI, M. & MIMORI, K. 2013. Tumor-derived tenascin-C promotes the epithelial-mesenchymal transition in colorectal cancer cells. *Anticancer Res*, 33, 1927-34.
- TANG, S., HOU, Y., ZHANG, H., TU, G., YANG, L., SUN, Y., LANG, L., TANG, X., DU, Y. E., ZHOU, M., YU, T., XU, L., WEN, S., LIU, C. & LIU, M. 2015a. Oxidized ATM promotes abnormal proliferation of breast CAFs through maintaining intracellular redox homeostasis and activating the PI3K-AKT, MEK-ERK, and Wnt-beta-catenin signaling pathways. *Cell Cycle*, 14, 1908-24.

- TANG, X., HOU, Y., YANG, G., WANG, X., TANG, S., DU, Y. E., YANG, L., YU, T., ZHANG, H., ZHOU, M., WEN, S., XU, L. & LIU, M. 2015b. Stromal miR-200s contribute to breast cancer cell invasion through CAF activation and ECM remodeling. *Cell Death Differ.*
- TARIN, D. & CROFT, C. B. 1969. Ultrastructural features of wound healing in mouse skin. *J Anat*, 105, 189-90.
- TAYLOR, R. W., GIORDANO, C., DAVIDSON, M. M., D'AMATI, G., BAIN, H., HAYES, C. M., LEONARD, H., BARRON, M. J., CASALI, C., SANTORELLI, F. M., HIRANO, M., LIGHTOWLERS, R. N., DIMAURO, S. & TURNBULL, D. M. 2003. A homoplasmic mitochondrial transfer ribonucleic acid mutation as a cause of maternally inherited hypertrophic cardiomyopathy. *J Am Coll Cardiol*, 41, 1786-96.
- TCHOU, J. & CONEJO-GARCIA, J. 2012. Targeting the tumor stroma as a novel treatment strategy for breast cancer: shifting from the neoplastic cell-centric to a stroma-centric paradigm. *Adv Pharmacol*, 65, 45-61.
- TEICHGRABER, V., MONASTERIO, C., CHAITANYA, K., BOGER, R., GORDON, K., DIETERLE, T., JAGER, D. & BAUER, S. 2015. Specific inhibition of fibroblast activation protein (FAP)-alpha prevents tumor progression in vitro. *Adv Med Sci*, 60, 264-272.
- TEJADA, S., LOBO, M. V., GARCIA-VILLANUEVA, M., SACRISTAN, S., PEREZ-MORGADO, M. I., SALINAS, M. & MARTIN, M. E. 2009. Eukaryotic initiation factors (eIF) 2alpha and 4E expression, localization, and phosphorylation in brain tumors. *J Histochem Cytochem*, 57, 503-12.
- THOREEN, C. C., CHANTRANUPONG, L., KEYS, H. R., WANG, T., GRAY, N. S. & SABATINI, D. M. 2012. A unifying model for mTORC1-mediated regulation of mRNA translation. *Nature*, 485, 109-13.
- TIMPL, R. & BROWN, J. C. 1994. The laminins. *Matrix Biol*, 14, 275-81.
- TIMPSON, P., MCGHEE, E. J., MORTON, J. P., VON KRIEGSHEIM, A., SCHWARZ, J. P., KARIM, S. A., DOYLE, B., QUINN, J. A., CARRAGHER, N. O., EDWARD, M., OLSON, M. F., FRAME, M. C., BRUNTON, V. G., SANSOM, O. J. & ANDERSON, K. I. 2011. Spatial regulation of RhoA activity during pancreatic cancer cell invasion driven by mutant p53. *Cancer Res*, 71, 747-57.
- TOCCHINI-VALENTINI, G. D., FRUSCOLONI, P. & TOCCHINI-VALENTINI, G. P. 2009. Processing of multiple-intron-containing pre-tRNA. *Proc Natl Acad Sci U S A*, 106, 20246-51.
- TOMASEK, J. J., GABBIANI, G., HINZ, B., CHAPONNIER, C. & BROWN, R. A. 2002. Myofibroblasts and mechano-regulation of connective tissue remodelling. *Nat Rev Mol Cell Biol*, 3, 349-63.
- TORRE, E. R. & STEWARD, O. 1992. Demonstration of local protein synthesis within dendrites using a new cell culture system that permits the isolation of living axons and dendrites from their cell bodies. *J Neurosci*, 12, 762-72.
- TRUITT, M. L., CONN, C. S., SHI, Z., PANG, X., TOKUYASU, T., COADY, A. M., SEO, Y., BARNA, M. & RUGGERO, D. 2015. Differential Requirements for eIF4E Dose in Normal Development and Cancer. *Cell*, 162, 59-71.
- TULLER, T., CARMİ, A., VESTSIGIAN, K., NAVON, S., DORFAN, Y., ZABORSKE, J., PAN, T., DAHAN, O., FURMAN, I. & PILPEL, Y. 2010. An evolutionarily conserved mechanism for controlling the efficiency of protein translation. *Cell*, 141, 344-54.
- TULLER, T., KUPIEC, M. & RUPPIN, E. 2007. Determinants of protein abundance and translation efficiency in *S. cerevisiae*. *PLoS Comput Biol*, 3, e248.

- ULRICH, T. A., DE JUAN PARDO, E. M. & KUMAR, S. 2009. The mechanical rigidity of the extracellular matrix regulates the structure, motility, and proliferation of glioma cells. *Cancer Res*, 69, 4167-74.
- UNTERGASSER, G., GANDER, R., LILG, C., LEPPERDINGER, G., PLAS, E. & BERGER, P. 2005. Profiling molecular targets of TGF-beta1 in prostate fibroblast-to-myofibroblast transdifferentiation. *Mech Ageing Dev*, 126, 59-69.
- VARSHAVSKY, A. 2011. The N-end rule pathway and regulation by proteolysis. *Protein Sci*, 20, 1298-345.
- VAZQUEZ-VILLA, F., GARCIA-OCANA, M., GALVAN, J. A., GARCIA-MARTINEZ, J., GARCIA-PRAVIA, C., MENENDEZ-RODRIGUEZ, P., GONZALEZ-DEL REY, C., BARNEO-SERRA, L. & DE LOS TOYOS, J. R. 2015. COL11A1/(pro)collagen 11A1 expression is a remarkable biomarker of human invasive carcinoma-associated stromal cells and carcinoma progression. *Tumour Biol*, 36, 2213-22.
- VELLING, T., RISTELI, J., WENNERBERG, K., MOSHER, D. F. & JOHANSSON, S. 2002. Polymerization of type I and III collagens is dependent on fibronectin and enhanced by integrins alpha 11beta 1 and alpha 2beta 1. *J Biol Chem*, 277, 37377-81.
- VIKESAA, J., HANSEN, T. V., JONSON, L., BORUP, R., WEWER, U. M., CHRISTIANSEN, J. & NIELSEN, F. C. 2006. RNA-binding IMPs promote cell adhesion and invadopodia formation. *EMBO J*, 25, 1456-68.
- VLODAVSKY, I. 1999. *Extracellular Matrix*, Current Protocols in Cell Biology, John Wiley & Sons, Inc. .
- WALDRON, C. & LACROUTE, F. 1975. Effect of growth rate on the amounts of ribosomal and transfer ribonucleic acids in yeast. *J Bacteriol*, 122, 855-65.
- WALKER, J. L., FOURNIER, A. K. & ASSOIAN, R. K. 2005. Regulation of growth factor signaling and cell cycle progression by cell adhesion and adhesion-dependent changes in cellular tension. *Cytokine Growth Factor Rev*, 16, 395-405.
- WALTER, P. & BLOBEL, G. 1982. Signal recognition particle contains a 7S RNA essential for protein translocation across the endoplasmic reticulum. *Nature*, 299, 691-8.
- WANG, K. X. & DENHARDT, D. T. 2008. Osteopontin: role in immune regulation and stress responses. *Cytokine Growth Factor Rev*, 19, 333-45.
- WANG, Z., BRYAN, J., FRANZ, C., HAVLIOGLU, N. & SANDELL, L. J. 2010. Type IIB procollagen NH(2)-propeptide induces death of tumor cells via interaction with integrins alpha(V)beta(3) and alpha(V)beta(5). *J Biol Chem*, 285, 20806-17.
- WANG, Z. & ROEDER, R. G. 1995. Structure and function of a human transcription factor TFIIB subunit that is evolutionarily conserved and contains both TFIIB- and high-mobility-group protein 2-related domains. *Proc Natl Acad Sci U S A*, 92, 7026-30.
- WATSON, J. D. & CRICK, F. H. 1953. Molecular structure of nucleic acids; a structure for deoxyribose nucleic acid. *Nature*, 171, 737-8.
- WEGENER, K. L., PARTRIDGE, A. W., HAN, J., PICKFORD, A. R., LIDDINGTON, R. C., GINSBERG, M. H. & CAMPBELL, I. D. 2007. Structural basis of integrin activation by talin. *Cell*, 128, 171-82.
- WEIDENDORFER, D., STOHR, N., BAUDE, A., LEDERER, M., KOHN, M., SCHIERHORN, A., BUCHMEIER, S., WAHLE, E. & HUTTELMAIER, S. 2009. Control of c-myc mRNA stability by IGF2BP1-associated cytoplasmic RNPs. *RNA*, 15, 104-15.

- WEK, S. A., ZHU, S. & WEK, R. C. 1995. The histidyl-tRNA synthetase-related sequence in the eIF-2 alpha protein kinase GCN2 interacts with tRNA and is required for activation in response to starvation for different amino acids. *Mol Cell Biol*, 15, 4497-506.
- WENDEL, H. G., SILVA, R. L., MALINA, A., MILLS, J. R., ZHU, H., UEDA, T., WATANABE-FUKUNAGA, R., FUKUNAGA, R., TERUYA-FELDSTEIN, J., PELLETIER, J. & LOWE, S. W. 2007. Dissecting eIF4E action in tumorigenesis. *Genes Dev*, 21, 3232-7.
- WHITE, D. P., CASWELL, P. T. & NORMAN, J. C. 2007. alpha v beta3 and alpha5beta1 integrin recycling pathways dictate downstream Rho kinase signaling to regulate persistent cell migration. *J Cell Biol*, 177, 515-25.
- WHITE, R. J. 1998. *RNA Polymerase III Transcription*, Springer-Verlag.
- WHITE, R. J. 2001. *Gene Transcription, Mechanisms and Control*, Blackwell Science.
- WHITE, R. J. 2002. *RNA Polymerase III transcription*, Springer.
- WHITE, R. J. 2004. RNA polymerase III transcription and cancer. *Oncogene*, 23, 3208-16.
- WHITE, R. J., TROUCHE, D., MARTIN, K., JACKSON, S. P. & KOUZARIDES, T. 1996. Repression of RNA polymerase III transcription by the retinoblastoma protein. *Nature*, 382, 88-90.
- WILL, C. L. & LUHRMANN, R. 2011. Spliceosome structure and function. *Cold Spring Harb Perspect Biol*, 3.
- WILLETT, M., BROCARD, M., DAVIDE, A. & MORLEY, S. J. 2011. Translation initiation factors and active sites of protein synthesis co-localize at the leading edge of migrating fibroblasts. *Biochem J*, 438, 217-27.
- WILLETT, M., BROCARD, M., POLLARD, H. J. & MORLEY, S. J. 2013. mRNA encoding WAVE-Arp2/3-associated proteins is co-localized with foci of active protein synthesis at the leading edge of MRC5 fibroblasts during cell migration. *Biochem J*, 452, 45-55.
- WILLETT, M., POLLARD, H. J., VLASAK, M. & MORLEY, S. J. 2010. Localization of ribosomes and translation initiation factors to talin/beta3-integrin-enriched adhesion complexes in spreading and migrating mammalian cells. *Biol Cell*, 102, 265-76.
- WILLIAMS, C. M., ENGLER, A. J., SLONE, R. D., GALANTE, L. L. & SCHWARZBAUER, J. E. 2008. Fibronectin expression modulates mammary epithelial cell proliferation during acinar differentiation. *Cancer Res*, 68, 3185-92.
- WILLIS, A. E. 1999. Translational control of growth factor and proto-oncogene expression. *Int J Biochem Cell Biol*, 31, 73-86.
- WILUSZ, J. E., WHIPPLE, J. M., PHIZICKY, E. M. & SHARP, P. A. 2011. tRNAs marked with CCACCA are targeted for degradation. *Science*, 334, 817-21.
- WINTER, A. G., SOURVINOS, G., ALLISON, S. J., TOSH, K., SCOTT, P. H., SPANDIDOS, D. A. & WHITE, R. J. 2000. RNA polymerase III transcription factor TFIIC2 is overexpressed in ovarian tumors. *Proc Natl Acad Sci U S A*, 97, 12619-24.
- WOLFE, A. L., SINGH, K., ZHONG, Y., DREWE, P., RAJASEKHAR, V. K., SANGHVI, V. R., MAVRAKIS, K. J., JIANG, M., RODERICK, J. E., VAN DER MEULEN, J., SCHATZ, J. H., RODRIGO, C. M., ZHAO, C., RONDOU, P., DE STANCHINA, E., TERUYA-FELDSTEIN, J., KELLIHER, M. A., SPELEMAN, F., PORCO, J. A., JR., PELLETIER, J., RATSCH, G. & WENDEL, H. G. 2014. RNA G-quadruplexes cause eIF4A-dependent oncogene translation in cancer. *Nature*, 513, 65-70.

- WONG, K. K., CHENG, R. S. & MOK, S. C. 2001. Identification of differentially expressed genes from ovarian cancer cells by MICROMAX cDNA microarray system. *Biotechniques*, 30, 670-5.
- WOODS, A. J., KANTIDAKIS, T., SABE, H., CRITCHLEY, D. R. & NORMAN, J. C. 2005. Interaction of paxillin with poly(A)-binding protein 1 and its role in focal adhesion turnover and cell migration. *Mol Cell Biol*, 25, 3763-73.
- WOODS, A. J., ROBERTS, M. S., CHOUDHARY, J., BARRY, S. T., MAZAKI, Y., SABE, H., MORLEY, S. J., CRITCHLEY, D. R. & NORMAN, J. C. 2002. Paxillin associates with poly(A)-binding protein 1 at the dense endoplasmic reticulum and the leading edge of migrating cells. *J Biol Chem*, 277, 6428-37.
- WYCKOFF, J. B., WANG, Y., LIN, E. Y., LI, J. F., GOSWAMI, S., STANLEY, E. R., SEGALL, J. E., POLLARD, J. W. & CONDEELIS, J. 2007. Direct visualization of macrophage-assisted tumor cell intravasation in mammary tumors. *Cancer Res*, 67, 2649-56.
- XU, J., RODRIGUEZ, D., PETITCLERC, E., KIM, J. J., HANGAI, M., MOON, Y. S., DAVIS, G. E. & BROOKS, P. C. 2001. Proteolytic exposure of a cryptic site within collagen type IV is required for angiogenesis and tumor growth in vivo. *J Cell Biol*, 154, 1069-79.
- YANG, Y. L., REIS, L. F., PAVLOVIC, J., AGUZZI, A., SCHAFER, R., KUMAR, A., WILLIAMS, B. R., AGUET, M. & WEISSMANN, C. 1995. Deficient signaling in mice devoid of double-stranded RNA-dependent protein kinase. *EMBO J*, 14, 6095-106.
- YAO, J., SASAKI, Y., WEN, Z., BASSELL, G. J. & ZHENG, J. Q. 2006. An essential role for beta-actin mRNA localization and translation in Ca²⁺-dependent growth cone guidance. *Nat Neurosci*, 9, 1265-73.
- YONEDA, A., USHAKOV, D., MULTHAUPT, H. A. & COUCHMAN, J. R. 2007. Fibronectin matrix assembly requires distinct contributions from Rho kinases I and -II. *Mol Biol Cell*, 18, 66-75.
- YOSHIHISA, T., YUNOKI-ESAKI, K., OHSHIMA, C., TANAKA, N. & ENDO, T. 2003. Possibility of cytoplasmic pre-tRNA splicing: the yeast tRNA splicing endonuclease mainly localizes on the mitochondria. *Mol Biol Cell*, 14, 3266-79.
- ZECH, T., CALAMINUS, S. D., CASWELL, P., SPENCE, H. J., CARNELL, M., INSALL, R. H., NORMAN, J. & MACHESKY, L. M. 2011. The Arp2/3 activator WASH regulates alpha5beta1-integrin-mediated invasive migration. *J Cell Sci*, 124, 3753-9.
- ZHENG, Y., RITZENTHALER, J. D., ROMAN, J. & HAN, S. 2007. Nicotine stimulates human lung cancer cell growth by inducing fibronectin expression. *Am J Respir Cell Mol Biol*, 37, 681-90.
- ZHENG, Z. Y., TIAN, L., BU, W., FAN, C., GAO, X., WANG, H., LIAO, Y. H., LI, Y., LEWIS, M. T., EDWARDS, D., ZWAKA, T. P., HILSENBECK, S. G., MEDINA, D., PEROU, C. M., CREIGHTON, C. J., ZHANG, X. H. & CHANG, E. C. 2015. Wild-Type N-Ras, Overexpressed in Basal-like Breast Cancer, Promotes Tumor Formation by Inducing IL-8 Secretion via JAK2 Activation. *Cell Rep*.
- ZHOU, L., YANG, K., ANDL, T., WICKETT, R. R. & ZHANG, Y. 2015. Perspective of Targeting Cancer-Associated Fibroblasts in Melanoma. *J Cancer*, 6, 717-26.
- ZHOU, Y., GOODENBOUR, J. M., GODLEY, L. A., WICKREMA, A. & PAN, T. 2009. High levels of tRNA abundance and alteration of tRNA charging by bortezomib in multiple myeloma. *Biochem Biophys Res Commun*, 385, 160-4.

- ZHU, G. G., RISTELI, L., MAKINEN, M., RISTELI, J., KAUPPILA, A. & STENBACK, F. 1995. Immunohistochemical study of type I collagen and type I pN-collagen in benign and malignant ovarian neoplasms. *Cancer*, 75, 1010-7.
- ZOU, X., FENG, B., DONG, T., YAN, G., TAN, B., SHEN, H., HUANG, A., ZHANG, X., ZHANG, M., YANG, P., ZHENG, M. & ZHANG, Y. 2013. Up-regulation of type I collagen during tumorigenesis of colorectal cancer revealed by quantitative proteomic analysis. *J Proteomics*, 94, 473-85.